B. Fischer-Tropsch Synthesis with Precipitated Iron Catalysts Using Hydrogen Rich Syngas

Introduction

The two most common sources of syngas proposed for Fischer-Tropsch synthesis are coal and natural gas. The FTS reaction requires a H_2/CO ratio greater than 2:1.

$$CO + (1+(x/2y))\ H_2 \rightarrow (1/y)\ C_yH_x + H_2O \quad (1)$$

Advanced coal gasifiers produce syngas that is deficient in hydrogen with respect to the FTS stoichiometry (1). Iron based FTS catalysts are capable of utilizing hydrogen lean syngas because they are also active for the water-gas shift reaction. Unconverted CO can react with H_2O generated by the FTS to produce additional H_2.

$$CO + H_2O \rightarrow CO_2 + H_2 \quad (2)$$

The overall effect is a decrease in catalyst efficiency because a significant amount of CO is converted to CO_2; however, the need for an external water-gas shift step is eliminated.

Cobalt catalysts have much lower water-gas shift activity than iron catalysts and are generally not suitable for FTS with coal derived syngas without an external water-gas shift step. Syngas derived from natural gas is more hydrogen rich than coal derived syngas and as a consequence is better suited for cobalt catalysts. Using iron based catalysts for the conversion of syngas derived from natural gas is more complicated because the water-gas shift is not needed to the same extent as with coal derived syngas and will result in lower catalyst efficiency. We have shown that when using hydrogen lean syngas, typical of that derived from coal, it is possible to decrease the water-gas shift rate relative to the FTS rate by operating at low to moderate conversion (30% to 50%) (2,3). At low conversion, the FTS rate is higher than the water-gas shift rate; as the conversion is increased, the water-gas shift rate approaches the rate of the FTS (Figure 1). For syngas with $H_2/CO=0.67$, the H_2/CO usage ratio is equal to the H_2/CO ratio of

the syngas at conversions between 40 and 70% (H_2 conversion = CO conversion, Figure 1) depending on the type and amount of promoters present. By running a low conversion with H_2/CO usage ratio equal to the H_2/CO ratio of the syngas it is possible to operate with recycle or with multiple reactors in series without having to adjust the syngas composition (4). Using recycle or multiple reactors allows for higher productivity and more efficient use of CO. In the present study we have conducted FTS on precipitated iron catalysts with syngas typical of that obtained from natural gas. The amount of potassium promoter and the reaction conditions (pressure, temperature, ghsv and H_2/CO ratio) were changed to optimize the catalyst efficiency.

Experimental

Catalysts were prepared by continuous precipitation from aqueous $Fe(NO_3)_3 \cdot 9H_2O$ (1.17 M) and concentrated NH_4OH (15.6M) in a continuous stirred tank reactor at pH 9.5. Hydrolyzed tetraethyl orthosilicate was added to the iron(III) nitrate solution to give an atomic ratio of 100Fe/4.6Si. The catalyst slurry was filtered continuously with one or more six inch rotary drum vacuum filters. The resulting catalyst cake was washed and filtered twice with a volume of distilled deionized water equal to the volume of the previous filtrate. A 5 kg catalyst batch was precipitated in this manner, oven dried in flowing air at 110°C and crushed to -325 mesh. The catalyst was calcined in air at 350°C for 4 hours. The 100Fe/4.6Si precursor was impregnated with aqueous $Cu(NO_3)_2 \cdot 3H_2O$ and dried at 110°C to give an atomic composition of 100Fe/4.6Si/2.0Cu. The catalyst was then impregnated with aqueous KNO_3 to give atomic compositions of 100Fe/4.6Si/2.0Cu/1.44K, 100Fe/4.6Si/2.0Cu/3.0K and 100Fe/4.6Si/2.0Cu/5.0K.

All FTS runs were conducted in a one liter autoclave operated as a continuous stirred tank reactor (CSTR). 5 g of each catalyst were suspended in 310 g of Ethylflo 164 hydrocarbon

oil (Ethyl Corporation) which is a 1-decene trimer. H_2 and CO flow rates were controlled by two mass flow controllers (Brooks Instruments) with the resulting synthesis gas composition regulated by adjusting the flow rate of the appropriate gas. The synthesis gas, after passing through a 2 L mixing vessel, was delivered to the catalyst slurry through a dip tube that extended to below the impeller blade. The reactor effluent exited the reactor and passed sequentially through two traps maintained at 60°C and 0°C. Accumulated reactor wax was removed daily through a tube fitted with a porous metal filter (0.5 μm). Uncondensed effluent was directed to an on-line Hewlett Packard 4 channel Quad Series Micro GC for determination of CO, H_2 , CO_2, CH_4 and C_2-C_8 alkanes and alkenes. Liquid samples were analyzed with a Hewlett-Packard 5890 GC equipped with a 60 m DB-5 capillary column.

All catalysts were activated with CO. CO flow (25 slph) was started at ambient temperature and 1.3 MPa and the temperature was increased to 270°C at 2°C min^{-1}. After reaching the activation temperature, the conditions were maintained for 24 h. Initial FTS conditions were 270°C, 1.3 MPa, H_2/CO=1.7 and ghsv=40 sl h^{-1} g-Fe^{-1}. Temperature, pressure, ghsv and H_2/CO feed ratio were changed periodically as outlined in Table 1.

Results

Condition 1, 270°C, 1.3 MPa, H_2/CO=1.7, ghsv=40 sl h^{-1} g-Fe^{-1}.

Syngas conversion data for the three runs are shown in Figure 2. Under the initial conditions, the syngas conversion ranged between 41 and 46% for the three catalysts which is indistinguishable within the expected experimental error. Hydrocarbon rates (Figure 3) were between 3.4 and 3.8 g h^{-1} g-Fe^{-1}. Methane selectivity (Figure 4) decreased with increasing potassium loading from 11 to 7 to 5% (carbon converted to hydrocarbon) for the 1.44K, 3.0K

and 5.0K loadings, respectively. The H_2/CO usage ratio increased with decreasing potassium loading; however, all were much lower than the H_2/CO feed ratio of 1.7 (Figure 5).

Condition 2, 270^{O}C, 1.3 MPa, H_2/CO=1.7, ghsv=65 sl h^{-1} g-Fe^{-1}.

In order to suppress the water-gas shift rate relative to the FTS rate and subsequently increase the H_2/CO usage ratio, the ghsv was increased from 40 to 65 sl h^{-1} g-Fe^{-1} for each catalyst. Increasing the ghsv caused the syngas conversion to decrease to 33%, 34% and 26% and the methane selectivity to decrease to 10%, 5.3% and 4.0% for the 1.44K, 3.0K and 5.0K catalysts, respectively. In addition, hydrocarbon rate increased for all catalysts. The ratio of water gas shift rate (rate of CO_2 production) to FT rate (rate of CO converted less CO_2) decreased (Figure 6); however, the H_2/CO usage did not increase significantly for any of the catalysts.

Condition 3, 250^{O}C, 1.3 MPa, H_2/CO=1.7, ghsv=22 sl h^{-1} g-Fe^{-1}.

The temperature was lowered to 250^{O}C and the ghsv was simultaneously lowered to 22 sl h^{-1} g-Fe^{-1} to maintain reasonable conversion. The syngas conversion increased slightly for each catalyst to 35%-39%. The ratio of water-gas shift rate to FT rate decreased (Figure 6) and the H_2/CO usage ratio increased for all catalysts (Figure 5). Hydrocarbon production rate decreased substantially from 4.6, 4.6 and 4.0 g h^{-1} g-Fe^{-1} to 1.75, 1.75 and 1.62 g h^{-1} g-Fe^{-1} for the 1.44K, 3.0K and 5.0K catalysts, respectively. Methane selectivity also decreased for each catalyst.

Condition 4, 250^{O}C, 2.5 MPa, H_2/CO=1.7, ghsv=22 sl h^{-1} g-Fe^{-1}.

The pressure was increased to 2.5 MPa and all other conditions were maintained. Syngas conversion (50 to 53%) and hydrocarbon productivity (2.26, 2.41 and 2.48 g h^{-1} g-Fe^{-1} for 1.44K, 3.0K and 5.0K, respectively) increased for each catalyst. Methane selectivity decreased for the 1.44K and 3.0K catalysts but increased for the 5.0K catalyst (Figure 4). The H_2/CO usage ratio

increased for all three catalysts; however, they remained well below the H_2/CO feed ratio of 1.7 (1.19, 1.44K; 0.99, 3.0K; 0.89, 5.0K).

Condition 5, 230^{O}C, 2.5 MPa, H_2/CO=1.7, ghsv=22 sl h^{-1} g-Fe^{-1}.

Temperature was decreased to 230^{O}C and all other reaction conditions were held constant. Syngas conversion and hydrocarbon production rate decreased for each catalyst; however, the largest drop was for the 5.0K catalyst (Figures 2-3). Methane selectivity decreased from 8.0% to 4.1% for the 1.44K catalyst, from 4.0% to 2.2% for the 3.0K catalyst and from 4.6% to 2.3% for the 5.0K catalyst. The relative water-gas shift rate decreased substantially for each catalyst and correspondingly the H_2/CO usage ratio increased to 1.46 (1.44K), 1.24 (3.0K) and 1.12 (5.0K).

Condition 6, 230^{O}C, 3.2 MPa, H_2/CO=1.7, ghsv=22 sl h^{-1} g-Fe^{-1}.

Increasing the pressure from 2.5 MPa to 3.2 MPa caused the syngas conversion and hydrocarbon production rate to decrease. Methane selectivity was not effected significantly for any K loading as was the case for the H_2/CO usage ratio.

Condition 7, 230^{O}C, 3.2 MPa, H_2/CO=1.4, ghsv=22 sl h^{-1} g-Fe^{-1}.

The H_2/CO feed ratio was decreased to 1.4. There was no appreciable effect on the syngas conversion or the hydrocarbon production rate. The H_2/CO usage ratio closely approached the feed ratio for the 1.44K catalyst (1.33); however, it was lower for the 3.0K (1.17) and 5.0K (1.09) catalysts. Methane selectivity decreased for each catalyst (Figure 4).

Condition 8, 230^{O}C, 3.2 MPa, H_2/CO=2.0, ghsv=22 sl h^{-1} g-Fe^{-1}.

Increasing the H_2/CO feed ratio to 2.0 had no effect on the syngas conversion or the hydrocarbon production rate as compared to the same conditions with H_2/CO feed ratio of 1.7. Methane selectivity increased with the increase in H_2/CO feed ratio. The H_2/CO usage ratio increased for each catalyst but was lower than the feed ratio (Figure 5).

Discussion

There was little difference in the FT activity of the 1.44K and 3.0K catalysts; however, the 5.0K catalyst had slightly lower syngas conversion and hydrocarbon production rate under most of the conditions studied. Increasing potassium decreased methane selectivity (Figure 4), increased the water-gas shift reaction rate relative to the FT rate (Figure 6) and decreased the H_2/CO usage ratio (Figure 5).

In an effort to make the H_2/CO usage ratio equivalent to the H_2/CO ratio of the syngas, reaction pressure, temperature and ghsv were varied. Increasing the ghsv (Condition 2) decreased the syngas conversion and increased the hydrocarbon production rate. The decrease in conversion caused the methane selectivity and relative water-gas shift reaction to decrease. Increasing the ghsv had little impact on the H_2/CO usage ratio. Increasing the reaction pressure (Conditions 4 and 6) had mixed results for the FT activity and product. When the pressure was increased from 1.3 MPa to 2.5 MPa at 250^{O}C (Condition 4) the syngas conversion and hydrocarbon productivity rate increased sharply for each catalyst. Despite the increase in conversion, methane selectivity decreased, the water-gas shift rate relative to the FT rate decreased and the H_2/CO usage ratio increased slightly. In contrast, increasing the pressure from 2.5 MPa to 3.2 MPa at 230^{O}C had very little effect on FT activity or selectivity. It is not clear from the current data if there is an optimum pressure or if pressure changes have a different effect at 250^{O}C and 230^{O}C. Reaction temperature also has a large impact on FT activity and selectivity. When the temperature was reduced from 250^{O}C to 230^{O}C (Condition 5) the syngas conversion and hydrocarbon production rate decreased as expected. There was a large decrease in methane selectivity and a substantial increase in H_2/CO usage ratio for all three catalysts.

The impact of changing the H_2/CO ratio of the syngas was also studied. Decreasing the H_2/CO syngas ratio from 1.7 to 1.4 (Condition 7) had no impact on the syngas conversion or the

hydrocarbon production rate; however, methane selectivity decreased appreciably for each catalyst. The 1.44K catalyst had a H_2/CO usage ratio of 1.33 while it was somewhat lower for the 3.0K (1.17) and 5.0K (1.09) catalysts. When the H_2/CO syngas ratio was increased to 2.0 (Condition 8) there was no significant change in FT activity and the methane selectivity increased. The H_2/CO usage ratio for each catalyst was below the H_2/CO syngas ratio: 1.54 for the 1.44K catalyst, 1.32 for the 3.0K catalyst and 1.20 for the 5.0K catalyst. Only the 1.44K catalyst operating at 230^{O}C, 3.2 MPa, H_2/CO=1.4 and ghsv=22 sl h^{-1} g-Fe^{-1} had a H_2/CO usage ratio comparable to the H_2/CO syngas ratio.

Conclusions

Potassium had little impact on FT activity but did effect selectivity and in particular the water-gas shift reaction. Potassium increased the water-gas shift rate relative to the FT rate and as a consequence decreased the H_2/CO usage ratio. Pressure and temperature can have significant effects on the activity and selectivity of iron based FT catalysts using syngas similar to that obtained from natural gas. By simultaneously decreasing temperature and increasing pressure it was possible to increase the H_2/CO usage ratio while also maintaining reasonable FT activity. Only the catalyst with atomic composition 100Fe/4.6Si/2.0Cu/1.44K was able to maintain a H_2/CO usage ratio similar to the H_2/CO syngas ratios. In general, the water-gas shift activity of the 100Fe/4.6Si/2.0Cu/3.0K and 100Fe/4.6Si/2.0Cu/5.0K catalysts was too high.

References

1. V. U. S. Rao, G. J. Steigel, G. J. Cinquegrane and R. D. Srivastava, *Fuel Proc. Tech.*, 1991, **30**, 83.

2. A. P. Raje and B. H. Davis, *Catal. Today*, 1997, **36**, 335.

3. A. P. Raje, R. J. O'Brien and B. H. Davis, *J. Catal.*, 1998, **180**, 36.

4. A. P. Raje, J. R. Inga, and B. H. Davis, *Fuel*, 1997, **76**, 273.

Table 1

FTS Conditions

Condition	Time (h)	Temperature (^{O}C)	Pressure (MPa)	ghsv (sl h^{-1} g-Fe^{-1})	H_2/CO
1	0-24	270	1.3	40	1.7
2	24-48	270	1.3	65	1.7
3	48-120	250	1.3	22	1.7
4	120-144	250	2.5	22	1.7
5	144-168	230	2.5	22	1.7
6	168-286	230	3.2	22	1.7
7	286-310	230	3.2	22	1.4
8	310-332	230	3.2	22	2.0

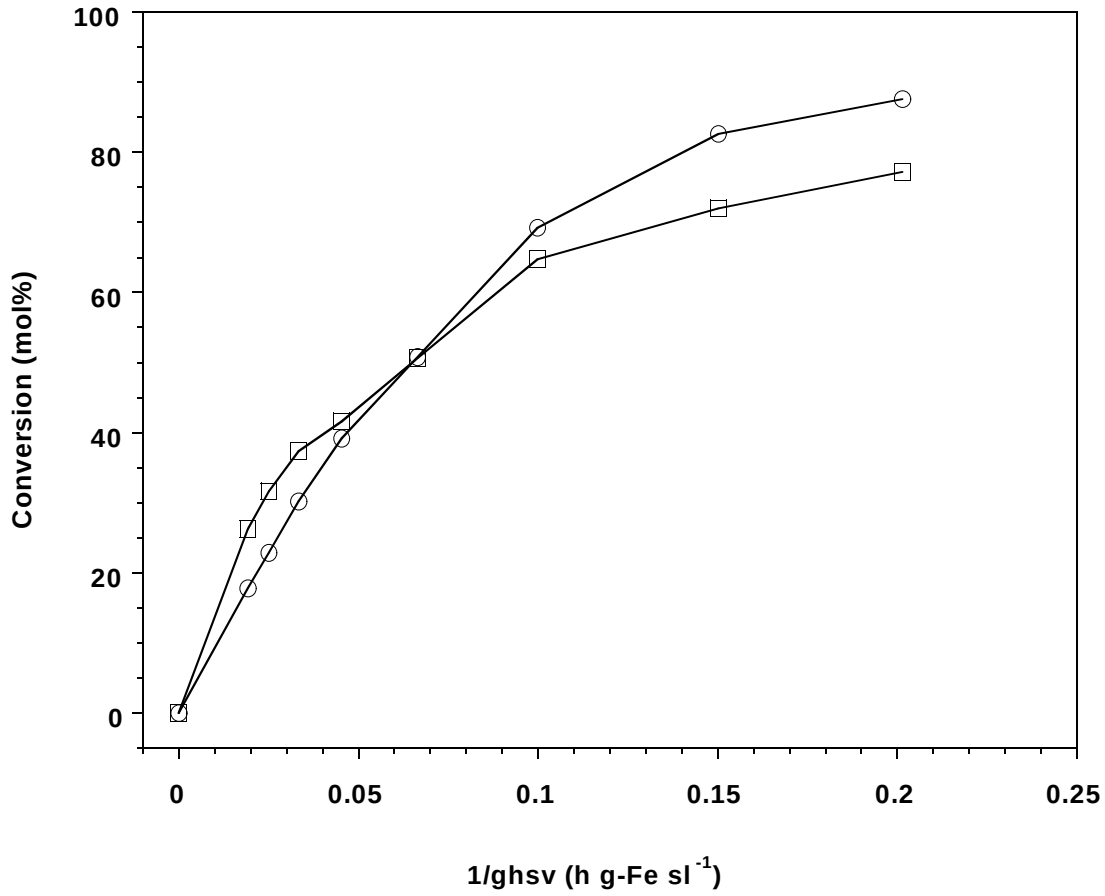

Figure 1. CO and H_2 conversion as a function of reciprocal space velocity for a 100Fe/4.6Si/2.2K catalyst. (F), CO conversion and (G), H_2 conversion.

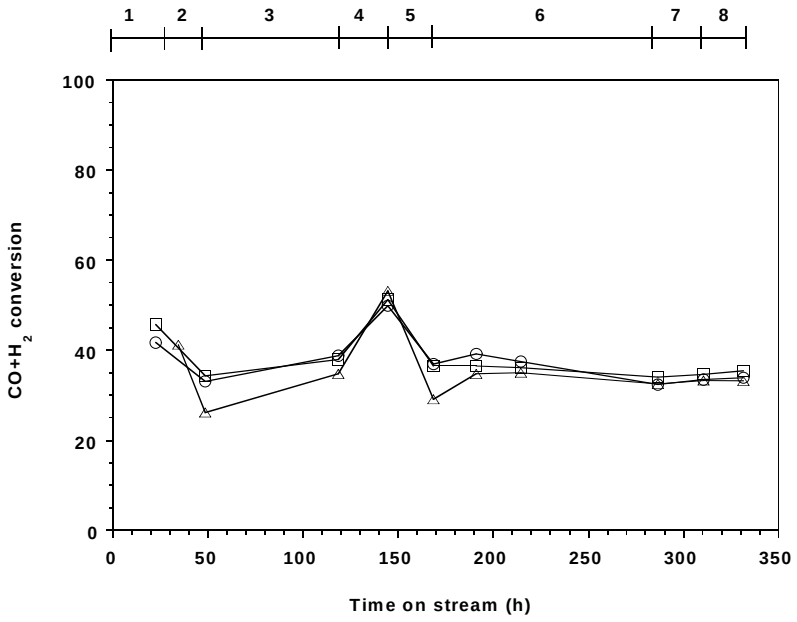

Figure 2. Syngas conversion as a function of time on stream for (F), 100Fe/4.6Si/2.0Cu/1.44K, (G), 100Fe/4.6Si/2.0Cu/3.0K and (△), 100Fe/4.6Si/2.0Cu/5.0K catalysts. Conditions are identified on time line above graph (as defined in Table 1).

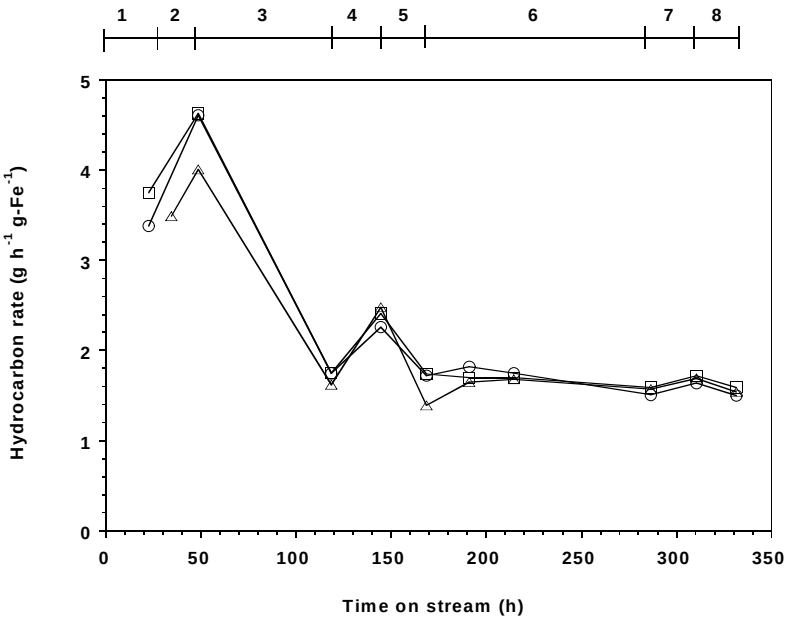

Figure 7. Hydrocarbon production rate as a function of time on stream for (F), 100Fe/4.6Si/2.0Cu/1.44K, (G), 100Fe/4.6Si/2.0Cu/3.0K and (△), 100Fe/4.6Si/2.0Cu/5.0K catalysts. Conditions are identified on time line above graph.

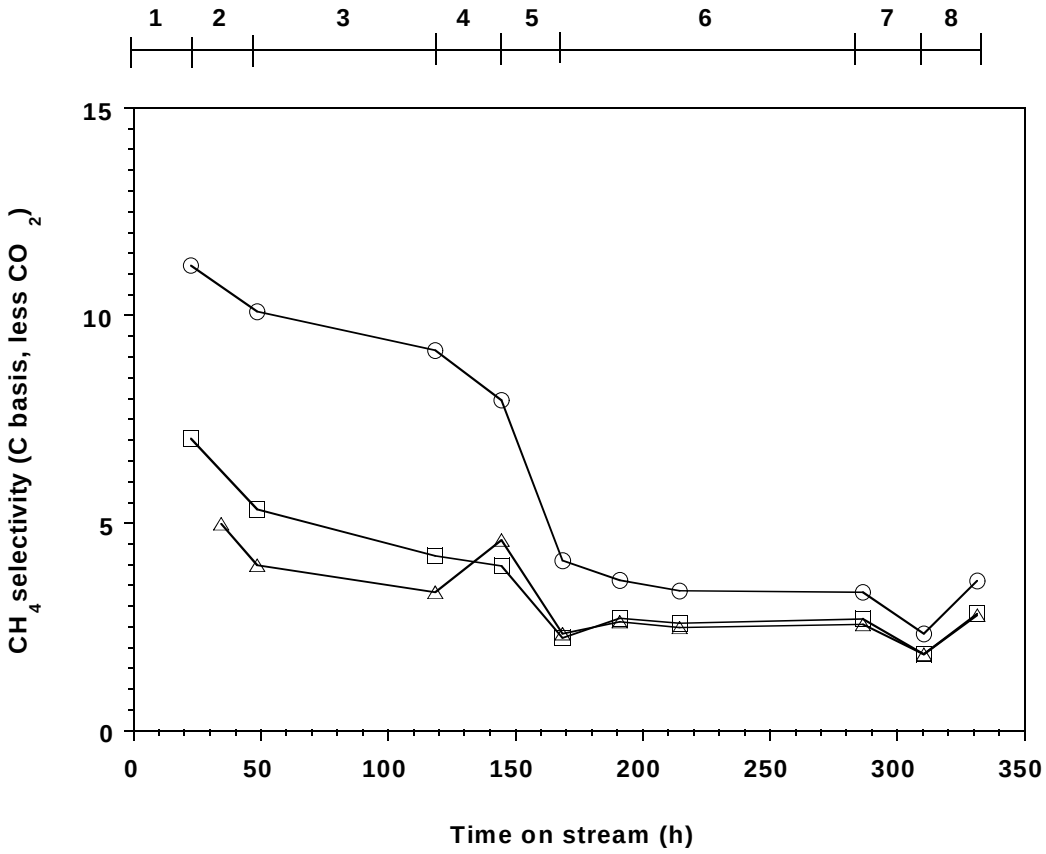

Figure 8. Methane selectivity as a function of time on stream for (F), 100Fe/4.6Si/2.0Cu/1.44K, (G), 100Fe/4.6Si/2.0Cu/3.0K and (△), 100Fe/4.6Si/2.0Cu/5.0K catalysts. Conditions are identified on time line above graph.

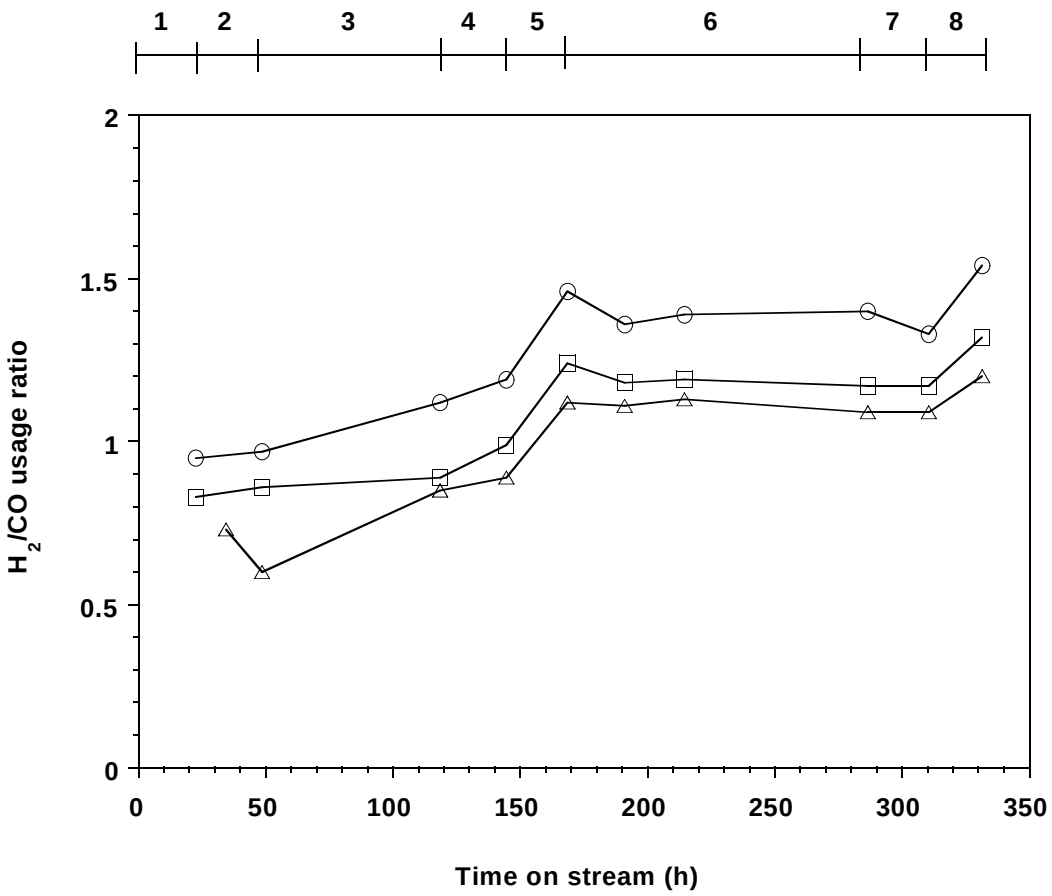

Figure 9. H_2/CO usage ratio as a function of time on stream for (F), 100Fe/4.6Si/2.0Cu/1.44K, (G), 100Fe/4.6Si/2.0Cu/3.0K and (△), 100Fe/4.6Si/2.0Cu/5.0K catalysts. Conditions are identified on time line above graph.

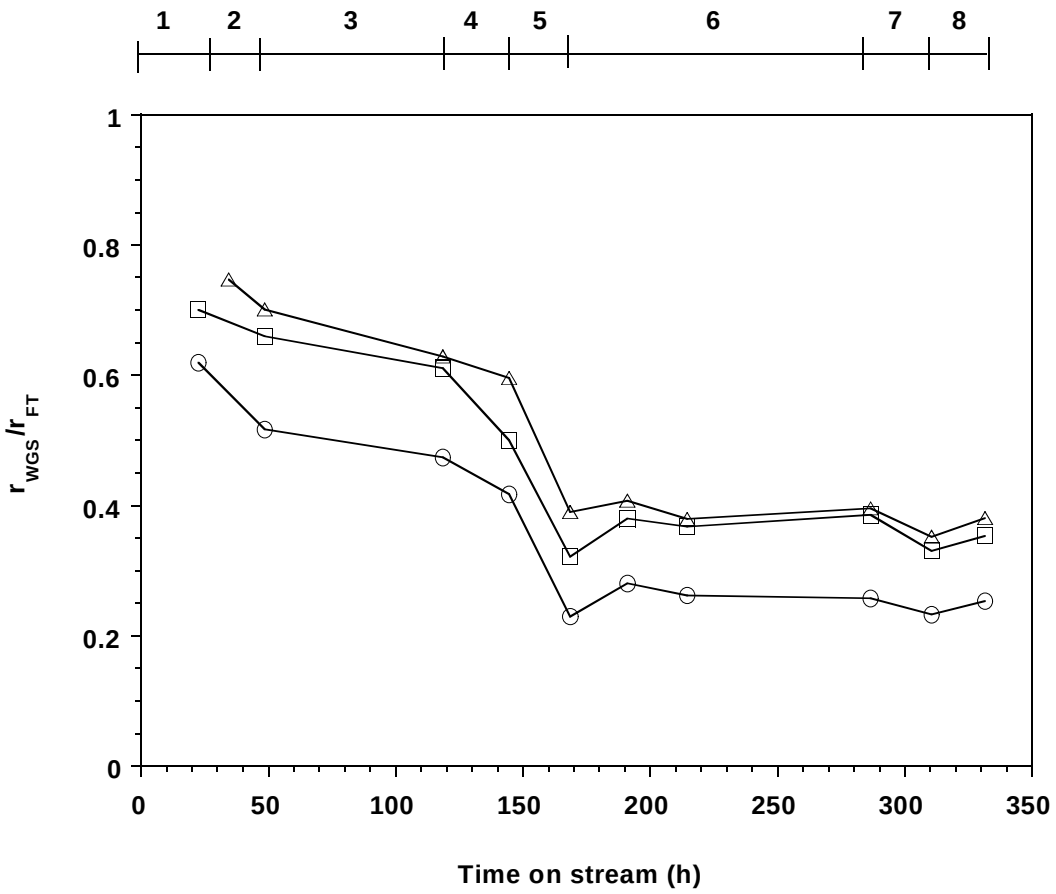

Figure 10. Ratio of water-gas shift rate to Fischer-Tropsch rate as a function of time on stream for (F), 100Fe/4.6Si/2.0Cu/1.44K, (G), 100Fe/4.6Si/2.0Cu/3.0K and (△), 100Fe/4.6Si/2.0Cu/5.0K catalysts. Conditions are identified on time line above graph.

C. Impact of Potassium on the Activation Energy of Precipitated FTS Catalysts

Several kinetic models have been proposed for iron based Fischer-Tropsch catalysts. Anderson (1) proposed a rate expression in which water inhibits the FT rate:

$$-R_{CO+H_2} = \frac{kP_{H_2}P_{CO}}{P_{CO} + bP_{H_2O}} \quad (1)$$

Anderson noted that at syngas conversion below 60%, the FT rate was first order with respect to hydrogen and zero order with respect to carbon monoxide (equation 2).

$$-R_{CO+H_2} = kP_{H_2} \quad (2)$$

Huff and Satterfield proposed a rate expression based on the carbide mechanism in which the rate limiting step was the hydrogenation of a surface carbide species (2). This model also accounted for inhibition by water (equation 3).

$$-R_{CO+H_2} = \frac{kP_{CO}P^2_{H_2}}{P_{CO}P_{H_2} + bP_{H_2O}} \quad (3)$$

Ledakowicz has proposed two rate expressions (3) in which the FT rate is inhibited by CO_2 adsorption (equation 4).

$$-R_{CO+H_2} = \frac{kP_{CO}P_{H_2}}{P_{CO} + cP_{CO_2}} \quad (4)$$

and a general rate expression which accounts for both H_2O and CO_2 inhibition (equation 5).

$$-R_{CO+H_2} = \frac{kP_{CO}P_{H_2}}{P_{CO} + aP_{H_2O} + cP_{CO_2}}$$

Using these and other rate equations, the activation energy of the FT reaction with iron catalysts has been determined to fall within a broad range of 71 to 103 kJ mol^{-1}. The impact of promoters on the activation energy has not been reported. Satterfield has reported an activation energy of 83 kJ mol^{-1} for a fused iron catalyst promoted with K, Ca, Si, and Al (2). Bukur has reported activation energies of for precipitated iron catalysts promoted with K, Cu and SiO_2 (4). A systematic study of the effect of potassium on the FT activation energy has not been reported. Potassium can either increase or decrease the activity of iron-based catalysts depending on the H_2/CO ratio of the syngas and the range of syngas conversion studied. Furthermore, the CO conversion increases, attains a maximum, and then decreases as the amount of potassium in the catalyst is increased. As a consequence it is possible that potassium will impact the activation energy of the FT reaction.

Experimental

Five catalysts with atomic composition 100Fe/4.6Si, 100Fe/4.6Si/0.36K, 100Fe/4.6Si/0.71K, 100Fe/4.6Si/1.4K and 100Fe/4.6Si/2.2K were studied. 15.0 g of catalyst and 290 g of C_{30} oil were loaded into 1000 ml autoclaves. The catalysts were activated with CO at 270^{O}C and 175 psig for 24 h. Initial FTS conditions were 270^{O}C, 175 psig, H_2/CO=0.67 and ghsv=5.0 sl h^{-1} g-Fe^{-1}. After the syngas conversion stabilized, the temperature was lowered to 250^{O}C for 24 hours and then to 230^{O}C for 24 hours. The temperature was then increased to 270^{O}C to determine whether catalyst deactivation had occurred.

Results

Syngas conversion profiles for each potassium loading are shown in Figures 1-5. Syngas conversion stabilized after about 120 hours on steam for each catalyst. After decreasing the temperature to 250^{O}C and then 230^{O}C, the temperature was increased to 270^{O}C. In each case the conversion was higher than before the temperature reductions. This occurred even after most of

the catalysts appeared to be deactivating slightly before the initial temperature reductions. In order to insure consistency, kinetic data were obtained from the initial temperature reductions. Syngas conversion as a function of potassium loading at each temperature is shown in Figure 6. The syngas conversion increased slightly when going from 0K to 0.36K at each temperature; however, there was essentially no effect on conversion with increasing potassium loading beyond 0.36K.

For the sake of simplicity the reaction was assumed to be first order in H_2 and zero order in CO (equation 2).

$$-R_{CO+H_2} = kP_{H_2}$$

Rate constants at each temperature for each potassium loading are shown in Table 1. There is approximately 5% relative error for the rate constant of the duplicate runs using 0K loading. Arrhenius plots for the different catalysts are shown in Figure 7. Activation energy as a function of potassium loading is shown in Figure 8. In general, the activation energy ranged between 64 kJ mol^{-1} and 82 kJ mol^{-1}. The activation energy decreased from 79 kJ mol^{-1} for the catalyst with no potassium to 64 kJ mol^{-1} for the catalyst with 0.36K; however, additional potassium caused the activation energy to increase up to 82 kJ mol^{-1} for the 2.2K catalyst. The activation energy for the catalyst without K was essentially the same for the duplicate runs; however, additional runs which repeat the runs with 0.36K and 2.2K should be completed before any conclusions can be reached about the effect (if any) of potassium on activation energy. No reason that the activation energy should have a minimum with respect to potassium loading is apparent. It may be that we are only seeing the effects of experimental error from the catalysts being incompletely activated (activity always increased after completing the series of temperature reductions and then returning to the original conditions). This is an important aspect and work continues on this.

References

1. Anderson, R. B. In “Catalysis,” Vol. 4; Emmett, P. H., Ed. Reinhold: New York, 1956.

2. Huff, G. A., Jr. and Satterfield, C. N. *Ind. Eng. Chem. Process Des. Dev.* **23** (1984) 696.

3. Ledakowicz, S., Nettelhoff, H., Kokuun, R., and Deckwer, W.-D. *Ind. Eng. Chem. Process Des. Dev.* **24** (1985) 1043.

4. Zimmerman, W. H. and Bukur, D. B. *Can. J. Chem. Eng.* **68** (1990) 292.

Table 1						
	k(mol h^{-1}g-$Fe^{-1}$$kPa^{-1}$)					
T (^{O}C)	**0K**	**0K**	**0.36K**	**0.72K**	**1.44K**	**2.18K**
230	1.32 x 10^{-4}	1.18 x 10^{-4}	1.93 x 10^{-4}	1.58 x 10^{-4}	1.36 x 10^{-4}	1.23 x 10^{-4}
250	2.79 x 10^{-4}	2.56 x 10^{-4}	3.37 x 10^{-4}	3.33 x 10^{-4}	2.88 x 10^{-4}	2.80 x 10^{-4}
270	5.31 x 10^{-4}	4.90 x 10^{-4}	6.17 x 10^{-4}	5.67 x 10^{-4}	5.64 x 10^{-4}	5.38 x 10^{-4}

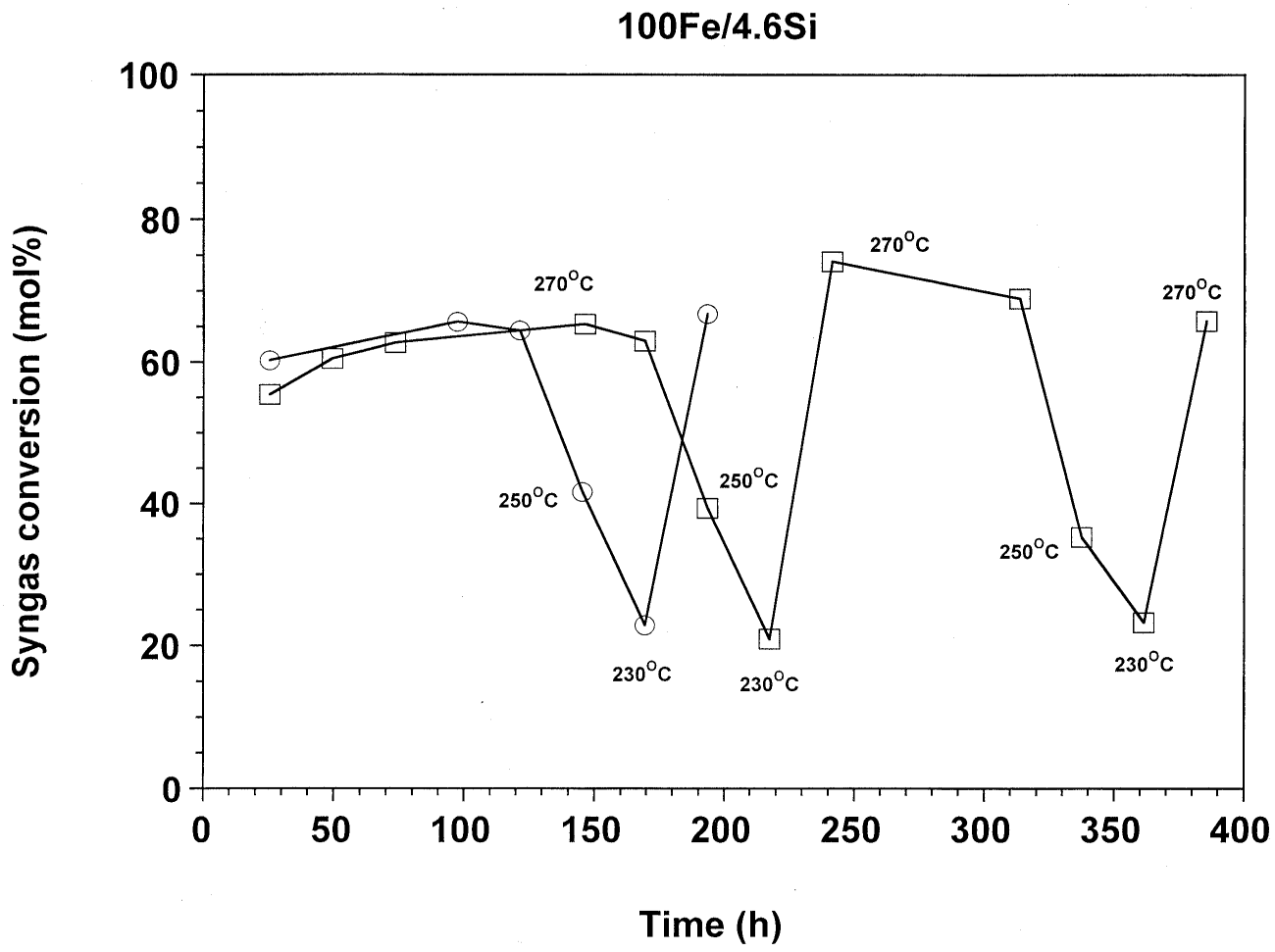

Figure 1. Conversion profile for 100Fe/4.6Si.

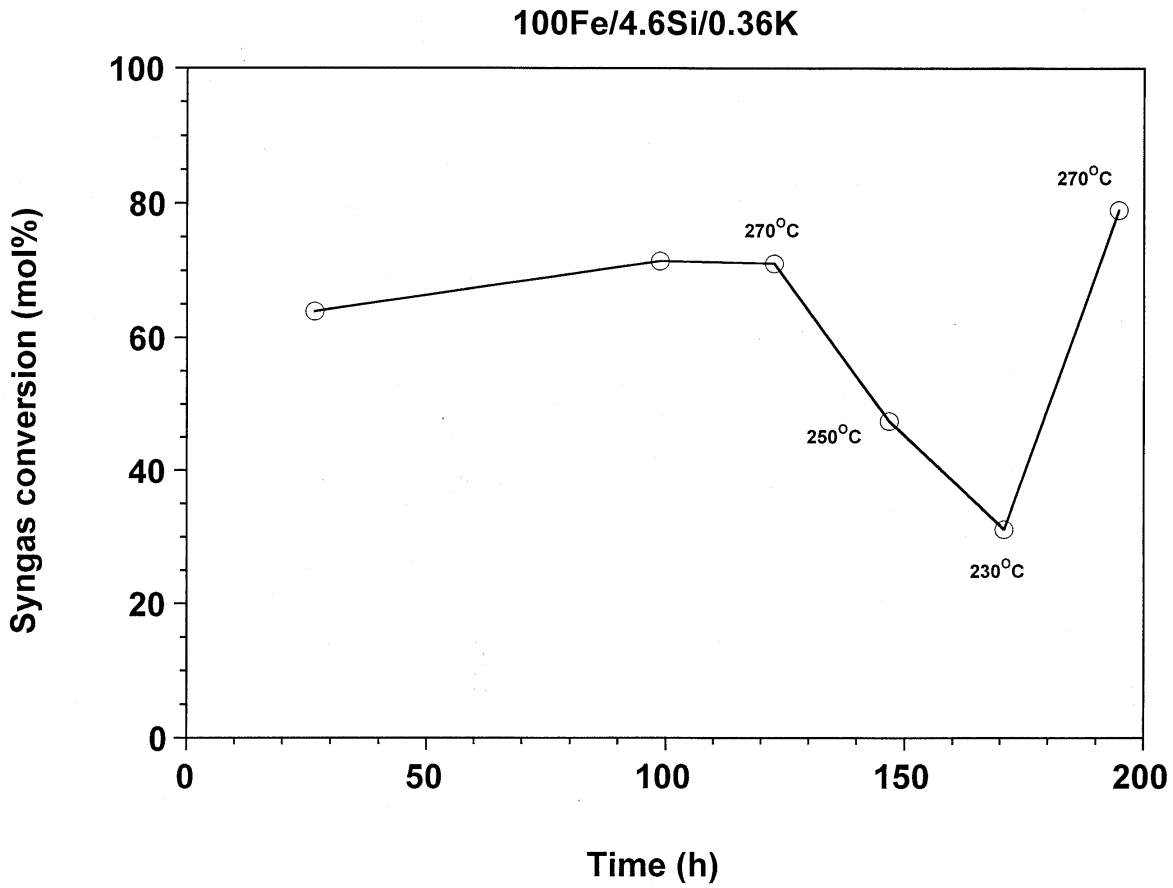

Figure 2. Conversion profile for 100Fe/4.6Si/0.36K.

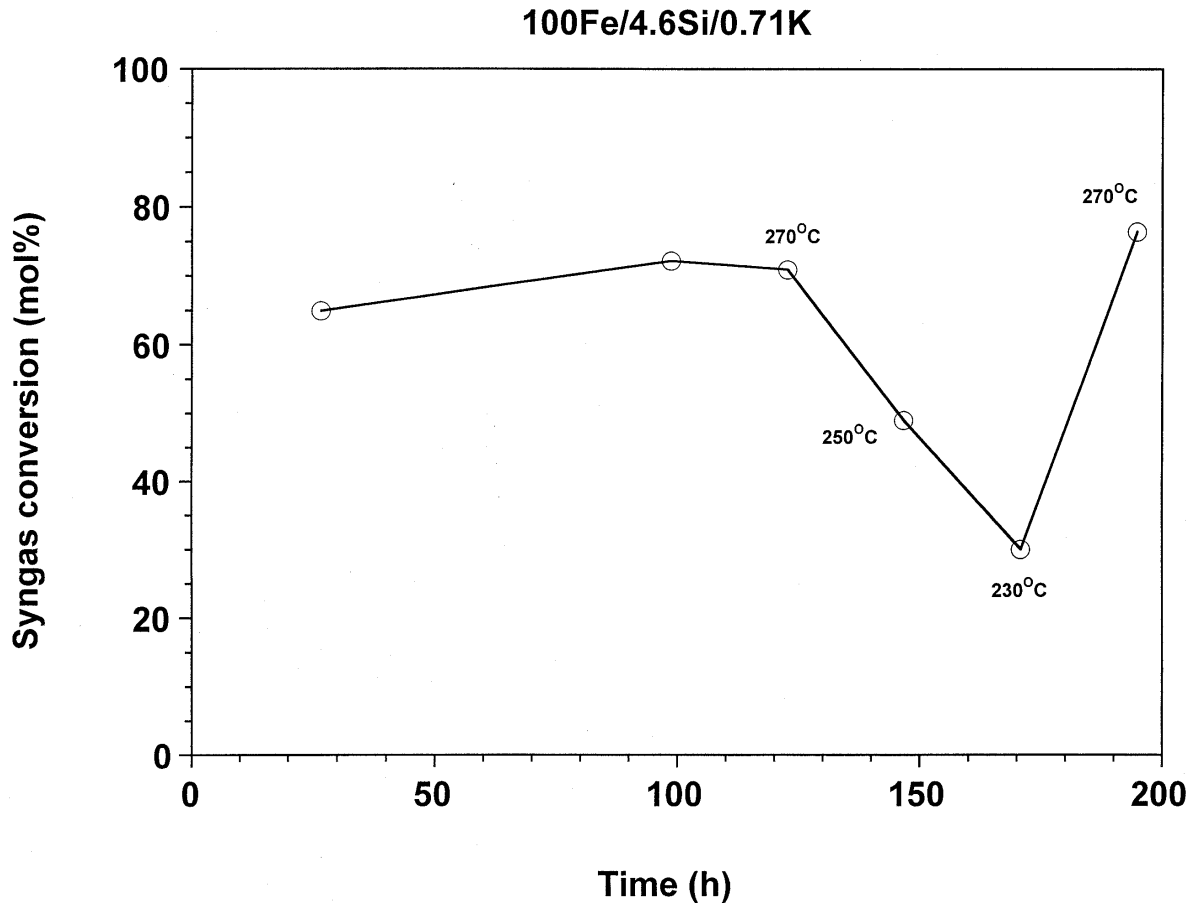

Figure 3. Conversion profile for 100Fe/4.6Si/0.71K.

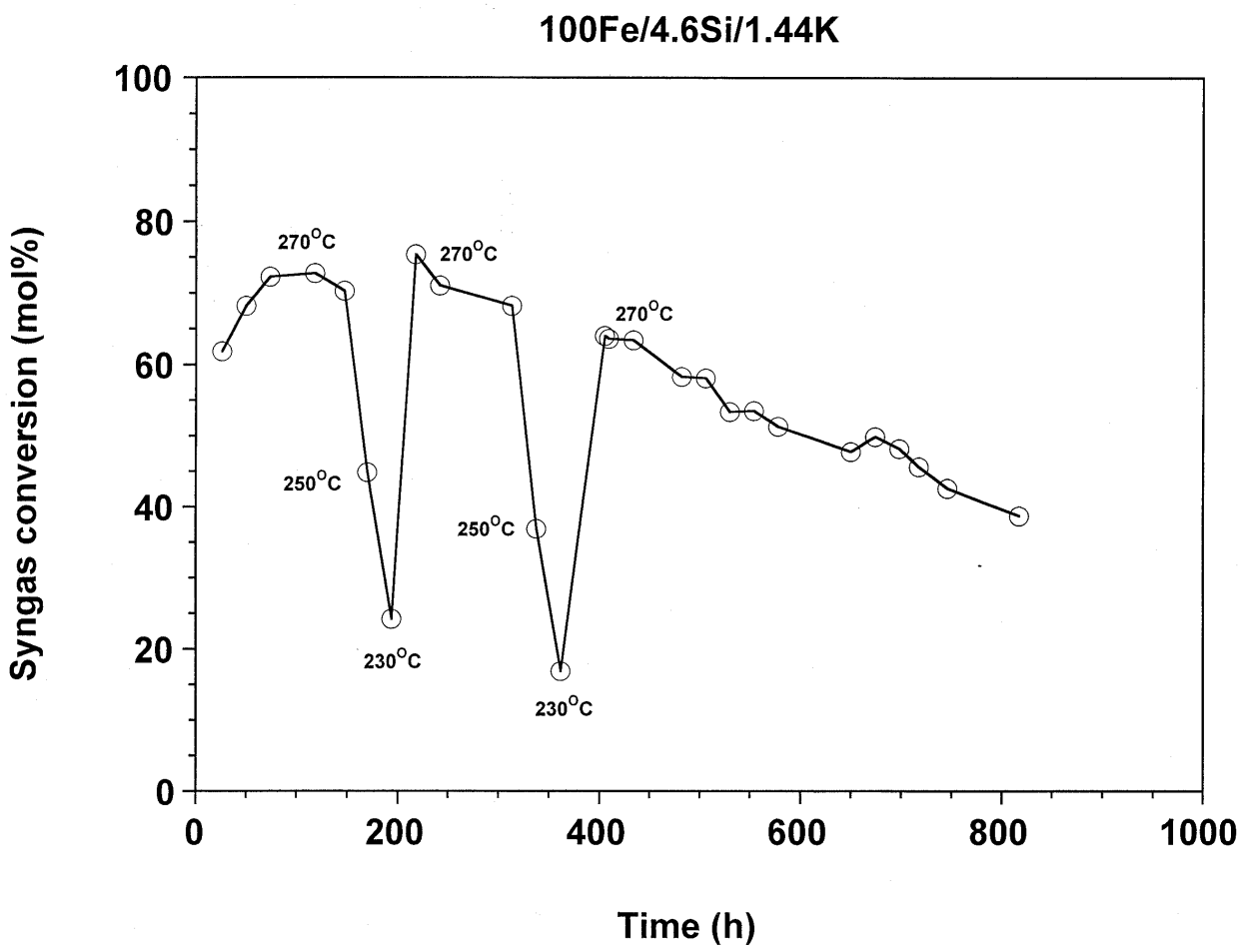

Figure 4. Conversion profile for 100Fe/4.6Si/1.44K.

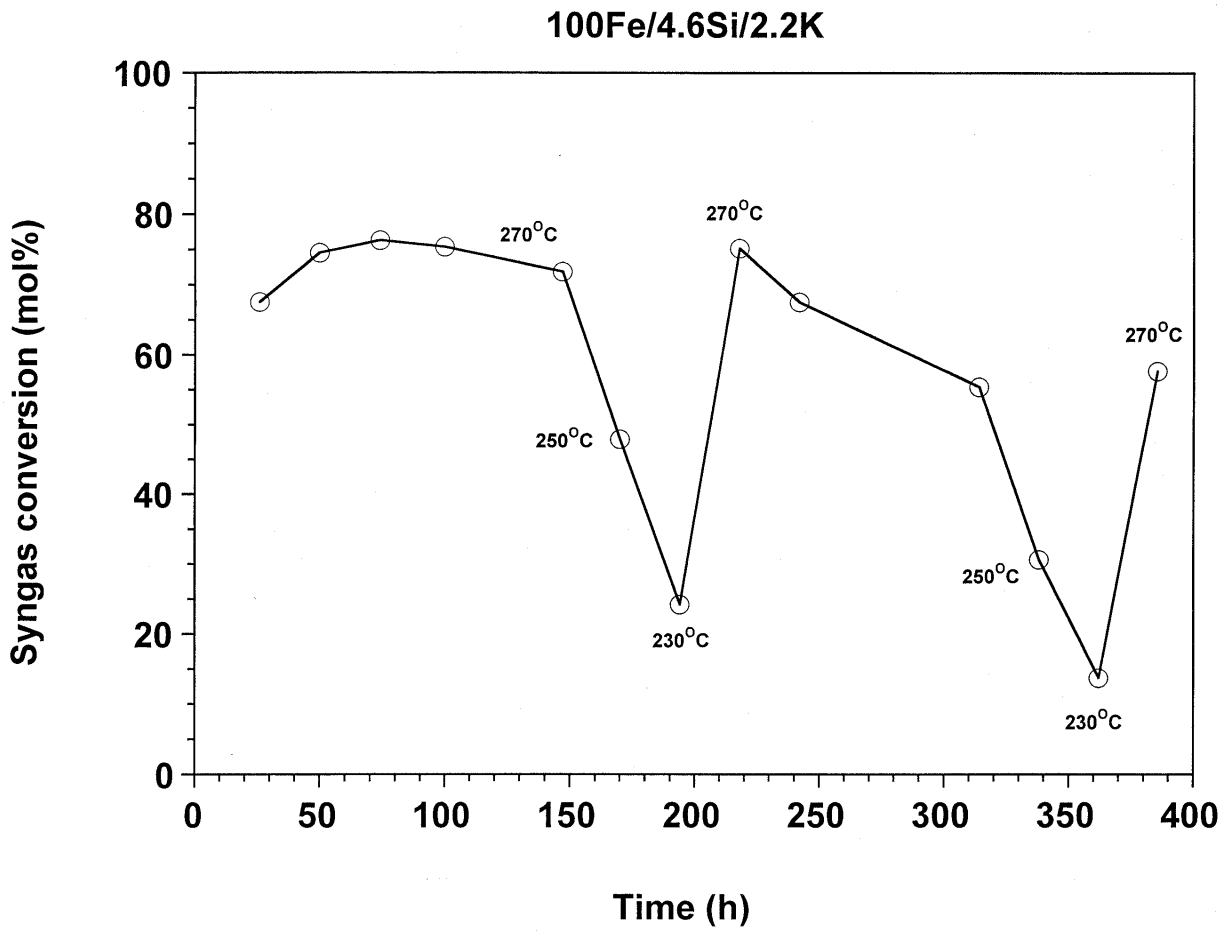

Figure 5. Conversion profile for 100Fe/4.6Si/2.2K.

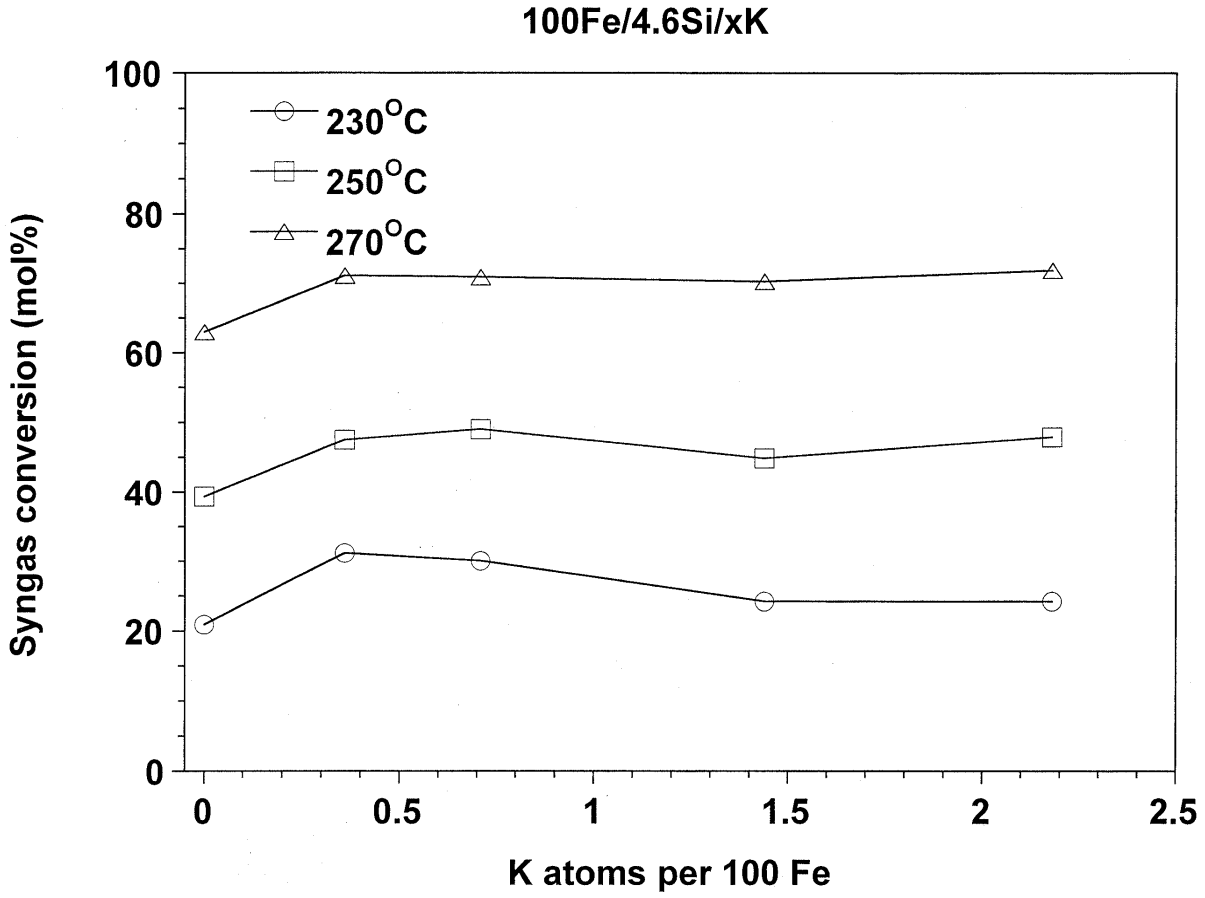

Figure 6. Syngas conversion as a function of K loading at each temperature.

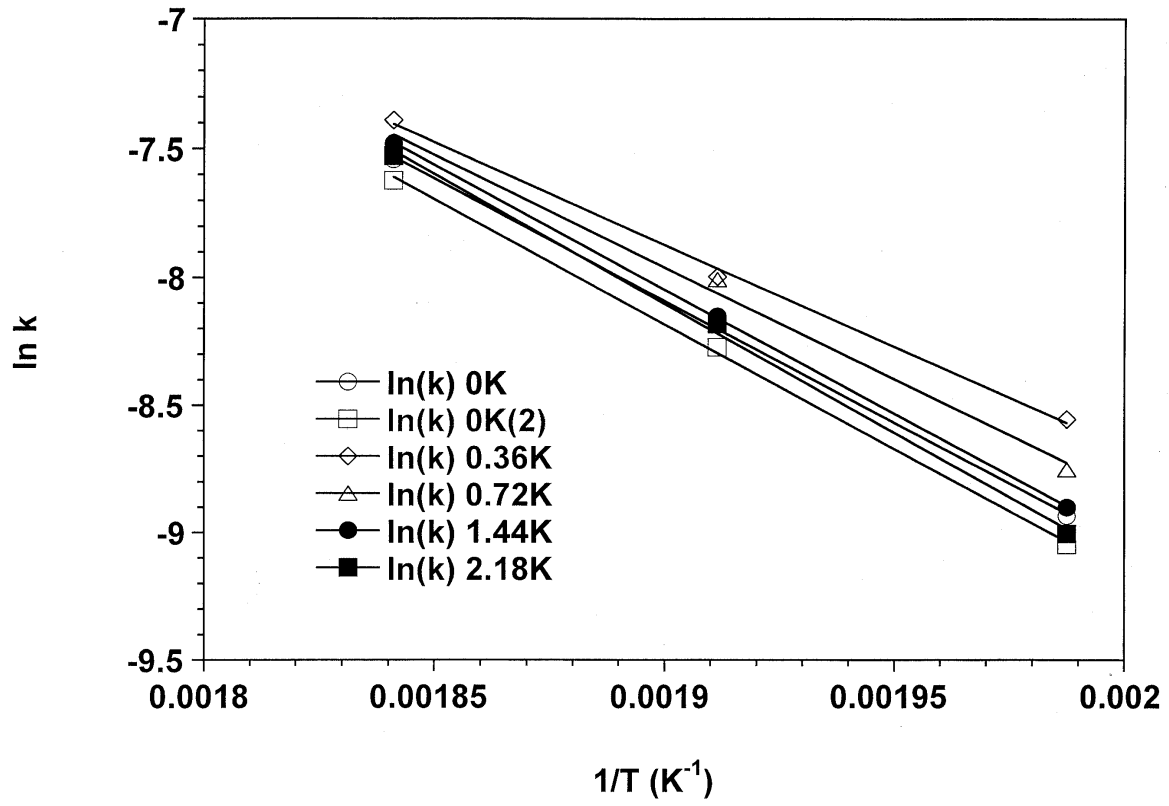

Figure 7. Arrhenius plot for the different K loadings.

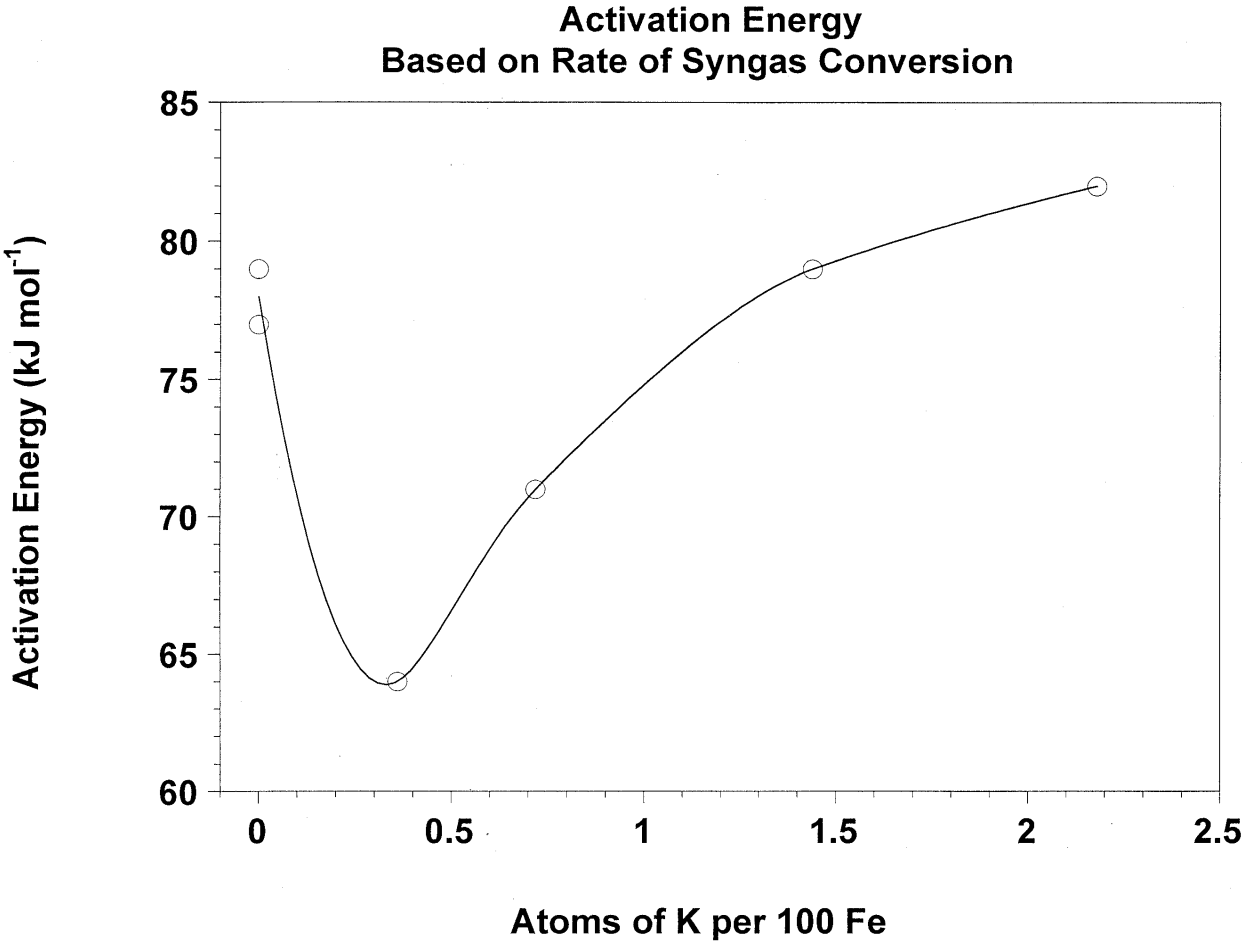

Figure 8. Activation energy as a function of the K loading.

D. Fischer-Tropsch Synthesis: Influence of Startup Media on Activity and Selectivity over Magnesium Iron Promoted Catalysts

Introduction

Fischer-Tropsch synthesis process converts CO and H_2 to liquid fuels, and the feedstock, a mixture of CO and H_2, can be produced from coal gasification. As a cleaner raw material source than coal, natural gas can also used for Fischer-Tropsch synthesis. One of the advantages of FTS is that the process can be designed to produce either gasoline, diesel and/or chemicals. There are two types of operation modes, the low temperature, which is for production of high wax, and the high temperature FTS, which is designed for production of gasoline and alkenes.

In an FTS process, the hydrocarbon is produced from CO and H_2, which can be expressed as

$$(2n+1)\ H_2 + n\ CO \rightarrow C_nH_{2n+2} + n\ H_2O$$

where n is defined as $n = 1/(1-\alpha)$ or it can be rearranged as $\alpha = 1 - (1/n)$ (1).

When an iron catalyst is used for FTS reactions, the water gas shift (WGS) reaction can also occur. This side reaction consumes CO and water produced in the FTS process and produces additional hydrogen.

$$H_2O + CO \rightarrow CO_2 + H_2$$

Potassium has long been used as a promoter for iron catalysts to increase the alkene yield and to decrease the CH_4 selectivity (2). It is also believed that potassium can also increase FTS and water-gas shift reaction activity (3).

Although catalyst play the most important role in FTS reactions, it is believed that startup media also had an innegligible influence on the activity and selectivity of the FTS reactions. The purpose of this study was to investigate the effect of the startup media, two different media were used, i.e., the liquid C-30 oil and solid granular parawax. Iron FTS catalysts promoted with

1.44% alkalis of magnesium and potassium were used in this study. A simulated synthesis gas of 40% hydrogen and 60% carbon monoxide was used in a one-liter CSTR slurry reactor. Liquid oil, water, heavy wax and gas samples from the FTS reactions were collected and analyzed with gas chromatographs (GC). Reaction conversion, product selectivity and other results were calculated by a database system.

Experimental

Preparation of alkali metal promoted catalysts

Iron catalyst promoted with Mg were prepared and tested in this study. Promoter was added at a 1.44:100 of promoter to iron atomic ratio. Precipitated iron catalysts were prepared with tetraethyl orthosilicate, iron nitrate. Ferric nitrate solution was first prepared by dissolving $Fe(NO_3)_3 \cdot 9H_2O$ in distilled and deionized water, and the amount of orthosilicate needed to make Si:Fe of 4.6 was added. The mixture was stirred vigorously until the tetraethyl orthosilicate has hydrolyzed. Tetraethyl orthosilicate and iron nitrate mixture was then added to a CSTR precipitator vessel together with ammonium hydroxide. By maintaining the slurry pH at 9 and an average residence time of 6 minutes, a base catalyst material with an iron to silicon molar ratio of 100:4.6 was obtained. The slurry was then filtered with a vacuum drum filter and washed twice with deionized water. The final filtration cake was dried in an oven with flowing air at $110^{O}C$ for 24 hours. The catalyst was crushed to approximately 60 μm and calcined in a $350^{O}C$ oven under an air flow for 4 hours.

In this study, the iron catalyst was impregnated with an aqueous nitrate solutions of magnesium for alkali metal promoted catalyst. Magnesium nitrate was added to obtain a promoter to iron atomic ratio of 1.44:100. The catalysts was dried at $110^{O}C$ overnight with good mixing following the impregnation. Thus, catalyst promoted with magnesium was prepared for FTS studies.

In-situ catalysts activation

The iron catalyst needs to be activated with either H_2, CO or synthesis gas. Activation procedures can have a significant effect on the selectivity and activity of iron catalyst (6, 7). It was reported that catalysts activated with CO yielded higher long-chain hydrocarbons than syngas and H_2 activated catalysts. In addition, activation conditions may also influence the performance of the iron catalyst. In this study, the potassium promoted iron catalysts were pretreated with CO at 270°C, 1.2 MPa for 24 hours. The reduction of Fe_2O_3 with CO occurs in two steps:

$$3Fe_2O_3 + CO \rightarrow 2Fe_3O_4 + CO_2$$

$$5Fe_3O_4 + 32CO \rightarrow 3Fe_5C_2 + 26CO_2$$

In addition, CO_2 may be formed by the Boudouard reaction:

$$2CO \rightarrow C + CO_2$$

Previous work in our lab showed that approximately 50 % to 75% more carbon was present in the catalyst mass than was needed to form Fe_5C_2 (8). Gradual oxidation of Fe_5C_2 to Fe_3O_4 was observed when iron catalyst was used in FTS. The results showed that at the end of the run an unpromoted iron catalysts had been completely oxidized to Fe_3O_4.

Reactor system

A one-liter continuous stirred tank reactor (CSTR) was used in this study. A sintered filter was installed to remove the wax samples from the catalyst slurry. The wax sample was extracted through the internal filter and collected in the hot trap (200°C). A warm trap (100°C) and cold trap (0°C) were used to collect oil, light wax and water samples. Tail gas from the cold trap was analyzed with an HP quick GC.

Gas mixer equipped with a CO and an H_2 mass controller was used to provide a simulated synthesis gas. After the catalysts was activated with CO, syngas was introduced at a

rate of 10 NL/hr/gram-catalyst. Then the gas space velocity was varied in the range of 3 to 60 sl/hr/g-Fe to collect kinetic data. Other reaction conditions were maintained at 270°C, 1.2 MPa and a stirrer speed of 750 rpm.

Product sampling and analysis

Daily gas, water, oil, light and heavy wax samples were collected and analyzed. Table 1 gives the summary of the instruments for gas and liquid product analysis. A heavy wax sample was taken from the 200°C hot trap connected to the filter. Vapor phase above the slurry phase passed to the warm (100°C) and the cold (0°C) traps outside the reactor. The light wax and water mixture was collected from the warm trap and an oil plus water sample from the cold trap. Tail gas from the cold trap was analyzed with an online HP Quad Series Micro GC. Molar compositions of C_1-C_7 olefins and paraffins were thus obtained. Hydrogen and carbon monoxide conversions were calculated based on the gas product GC analysis results and the gas flow measured at reactor outlet. Hydrogen, carbon monoxide and syngas conversion were obtained using the following formula:

$$\text{Conversion} = \frac{(N_{in} - N_{out})}{N_{in}} \times 100\%$$

The Oil and light wax samples were mixed before analyzed with an HP 5790A GC. The heavy wax was analyzed with an HP5890 Series II Plus GC while the water sample was run with an HP5890 GC.

Results and Discussion

Effect on Fischer-Tropsch synthesis activity

Two parallel Fischer-Tropsch reactions were carried out in a CSTR using two different startup media, i.e., C-30 oil (liquid oil) and parawax (granular solid polymer). Figure 1 shows

the CO conversion results from the two reactions. With C-30 oil, higher CO conversion was obtained than in a parawax medium. As the reaction proceeds, the difference in CO conversion between the two startup media becomes more pronounced. Initial conversion were at about 37% in both media, after 150 hours of reaction, CO conversion in C-30 oil stablized at 56% while the conversion in parawax decreased to 32%. This results suggest that in FTS reaction system, heavier startup media may have a detrimental effect on the catalyst activity due to the negative effect by the parawax in the mass transport process in the solid-liquid-gas slurry.

Figure 2 gives the results of FTS rate, which is calculated by the following equation:

$$\text{FTS rate} = \text{Rate [CO]} - \text{Rate [CO}_2\text{]} \quad \text{(mol/hr/g-Fe)}$$

Regardless of the space time, C-30 oil produced a higher FTS rate than parawax. At a short space time C-30 oil generated twice as much hydrocarbon as parawax but the difference in hydrocarbon rate was insignificant at a higher space time.

Effect on Fischer-Tropsch synthesis selectivity

Figure 3 gives the methane selectivity and the alpha values from the FTS reactions using two different startup media. Methane selectivity from the FTS using C-30 oil was significantly higher than that in a parawax. A 7.12% methane selectivity was obtained in a C-30 oil while only a 4.87% was obtained in a parawax medium. In the meantime, C-30 oil showed a slightly lower alpha value than parawax.

Olefin ratio was calculated from the following equation:

$$\text{Olefin ratio} = \frac{Olefin}{(Olefin + Paraffin)} \times 100\%$$

Olefin ratios of C_2 to C_20 were shown in Figure 4 and it was found that two lines were overlapped in the whole range of the data. The results indicates that the startup media did not have any influence on olefin ratio of the FTS product.

Figure 5 gives the results of hydrocarbon fractions from the FTS reactions. It is shown that C-30 oil generated more gas (C_1-C_4) and gasoline (C_5-C_{11}) products and less diesel (C_{12}-C_{18}) and C_{19+} products than parawax. As shown in both Figure 3 and Figure 5, C-30 oil produced a slightly heavier products or higher alpha value than parawax.

Effect on product partial pressure and water gas shift activity

Water partial pressure was given in Figure 6 and it shows that at a low space time, C-30 oil produced a higher water partial pressure than parawax while at a higher space time, the opposite result was obtained. Figure 7 shows the partial pressure of CO_2 at different space time, C-30 oil always yielded a higher CO_2 partial pressure than parawax, indicating that water-gas shift reaction activity was affected by the startup media. Heavy medium inhibited the WGS reaction and as the space time increase, the detrimental effect became more and more pronounced.

Figure 8 shows the partial pressure of hydrocarbon at different space time. Similar to CO_2 partial pressure, hydrocarbon partial pressure from FTS using C-30 oil was higher than that in a parawax startup medium. This suggests that heavy startup medium inhibits the mass transport between the gas reactants and the surface species on the solid catalyst surface; thus a lower hydrocarbon yield was resulted in a parawax medium than that in C-30 oil.

Figure 9 gives the result of water gas shift quotient, which is calculated from the following equation:

$$\text{Water gas shift quotient} = \frac{P_{[CO2]} \cdot P_{[H2]}}{P_{[CO]} \cdot P_{[H2O]}}$$

Water-gas shift quotient measures the water gas shift reaction extent. Similar to the CO_2 partial pressure, WGS quotient from reaction in C-30 oil was higher than that in parawax medium. At a low space time, the two media showed little difference in WGS quotient, but the difference between the two media becomes more and more greater at higher space time. It is also found that the WGS quotient remained stable in parawax medium regardless of the space velocity while the WGS quotient increased appreciably as the space time increase.

Conclusion

Startup media showed an innegligible influence on FTS reactions over iron FTS catalysts promoted with magnesium. Although startup media had little effect on olefin ratio, alpha value and gasoline faction of the hydrocarbon products, they had a significant influence on CO conversion, methane selectivity, hydrocarbon fractions other than gasoline, partial pressure of CO_2, water, and the water-gas shift quotient. The effect of startup media depends on the space time applied in the FTS reactions. Greater influence on CO conversion, water-gas shift activity, hydrocarbon and CO_2 partial pressure was observed at a high space time than at a low space time. This study suggests that C-30 oil yielded a better CO conversion, hydrocarbon rate but higher CO_2 and methane byproduct and slightly lighter hydrocarbon products. Thus a heavy parawax startup medium is not recommended for FTS reactions in a CSTR due to the detrimental effect on mass transport property.

Acknowledgment

Funding from the Department of Energy (DE-FC-26-98FT40308) and the Commonwealth of Kentucky are acknowledged.

References

1. X. Zhan, B. H. Davis, 1999 Spring Symposium of The Tri-State Catalysis Society, Apr. 20-21, Louisville, KY, (1999).
2. M. E. Dry, in Catalysis Science and Technology, Vol. 1, 159-255, (1981).
3. D. B. Bukur, D. Mukesh, and S. A. Patel, Ind. Eng. Chem. Res., 29, 194 (1990).
4. D. B. Bukur, L. Nowichi and X. Lang, Energy and Fuels, 9 620 (1995).
5. R. J. O'Brien, L. Xu, R. L. Spicer and B. H. Davis, accepted by Energy and Fuels.
6. R. J. O'Brien, Y. Zhang, H. H. Hamdeh, B. H. Davis, "Mossbauer study of precipitated unpromoted iron Fischer-Tropsch catalyst," Preprints, 44(1) ACS, Division of Petroleum Chemistry, Mar. 21-25, Anaheim, CA, 100-102, (1999).

Table 1. Analyzers for FTS Products

Analyzer	Sample	GC Detector
HP Quad Series Micro GC	Gas	TCD
HP 5790A GC	Water	FID
HP5890 GC	Oil+light Wax	TCD
HP5890 Series II Plus	Heavy Wax	FID

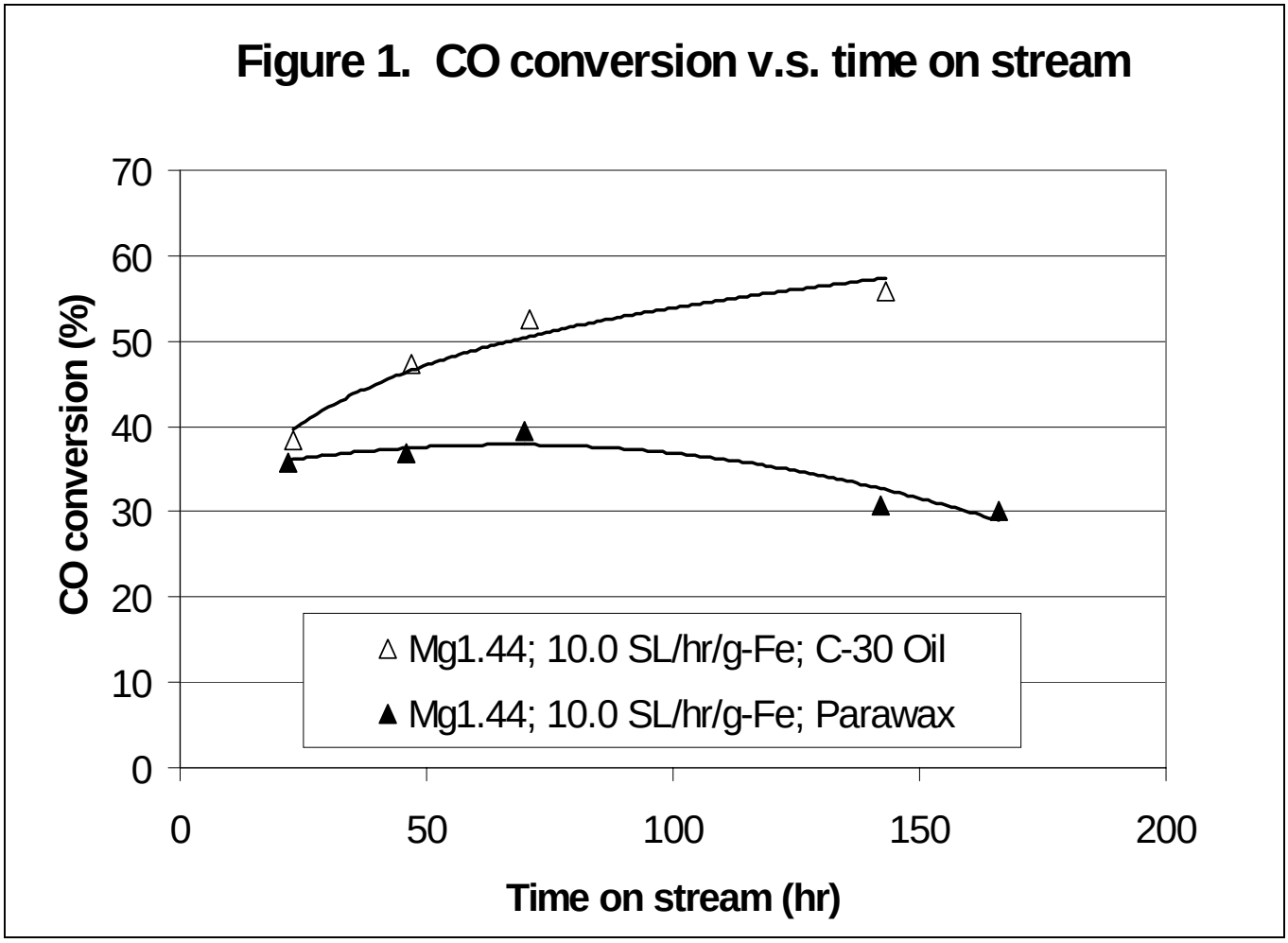
Figure 1. CO conversion v.s. time on stream
CO conversion (%)
70
60
50
40
30
20
10
0
0
50
100
150
200
Time on stream (hr)
Mg1.44; 10.0 SL/hr/g-Fe; C-30 Oil
Mg1.44; 10.0 SL/hr/g-Fe; Parawax

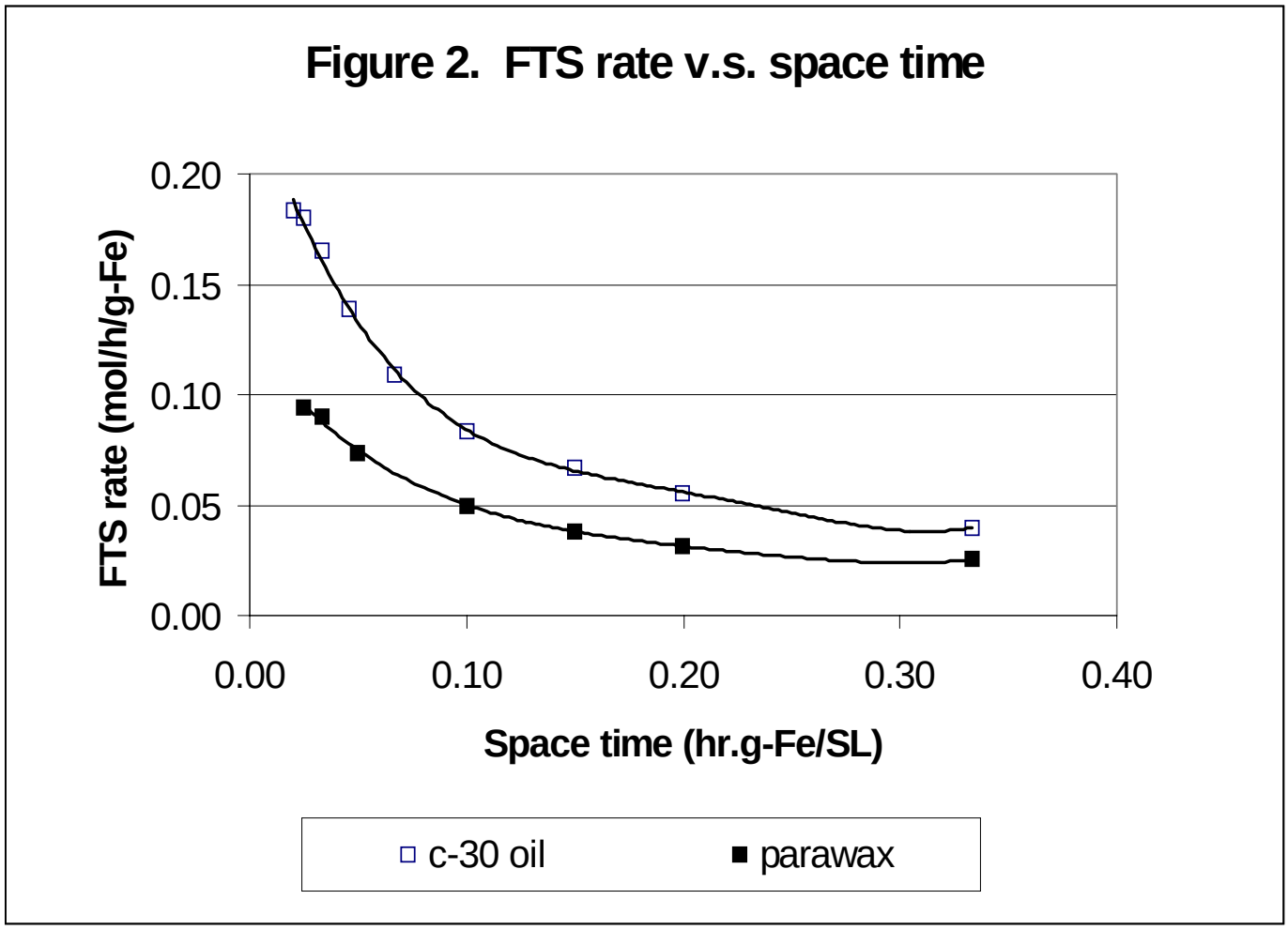
Figure 2. FTS rate v.s. space time
FTS rate (mol/h/g-Fe)
0.20
0.15
0.10
0.05
0.00
0.00
0.10
0.20
0.30
0.40
Space time (hr.g-Fe/SL)
c-30 oil
parawax

Figure 3. Methane selectivity and alpha value

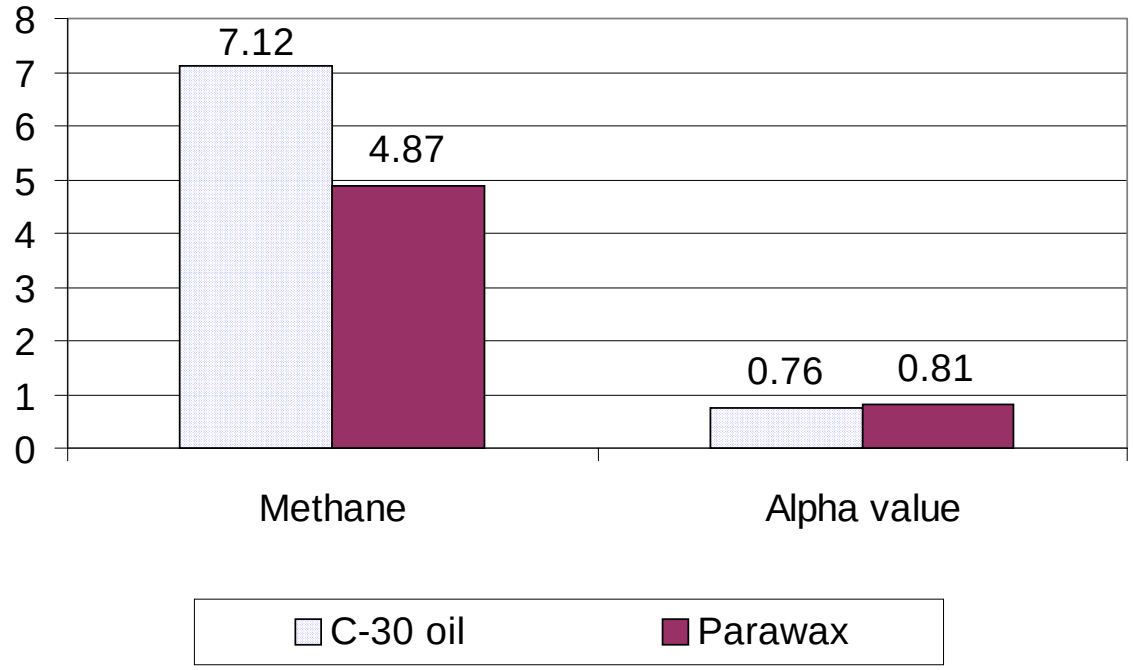

Figure 4. Olefin ratio v.s. carbon number

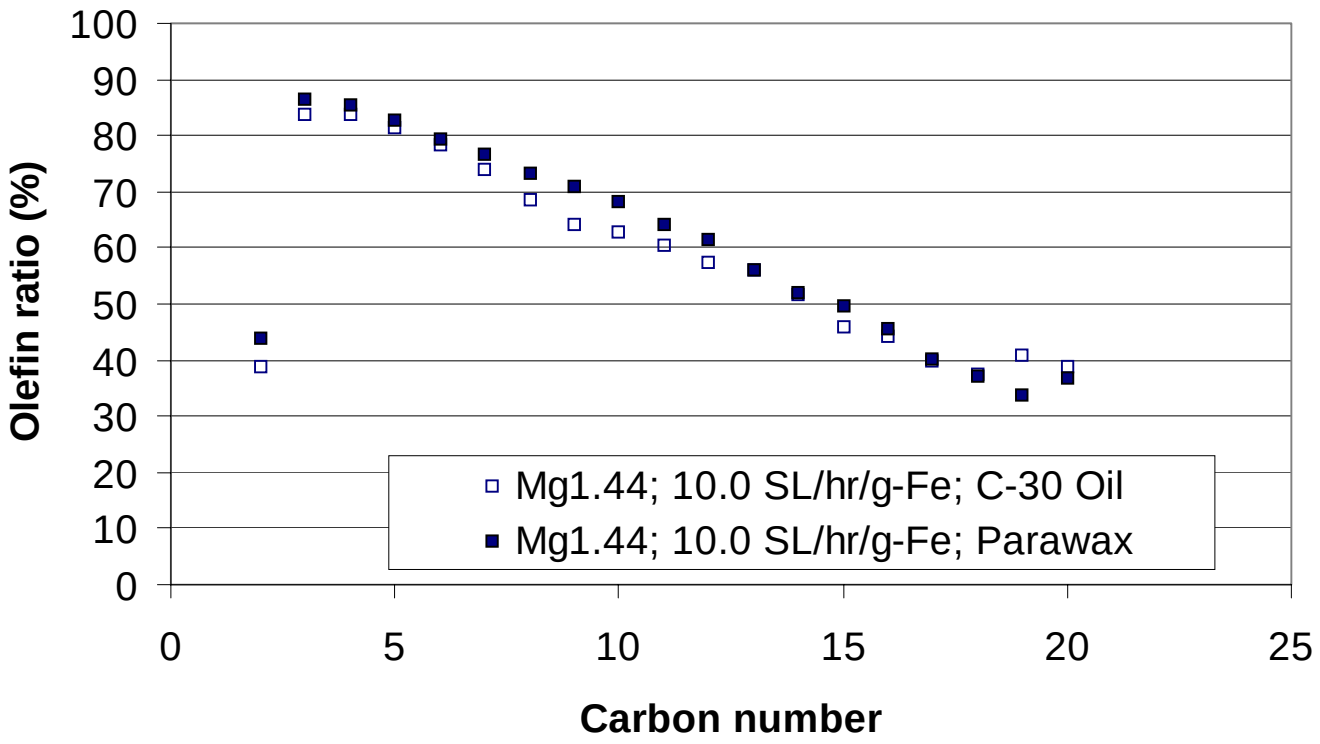

Figure 5. Hydrocarbon fractions

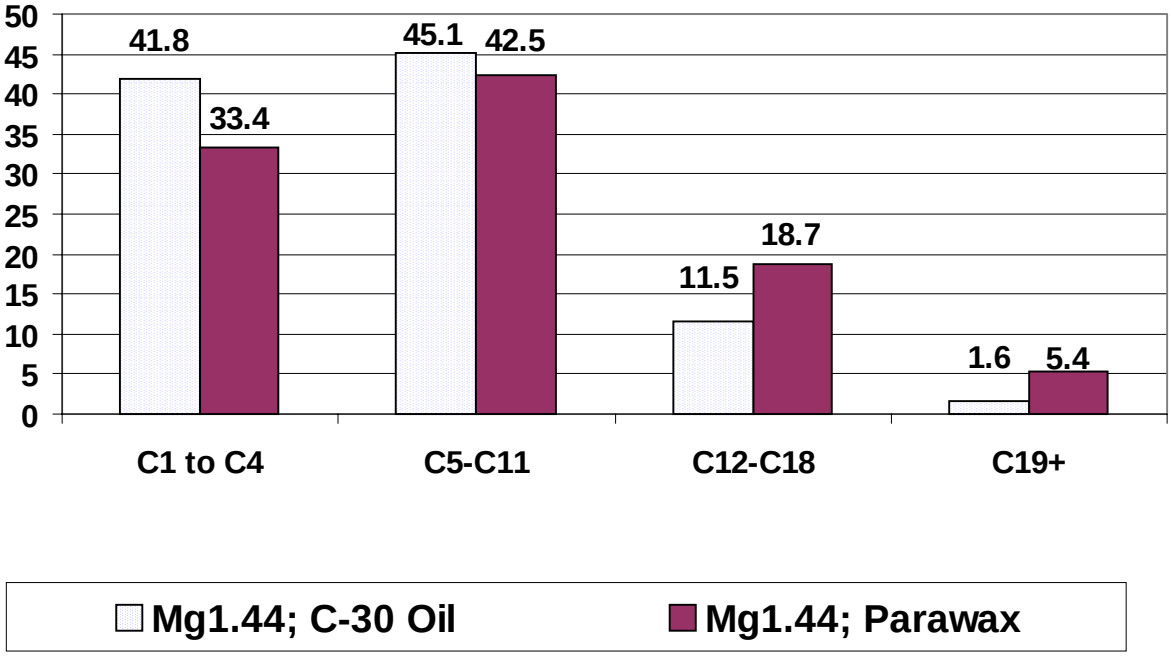

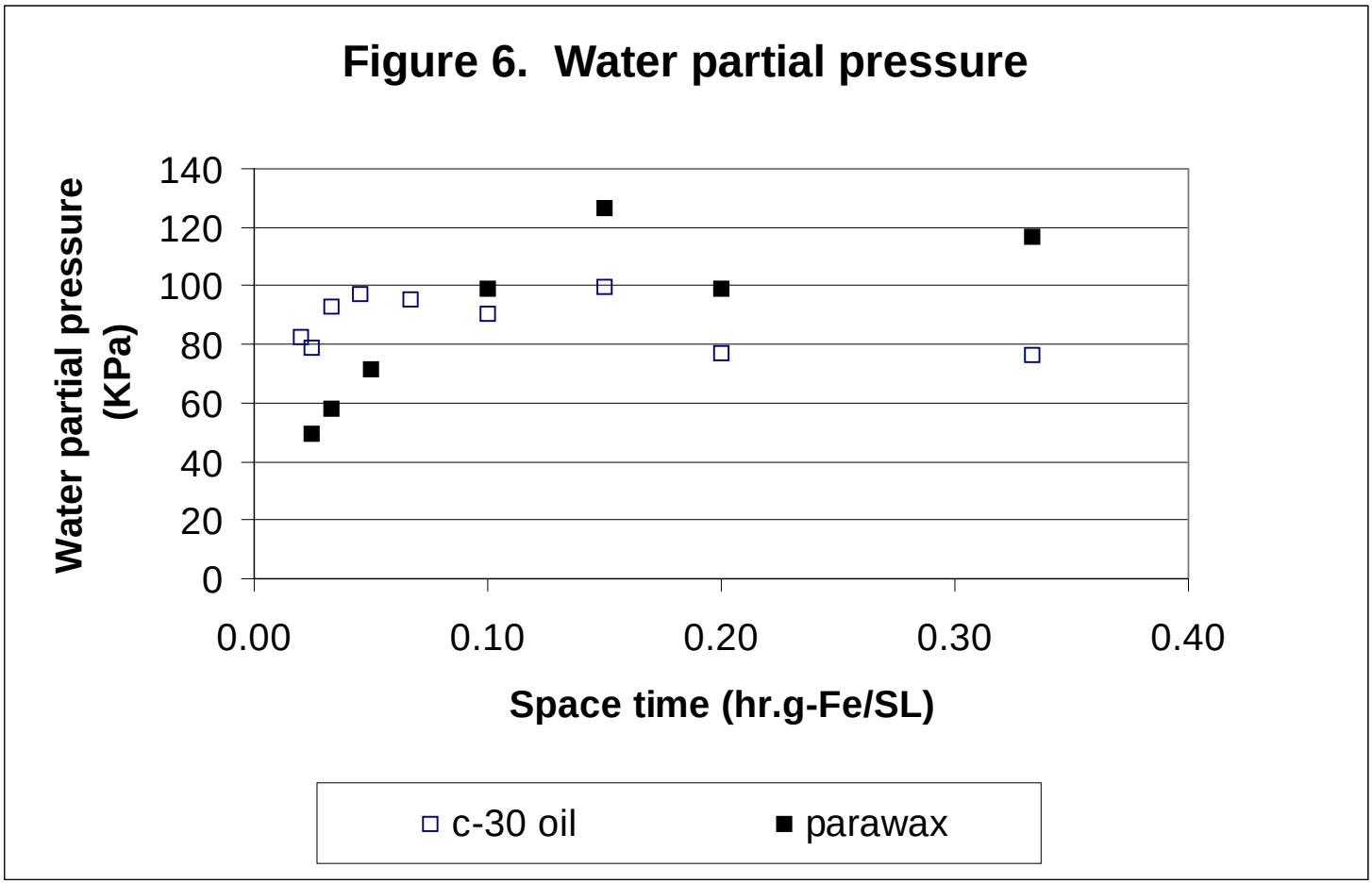
Figure 6. Water partial pressure
Water partial pressure (KPa)
140
120
100
80
60
40
20
0
0.00
0.10
0.20
0.30
0.40
Space time (hr.g-Fe/SL)
c-30 oil
parawax

Figure 7. Carbon dioxide partial pressure

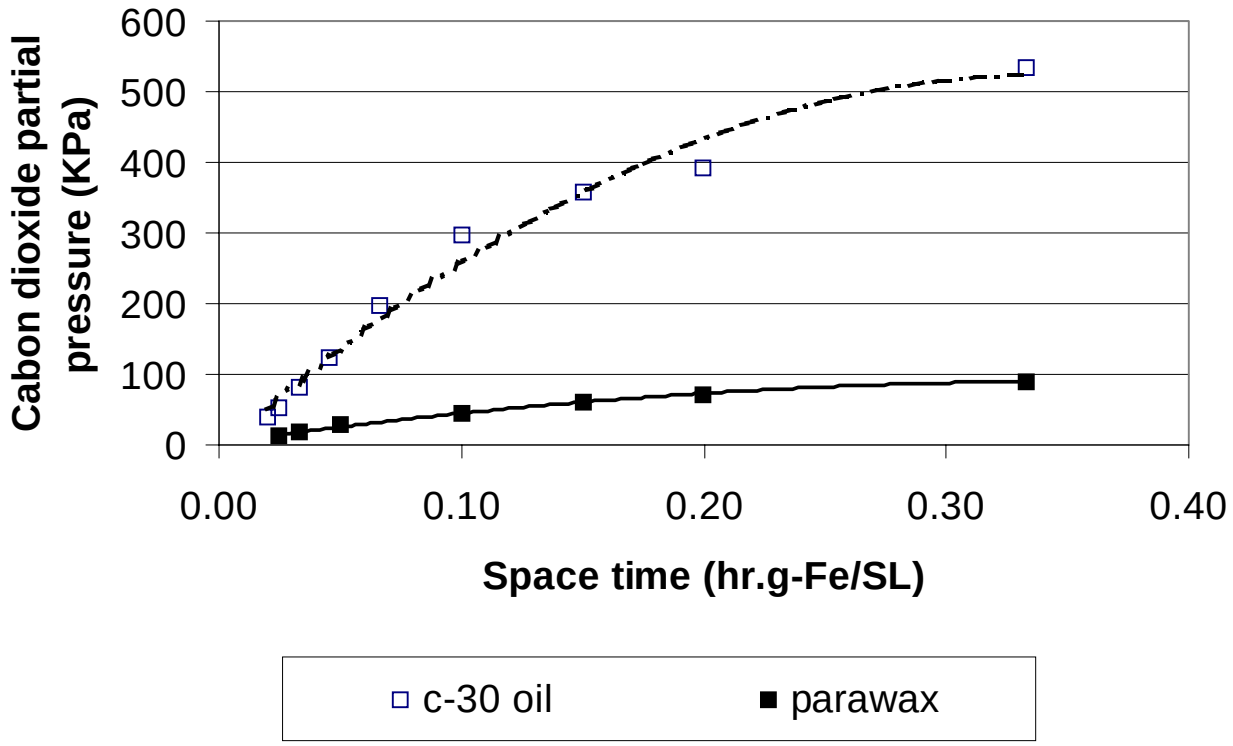

Figure 8. Hydrocarbon partial pressure

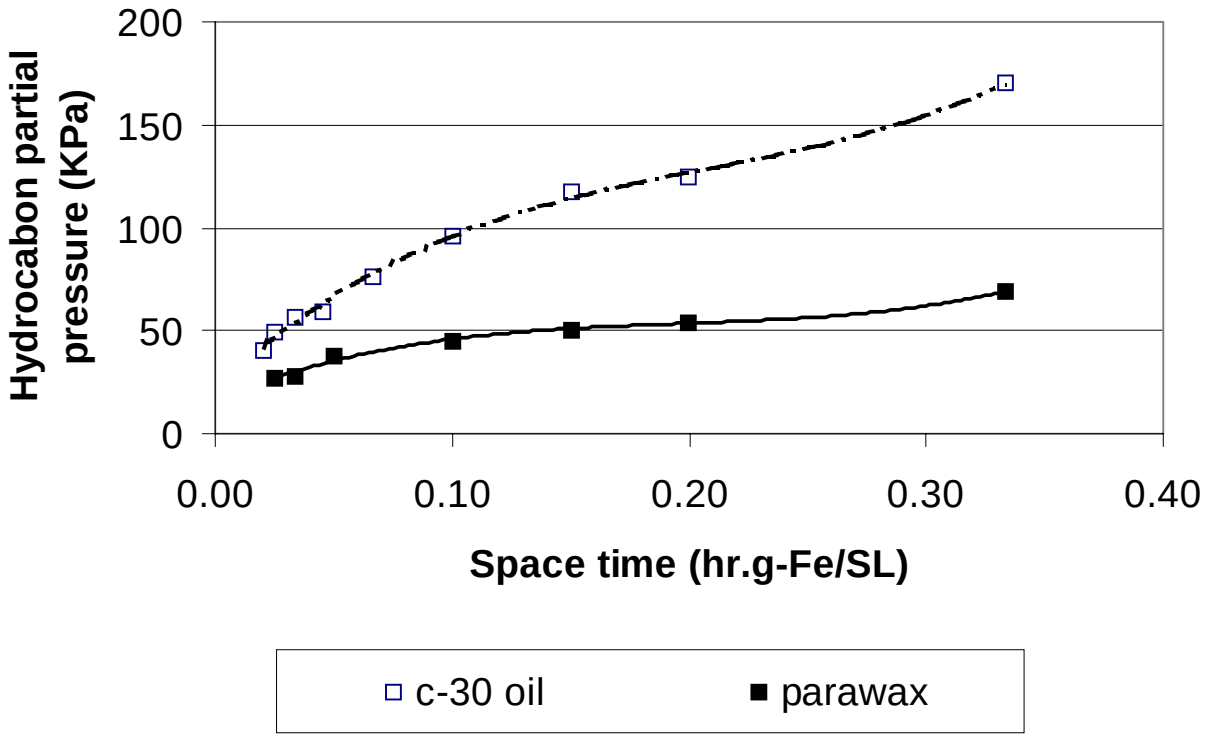

Figure 9. Water-gas shift qotient

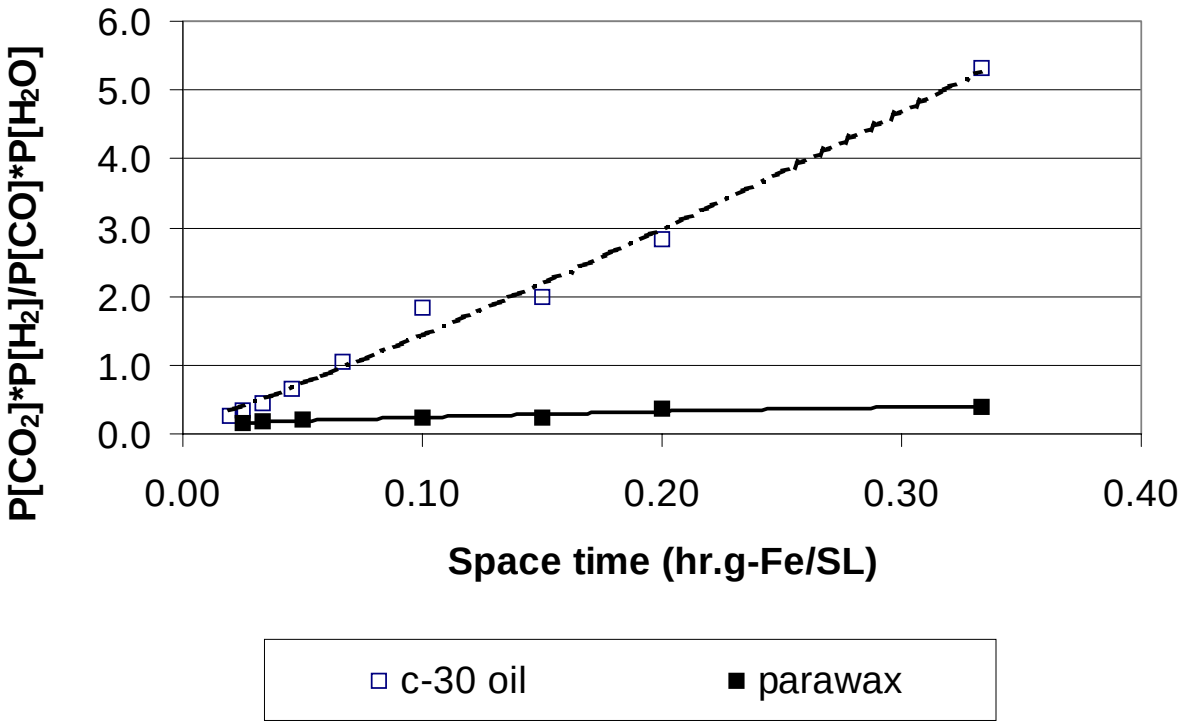

E. Two Alpha Fischer-Tropsch Product Distribution. A Role for Vapor Liquid Equilibrium?

Abstract

The simple polymerization mechanism for the Fischer-Tropsch synthesis produces products which follows an Anderson-Schulz-Flory distribution. Thus, plotting the logarithm of the mole fraction versus carbon number will produce a straight line whose slope is related to alpha which is determined by the chain termination and propagation probabilities. In contrast, the products from laboratory and large commercial plants exhibit a two-alpha plot. Vapor-liquid calculations show that product accumulation cannot be responsible for the two-alpha plot when the alpha value is large enough to produce liquid products at the reaction temperature. Only in the case where alpha is small and all products are in the vapor phase, allowing evaporation of the startup solvent and a "drying out" of the reactor can a product accumulation produce a two-alpha plot.

Introduction

By 1950, it was recognized that a simple polymerization mechanism should describe the Fischer-Tropsch synthesis product distribution, the so-called Anderson-Schulz-Flory (ASF) distribution (1-3). Thus, a plot of the logarithm of the molar concentration versus the carbon number would produce a straight line plot whose slope is related to alpha, the chain propagation probability. While this description has become widely accepted, it was also recognized at that time that the actual products, when higher carbon-number products were included, could not be described by a single alpha value. The so-called two-alpha distribution of products from several larger-scale plants in Germany and the U.S. were demonstrated in a plots by Anderson (4). In each of these and subsequent plots it has been shown that the break occurs in the range of carbon numbers 8 to 14.

Several models have been proposed to account for the two, or even more, alpha values (5). One that is frequently cited is the operation of two or more chains that undergo propagation independently (6-8). Another reason frequently cited for the two alpha distribution is the impact of diffusion and reincorporation of higher carbon number alkenes (9-14). It has become apparent that the ^{14}C-distribution in the products when labeled alcohols or alkenes are added to the synthesis gas fed to a continuous stirred tank reactor (CSTR) are impacted by accumulation of heavier products in the liquid in the reactor (15). Bell, among others, has shown that the initial gas phase products are depleted of higher carbon number products during the Fischer-Tropsch synthesis in a CSTR (16). For a catalyst that exhibits a constant conversion for some period and then declines in activity, the accumulation effects can provide a two alpha plot since the increasing gas flow carries accumulated products from the reactor in higher concentrations than they are formed (17). It was therefore of interest to learn whether a two alpha plot could be obtained when a catalyst with constant activity was utilized in a slurry reactor. Results of calculations for vapor-liquid equilibrium models corresponding to the operation of a Fischer-Tropsch catalyst with a single alpha value was utilized in a CSTR are provided in this manuscript.

Continuous Stirred Tank Reactor

The continuous stirred tank reactor provides the advantage that all catalyst particles have the same average catalyst life (based on usage), all catalyst particles are exposed to the same synthesis gas composition, and the reaction temperature is uniform in the catalyst slurry. Thus, the typical CSTR for Fischer-Tropsch synthesis is operated under constant temperature, pressure and reactant compositions. A certain amount of paraffin is charged to the reactor as starting solvent to provide a slurry phase. Reactant gases, i.e., CO and H_2, continuously flow into the reactor at constant rates. Vapor phase products, i.e., unconverted CO and H_2, CO_2, water, and

volatile hydrocarbons, continuously flow out. Liquid phase products are either removed continuously or allowed to accumulate in the reactor for some time interval. In the latter mode of operation, the excess reactor liquid is drained periodically, as necessary, so that the reactor is operated at a nearly constant liquid level. The drained liquid is added to the vapor phase product to obtain the total reaction product for the sampling period.

For the development of VLE model for Fischer-Tropsch synthesis, it is convenient to divide a CSTR reactor into two operational parts, i.e., reaction and separation, as illustrated schematically in Figure 1, where,

F_{CO}, F_{H_2}, F : molar flow rate of feed CO, feed H_2, and total flow after reaction, respectively

X_{CO} : CO conversion to hydrocarbons

x_i, y_i, z_i: individual hydrocarbon molar fraction in reactor slurry, vapor stream, and the combined streams after reaction, respectively

k_i : vapor-liquid equilibrium constant

L: moles of reactor liquid

V: molar flow rate of vapor stream

Fischer-Tropsch Reaction

For the Fischer-Tropsch reaction, it is assumed that CO and H_2 react stoichiometrically to produce hydrocarbons (exclusively paraffins for simplicity) and water following a single α ASF distribution and constant catalyst activity. Also, the fraction of CO converted to hydrocarbons (X_{CO}) is assumed to be constant through any reaction time period. Therefore, with constant reactant flow rates, the total flowrate of the stream after reaction (F) is constant. In addition, the each component in the reactor effluent (z_i) is constant with time. The water gas shift reaction,

which is significant with an iron catalyst, is not included explicitly in this model because it is an equal molar reaction that does not impact the total reactor effluent flow. This reaction does not affect hydrocarbon product distribution if the gases are insoluble, or of limited solubility, in the reactor liquid.

Based on the above assumptions, the Fischer-Tropsch reaction can be written as

$$(2n+1)\ H_2 + n\ CO \rightarrow C_nH_{2n+2} + nH_2O \quad (\ n = 1/(1-\alpha)\ ) \tag{1}$$

and the composition of each hydrocarbon produced by the reaction

$$Z_i = (1-\alpha)^2\ \alpha^{i-1}\ F_{co}\ X_{co} / F \tag{2}$$

Vapor-Liquid Separation

In the vapor-liquid separation component, the input is the stream leaving the reaction component. Here, the input stream is separated into liquid and vapor, which are assumed to be in thermodynamic equilibrium at reaction temperature and pressure (Eq. (3)). Equations (4) and (5) are used to describe the material balance for the separation process.

$$y_i = k_i x_i \tag{3}$$

$$\frac{dL}{dt} = F - V \tag{4}$$

$$\frac{d(Lx_i)}{dt} = Fz_i - Vy_i \tag{5}$$

The above equations can be solved numerically. For an infinitesimally small time interval, Δt, equations (3) - (5) can be combined to give

$$x_i = \frac{Fz_i\Delta t + (Lx_i)_{prev}}{L + k_i(F\Delta t - L + L_{prev})} \tag{6}$$

Equation (6) allows the calculation of the composition, x_i, and amount, L, of liquid in the reactor at any time interval within the constraint of Equation (7).

$$\Sigma x_i = 1 \tag{7}$$

With a knowledge of the initial reaction conditions, the liquid composition, vapor composition, vapor flow rate, and the amount of liquid in the reactor can be calculated at any time-on-stream.

Model Simulation

Based on the above model, the simulation is performed using a computer program developed in our lab. For simplicity of simulation, it was further assumed that hydrocarbon products are linear paraffins from C_1 to C_{100} whose relative concentrations follow a single α ASF distribution. Also for simplicity, CO, H_2, and H_2O are assumed to be insoluble in reactor liquid. All vapors are assumed to be idea gases and the liquid is assumed to be an idea solution; their compositions are related by Roult's law:

$$y_i = k_i x_i = \frac{P_i^s}{P} x_i \tag{8}$$

In the simulations, unless noted otherwise, the saturation vapor pressures of the Caldwell and Van Vuuren paraffins in Equation (8) are calculated using Equation (9) obtained from the literature (18). In this correlation, the unit for vapor pressure is atm and the unit for temperature is Kelvin.

$$P_i^s = 176.0452\exp(-427.218(\frac{1}{T} - 1.029807 \times 10^{-3})) \tag{9}$$

The paraffin vapor pressure was also estimated using Antoine's equation whose constants are obtained from API Project 44 (19). The difference between vapor pressure from these two sources and their impact on FT product distribution will be discussed later. A temperature

dependent correlation from the literature (20) is used to estimate the partial molar volumes of paraffins in the FT liquid. Other conditions for simulation are Newton's method for iteration of Equation (6), accuracy of the sum of liquid molar fraction of 0.0001 (Eq. (7)), and time interval of 0.01h for each numerical calculation.

Before reaction, a certain amount of C_{28} paraffin is added to the reactor as start-up solvent. This volume is used as the liquid volume to be maintained in the reactor. The catalyst volume is ignored in this simulation. The reaction effluent enters the separator, with vapor products leaving continuously and liquid products accumulating for some time interval. The amount of liquid in the reactor is examined at each time interval. If the liquid level is higher than that to be maintained, the extra volume is drained instantaneously so that the liquid level is constant throughout the simulation. The liquid drained from the reactor, if there is any, is added to the vapor stream as the total reaction products generated during that sampling period. Vapor products collected include water, unconverted H_2 and CO, and hydrocarbons. The flowrate of the vapor stream and its compositions are normalized to those of pure hydrocarbons for further calculations. Since C_{28} paraffin is used as the start-up solvent, its composition in both liquid and vapor are substantially higher than they should be in the Fischer-Tropsch product. Therefore, C_{28} is removed from vapor product as it does not represent what is produced by the reaction. Its composition in the vapor is determined from the amount of C_{27} and C_{29} using single α distribution rule. The same method is used for the liquid which is drained from the reactor and is added to the vapor stream to obtain the total reaction product.

The following seven (7) parameters are required as input to the simulation program: reaction temperature (^oC), reaction pressure (atm), H_2 flowrate (SL/h), CO flowrate (SL/h), CO conversion (mole%), amount of C_{28} starting solvent (g), and the single α value.

Simulation Results

Two sets of reaction conditions are used to illustrate the effect of VLE on the FT product distribution. The common conditions are temperature (270°C), pressure (12.9 atm), hydrogen flow rate (F_{H_2}; 23 SL/h), CO flow rate (F_{CO}; 33 SL/h), conversion of CO to hydrocarbons (X_{CO}; 40%), and the amount of C_{28} starting solvent (300g). The only difference is single α value; α=0.85 represents normal operating condition with liquids accumulation and α=0.65 which represents a drying out condition due to excessive evaporation of the starting solvent.

Figures 2 through 4 shows the hydrocarbon product distribution with an α value of 0.85 when the reactor is operated under normal conditions without drying out. In Figure 2 and the liquid phase plots thereafter, the composition of starting solvent (C_{28}) is not shown since it is not representative. The composition of a hydrocarbon in both liquid phase (Figure 2) and vapor phase (Figure 3) increases with time-on-stream before leveling off. The higher the carbon number, the longer time-on-stream it takes to attain the "steady-state" composition. After 5000 hours on stream, both liquid and vapor compositions become stable and are no longer affected by reaction time. For vapor phase composition, there is always a negative deviation from the ASF distribution for about C_{20}+ products, due to the thermodynamic effect. When the drained reactor liquid is added to the vapor stream to obtain the total reaction product, as shown in Figure 4, the product distribution approaches a single α distribution, although there is still a negative deviation before steady state. Also shown in Figure 4 are two dashed lines for liquid and vapor phases at 100 h to illustrate how they are combined to generate the total reaction product distribution. Once the reactor reaches steady state, the total reaction product distribution is represented by a single α distribution and without deviation. Longer reaction times up to 10,000 hours do not

change this distribution. It appears that, with a single α chemistry, vapor/liquid separation and/or accumulation is not responsible for the two α observation.

Figures 5 and 6 show the simulation results with α=0.65 when the reactor is drying-out at 508 h due to excessive evaporation of the start-up solvent. The vapor stream is the only product collected since the reactor liquid level decreases with time-on-stream, and hence no liquid can be drained from the reactor. As shown in Figure 5, the hydrocarbon fraction in the reactor liquid decreases with carbon number except when the reactor is close to drying-out, in contrast to normal operation (Figure 2) in which liquid fraction increases with carbon number and then decreases after reaching a maximum. Figure 6 shows the vapor phase composition, together with the theoretical ASF plot (dotted line). It is interesting to note that after some time on stream (e.g., 400 h), the vapor composition begins to show positive deviation from the ASF distribution. Obviously, this is due to the flashing-off of previously-accumulated heavier hydrocarbons, in agreement with earlier observations (17). Misinterpretation of this phenomena may lead to the conclusion of a two α product distribution. It should be noted that, with single α chemistry, positive deviation is possible only under drying-out conditions. Under the extreme situation when the reactor is dry (508 h, liquid level 0.1% of initial level in this simulation), an abnormal phenomena occurs. The plot at this time on stream indicates that the α value can be larger than unity over a range of carbon numbers, which is impossible from the chemical reaction stoichiometry.

As mentioned previously, a correlation from the literature is used to calculate the paraffin vapor pressure for vapor/liquid separation. Data from other sources may lead to different product distribution. Figure 7 compares the differences for the paraffin vapor pressure at 270^{o}C from two sources, the one used in this simulation and the other one from API Project 44 (19). For carbon numbers higher than about 40, the vapor pressure deviates from each other, and the

deviation becomes greater with increasing carbon number. As a result, predicted product distribution in both vapor phase and liquid phase depend on the data used. For the example shown in Figure 8, vapor pressure from API Project 44 predicts higher concentration of C_{30+} paraffins in the vapor phase, and a lower concentration in liquid phase. However, when the reactor reaches "steady-state", the total reaction product distribution is represented by a single α straight line. The dependence of vapor and liquid on vapor pressure is canceled out when the drained liquid is added to the vapor to produce the total reaction product. It is therefore reasonable to predict that as long as the reactor is operated under normal conditions, the total reaction product distribution is independent of the vapor-liquid equilibrium constant (k value), although vapor and liquid compositions will vary.

Conceptual Illustration

The above discussion is based on computer simulation involving 100 components with assumptions such as ideal gases, idea solution, and vapor/liquid separation at equilibrium. In fact, whether two α observation in FT synthesis can, or cannot, be attributed to vapor-liquid separation can be understood conceptually from separation principles.

A binary system shown in Figure 9 is used to illustrate the composition change with time. Pure component A continuously flows into the tank initially containing A_0 amount of A and B_0 amount of non-volatile component B. The objective is to examine if there is any chance that the amount of A in the output (vapor + drained liquid) be more than its input, due to accumulation of A in the liquid phase over time. A positive answer will lead to the vapor/liquid separation being responsible for the two α product distribution in the FT synthesis.

For easier discussion, it is assumed that the liquid phase density is constant so that its volume is directly proportional to its mass. The vapor phase and liquid phase are not necessarily

in equilibrium, nor do they need to be an idea mixture. This binary separation process can be described as:

1) During any time interval Δt_i (t_i - t_{i-1}) , F amount of A flows in, V_i amount of A flows out, and Δ_i is the amount of A leftover in the liquid phase.

2) Vapor flows out continuously, but the liquid level might increase due to accumulation of A. The liquid is drained to the level of L_0 instantaneously or at time t_n , if L_n is higher than L_0.

These two liquid draining cases will be discussed separately in the following section.

Liquid Allowed to Accumulate over a Time Period This is the most common operation practice for FT synthesis in a CSTR. Typically, exit vapor is collected in a condenser vessel during the sampling period, e.g., each 24 hours. The reactor liquid level is allowed to increase during this period before draining the reactor to the desired level. The drained reactor liquid is then added to the vapor condensate to obtain the total reaction product for this period. Therefore, the product distribution is actually the average of the sampling period. For the binary system discussed here, the sampling period is divided into **n** time intervals, each being of differential scale theoretically. The amount of A in vapor and liquid at each time interval is shown in Table 1. At the end of the sampling period, t_n, the reactor liquid is drained to the initial level of L_0. The total amount of A in output (F_{out}) is the sum of A in the drained liquid and the amount of A in vapor, shown as follows:

Total component A collected in vapor phase:

$$V = \sum V_i = nF - \sum \Delta_i = F_{in} - \sum \Delta_i$$

Total component A drained from liquid phase:

$$L = (L_n - L_0)C_n = (\sum \Delta_i) (A_0 + \sum \Delta_i)/(L_0 + \sum \Delta_i)$$

Total A sampled

$$
\begin{aligned}
F_{out} &= V + L \\
&= F_{in} - \Sigma\Delta_i + \frac{(\Sigma\Delta_i)(A_0 + \Sigma\Delta_i)}{L_0 + \Sigma\Delta_i} \\
&= F_{in} - \frac{B_0 \cdot \Sigma\Delta_i}{L_0 + \Sigma\Delta_i}
\end{aligned}
\tag{10}
$$

In Equation (10), F_{in} and F_{out} are the input and output of A during the sampling period, respectively. The amount of A in output depends on the following four cases:

1) $\sum\Delta_i > 0$, $F_{out} < F_{in}$, accumulation of A in liquid phase, negative deviation

2) $\sum\Delta_i = 0$, $F_{out} = F_{in}$, no accumulation of A in liquid phase, single α observation

3) $\sum\Delta_i < 0$ & $(-\sum\Delta_i) < L_0$, $F_{out} > F_{in}$, drying-out, false two α observation

4) $\sum\Delta_i < 0$ & $(-\sum\Delta_i) \rightarrow L_0$, $F_{out} \rightarrow \infty$, almost dry, hump observed, $\alpha > 1$

Case 1 is an unsteady state process for component A which accumulates in the separation tank. In FT synthesis, product distribution will show negative deviation from ASF distribution in this case. Case 2 is a "steady state" when the amount of A that accumulates during the sampling period equals the amount drained so that there is no net accumulation of A. These two cases are under normal operating conditions corresponding to Figure 4 in FT synthesis. In cases 3 and 4, the negative accumulation of A indicates that more material is collected in output than added in the input. This is possible only when the previously accumulated A in the tank is carried out by the flowing vapor. In FT synthesis, product distribution will exhibit positive deviation from ASF distribution. When the reactor is nearly dry (Case 4), F_{out} in much larger than F_{in}, which explains the "hump" in Figure 6.

Liquid Sampling Instantaneously (constant liquid level)

In this case, liquid level is kept constant by draining extra liquid instantaneously at each time interval. The liquid level is kept at the amount of L_0 after liquid draining. Table 2 shows

the material balance of component A at each time interval. Similar to the above example where liquid is allowed to accumulate, the amount of A in output cannot be higher than its input unless under drying out conditions.

Summary

From the above computer simulation and the conceptual discussion, it is concluded that under normal operating conditions, the observation of two α values for the Fischer-Tropsch synthesis cannot be due to VLE of reaction products. A positive deviation from ASF distribution is possible only when the reactor is drying-out. This false two α distribution should not be interpreted as the responsibility of VLE for normal operation.

References

1. R. B. Anderson, H. Friedel and H. H. Scorch, Fischer-Tropsch reaction mechanism involving stepwise growth of carbon chain, J. Chem. Phys., **19**, 313-319 (1951); R. A. Friedel and R. B. Anderson, J. Am. Chem. Soc., **72**, 1212, 2307 (1950).
2. E. F. G. Herington, Chem. Ind. (London), **(1946)**, 347.
3. S. Weller and R. A. Friedel, Isomer distribution in hydrocarbons from Fischer-Tropsch process, J. Chem. Phys., **17**, 801 (1949).
4. R. B. Anderson in "Catalysis," (P. H. Emmett, Ed.) Reinhold Pub. Co., New York, 1956, pp 208, 209.
5. B. H. Davis, The two-alpha value for iron Fischer-Tropsch catalysts: fact or fiction?, ACS Div. Fuel Chem. Preprints, 37, 172 (1992).
6. L.-M. Tau, H. Dabbagh, S. Bao and B. H. Davis, Fischer-Tropsch Synthesis: Evidence for two chain growth mechanisms, Catal. Letters, 7 127 (1990).
7. L. Konig and J. Gaube, The influence of water and of alkali promoter on the carbon number distribution of FT products formed over iron catalysts, Ber. Bunsenges. Phys. Chem. 9l (l987) ll6.
8. T. J. Donnelly, I. C. Yates and C. N. Satterfield, Analysis and prediction of product distributions of the Fischer-Tropsch synthesis, Energy Fuels, 2, 734-739 (1988).
9. E. Iglesia, S. C. Reyes and R. J. Madon; Transport-enhanced alpha-olefin readsorption pathways in Ru catalyzed hydrocarbon synthesis; J. Catal., 129 (1991) 238-256.
10. R. J. Madon, E. Iglesia and S. C. Reyes; Non-Flory product distributions in Fischer-Tropsch synthesis catalyzed by ruthenium, cobalt and iron; ACS Symp. Series, 517 (1993) 383-396.

11. E. Iglesia, S. C. Reyes and S. L. Soled; Reaction-transport selectivity models and the design of Fischer-Tropsch catalysts; "Computer-Aided Design of Catalysts and Reactors," (E. R. Becker and C. J. Pereira, Eds.), Marcel Dekker, Inc., 1992.

12. K. Fujimoto, L. Fan and K. Yoshii; New controlling method for product distribution in Fischer-Tropsch synthesis reaction; Topics in Catal., 2, 259-266 (1995).

13. S.-R. Yan, L. Fan, Z.-X. Zhang, J.-L. Zhou and K. Fujimoto; Effect of 1-olefin addition on supercritical phase Fischer-Tropsch synthesis over Co/SiO_2 catalyst; 14th Ann. Int. Pittsburgh Coal Conf., Proc., 1997.

14. E. W. Kuipers, C. Scheper, J. H. Wilson, I. H. Vinkenburg and H. Oosterbeek; Non-ASF product distributions due to secondary reactions during Fischer-Tropsch synthesis; J. Catal., 158 (1996) 283-300.)

15. B. Shi, L.-M. Tau, H. Dabbagh, J. Halasz and B. H. Davis, submitted.

16. D. Stern, A. T. Bell and H. Heinemann; Experimental and theoretical studies of Fischer-Tropsch synthesis over ruthenium in a bubble-column reactor; Chem. Eng. Sci., 40 (1985) 1917-1924.

17. A. P. Raje and B. H. Davis, Effect of vapor-liquid equilibrium on Fischer-Tropsch hydrocarbon selectivity for a deactivating catalyst in a slurry reactor, Energy & Fuels, 10, 552 (1996).

18. L. Caldwell and D.S. van Vuuren; On the formation and composition of the liquid phase in Fischer-Tropsch reactors; Chem. Eng. Sci., 41 (1986) 89-96.

19. Thermodynamic Research Center, Texas A&M University; Selected values of hydrocarbons and Related compounds; API Project 44, 1983.

20. J.J. Marano and G.D. Holder; Characterization of Fischer-Tropsch liquids for vapor-liquid equilibria calculations; Fluid Phase Equilibria, 138 (1997) 1-21.

Table 1

Amount of Component A at Any Time Interval when the Liquid is Allowed to Accumulate

Time	A in Vapor	Amount of Liquid Phase	Concentration of A in Liquid Phase
0		L_0	A_0/L_0
t_1	$V_1 = F - \Delta_1$	$L_1 = L_0 + \Delta_1$	$C_1 = \frac{A_0 + \Delta_1}{L_1} = \frac{A_0 + \Delta_1}{L_0 + \Delta_1}$
t_2	$V_2 = F - \Delta_2$	$L_2 = L_0 + \Delta_1 + \Delta_2$	$C_2 = \frac{A_0 + \Delta_1 + \Delta_2}{L_2} = \frac{A_0 + \Delta_1 + \Delta_2}{L_0 + \Delta_1 + \Delta_2}$
t_3	$V_3 = F - \Delta_3$	$L_3 = L_0 + \Delta_1 + \Delta_2 + \Delta_3$	$C_3 = \frac{A_0 + \Delta_1 + \Delta_2 + \Delta_3}{L_3} = \frac{A_0 + \Delta_1 + \Delta_2 + \Delta_3}{L_0 + \Delta_1 + \Delta_2 + \Delta_3}$
. . . . .			
t_i	$V_i = F - \Delta_i$	$L_i = L_0 + \Delta_1 + \Delta_2 + \ldots \Delta_i$	$C_i = \frac{A_0 + \Delta_1 + \Delta_2 + \ldots \Delta_i}{L_i} = \frac{A_0 + \Delta_1 + \Delta_2 + \ldots \Delta_i}{L_0 + \Delta_1 + \Delta_2 + \ldots \Delta_i}$

Table 2

Amount of Component A at Any Time Interval when Liquid is Drained Instantaneously

Time	A in Vapor	Concentration of A in Liquid Phase	Total A Collected (vapor + drained liquid)
0		A_0/L_0	
t_1	$V_1 = F - \Delta_1$	$C_1 = \frac{A_0 + \Delta_1}{L_0 + \Delta_1} = 1 - \frac{B_0}{L_0 + \Delta_1}$	$F_1 = V_1 + \Delta_1 C_1$ $F_1 = V_1 + \Delta_1\left(\frac{A_0 + \Delta_1}{L_0 + \Delta_1}\right) = F - \frac{\Delta_1 B_0}{L_0 + \Delta_1}$
t_2	$V_2 = F - \Delta_2$	$C_2 = \frac{\Delta_2 + \left(\frac{A_0+\Delta_1}{\Delta_1+L_0}\right)\cdot L_0}{L_0 + \Delta_2}$ $= 1 - \frac{L_0 B_0}{(L_0 + \Delta_1)(L_0 + \Delta_2)}$	$F_2 = V_2 + \Delta_2 C_2$ $F_2 = F - \Delta_2 + \Delta_2\left(1 - \frac{L_0 B_0}{(L_0+\Delta_1)(L_0+\Delta_2)}\right)$ $= F - \frac{\Delta_2 L_0 B_0}{(L_0 + \Delta_1)(L_0 + \Delta_2)}$
t_3	$V_3 = F - \Delta_3$	$C_3 = 1 - \frac{L_0^2 B_0}{(L_0 + \Delta_1)(L_0 + \Delta_2)(L_0 + \Delta_3)}$	$F_3 = F - \frac{\Delta_3 L_0^2 B_0}{(L_0 + \Delta_1)(L_0 + \Delta_2)(L_0 + \Delta_3)}$
. . . . .			
t_i	$V_i = F - \Delta_i$	$C_i = 1 - \frac{L_0^{i-1} B_0}{(L_0 + \Delta_1)(L_0 + \Delta_2)\ldots(L_0 + \Delta_i)}$	$F_i = F - \frac{\Delta_i L_0^{i-1} B_0}{(L_0 + \Delta_1)(L_0 + \Delta_2)\ldots(L_0 + \Delta_i)}$

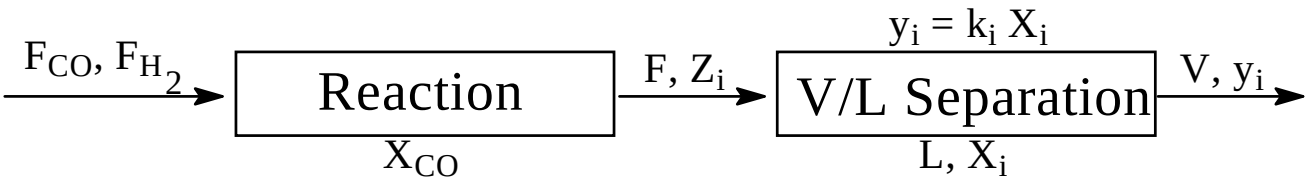

Figure 1. Schematic diagram of VLE mode for Fischer-Tropsch synthesis in a CSTR.

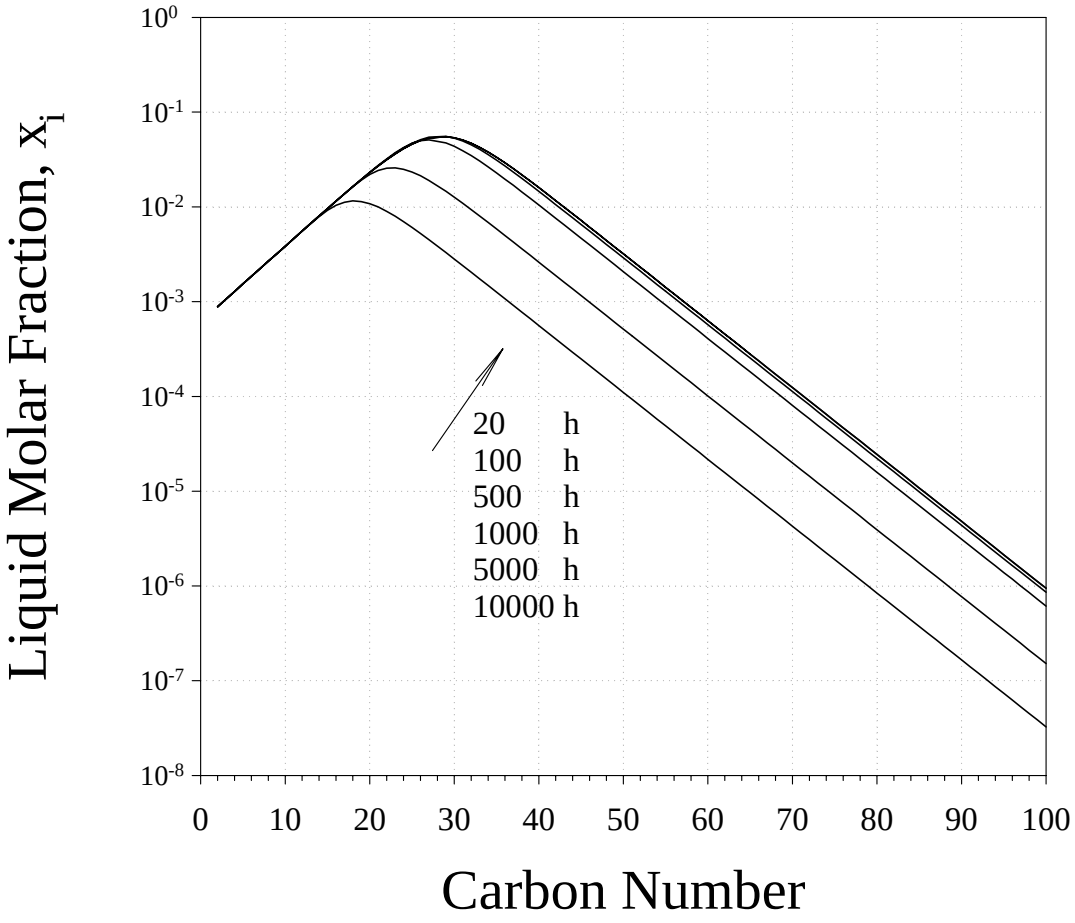

Figure 2. Hydrocarbon molar fraction in reactor liquid with α=0.85.

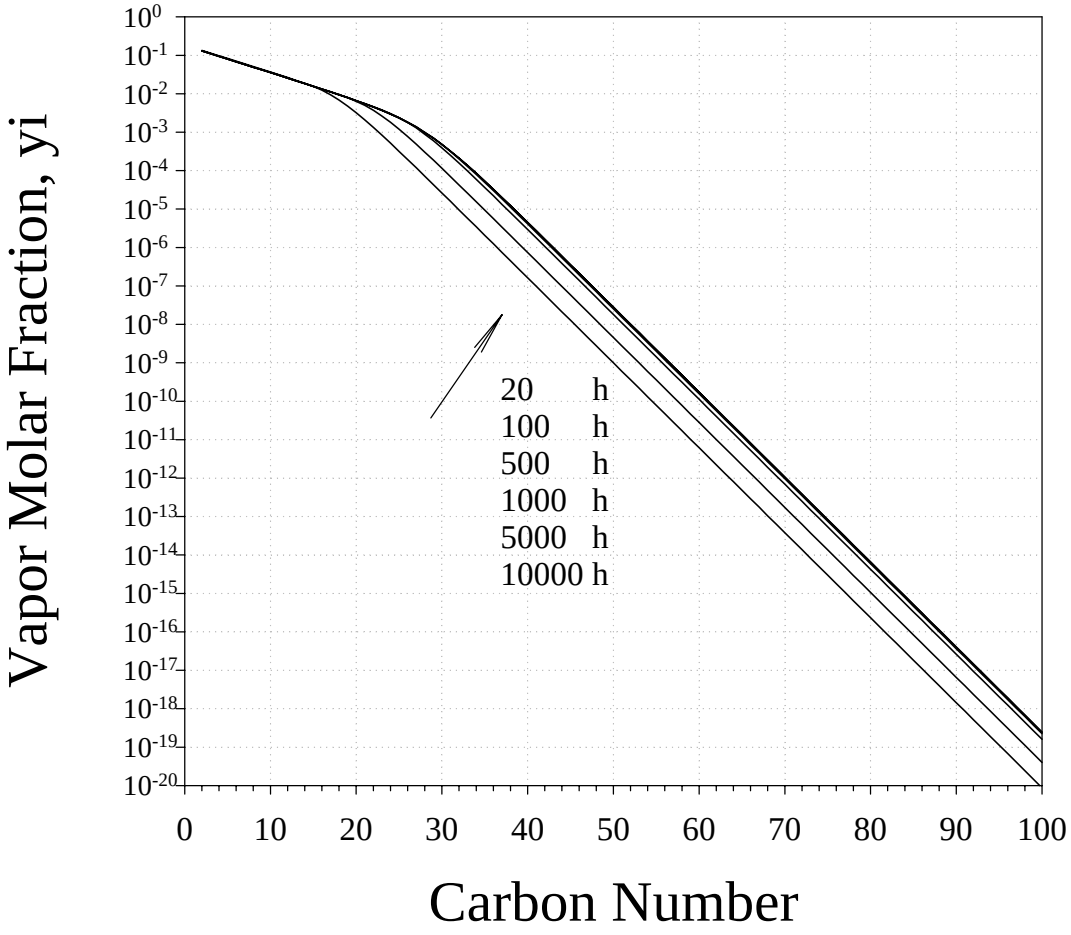

Figure 3. Hydrocarbon molar fraction in vapor phase with α=0.85.

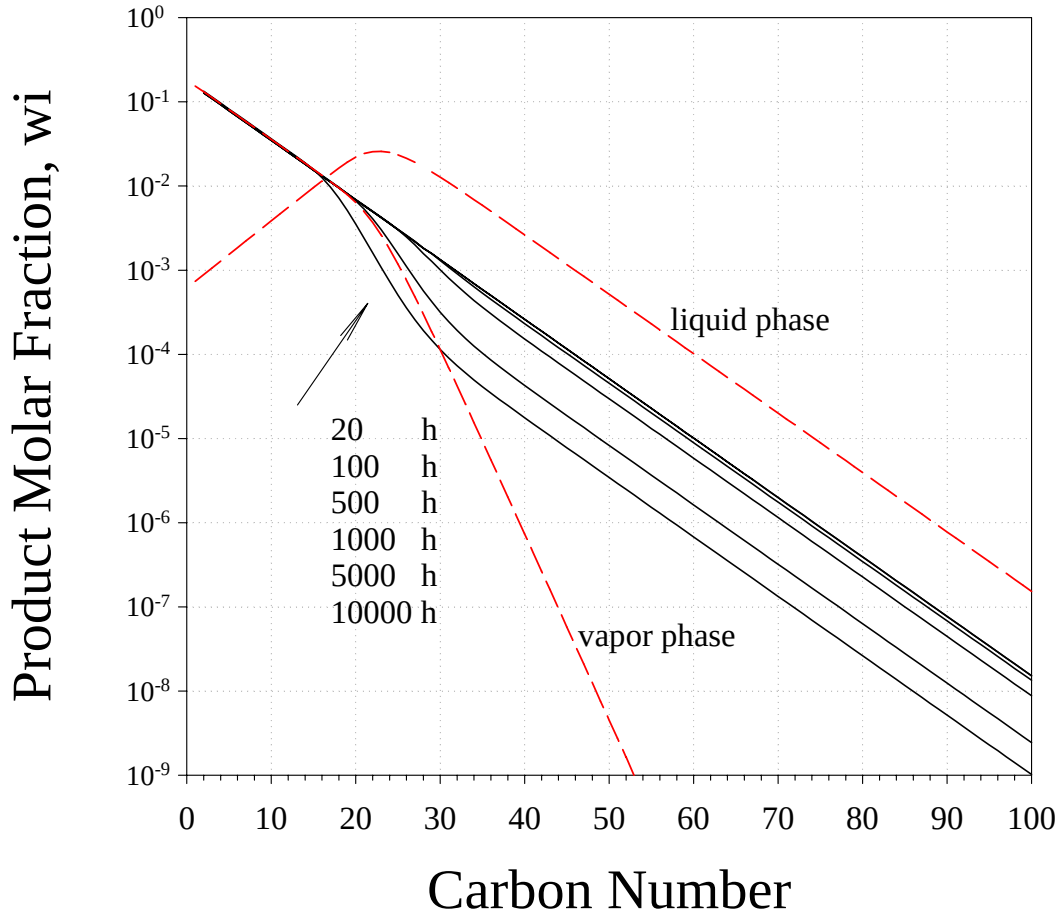

Figure 4 Hydrocarbon molar fraction in total reaction product with α=0.85 (solid line). Dashed lines are liquid phase and vapor phase compositions at 100 h.

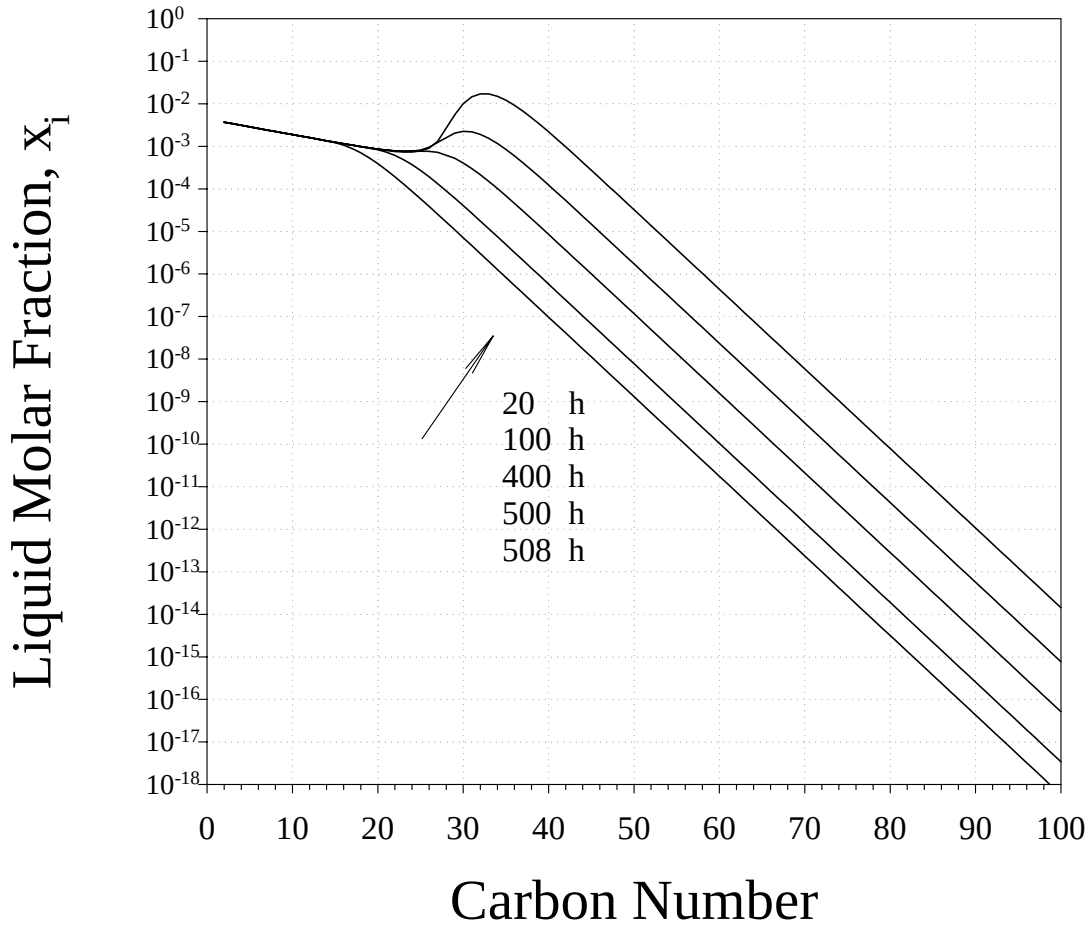

Figure 5 Hydrocarbon molar fraction in liquid phase with α=0.65

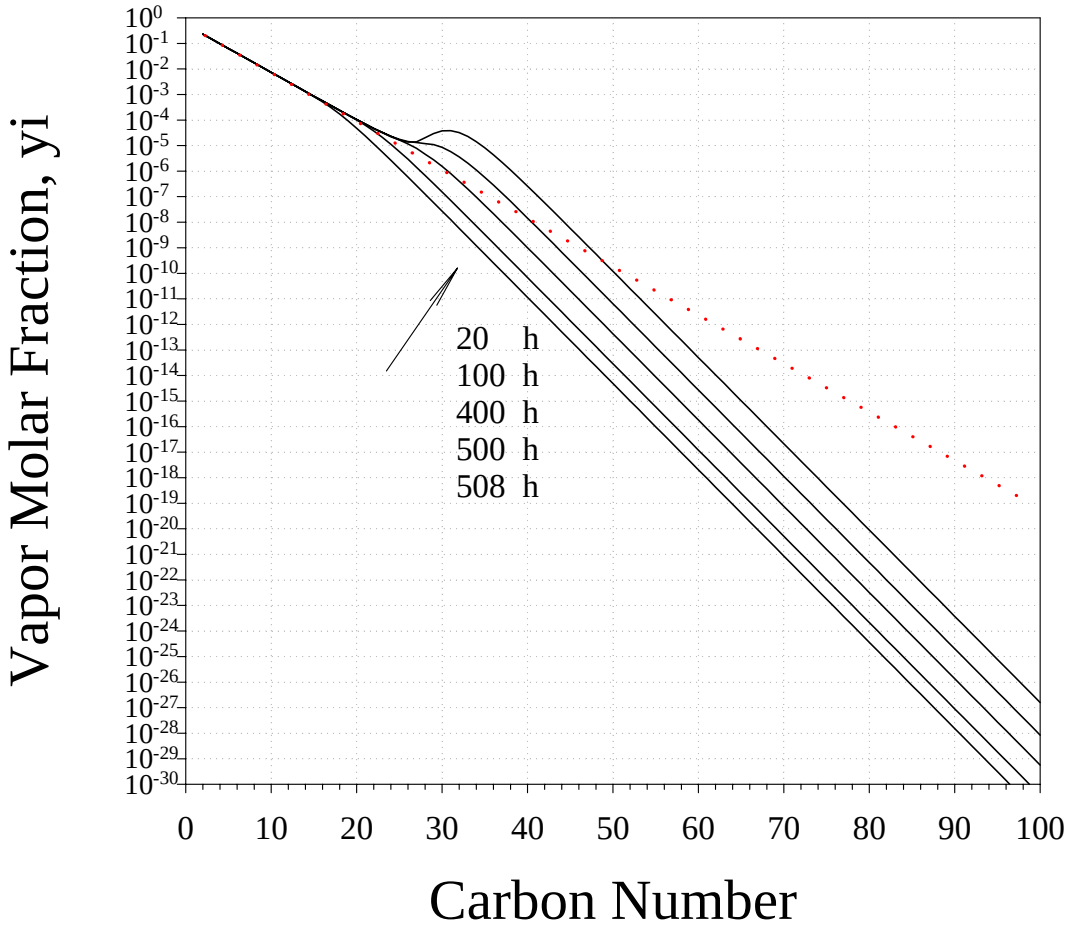

Figure 6 Hydrocarbon molar fraction in vapor phase with α=0.65
(Dotted line is ASF plot)

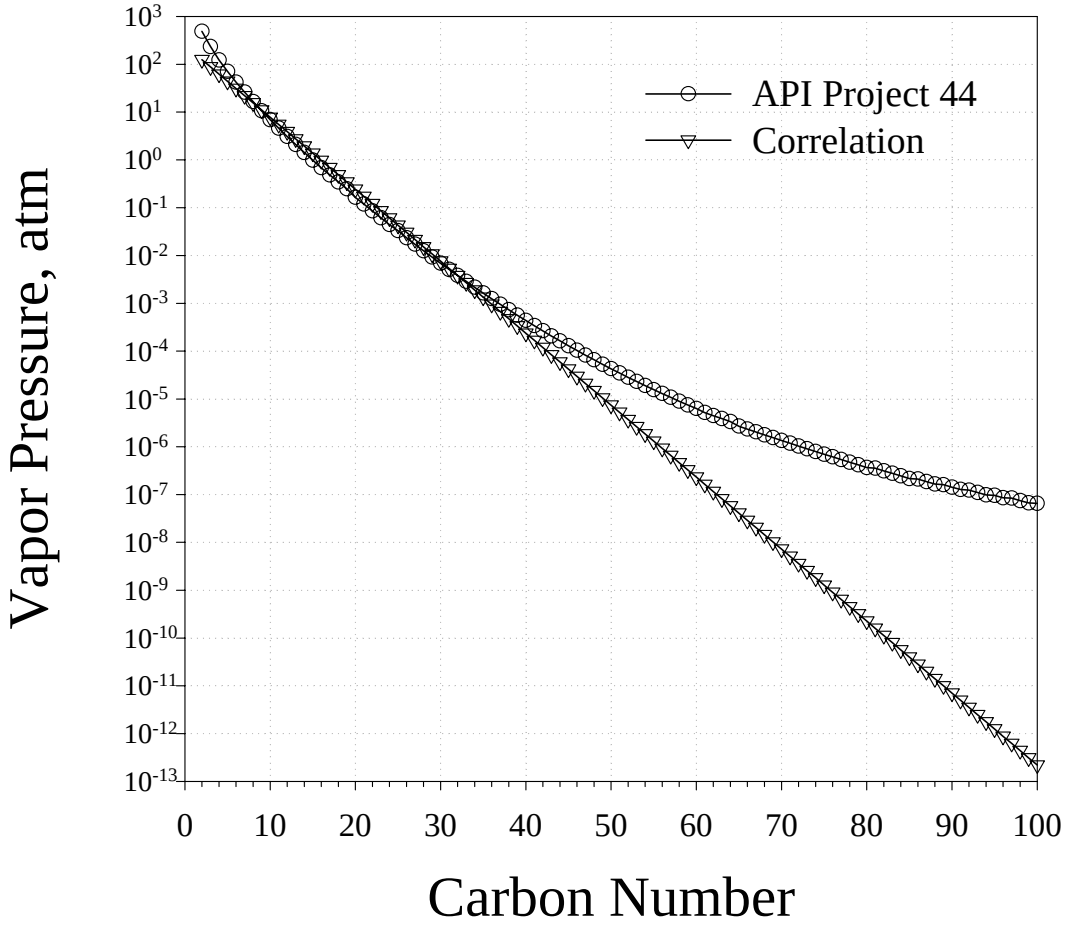

Figure 7 Comparison of paraffin saturation vapor pressure from different sources (270 ^{o}C)

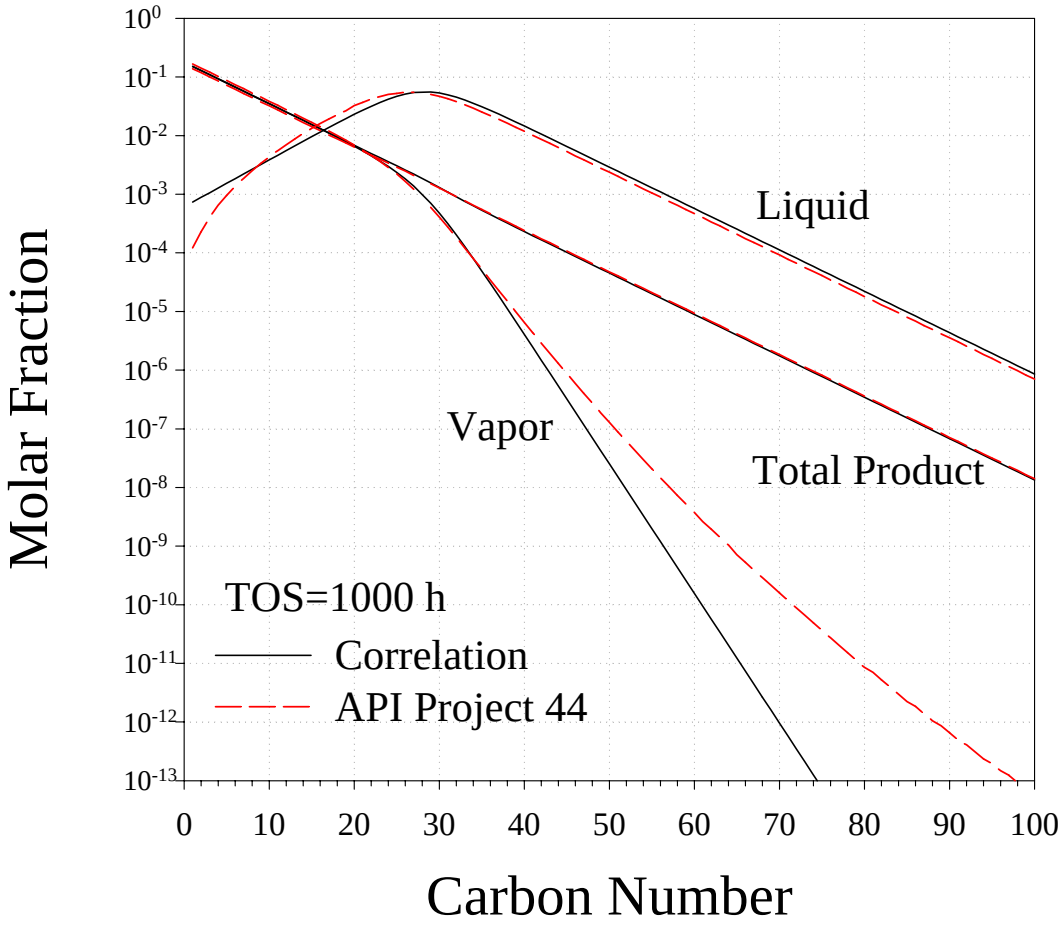

Figure 8 Effect of vapor pressure source on hydrocarbon molar fraction with α=0.85

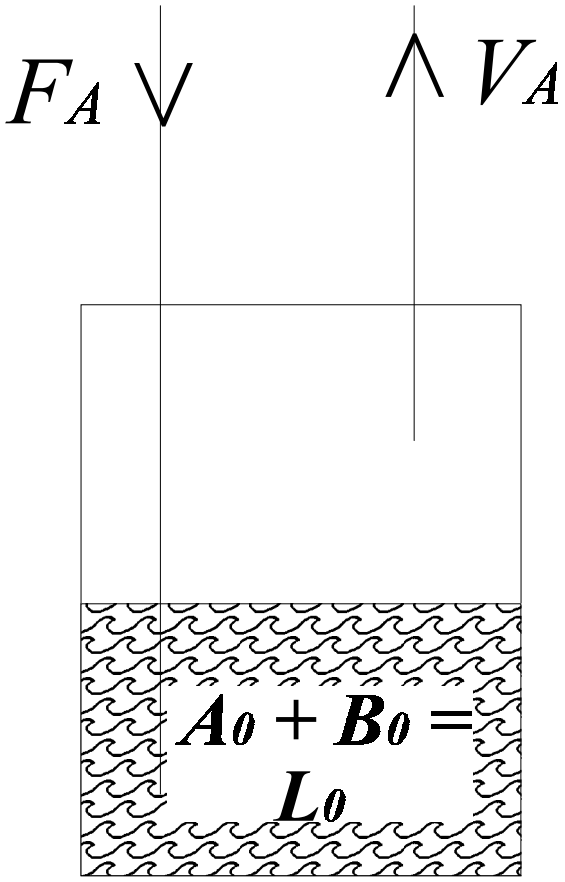

Figure 9. Schematics of a binary separation system.

F. Fischer-Tropsch Synthesis: Induction and Steady-State Activity of High-Alpha Potassium Promoted Iron Catalysts

Abstract

Iron Fischer-Tropsch synthesis (FTS) catalysts with different potassium loadings showed different induction periods during which the conversion increased from a low initial level to a peak value before declining to attain a lower stable activity at the same reaction conditions. A lower K loading produced a slightly higher peak conversion and a shorter induction period. Although the induction period and the peak conversion were slightly dependent on the K loading for the iron catalyst, the stabilized conversions and the stabilization periods were independent of potassium content. The C_2-C_4 olefin to paraffin ratio of the gaseous products and the CO_2 selectivity did not change significantly as the potassium content increased from 5 to 10%. An increase in reaction temperature produced a new induction period and a higher conversion than was obtained before the reaction temperature was increased. The H_2:CO ratio also had an important influence on FTS conversions. Increasing the H_2:CO ratio in the feed gas lowered the H_2 utilization. A higher H_2:CO ratio feedstock gas produced lower FTS catalyst activity compared to a low H_2:CO ratio gas.

Keywords: Catalyst, iron; Fischer-Tropsch Synthesis; Promoter, K; induction period; catalyst activation

Introduction

In a FTS process, the hydrocarbon is produced from CO and H_2 by a reaction which can be expressed as

$$(2n+1)\ H_2 + n\ CO \rightarrow C_nH_{2n+2} + n\ H_2O \qquad (1)$$

where the average value of n is defined as $\bar{n} = 1/(1-\alpha)$ or it can be rearranged as $\alpha = 1 - (1/\bar{n})$ where α is the ratio of chain termination to chain propagation [1]. When an iron catalyst is used for FTS reactions, the water gas shift (WGS) reaction can also occur. This side reaction consumes CO and water formed by the FTS reaction and produces additional hydrogen and carbon dioxide.

$$H_2O + CO \rightarrow CO_2 + H_2 \quad (2)$$

Potassium has long been used as a promoter for iron catalysts. It provides an increase in the alkene yield and a decrease in the fraction of CH_4 that is produced [2,3]. Potassium can also increase the catalytic activity for FTS and water-gas shift (WGS) reactions [4]. Activation of low alpha FTS with iron catalysts that are similar, except they have K to Fe atomic ratios less than 2, have been described earlier [5].

Dry reported the effect of K_2O on iron catalysts utilized in a fixed bed and a fluidized bed reactor that operated at different temperatures [3]. According to Dry, the low temperature FTS catalytic activity decreased as the loading of K_2O increased but the high temperature reaction showed the opposite effect. As shown in Figure 1, at 200°C, the relative catalyst activity decreased from 64 to 29 when the relative K_2O content increased from 0 to 2.6. At 330°C, the catalytic activities first increased and then stabilized at a certain level as the relative K_2O content was above 2 to 3. For use at high temperature conditions, Figure 1 indicates that the catalytic activity can be enhanced by potassium when its loading was lower than 3 relative to Fe, but a further increase in K_2O loading does not enhance the iron catalytic activity.

The influence of potassium on iron catalysts has also been investigated by other researchers [e.g., 6-8]. It is believed that strong bases of Group I metals have significant effects on both FTS activity and product selectivity. Bell and coworkers found that potassium enhances

the adsorption of CO but decreases the adsorption of H_2; therefore, potassium decreases olefin hydrogenation [14,15]. As the most effective promoter, potassium salts are widely used in iron catalysts; however, the readiness to form an alkali compound with common catalyst supports, or structural promoters such as alumina or silica, complicates the situation.

Although potassium enhanced the FTS activity and heavy product fraction, high potassium loadings may cover too large of a fraction of the surface of the iron catalyst, resulting in a limited promotion effect or even a decrease in FTS conversions. In our study, a potassium loading resulting in K to Fe atomic ratio of greater than 5 failed to further enhance the CO conversion.

Bonzel and Kerbs [9] claimed that potassium lowered the methane formation rate and increased the carbon deposition rate. It was also found that the deposited carbon was covered by potassium compounds rather than carbon sitting on top of the promoter. Huang et al. [6] studied potassium promoted iron catalysts with XPS and found that two-thirds of the catalyst surface was covered by K_2O and SiO_2. Wang, et al. [7] applied the temperature programmed reduction (TPR) technique to study the effects of potassium. They suggested that potassium facilitates the desorption process of carbon monoxide and strengthens the Fe-C bond. Thus, potassium enhanced the selectivity of long-chain products; i.e., it resulted in a high alpha product distribution. Copper is widely used as a promoter for iron FTS catalyst. It was believed that copper can facilitate the activation process. Copper can also minimize the sintering of iron catalysts by lowering the reduction temperature [3].

"In 1944, Hofer made an attempt to correlate the more reliable of the existing data of interest in connection with the Fischer-Tropsch synthesis [L. J. E. Hofer, "The Preparation and Properties of Metal Carbides," Report of Investigations 3770, U.S. Bureau of Mines, Washington. DC, July 1944]. Some 20 years later, Hofer reported that up to then (1966) little

work had been done on the action of CO on iron oxide [L.J.E. Hofer, "Nature of the Carbides of Iron," Bulletin 631, U.S. Bureau of Mines, Washington, DC, 1966]. During the 1940s, testing of iron catalysts prepared by six German organizations was conducted; these utilized the best activation procedure practiced by each organization and these varied widely [Anon., "Report on the Petroleum and Synthetic Oil Industry of Germany," Ministry of Fuel and Power, His Majesty's Stationery Office, London, 1946, pp 96-100.] While some utilized reduction in hydrogen, others indicated that activation in CO was preferred. Some of these early studies indicated that the catalyst activity and/or stability depended upon the amount of free carbon that was incorporated into the catalytic material during the induction period [L.J.E. Hofer, E. M. Cohn and W. C. Peebles, J. Am. Chem. Soc., 71, 189 (1949); H. Pichler and H. Merkel, "Chemical and Thermomagnetic Studies on iron catalysts for Synthesis of Hydrocarbons," Technical Paper 718, U.S. Bureau of Mines, Washington, DC, 1949 (based on thesis by H. Merker)]. Dry [M. E. Dry in "Catalysis-Science and Technology," (J. R. Anderson and M. Boudart, Eds.), Vol. 1, 160-255 (1981)] summarized much of the work on catalyst activation that was conducted during the commercialization of Fischer-Tropsch synthesis at Sasol; however, much of this work was applicable to the high temperature conditions and not the lower temperatures utilized in this study. More recent work has utilized conditions that are applicable to low temperature Fischer-Tropsch synthesis but much of this has been accomplished at low conversion conditions or at short times on stream [Bukur, Dragomir; X. Lang, et al; IEC Res. 28 (1989) 1130-1140; Niemantsverdriet, J.W.; A. van der Kraan; J. Catal. 72 (1981) 385-388; Sancier, K.M.; W.E. Isakson, H.Wise; Adv. Chem. Ser., 178, 129-45 (1979); Pennline, Henry; M. Zarochak, J. Stencel, J. Diehl; IEC Res. 26 (1987) 595-60l; Sault, Allen G.; J. Catal. 140 (1993) 121-135; Sault, Allen G.; A. Datye; J. Catal. 140 (1993) 136-149; Ameise, J. A., J. B. Butt and L. H. Schwartz; J. Phys. Chem., 82, 558, (1978); Pijolat, M, V. Perrichon and P.

Bussiere; J. Catal., 107, 82-91 (1987); Kock, A. J. H. M., H. M. Fortuin and J. W. Geus; J. Catal; 96, 261-275 (1985).]. This early work as well as work as well as more recent work has been reviewed recently [B. H. Davis, Technology Development for Iron Fischer-Tropsch Catalysts, Final Report, 1996, DoOE/PC90056-T17, 1100 pp (available at www.Fischer-Tropsch.org maintained by Syntroleum).].

In this study, three potassium promoted iron catalysts were prepared and tested at low temperatures to investigate the effect of potassium at a high level of K to Si atomic ratio of 0.05 to 0.10 on the selectivity and activity of Fischer-Tropsch synthesis. Influences of reaction conditions and gas compositions were also studied in this work.

Experimental

Preparation of Catalyst

In this study three catalysts, containing 0.05, 0.075 and 0.10 atomic ratio of K relative to iron, have been utilized. Precipitated iron catalyst precursors were precipitated from a ferric nitrate solution that was prepared by dissolving $Fe(NO_3)_3 \cdot 9H_2O$ in distilled and deionized water, and then an amount of tetraethyl orthosilicate needed to make a Si/Fe atomic ratio of 4.6 was added. The mixture was stirred vigorously until the tetraethyl orthosilicate had hydrolyzed. A stream of the tetraethyl orthosilicate and iron nitrate mixture was added to a continuous stirred tank reactor (CSTR) precipitation vessel and a separate stream of 30% ammonium hydroxide was added at a rate to maintain a pH of 9.0. By maintaining the slurry pH at 9 and an average residence time of 6 minutes, a base catalyst material with an iron to silicon atomic ratio of 100:4.6 was obtained. The slurry from the CSTR was filtered using a vacuum drum filter and washed twice with deionized water. The final filter cake was dried for 24 hours in an oven at $110^{O}C$ with flowing air. The catalyst was crushed to approximately 60 μm sized particles and then calcined at $350^{O}C$ in an air flow for 4 hours.

The 100Fe/4.6Si catalyst base powder was impregnated with the proper amount of $Cu(NO_3)_2 \cdot 3H_2O$ to give an atomic composition of 100Fe/4.6Si/2.0Cu. The amount of $Cu(NO_3)_2 \cdot 3H_2O$ added will depend on the iron content of the base catalyst following calcination. In addition to copper, potassium was also added as a promoter for the iron catalyst. Although most researchers use the carbonate, it is believed other potassium salts, such as nitrate, hydroxide, fluoride, silicate or permanganate, produce equal results [3]. In this study, the iron catalyst was impregnated with an aqueous K_2CO_3 solution to give the desired K-content in the final catalyst. The catalyst was dried at $110^{O}C$ overnight with good mixing following the impregnation. Thus, catalysts with three different potassium loading of K/Fe = 0.05, 0.075 and 0.10 (atomic ratio) were prepared for FTS studies.

In-situ Activation of Catalysts

The iron catalyst needs to be activated with H_2, CO or synthesis gas. Activation procedures can have a significant effect on the selectivity and activity of iron catalyst [8,10]. It was reported that catalysts activated with CO yielded higher amounts of long-chain hydrocarbons than catalysts activated with syngas or with H_2. Hydrogen activation followed by CO activation was reported by Bell [15] and by Anderson [16]. In addition, activation conditions may also influence the performance of the iron catalyst during the course of the run.

In this study, the potassium promoted iron catalysts were pretreated with 24NL/h CO at 270°C and 1.2 MPa for 24 hours. The CO flowed through a catalyst slurry containing 10% solids suspended in 300 mL of Ethylflow (a mixture of decene trimers). The reduction of Fe_2O_3 with CO occurs in two steps:

$$3Fe_2O_3 + CO \rightarrow 2Fe_3O_4 + CO_2 \quad (3)$$

$$5Fe_3O_4 + 32CO \rightarrow 3Fe_5C_2 + 26CO_2 \quad (4)$$

In addition, CO_2 may be formed by the Boudouard reaction:

$$2CO \rightarrow C + CO_2 \quad (5)$$

Previous work in our lab showed that approximately 50 % to 100% more carbon was present in the activated catalyst mass than was needed to form Fe_5C_2 [10]. Gradual oxidation of Fe_5C_2 to Fe_3O_4 was observed when this iron catalyst was used in FTS. It is believed that reaction system becomes more oxidizing and magnetite is usually formed at a high CO conversion [16].

Reactor System

A one-liter CSTR was used in this study (Figure 2). A sintered metal filter was installed to remove wax samples from the catalyst slurry. The wax sample was extracted through an internal filter and collected in a hot trap held at 200°C. A warm trap (100°C) and cold trap (0°C) were used to collect light wax and the water plus oil samples, respectively, by condensing from the vapor phase that was continuously withdrawn from the reactor vapor space.

CO and H_2 mass flow controllers were used to provide a simulated synthesis gas of the desired composition. After the catalysts was activated with CO, syngas was introduced at a rate of 3.1 NL/hr/gram-Fe. Reaction conditions were 230°C, 1.2 Mpa, $H_2/CO = 0.67$, and a stirrer speed of 750 rpm.

Product Sampling and Analysis

Daily gas, water, oil, light and heavy wax samples were collected and analyzed. Table 1 gives a summary of the instruments for gas and liquid product analysis. A heavy wax sample was taken from the 200°C hot trap connected to the filter. The vapor phase above the slurry passed continuously to the warm (100°C) and the cold (0°C) traps outside the reactor. The light wax and water mixture was collected from the warm trap and an oil plus water sample from the cold trap. Tail gas from the cold trap was analyzed with an online HP Quad Series Micro GC, providing molar compositions of C_1-C_7 olefins and paraffins as well as for H_2, CO and CO_2. Hydrogen and carbon monoxide conversions were calculated based on the gas product GC

analysis results and the gas flow measured at the reactor outlet. Hydrogen, carbon monoxide and syngas conversion were obtained using the following formula:

$$\text{Conversion} = 100\% \times (N_{in} - N_{out}) \div N_{in} \quad (6)$$

The oil and light wax samples were mixed before analysis using an HP 5790A GC. The heavy wax was analyzed with an HP5890 Series II Plus GC while the water sample was analyzed using an HP5890 GC.

Results and Discussion

Potassium Effect on Fischer-Tropsch Synthesis Activity

In this study, a CSTR reactor was used under the conditions of 230°C and 175psig (1.20 MPa). Simulated synthesis gas was prepared by mixing CO and H_2 to produce a H_2:CO ratio of 0.67. Gas feed flow rate was controlled at 3.1 NL/h/g-iron. To study the effect of potassium on iron catalyst activities, two series of catalysts were used to produce low and high wax Fischer-Tropsch synthesis products. Low wax (low alpha) iron catalysts were prepared to obtain a potassium to iron atomic ratio of 0.07 and 0.02 while high alpha catalysts had ratios of 0.05, 0.75 and 0.10.

The results (Figure 3) show that potassium has a significant effect on FTS catalyst activity when potassium loading was relatively low. Carbon monoxide conversions increased from 14% to 25% as the potassium to iron atomic ratio increased from K/Fe = 0.0 to 0.02. However, potassium, when added at levels higher than about K/Fe = 0.050 it did not affect the CO conversion. All three higher potassium-containing catalysts used in this study yielded a stabilized CO conversion of 40%. This shows that the potassium promotion effects for synthesis at 230°C for an iron FTS catalyst activity reached a maximum at a K loading of K/Fe = 0.050 or less. This contrasts to the results shown in Figure 1 since it is anticipated that similar activity patterns should be obtained at 200°C and 230°C.

Figure 4 gives the relation of potassium loading and FTS alpha values, which was calculated using all gas, oil and wax analysis data. A lower level of K loading significantly increased the alpha value. An increase in K loading from K/Fe = 0.0 to 0.02 raised the alpha value from 0.71 to 0.85. A further increase to a K/Fe loading of 0.050 increased the alpha value to 0.91; however, a further increase in potassium loading did not increase the alpha value further.

Induction Period

The induction periods for three potassium promoted iron catalysts were obtained under the same conditions of 1.2 MPa and 230°C. A mixture of known CO and H_2 composition was used as a simulated synthesis gas. Figures 5 and 6 show the CO and H_2 conversion results obtained from these tests. All three higher K-containing catalysts used in this study showed a similar behavior for both hydrogen and carbon monoxide conversions. For hydrogen conversion, all catalysts showed an induction period in which the catalysts effected increasing conversion from a low initial point to a peak value before declining to a lower but stable level. The lower potassium loaded catalyst, K/Fe = 0.05, produced a slightly higher maximum conversion, and at a shorter induction period. The peak hydrogen conversion for the K/Fe = 0.050 catalyst was as high as 50% while the K/Fe = 0.10 yielded a 45% peak conversion (Figure 5). While the induction period and the peak conversion values for hydrogen are slightly dependent of the K loading, the stabilized conversions and the stabilization periods are independent of the potassium content. All three higher potassium promoted catalysts yielded the same stabilized hydrogen conversion at about 400 hours of total on-stream time.

Carbon monoxide conversions showed a behavior that is similar to hydrogen conversions using these K-promoted catalysts (Figure 6). The K/Fe = 0.0144 catalyst showed an induction period of 25 hours while the K/Fe = 0.05, 0.075 and 0.10 catalysts yielded induction periods of 80, 120 and 150 hours, respectively. When high alpha catalysts were used, stable CO

conversions were obtained after about 400 hours of reaction time. Figure 6 showed only a slight difference in stabilized CO conversions for catalysts with different potassium loadings. The K/Fe = 0.075 catalyst yielded a 40% CO conversion while the K/Fe = 0.05 and 0.10 catalysts produced a CO conversion of 36% and 38%, respectively.

Selectivity

Table 2 shows the productivity and selectivity of the FTS reactions catalyzed by these high-alpha iron catalysts. Hydrocarbon productivity, CO_2 selectivity and the water gas shift reaction were not significantly influenced by the potassium content at the three higher loadings. Only a slight improvement in methane selectivity, water gas shift reaction and hydrogen productivity was observed when potassium content increased from K/Fe of 0.05 to 0.075. A further increase in potassium content did not enhance the productivity and the selectivity of FTS. Gas (C_2-C_4) analysis results indicate that the percentage of olefins for each carbon number were in the range of 82 to 87% for all three catalysts (Figures 7 and 8). The data (Table 2) also indicate that, as potassium content increased from K/Fe of 0.075 to 0.10, long-chain hydrocarbons (C_{19+}) yield increased significantly from 17.7% to 44.9%. The amount of the gas fraction with increasing potassium content (C_1-C_4) decreased by 61% and gasoline (C_5-C_{11}) fraction decreased by over 50% when increased from 0.05 to 0.07 K/Fe. These results are consistent with the findings by other researchers [3,14,15].

Dry reported that formation of methane is inversely proportional to the concentration of water and carbon dioxide [3], although others believed that CO_2 and water favor the formation of methane [13]. Figures 9 and 10 show the influence of high loadings of potassium on CO_2 and CH_4 selectivity for low temperature synthesis. Similar to the CO conversion profile, CO_2 selectivity also shows an induction period. The CO_2 selectivity for all three catalysts went through a rapid initial period of increase; however, the induction period for CO_2 is shorter than it

is for hydrocarbon formation. The CO_2 selectivity declined from its peak value of 42% to a stable level of 39%. Potassium had little effect on CO_2 selectivity for iron catalysts with K/Fe = 0.05 to 0.10. Figure 10 shows an initial decline in methane selectivity during the first 200 hours of the run. The content of potassium had little effect on the methane selectivity. All three catalysts yielded a stable methane selectivity of 1.5% after the first 200 hours of run. The results shown in Figures 9 and 10 suggest that the surface structure and/or composition changes in the first 250 hours of the reaction so that it favors the formation of CO_2 and inhibits the formation of methane. This is opposite the expectation since a slower CO_2 content produces a lower H_2/CO ratio and this is expected to produce less methane, in contrast to the higher methane fraction.

Reaction Conditions

After both hydrogen and the carbon monoxide conversions were stabilized, the FTS reaction temperature was changed from 230 to 250°C using the K/Fe = 0.10 promoted catalyst. As shown in Figure 11, both conversions went through a new induction period and then rapidly reached a stable conversion level. A 20°C temperature increase resulted in a hydrogen conversion change from 36% to a stable level of 50%. Similarly, CO conversion increased from 37% to 47%.

In addition to reaction temperature, total pressure and the H_2:CO ratio also had an important influence on FTS conversions. A test was conducted using an iron catalyst (K/Fe = 0.075) to study the effect of H_2:CO ratio on the catalyst activity. Initial reaction conditions were 175psig, 230°C and H_2:CO ratio of 0.67. After FTS conversions became stable after 500 hours of reaction time, the pressure was increased to 350psig and the H_2:CO ratio to 1.7. Figure 12 show that a change of the H_2:CO ratio did not yield stable conversions for H_2 and CO in the initial 200 hours of reaction following the changes in reaction conditions. Immediately after the H_2:CO ratio was changed, the H_2 conversion decreased significantly from 40% to less than 30%,

and then the H_2 conversion declined linearly from 30 to 22% before it approached a stable level. Although carbon monoxide conversion showed an initial increase, it then decreased at a similar rate as the H_2 conversion did.

The results show, as expected, that an increase of the H_2:CO ratio in the feed gas lowered the H_2 utilization rate. Higher H_2:CO ratio feedstock gas and/or the higher partial pressures lowered the FTS catalyst activity, apparently due a slower replenishment of the iron carbide surface than when a lower H_2:CO ratio gas was used. CO_2 selectivity decreased from 40% to 30% immediately after the gas ratio and pressure were changed, suggesting that water gas shift reaction can be inhibited due to the higher H_2 content in the gas (H_2:CO = 1.7); however, this may be due to changes of the surface composition. The data in Figure 12 also showed a new induction period after the reaction temperature changed from 230 to 270°C. A new stabilized conversion may be expected that is similar to the result given by Figure 11.

Conclusion

Promoted iron FTS catalysts showed a significant increase in CO conversion up to about K:Fe ratio of 5:100. An increase in K loading K/Fe = 0.0144 to 0.020 increased the alpha value from 0.71 to 0.85; a further increase to K/Fe = 0.050 increased the alpha value to 0.91. Catalysts with different potassium loadings showed different lengths of induction period, in which the FTS reaction showed increasing conversion from a low initial value to a peak value before declining to a stable activity level. Lower potassium loadings produced a higher maximum conversion and a shorter induction period. Although the induction period and the peak conversion values were dependent of the catalysts with higher K loading, the stabilized conversions and the stabilization period were independent of potassium content. All three of the higher level potassium promoted catalysts yielded a stabilized hydrogen conversion at about 400 hours of total on-stream time.

An increase in potassium content to K/Fe = 5:100 substantially enhanced the long-chain hydrocarbon yield with a concurrent decrease in the gas fraction (C_1-C_4) by nearly 50% and the gasoline(C_5-C_{11}) fraction by over 40%. Further increase in potassium iron ratio from K/Fe = 0.075 to 0.10 did not further enhance the production of the heavy fraction. Similar to the CO conversion profile, CO_2 selectivity also shows an induction period. The CO_2 selectivity for all three catalysts went through a rapid initial period of increase and then declined from its peak value of 42% to a stable level of 39%. Potassium had little effect on CO_2 selectivity for K/Fe ratios in the range of 5:100 to 10:100 for the potassium promoted catalysts. Methane selectivity declined gradually during the first 250 hours of run. All three higher potassium-containing catalysts yielded a stable methane selectivity of 1.5% after the first 250 hours of run. The surface structure and/or composition changes in the first 250 hours of reaction increases the formation of CO_2 but inhibits the formation of methane. All three potassium promoted catalysts yielded a stable CO_2 selectivity of 38-39% and methane yield of 1.5 mole %.

Increase in reaction temperature resulted in a new induction period and a new higher activity than that before the reaction temperature was increased. In addition to reaction temperature and pressure, H_2:CO ratio also had an important influence on FTS conversions. Increase of the H_2:CO ratio in the feedstock gas lowered the H_2 utilization rate. Higher H_2:CO ratio feedstock gas lowered the FTS catalyst activity presumably due to the lower iron carbide formation rate than that when a low H_2:CO ratio gas was used. CO_2 selectivity decreased immediately after the H_2:CO ratio increased, suggesting that water gas shift reaction be inhibited due to the higher H_2 content in the gas of H_2:CO ratio of 1.7.

Acknowledgment

Funding from the Department of Energy (DE-FC-26-98FT40308) and the Commonwealth of Kentucky are acknowledged.

References

1. R. B. Anderson, “The Fischer-Tropsch Synthesis,” Academic Press, New York, 1984.
2. R. J. O’Brien, L. Xu, R. L. Spicer and B. Davis, Symposium on Syngas Conversion to High Value Chemcials, 252-253, Presented at the 211th ACS Annual Meeting, New Orleans, March 24-29, (1996).
3. M. E. Dry, in Catalysis Science and Technology, Vol. 1, 1981, 159-255.
4. D. B. Bukur, D. Mukesh, and S. A. Patel, *Ind. Eng. Chem. Res.*, **29**, 1990, 194.
5. R. J. O’Brien, L. Xu, R. L. Spicer and B. H. Davis, *Energy & Fuels*, **10**, 1996, 921.
6. Z. E. Huang, Ran Liao Hua Xue Xue Bao, **18**, 1990, 143.
7. X. Z. Wang, Ran Liao Hua Xue Xue Bao, **18**, 1990, 137.
8. D. B. Bukur, L. Nowichi and X. Lang, *Energy & Fuels*, **9**, 1995, 620.
9. H. P. Bonzel, H. J. Kerbs, *Surface Science*, **109**, 1981, L527.
10. R. J. O'Brien, Y. Zhang, H. H. Hamdeh, B. H. Davis, "Mossbauer study of precipitated unpromoted iron Fischer-Tropsch catalyst," Preprints, 44(1) ACS, Division of Petroleum Chemistry, Mar. 21-25, Anaheim, CA, 1999, 100-102.
11. A. P. Raje, R. J. O’Brien and B. H. Davis, *J. Catal.*, **180**, 1998, 36.
12. M. E. Dry, *Appl. Catal. A: General*, **189**, 1999, 1850.
13. A J. Forney, W. P. Haynes, J. J. Elliot, Zarochak, *Am. Chem. Soc., Div. Fuel*, **20**, 1975, 3.
14. H. Arakawa and A. T. Bell, *I & EC Proc. Des. Dev.*, **22**, 97 (1983).
15. A. D. Ronald and A. T. Bell, *J. Catal*., **97**, 121 (1986).
16. R. B. Anderson, in P. H. Emmett (Editor), Catalysis, Vol. 4, Van Nostrand-Reinhold, New York, 1956, p. 29.
17. M. E. Dry, in Catalysis Science & Technology, Vol. 1, Springer, Berlin (1981) 191-192.

Table 1

Analyzers for FTS Products

Analyzer	Sample	GC Detector
HP Quad Series Micro GC	Gas	TCD
HP 5890 GC	Water	FID
HP 5790A GC	Oil + Light Wax	TCD
HP 5890 Series II Plus	Heavy Wax	FID

Table 2

Productivity and Selectivity for Potassium Promoted Catalysts

Catalyst	5.0%	7.5%	10.0%
Conversion			
CO	38	41	39
H_2	40	40	39
Syngas	39	40	39
Productivity			
Hydrocarbon, g/hr/g-Catalyst	0.28	0.29	0.28
Hydrocarbon, g/h/Nm^3-	145	153	148
Syngas	0.279	0.329	0.318
Methane, mol/h	0.181	0.213	0.210
Ethene, mol/h	0.032	0.040	0.040
Ethane, mol/h	0.196	0.023	0.225
Propene, mol/h	0.029	0.003	0.035
Propane, mol/h	0.113	0.144	0.124
Butene, mol/h	0.022	0.053	0.027
Butane, mol/h			
Water-Gas Shift			
K_p[a]	2.0	2.3	2.1
H_2:CO usage[b]	0.72	0.66	0.67
Selectivity			
CO_2, mol%[c]	38	40	39
CH_4, mol%[d]	1.43	1.44	1.61
Olefin ratio[e]			
C_2	85	85	84
C_3	87	87	87
C_4	84	87	82
Product Composition (Wt.%)			
C_1-C_4	30.06	11.64	14.74
C_5-C_{11}	31.28	15.43	21.64
C_{12}-C_{18}	27.41	55.29	18.71
C_{19+}	11.25	17.65	44.92

a. $K_p = [P_{H_2} P_{CO_2}]/[P_{CO} P_{H_2O}]$

b. $Usage = r_{H_2}/r_{CO}$

c. CO_2 mole% = CO_2 formed/CO converted.

d. CH_4 mole% = CH_4/all hydrocarbons.

e. Olefin ratio = olefin/[olefin + paraffin].

Figure 1. Potassium Effect on Relative Activity (draw from data in reference17)

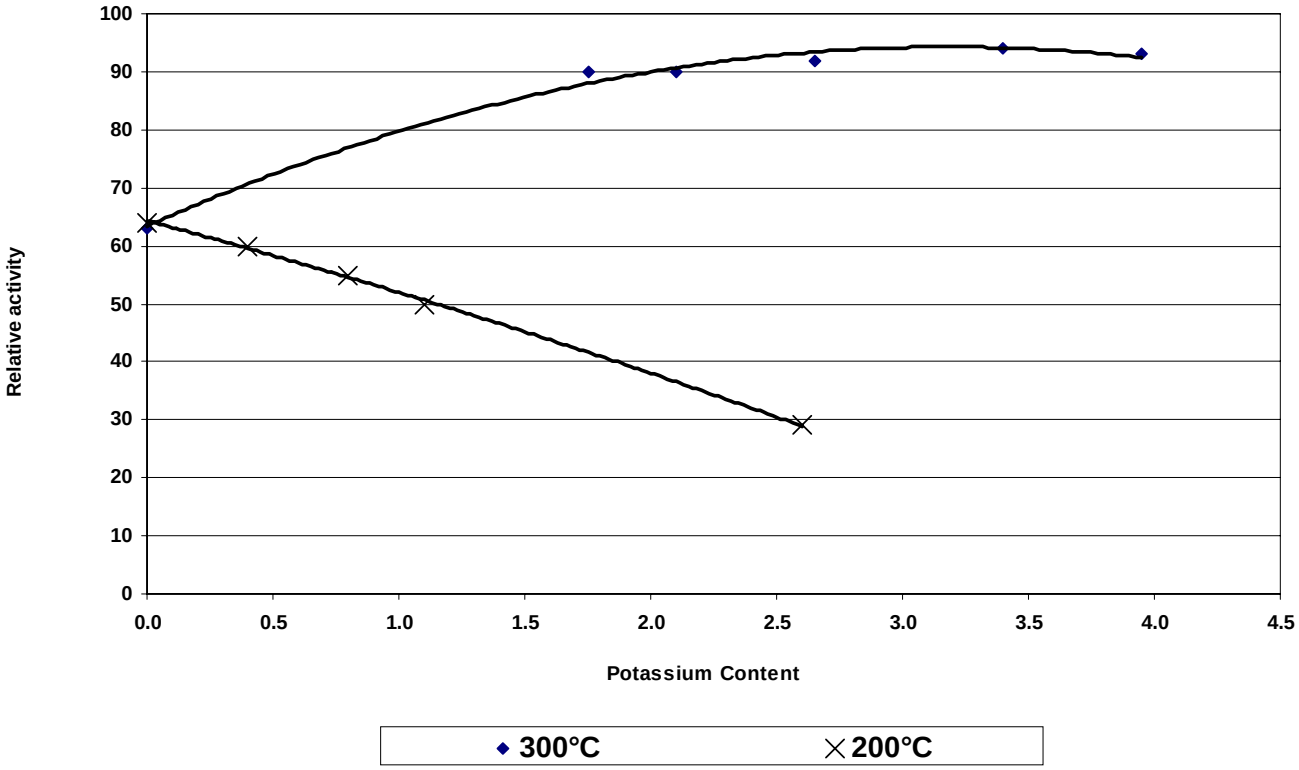

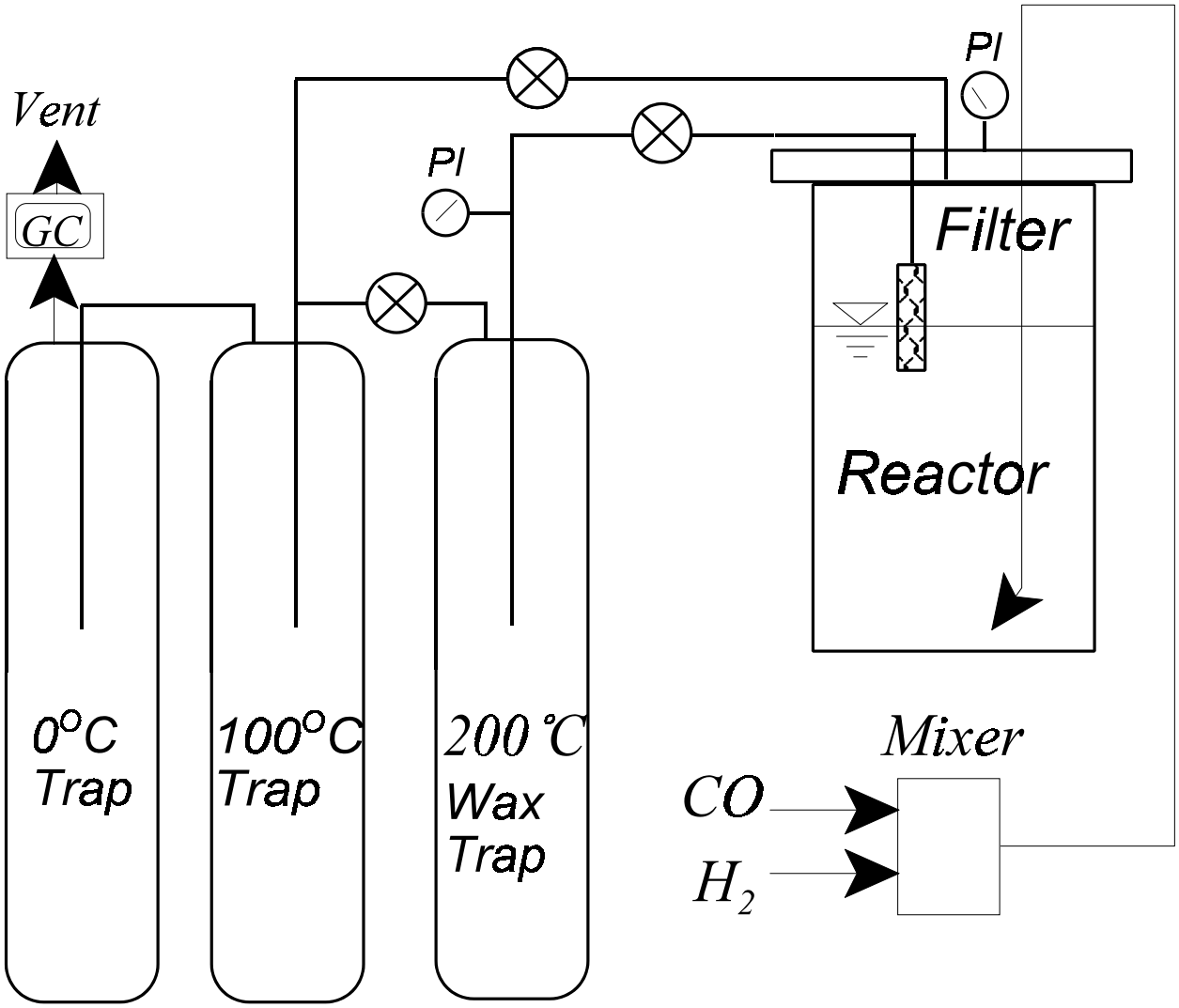

Figure 2. Schematic of the CSTR reactor system.

Figure 3. Potassium Effect on Fe Catalyst Activity
(230°C, 1.3MPa, H_2/CO=0.7 and 3.1 NL/gFe/hr)

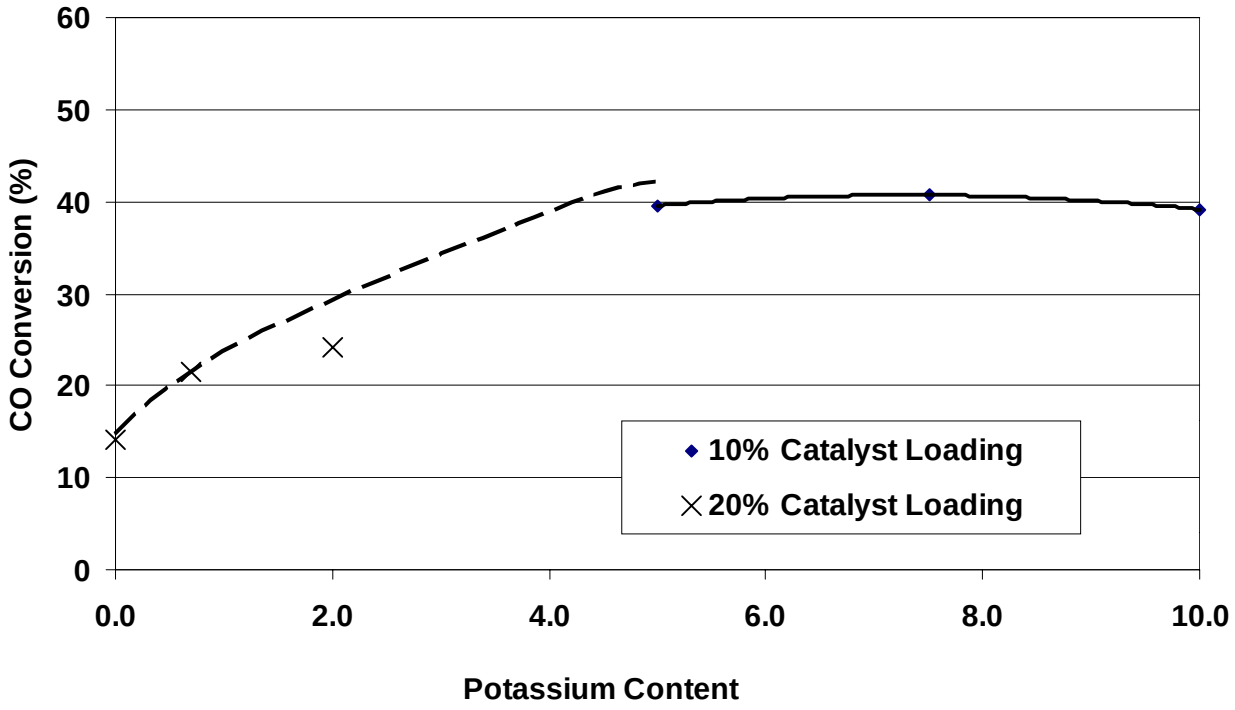

Figure 4. Potassium Effect on Alpha Values

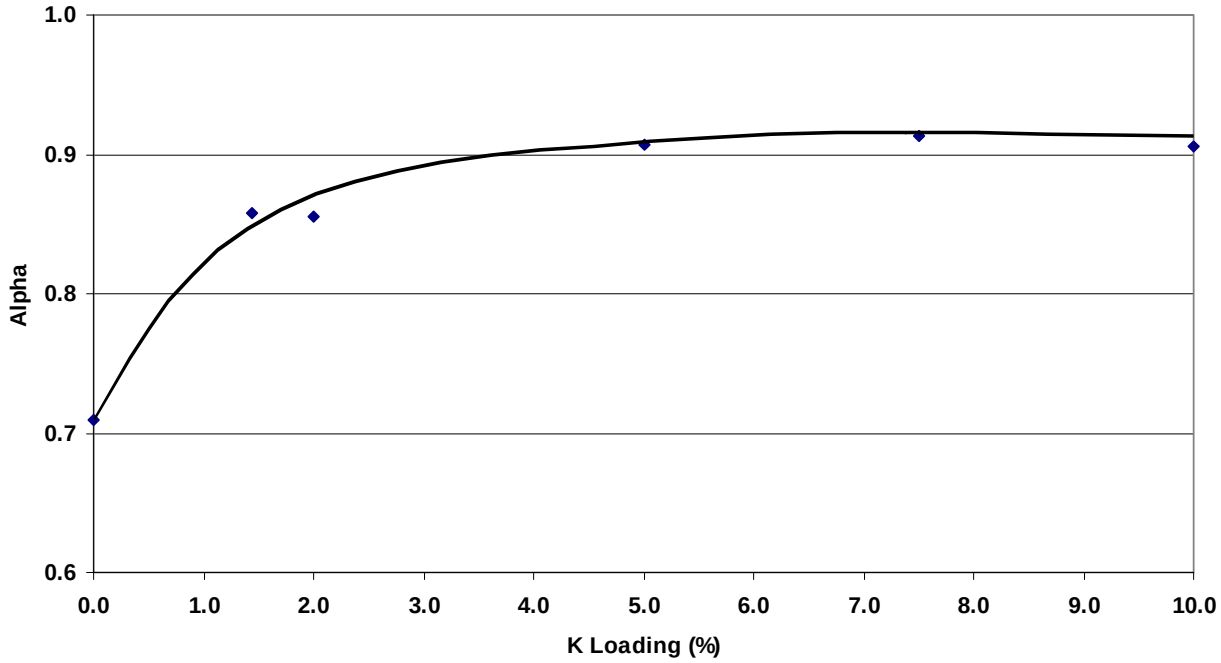

Figure 5. Potassium Effect on H_2 Conversion

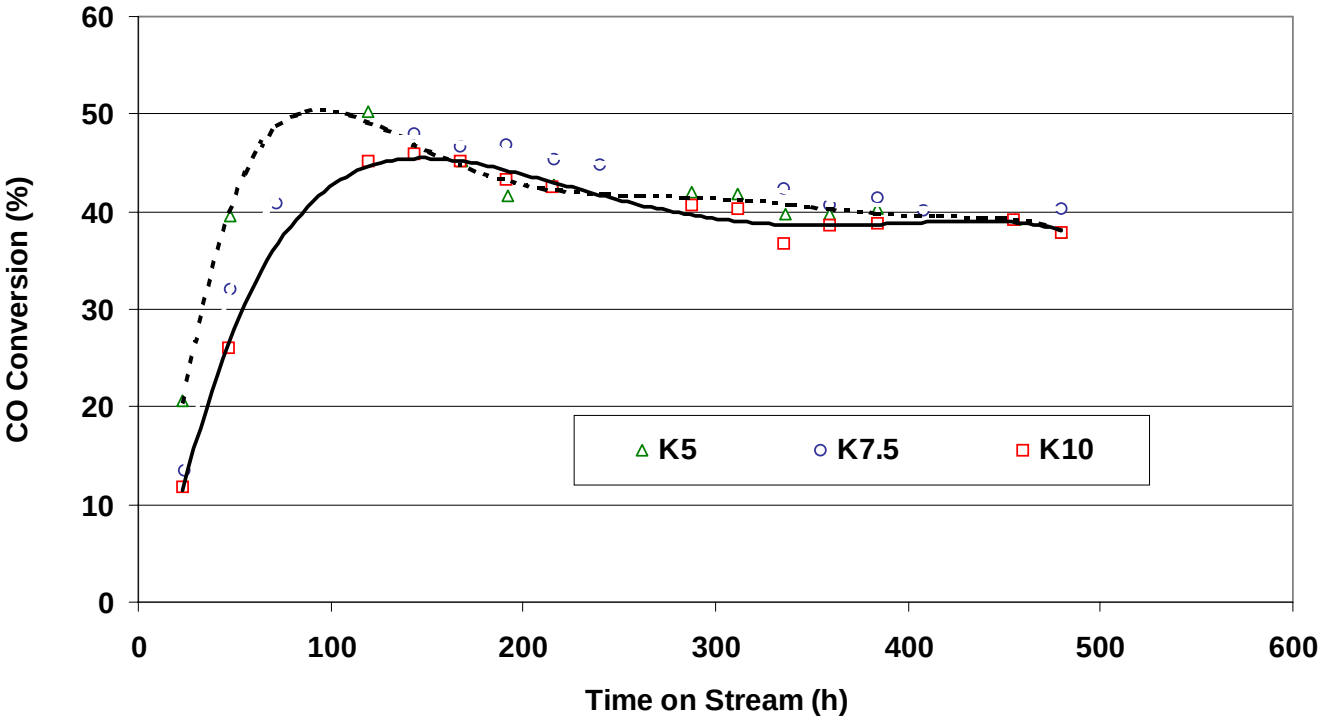

Figure 6. Potassium Effect on CO Conversion

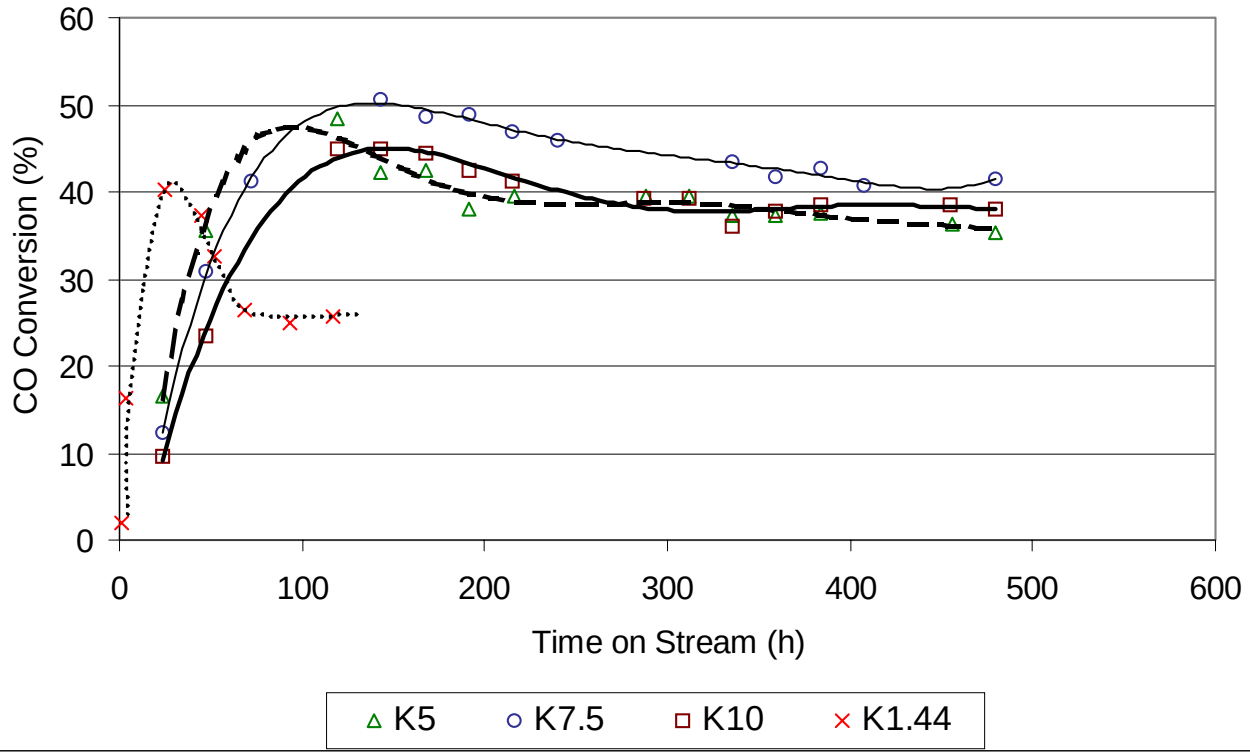

Figure 7. Olefin Ratio (C_2)

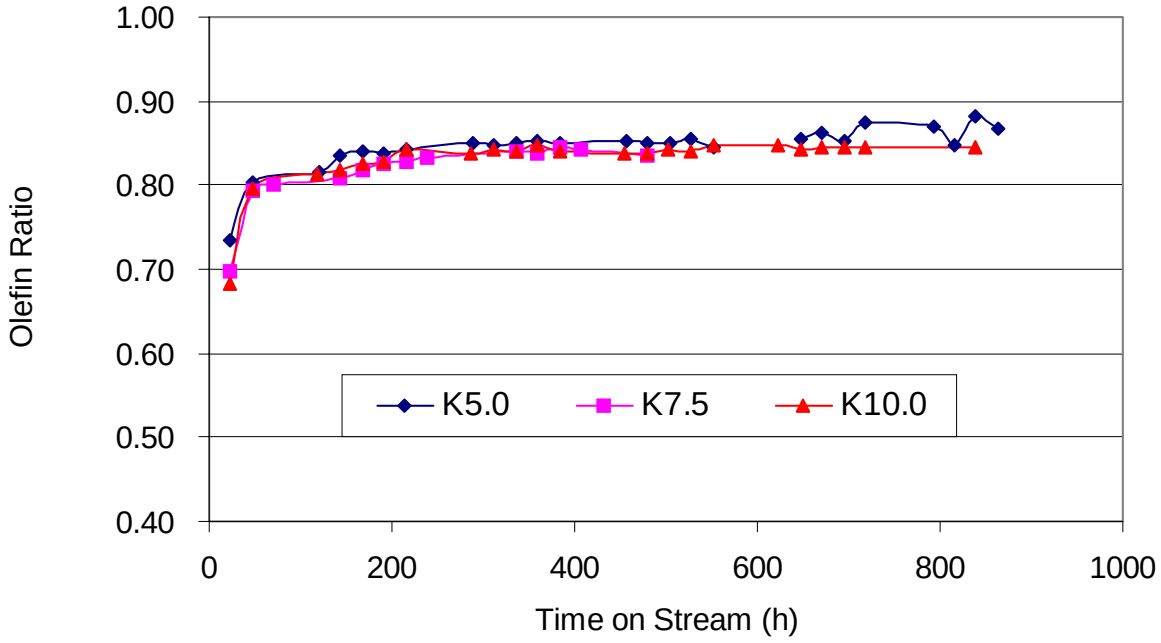

Figure 8. Olefin Ratio (C_4)

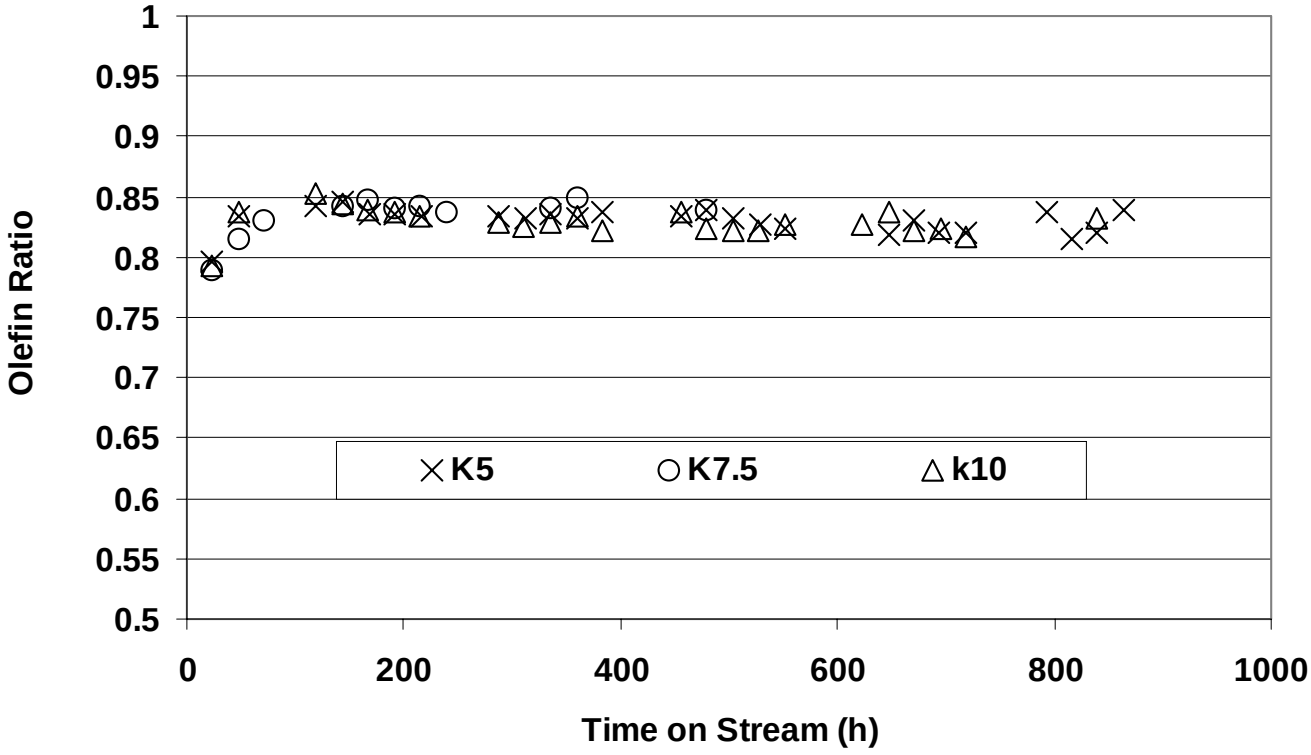

Figure 9. Potassium Effect on CO_2 Selectivity

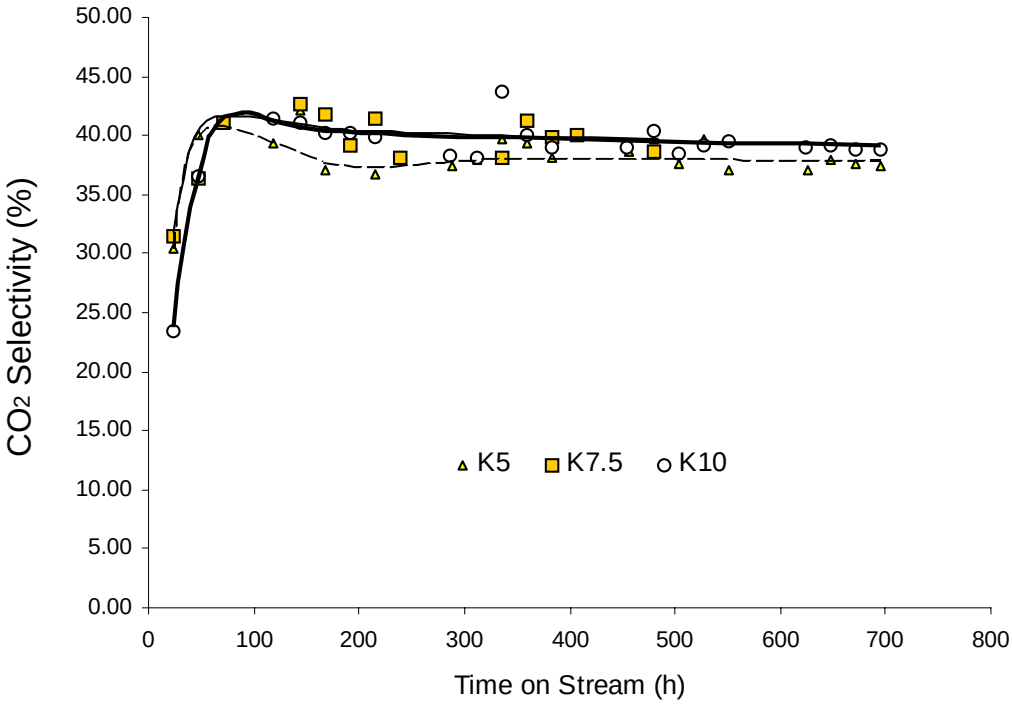

Figure 10. Potassium Effect on CH_4 Selectivity

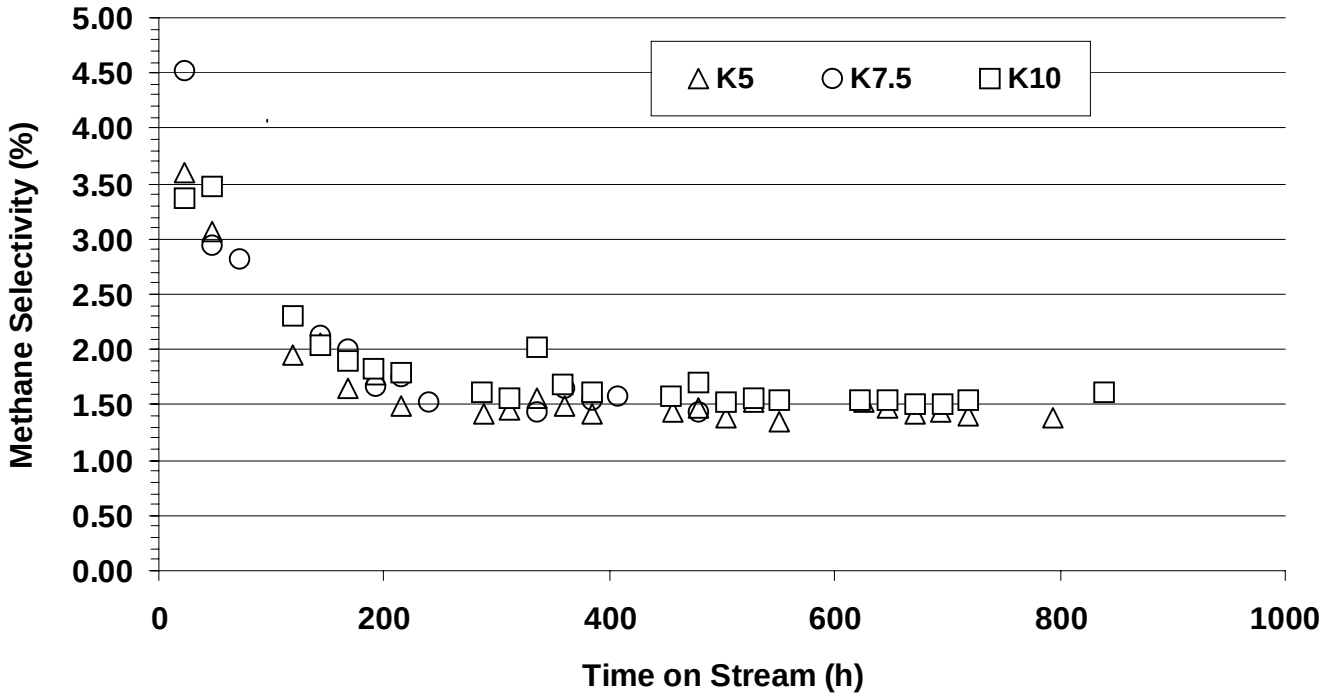

Figure 11. Effect of Temperature on FTS Conversions

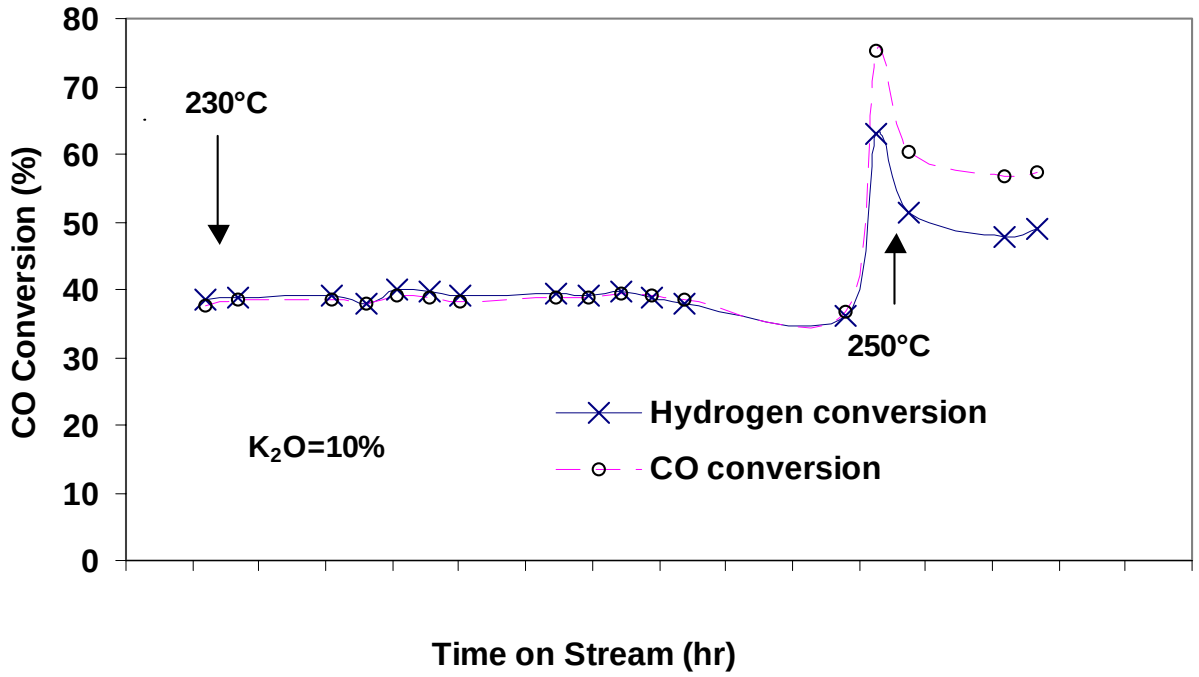

Figure 12. Effect of Gas Composition and Temperature on FTS Conversions

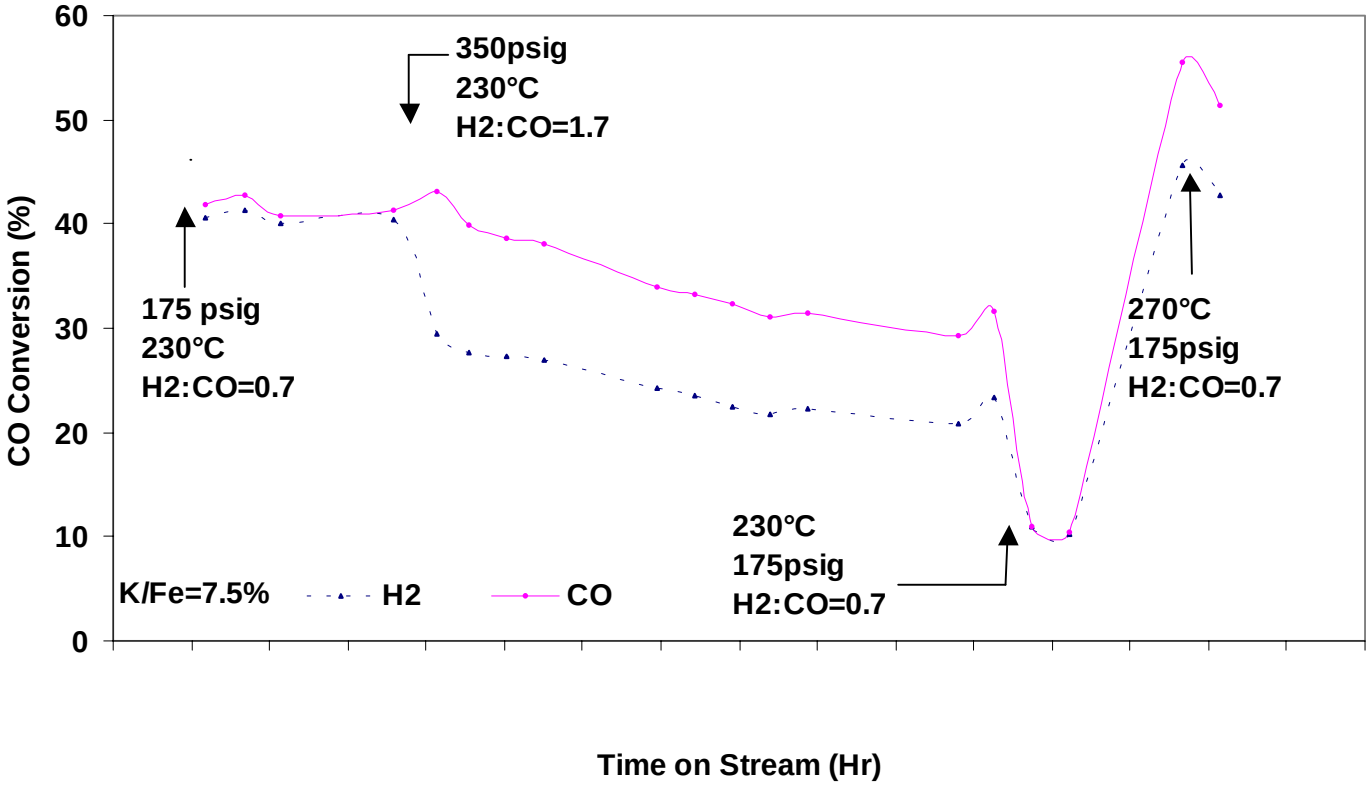

G. Study of deactivation of iron based Fischer-Tropsch synthesis catalysts

Abstract

Attempts to correlate the catalytic activity of unpromoted and potassium-promoted iron Fischer-Tropsch catalysts to their bulk phase compositions as determined using Mössbauer spectroscopy are reported. The CO-conversion of both catalysts declined with time-on-stream. Samples of the unmpromoted catalyst were primarily Fe_5C_2 and this phase gradually decreased to become essentially pure Fe_3O_4 after 450 hours time-on-stream. In contrast, the potassium-promoted catalyst was primarily $Fe_{2+}C$ after pretreatment and remained this phase during 400 hours of synthesis. Thus, both Fe_5C_2 and $Fe_{2+}C$ phases are about equally active for Fischer-Tropsch synthesis but exhibit much different stability during the course of the synthesis reaction.

Introduction

Iron-based Fischer-Tropsch (FT) catalysts undergo a series of phase transformations during activation and use (1). Activation with carbon monoxide or syngas typically results in the conversion of Fe_2O_3 to Fe_3O_4 and ultimately to one or more iron carbides (2). During FT synthesis, iron carbides can be oxidized to Fe_3O_4 if the H_2O/H_2 or CO_2/CO ratios are high enough (1). There has been considerable debate about the active phase of the FT synthesis. Some studies have indicated an active oxide species (3) while most have supported a carbide species (2,4). Mössbauer spectroscopy has proven to be an effective technique for the analysis of iron-based FT catalysts. *In situ* Mössbauer studies have been reported (5,6); however, these studies have been performed at low pressure and low conversions. Studies performed at industrially relevant conditions have generally involved removing the catalyst from the reactor followed by passivation (7) which, if not performed properly, will oxidize the catalyst (4).

The early work directed toward defining the role of different carbide species that are present during CO hydrogenation have been reviewed (8,9). It has been suggested that the ϵ and

ϵ'-carbide (Fe_2C and $Fe_{2.2}C$, respectively) are responsible for catalysis following CO dissociation (10). Häag carbide formation has been considered to decrease the activity of the catalyst (6). On the other hand, it has been claimed that the deactivation of iron catalysts in FT synthesis is associated with the transformation of the highly active Hägg carbide to a less active epsilon-carbide and to the formation of a highly ordered graphite on the surface of the catalyst (11).

Tau et al. (12) utilized an in-situ Mössbauer cell to follow changes in a 10% Fe-Sl_2O_3 (Alon-C) and 10% Fe-SiO_2 (Cab-O-Sil catalysts. Using Niemantsverdret's nomenclature (13), the progressive carburization in 10%CO/H_2 at 285°C, following reduction in H_2 at 450°C, produced the following progression: Fe → Fe_xC → $\varkappa$-$Fe_{2.5}C$ → ϵ'-$Fe_{2.2}C$. The authors cautioned that this sequence was not followed for an unsupported iron catalyst (13) nor for a supported catalyst that was similar to the one they used (14). Their composition was not consistent with the usual order of stability of the carbides where the ϵ'-$Fe_{2.2}C$ form, when heated, loses carbon to form the $\varkappa$-form and then the θ-form. After 30 min time the bulk of the iron is about 74% carburized to a mixture of $\varkappa$-$Fe_{2.5}C$ and ϵ'-$Fe_{2.2}C$ (15). They reported that at longer synthesis times, the ϵ'-$Fe_{2.2}C$ form predominates.

Gatte and Phillips (16) evaluated the modeling routine used to obtain the iron phases from Mössbauer spectra and concluded that this is fraught with difficulties. In spite of this, they conclude that there is ample evidence to support the conclusion that at least one phase of octahedral carbide, normally called ϵ' carbide, forms during Fischer-Tropsch synthesis; however, they cautioned that the spectra of ϵ'-carbide probably consists of at least two sextuples.

Herein are reported Mössbauer results obtained for an unpromoted and potassium promoted precipitated iron catalyst that was activated and used for synthesis in a slurry phase, continuous stirred tank reactor at high conversion and under industrially relevant conditions. Strict measures were observed to prevent oxidation of the catalyst samples. The results reported

here compare the iron phases present initially and as the two iron catalysts are utilized for FT synthesis.

Experimental

Catalysts was prepared by a previously described procedure (2). An aqueous solution of $Fe(NO_3)_3 \cdot 9H_2O$ (Johnson Matthey Co., 98+% metals basis, 1 M) at a feeding rate of 157 cm^3/min was precipitated with concentrated NH_4OH (VW, reagent grade, 28-30 wt.%) of 71 cm^3/min. The pH of the slurry was 9.3 and the residence time in the reactor was 300 s. This resulted in a total slurry volume of 34.4 liters. After the initial filtration, the filtrate was washed by re-slurring the filtrate in the amount of distilled, de-ionized water required to bring the total volume of the re-slurried material back to 34.4 liters for each of the two washings. Each of the filtrations was done with rotary drum filters. The washed filter cake was dried in air at 373 K overnight. The dried catalyst was ground using mortar and pastel to particles of ~0.15 mm and then treated in stagnant dry air at 623 K for 4 h. A comparable promoted catalyst was obtained by impregnating the calcined material with sufficient potassium nitrate solution to yield a finished catalyst with Fe:K = 100:0.71.

Activation and FTS Reaction

All FTS runs were conducted in a 1 L continuous stirred tank reactor (CSTR). The catalyst precursor (64.44 g) was suspended in C-30 oil (Ethylflow, a decene trimer obtained from the Ethyl Corp.; 290 g) and it was pretreated with CO at 543 K at 1.22 MPa for 24 h. The CO flow (58.7 sl/h g-Fe) was started at ambient conditions (298 K and 0.1 MPa), the pressure was raised to 1.22 MPa, and the reactor was ramped to 543 K at 2 K/min and maintained at this temperature for 24 h. Following the activation treatment, the reactor was brought to reactions conditions, which were 543 K, 1.22 MPa , H_2/CO ratio of 0.68, and a total flow ($CO+H_2$) rate of 3.1 SL/h g-Fe.

Reaction products were analyzed using several chromatographs. Gas products were analyzed using a Hewlett-Packard Quad-Series Refinery Gas Analyzer Micro Gas Chromatograph (QRGA). The analysis of the aqueous phase collected beyond the reactor used a Hewlett-Packard 5790 GC with a thermal conductivity detector and a Porapak Q column. Oil and wax were combined and analyzed with a Hewlett-Packard 5890 GC with a flame ionization detector and a 60 m DB-5 column. The reactor wax was analyzed on a Hewlett-Packard 5890 High Temperature GC with an flame ionization detector and a 30 m alumina clad HT-5 column.

Catalyst samples were extracted from the autoclave during reaction using a dip tube blanketed with an inert gas. All subsequent handling of the used catalysts was carried out under an inert gas within a glove box. A total of 20 samples were withdrawn from the reactor during the 452 hour run for the unpromoted sample and 17 samples during 400 hours for the potassium promoted catalyst.

Mössbauer Spectroscopy Measurement

The Mössbauer experiments used a constant acceleration spectrometer. The radioactive source comprised 50-100 mCi of ^{57}Co in a Pb matrix. The samples in the reactor wax form were loaded into Plexiglass compression holders presenting a thin sample to the beam. All spectra were analyzed by a least-squares fitting procedure, which attempts to describe the spectra as a series of Lorentzian peaks corresponding to the Mossbauer spectra of known Fe compounds. The fraction of the Fe atoms in each of the known phases is reported as the contributions of each of these known phases to the experimental spectrum.

Results

Unpromoted Iron Catalyst

Table 1 contains a description of the unpromoted iron samples that were used and the Mössbauer data showing the catalyst composition as a function of time-on-stream. Samples 1, 3,

10, and 20 are the used samples after various FTS reaction times. The Fe_5C_2 phase was established from the measured hyperfine parameters, although the measured fraction ration (Fe_I:Fe_{II}:Fe_{III}) did not conform to the expected ratio of (2:2:1). In large-crystal samples of the carbide, the ratio frequently differs from (2:2:1) due to the variable concentration of carbide carbon. Here, however, the deviation is more profound and indicates that crystallization is not complete. In spite of this, Fe_5C_2 is the only iron carbide that can be discerned from the Mössbauer measurements.

Table 1. Mössbauer structural analysis results for unpromoted iron sample

Sample	1	2	3	4
FTS reaction time (hr)	0	23	168	452
Fe_5C_2 (atom %)	94	83	42	0
Fe_3O_4 (atom %)	6	17	58	100

Unpromoted iron catalyst samples for Mössbauer spectroscopy were withdrawn immediately after activation and at 23 h, 168 h and 453 h of FT synthesis. The distribution of iron in the catalyst after activation with carbon monoxide was 94 % χ-Fe_5C_2 and 6 % Fe_3O_4. Exposure to syngas initiated oxidation of the χ-Fe_5C_2 to Fe_3O_4. After 23 hours of FT synthesis, 83 % of the iron was present as χ-Fe_5C_2 and the balance was Fe_3O_4. The amount of iron present as χ-Fe_5C_2 had decreased to 18 % after 168 hours of FT synthesis. The only detectable phase after 453 hours of FT synthesis was Fe_3O_4.

Syngas conversion and carbide-phase versus time-on-stream for the unpromoted iron catalyst are shown in Figure 1. Syngas conversion after 24 hours of FT synthesis was above 84% as is in excellent agreement with a similar catalyst whose results were reported earlier (17). The catalyst activity declined steadily throughout the run with an average rate of deactivation of

0.16 % h^{-1} and when the conversion is corrected for catalyst withdrawal the decline is even more rapid.

Potassium Promoted Iron Catalyst

The Mössbauer spectrum of the potassium-promoted sample taken at the earliest time-on-stream is more complex than the others and indicates that the sample contains 42 atomic% of a superparamagnetic phase (Figure 2). The Mössbauer line widths are relatively sharp for the spectra recorded for the potassium-promoted samples that were withdrawn later in the run (Figure 3). The data for five samples are summarized in Table 2. If this portion of the sample follows the pattern of another sample; the low temperature spectrum, still to be obtained, will show that the superparamagnetic contribution is due to both Fe_3O_4 and iron carbide phases. The data for sample 3 suggest that the carbiding of the promoted iron catalyst is incomplete at the end of 24 hours and continues during the early stages of the synthesis. However, after about 100 hours-on-stream, the iron is present essentially as carbide phases. Thus, the latter four samples could be fitted to four sextets (sub-spectra), as shown by the deconvolution curves. For sample 3, an additional collapsing spectrum, which originates from the superparamagnetic fine clusters, is necessary. It is reasonable to assign the major sextet (HMF 168-170 kG) to ϵ-Fe_2C. The minor sextet (HMF 217-221 kG) is assigned to a phase with an excess of Fe and this phase may be designated as ϵ-$Fe_{2+}C$.

Table 2. Mössbauer structural analysis for potassium-promoted iron samples.

Sample	Time-on-stream, h	HNF[a]	Atomic Aeral Fraction, %	Phase
3	48	491	6	A-site Fe_3O_4
		457	9	B-site Fe_3O_4
		219	6	$Fe_{2+}C$
		170	36	$Fe_{2+}C$
		Unknown	42	Superparamagnetic
5	97	490	3	A-site Fe_3O_4
		453	5	B-site Fe_3O_4
		228	6	$Fe_{2+}C$
		168	86	$Fe_{2+}C$
8	167	491	1	A-site Fe_3O_4
		457	2	B-site Fe_3O_4
		219	3	$Fe_{2+}C$
		170	93	$Fe_{2+}C$
11	259	493	2	A-site Fe_3O_4
		454	3	B-site Fe_3O_4
		217	2	$Fe_{2+}C$
		168	93	$Fe_{2+}C$
16	394	490	2	A-site Fe_3O_4
		453	2	B-site Fe_3O_4
		221	3	$Fe_{2+}C$
		168	93	$Fe_{2+}C$

a. HNF = hyperfine magnetic field.

The conversion with time-on-stream and the fraction of the iron present as the carbide phase are shown in Figure 4. The CO conversion is high for both the promoted and unpromoted iron catalyst at the early time-on-stream. For both catalysts, the activity remains nearly constant for a brief time and then begins to decline to a low (<20%) level at later times-on-stream. While there is uncertainty about the amount of catalyst withdrawn for each sample and the impact that this has on the contact times, and therefore the CO conversion, it appears that the CO conversion for the promoted iron catalyst declines slightly more rapidly than for the unpromoted sample. The relative activity decline for these two catalysts is similar to the ones reported earlier (17).

Discussion

Based on data generated from several catalysts, a model of the working FT catalyst was developed. In this model, the initial catalyst was essentially comprised of a mixture of iron carbides. As the reaction progressed, the carbide fraction decreased to attain a value of about 30-40% (18). During this phase change, the conversion did not decrease appreciably. To account for the nearly constant activity while the iron phases changed, a model was proposed. This model had the core of each catalyst particle, initially consisting of an iron carbide phase, oxidizing to form Fe_3O_4 and an outer layer that remains as a carbide form; thus, the surface of the catalyst remained essentially the carbide form while the ratio of oxide/carbide increased as the core consisting of Fe_3O_4 expanded to approach a "steady state" carbide/oxide ratio. The constant conversion while the bulk carbide/oxide ratio changed seems to dictate that the surface composition remain essentially constant throughout the run.

The results with the unpromoted iron catalyst do not agree with this model. Instead, it appears that the catalyst particles convert from the carbide to the oxide form in parallel with the decline in conversion. Thus, it appears that a steady-state surface carbide phase/core Fe_3O_4 phase is not formed for the unpromoted iron catalyst. One explanation to account for this is that the rate of iron carbide oxidation is dependent upon the particle size for the unpromoted catalyst.

The results for the potassium-promoted iron catalyst provide a third model for the iron Fischer-Tropsch catalyst as it is used for longer times-on-stream. Initially, the catalyst activity is high and the catalyst is incompletely carbided. As the time-on-stream increases with the unpromoted catalyst, it is oxidized to the Fe_3O_4 phase in parallel with the decline in CO conversion. On the other hand, the potassium-promoted iron catalyst continues to form the iron carbide phase during the initial time-on-stream and the material remains as the carbide phase even though the activity declines with time-on-stream much like the unpromoted iron catalyst.

These results make it clear that relating the catalyst composition to the catalytic activity of an iron Fischer-Tropsch synthesis catalyst will be a demanding task. It appears that the carbide phase is more active than the oxide phase. Furthermore, the data for the promoted and unpromoted show that the initial activity of the χ-Fe_5C_2 phase is as great as the ϵ or ϵ'-carbide (Fe_2C to $Fe_{2.2}C$) phases. The present data do not allow us to decide whether it is the presence of potassium or the stability of the iron carbide phases that allows the ϵ or ϵ'-carbide (Fe_2C to $Fe_{2.2}C$) phases to remain as the conversion declines to a low level while the χ-Fe_5C_2 oxidizes as the conversion decreases.

Acknowledgment

This work was supported by U.S. DOE contract number DE-FC26-98FT40308 and the Commonwealth of Kentucky.

References

1. Dry, M. E. In Catalysis-Science and Technology; Anderson, J. R., Boudart, M. Eds.; Springer-Verlag: New York, 1981; Vol. 1, pp 196-198.
2. O'Brien, R. J., Xu, L., Spicer, R. L., Davis, B. H., Energy & Fuels, 10, 921 (1996).
3. Reymond, J. P., Mériaudeau, P., Teichner, S. J., J. Catal., 75, 39 (1982).
4. Shroff, M. D., Kalakkad, D. S., Coulter, K. E., Köhler, S. D., Harrington, M. S., Jackson, N. B., Sault, A. G., Datye, A., J. Catal., 156, 185 (1995).
5. Berry, F. J., Smith, M. R., J. Chem. Soc. Faraday Trans., 85, 467 (1989).
6. Raupp, G. B., Delgass, W. N., J. Catal., 58, 361, (1979).
7. Huang, C. S., Ganguly, B., Huffman, G. P., Huggins, F. E., Davis, B. H., Fuel Sci. Technol. Int., 11, 1289 (1993).
8. Guczi, L., Catal. Rev.-Sci. Eng., 23, 329 (1981).

9. Le Caër, G., Dubois, J. M., Pijolat, M., Perrichon, V., Bussiere, P. J. Phys. Chem., 86, 4799 (1982).

10. Amelse, J. A., Butt, J. B., Schwartz, L. H., J. Phys. Chem., 82, 558 (1978).

11. Eliason, S. A. and C. H. Bartholomew, "Catalyst Deactivation 1997," (C. H. Bartholomew and G. A. Fuentes, Eds.) Elsevier, 1997, 517-526.

12. Tau, L.-M., Borcar, S., Bianchi, D., Bennett, C. O. J. Catal., 87, 36 (1984).

13. Niemantsverdriet, J. W., van der Kraan, A. M., van Dijk, W. L. J. Phys. Chem., 84, 3363 (1980).

14. Nahon, N., Thesis, Lyon, 1979.

15. Bianchi, D., Borcar, S., Teule-Gay, F., Bennett; C. O. J. Catal., 82, 442 (1983).

16. Gatte, R. R., Phillips, J. J. Catal., 104, 365 (1987).

17. A. Raje, R. J. O'Brien, L. Xu and B. H. Davis, Catalyst Deactivation 1997 (Studies in Surface Science Catalysis), (C. H. Bartholomew and G. A. Fuentes, eds.) 111, 527 (1997).

18. “Technology Development for Iron Fischer-Tropsch Catalysis,” DOE contract #DE-AC22-94PC94055, Final Report, March, 1999.

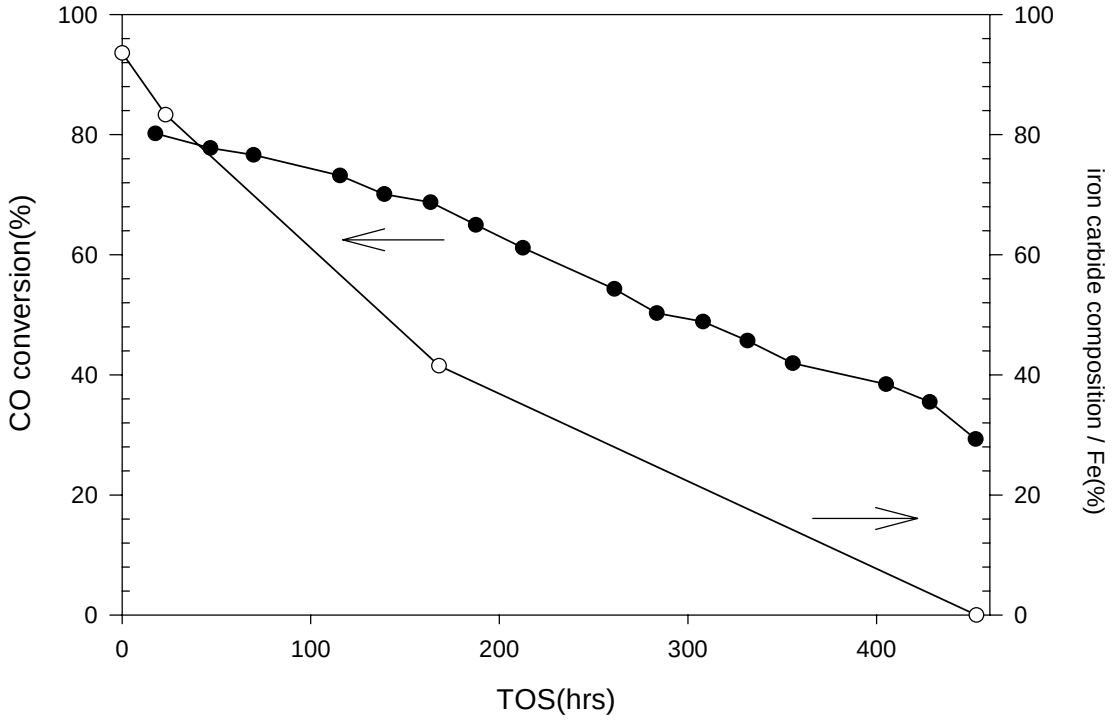

Figure 1. The changes in CO conversion (!) and total iron carbide phases (") for a precipitated, unpromoted iron catalyst, activated in CO, during synthesis.

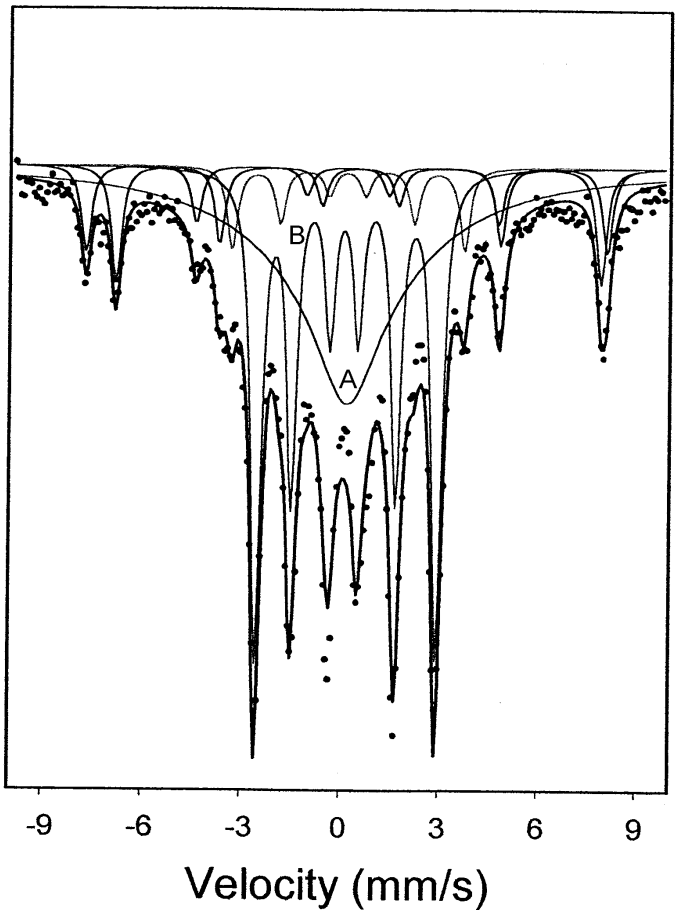

Figure 2. Mössbauer data (experimental points) and fitted spectra (A, superparamagnetic contribution, ϵ-Fe_2C).

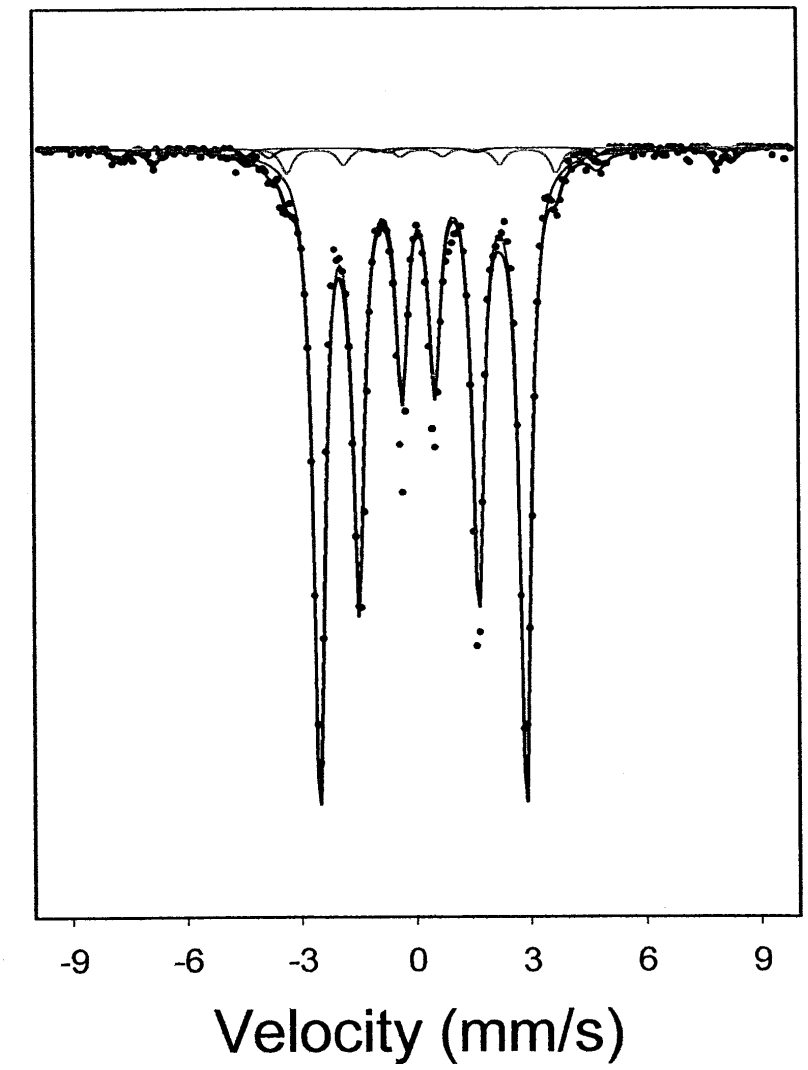

Figure 3. Mössbauer data (experimental points) and fitted spectra (see text for identification).

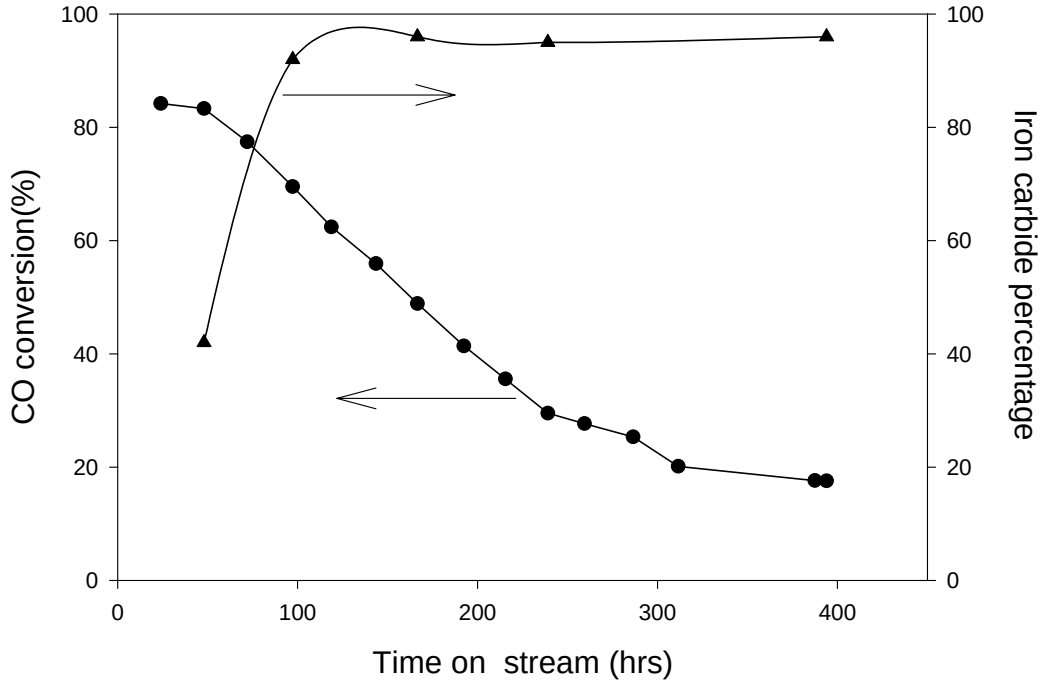

Figure 4. CO conversion and $Fe_{2+}C$ percentage as a function of time-on-stream.

H. Deactivation and Regeneration of Alkali Metal Promoted Iron Fischer-Tropsch Synthesis Catalysts

Abstract

Iron Fischer-Tropsch synthesis (FTS) catalysts promoted with potassium or beryllium showed a superior deactivation property. Potassium promoted iron FTS catalyst showed a low deactivation rate of 0.59% CO conversion/week after passing an initial conditioning period of 300 hours. Beryllium promoted iron catalyst produced an even more stable activity than potassium. A deactivation rate as low as 0.43% CO conversion/week was obtained from beryllium promoted catalyst. Higher temperature generated a shorter conditioning period for potassium promoted catalyst. The FTS activity began to decrease when the bulk phase of the catalyst changed from 100% carbide to iron oxides. Although the initial activity changed rapidly, little change occurred in the bulk phase of the catalyst. For potassium promoted catalyst, FTS activity, CO_2 selectivity, hydrocarbon productivity and water gas shift activity showed the same conditioning period of 300 hours of time on stream after passing a peak value at about 120 hours of reaction time. A higher water gas shift activity, higher CO_2 and CH_4 selectivity by beryllium promoted catalyst than those by potassium were also found in an FTS process. Beryllium promoted catalyst also showed a superior regenerability when either H_2 or CO was utilized. When rejuvenated with CO a better activity recovery was achieved than that with H_2.

Introduction

Hydrocarbons of various chain length can be produced from CO and H_2 in Fischer-Tropsch synthesis process, which can be expressed as

$$(2n+1)\ H_2 + n\ CO \rightarrow C_nH_{2n}+2 + n\ H_2O \qquad [1]$$

When an iron catalyst is used for FTS reactions, the water gas shift (WGS) reaction can also occur. This reaction consumes CO and water formed by the FTS reaction and produces additional hydrogen and carbon dioxide.

$$H_2O + CO \rightarrow CO_2 + H_2 \quad [2]$$

Potassium has long been used as a promoter for iron catalysts. It provides an increase in the alkene yield and a decrease in the CH_4 selectivity (1,2,3). Potassium can also increase the catalytic activity for FTS and water-gas shift (WGS) reactions (4). The influence of potassium on iron catalysts has been investigated by other researchers (e.g., 5-8). It is believed that alkali metals have significant effects on both FTS activity and product selectivity. As the most effective promoter, potassium salts are widely used in iron catalysts; however, the readiness to form an alkali compound with common catalyst supports, or structural promoters such as alumina or silica, complicates the situation. Although potassium enhanced the FTS activity and heavy fraction product distribution, high potassium loadings may cover too large of a fraction of the surface of the iron catalyst, resulting in a limited promotion effect or even a decrease in FTS conversions. Bonzel and Kerbs (9) claimed that potassium lowered the methane formation rate and increased the carbon deposition rate. It was also found that the deposited carbon was covered by potassium compounds rather than carbon sitting on top of the promoter. Huang et al. (6) studied the potassium promoted iron catalysts with XPS and found that two-thirds of the catalyst surface was covered by K_2O and SiO_2. Wang, et al. (7) applied the temperature programmed reduction (TPR) technique to study the effects of potassium. They suggested that potassium facilitates the desorption process of carbon monoxide and strengthens the Fe-C bond. Thus, potassium enhanced the selectivity of long-chain products; i.e., it resulted in a high alpha product distribution. Copper, as a secondary promoter, can facilitate the activation process.

Copper can therefore minimize the sintering of iron catalysts by lowering the reduction temperature (3).

Experimental

Catalyst

Two iron FTS catalysts with an atomic ratio of K:Fe=10:100 and Be:Fe=1.44:100 were prepared and utilized in this study. Precipitated iron catalysts were prepared using $Fe(NO_3)_3 \cdot 9H_2O$ tetraethyl orthosilicate, $Cu(NO_3)_2 \cdot 3H_2O$, and K_2CO_3 or $Be(NO_3)_2$ was used as the promoter precursor. Details of the preparation procedure was given elsewhere (5). The iron catalyst needs to be activated with H_2, CO or synthesis gas. Activation procedures can have a significant effect on the selectivity and activity of iron catalyst (8,10). It was reported that catalysts activated with CO yielded higher amounts of long-chain hydrocarbons than catalysts activated with syngas or with H_2. In addition, activation conditions may also influence the performance of the iron catalyst during the course of the run. In this study, the potassium promoted iron catalysts were pretreated with CO at 270°C and 1.2 MPa for 24 hours. The CO flowed through a catalyst slurry in 300 ml of Ethylflow oil. The reduction of Fe_2O_3 with CO occurs in two steps:

$$3Fe_2O_3 + CO \rightarrow 2Fe_3O_4 + CO_2 \quad [3]$$

$$5Fe_3O_4 + 32CO \rightarrow 3Fe_5C_2 + 26CO_2 \quad [4]$$

Reactor System

A one-liter continuous stirred tank reactor (CSTR) was used in this study. A sintered metal filter was installed to remove the wax samples from the catalyst slurry. The wax sample was extracted through the internal filter and collected in the hot trap held at 200°C. A warm trap (100°C) and cold trap (0°C) were used to collect light wax and the water plus oil samples, respectively, by condensing from the vapor phase that was continuously withdrawn from the

reactor vapor space. CO and H_2 mass flow controllers were used to provide a simulated synthesis gas of the desired composition. After the catalysts was activated with CO, syngas was introduced into the CSTR with a stirrer speed of 750 rpm. Reaction conditions were 1.2 Mpa, H_2/CO = 0.67, 230°C for potassium promoted catalyst and 270˚C for beryllium promoted catalyst.

Product Sampling and Analysis

Daily gas, water, oil, light and heavy wax samples were collected and analyzed. A heavy wax sample was taken from the 200°C hot trap connected to the filter. The vapor phase above the slurry passed continuously to the warm (100°C) and the cold (0°C) traps outside the reactor. The light wax and water mixture was collected from the warm trap and an oil plus water sample from the cold trap. Tail gas from the cold trap was analyzed with an online HP Quad Series Micro GC, providing molar compositions of C_1-C_7 olefins and paraffins as well as for H_2, CO and CO_2. Hydrogen and carbon monoxide conversions were calculated based on the gas product GC analysis results and the gas flow measured at reactor outlet. The oil and light wax samples were mixed before analysis with an HP 5790A GC. The heavy wax was analyzed with an HP5890 Series II Plus GC while the water sample was analyzed using an HP5890 GC.

Results and Discussion

Activation, conditioning and deactivation of potassium promoted catalyst

In this study, a potassium promoted iron FTS catalysts with an atomic ratio of Fe:K=100:10 was used. Reaction was carried out at 230˚C, 1.2 MPa at a space velocity of 3.1 sl/h/g-iron. The results (Figure 1) show that a conditioning period, in which CO conversion increased from below 10% to a peak value of 45% at 120 hours of time on stream and then gradually decreased to a stable level at 300 hours of reaction time. As indicated in the figure, a deactivation rate of 0.827% per day was observed from the peak CO conversion during the

conditioning period. Then a very low deactivation rate of 0.0834% per day was obtained following the initial conditioning period. Although CO conversion increased rapidly during the initial conditioning phase, Mossbauer spectroscopy analysis shows that the bulk phase iron carbide did not change. Almost all iron was converted during the in-situ catalyst activation prior to the FTS reaction. As carbon monoxide conversion decreased from the maxima, Fe_3O_4 started to appear in the bulk phase of the catalyst. This result suggests that as both the FTS and WGS reactions proceeds, increasing carbon dioxide and water partial pressure changed the reaction sytem to a more oxidizing environment and thus cause the formation of iron oxide, which subsequently cause the CO conversion decrease. A stabilized activity may obtained after the iron oxides-carbides phase or the three-phase reaction system thermodynamic equilibrium was reached. Figure 1 also shows that a temperature increase caused a new conditioning period, in which CO conversion reached a maxima of 75% before it stabilized at about 57%. This new conditioning period (250˚C) appeared more sharply than that over the fresh catalyst at 230˚C, suggesting that at a higher temperature, the new equilibrium on the catalyst surface is easier to established than that at a lower temperature.

Selectivity and productivity of potassium promoted iron catalyst

Figure 2 gives the CO_2 and CH_4 selectivity over the potassium promoted catalyst. Methane selectivity decreased from 3.5% at 24 hours of reaction time to a stable level of 1.6% in 300 hours of time on stream. While methane selectivity decreased monotonously, carbon dioxide went through a conditioning period similar to that of CO conversion. The CO2 selectivity started from 23% at 24 hours of time on stream and decreased from its maxima of 43% to a stabilized level of 39% in 300 hours of time on stream. Hydrocarbon rate showed a similar trend to that of CO conversion and CO2 selectivity, as indicated in Figure 3. The rate

rapidly increased from below 0.1g/h/g-iron to a peak value of 0.32 g/h/g-iron before reaching a stabilized level of 0.28 g/h/g-iron in 300 hours of time on stream.

Water gas shift activity over potassium promoted catalyst

When iron catalyst was utilized in an FTS process, water gas shift as expressed by equation [2] is always an important reaction involved. This property makes the iron catalyst more suitable for a carbon-rich syngas produced from coal. A water gas shift coefficient was calculated by the following equation to evaluate the WGS activity:

$$K_{WGS} = \frac{P_{[H_2]} \bullet P_{[CO_2]}}{P_{[CO]} \bullet P_{[H_2O]}} \qquad [5]$$

Figure 4. gives the results of WGS coefficient and an initial conditioning period similar to the ones for CO conversion and CO_2 selectivity was found. The water gas shift activity rapidly increased from an initial value of 1.2 and then gradually decreased from it maxima of 2.8 to a stable level of 2.3. It indicates that potassium promoted iron catalyst showed a similar FTS and WGS activity trend.

Deactivation and Regeneration of beryllium promoted iron catalyst

A beryllium promoted iron catalyst with an atomic ratio of Fe:Be=100:1.44 was prepared and tested in this study. FTS was carried our at 270˚C, 1.2MPa and 10 sl/h/g-iron. Table 1 gives the summary of results from the FTS reaction over beryllium promoted iron catalyst. At 270˚C, a CO conversion of 51% and a CO2 selectivity of 45% were obtained; however, a higher methane selectivity of 8.14% than that over the potassium promoted catalyst at 230˚C. In addition, a higher hydrocarbon rate and higher water gas shift activity were produced over beryllium promoted catalyst at 270˚C. Figure 5 gives the results of CO conversion and deactivation rate from the FTS reaction over the beryllium promoted iron catalyst. After passing

an initial conditioning period, CO conversion stabilized at 50% in the first 500 hours of time on stream. As indicated in Figure 4, a deactivation rate as low as 0.0062% during the first 500 hours of time on stream, suggesting that a superior stability was achieved over beryllium promoted iron FTS catalyst.

The reaction was operated at a series of low space velocity at 500 hours and thus the catalyst deactivated significantly. Regeneration with hydrogen was carried out at the same temperature as the FTS but zero gauge pressure for 24 hours. As shown in the figure, CO conversion increased from 37.03% to 45.35% after hydrogen regeneration. Another regeneration with CO further improved the activity by almost 10% to 55.20%. This rejuvenated activity was maintained in the next 150 hours of time on stream. These results indicated that beryllium promoted catalyst showed a good regenerability and CO is a more efficient regeneration reagent than H_2.

Conclusion

Potassium promoted iron FTS catalyst showed a low deactivation rate of 0.083% per day after passing an initial conditioning period of 300 hours. Higher temperature generated a shorter conditioning period. The FTS activity began to decrease when the bulk phase of the catalyst changed from 100% carbide to iron oxides. Beryllium promoted iron catalyst produced an even more stable activity than potassium. A deactivation rate as low as 0.0062% per day was obtained from beryllium promoted catalyst. Although the initial activity changed rapidly, little change occurred in the bulk phase of the catalyst, suggesting only the surface change may attribute to the activity change in the initial conditioning period. For potassium promoted catalyst, FTS activity, CO_2 selectivity, hydrocarbon productivity and water gas shift activity showed the same conditioning period of 300 hours of time on stream after passing a peak value

at about 120 hours of reaction time. Methane selectivity, however, showed a monotonous decrease from an initial maxima to a stable level of 1.6%.

Beryllium promoted iron catalyst showed a better deactivation property than potassium promoted catalyst, even operated at a higher reaction temperature than that over the potassium promoted catalyst. A higher water gas shift activity, higher CO2 and CH4 selectivity by beryllium promoted catalyst than those by potassium were also found in an FTS process. Beryllium promoted catalyst also showed a superior regenerability when either H_2 or CO was utilized. Carbon monoxide rejuvenation generated a better CO conversion recovery than hydrogen.

Acknowledgment

Funding from the Department of Energy (DE-FC-26-98FT40308) and the Commonwealth of Kentucky are acknowledged.

References

1. X. Zhan, B. H. Davis, 1999 Spring Symp. of the Tri-State Catalysis Society, April 20-21, Louisville, KY, 1999.
2. R. J. O'Brien, L. Xu, R. L. Spicer and B. Davis, Symposium on Syngas Conversion to High Value Chemcials, 252-253, Presented at the 211th ACS Annual Meeting, New Orleans, March 24-29, (1996).
3. M. E. Dry, in Catalysis Science and Technology, Vol. 1, 159-255, (1981).
4. D. B. Bukur, D. Mukesh, and S. A. Patel, *Ind. Eng. Chem. Res.*, **29**, 194 (1990).
5. R. J. O'Brien, L. Xu, R. L. Spicer and B. H. Davis, *Energy & Fuels*, **10**, 921 (1996).
6. Z. E. Huang, Ran Liao Hua Xue Xue Bao, **18** 143 (1990).
7. X. Z. Wang, Ran Liao Hua Xue Xue Bao, **18** 137(1990).
8. D. B. Bukur, L. Nowichi and X. Lang, *Energy & Fuels*, **9**, 620 (1995).
9. H. P. Bonzel, H. J. Kerbs, *Surface Science*, **109**, L527 (1981).
10. R. J. O'Brien, Y. Zhang, H. H. Hamdeh, B. H. Davis, "Mossbauer study of precipitated unpromoted iron Fischer-Tropsch catalyst," Preprints, 44(1) ACS, Division of Petroleum Chemistry, Mar. 21-25, Anaheim, CA, 100-102, (1999).
11. A. P. Raje, R. J. O'Brien and B. H. Davis, *J. Catal*., **180**, 36 (1998).
12. M. E. Dry, *Appl. Catal. A: General*, **189**, 1850 (1999).
13. A. J. Forney, W. P. Haynes, J. J. Elliot, Zarochak, *Am. Chem. Soc., Div. Fuel*, **20**, 3 (1975).

Table 1

Productivity and Selectivity for Beryllium Promoted Catalysts

Conversion (%)	
CO	51.21
H_2	61.98
Syngas	55.53
Product distribution (%)	
C_1	10.11
C_2-C_4	35.61
C_5-C_{11}	31.80
C_{12}-C_{18}	11.56
C_{19+}	10.92
Hydrocarbon rate, g/hr/g-iron	1.08
Water-Gas Shift	
K_p [a]	1.76
H_2:CO usage[b]	0.81
Selectivity (%)	
CO_2	45.00
CH_4	8.14

a. $Kp = [P_{H2}\ P_{CO2}]/[P_{H2O}\ P_{CO}]$.
b. Usage = r_{H2} / r_{CO}.

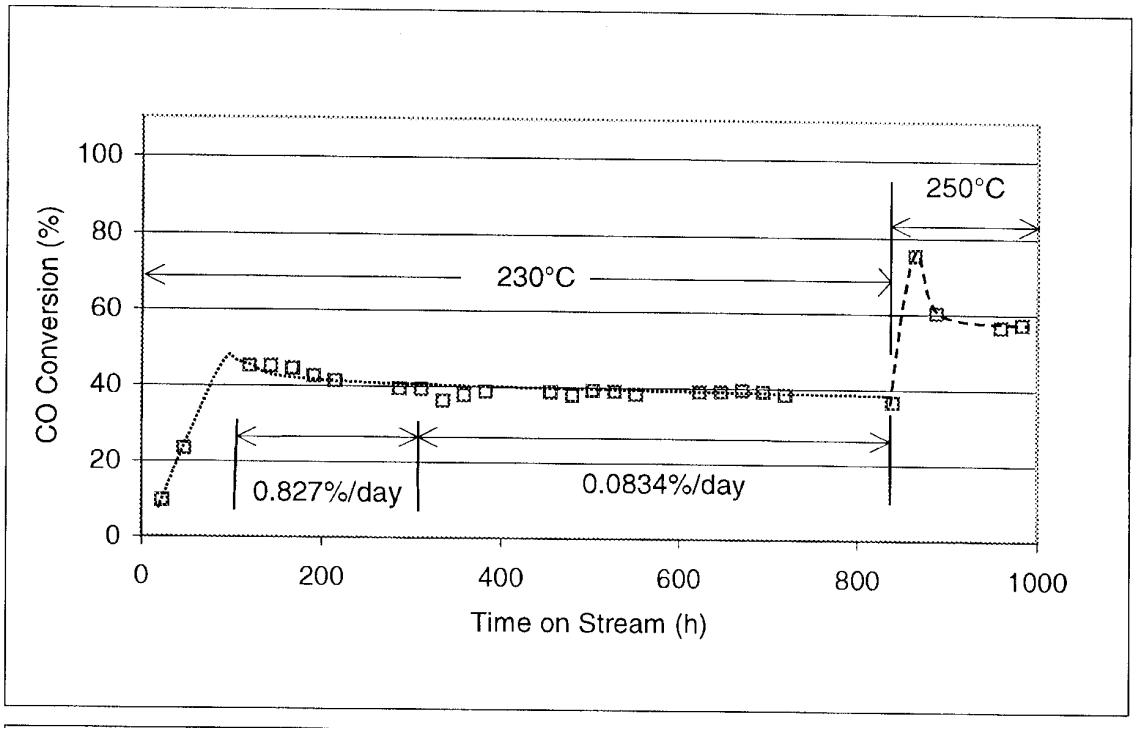

Figure 1. Deactivation rate over potassium promoted iron FTS catalyst.

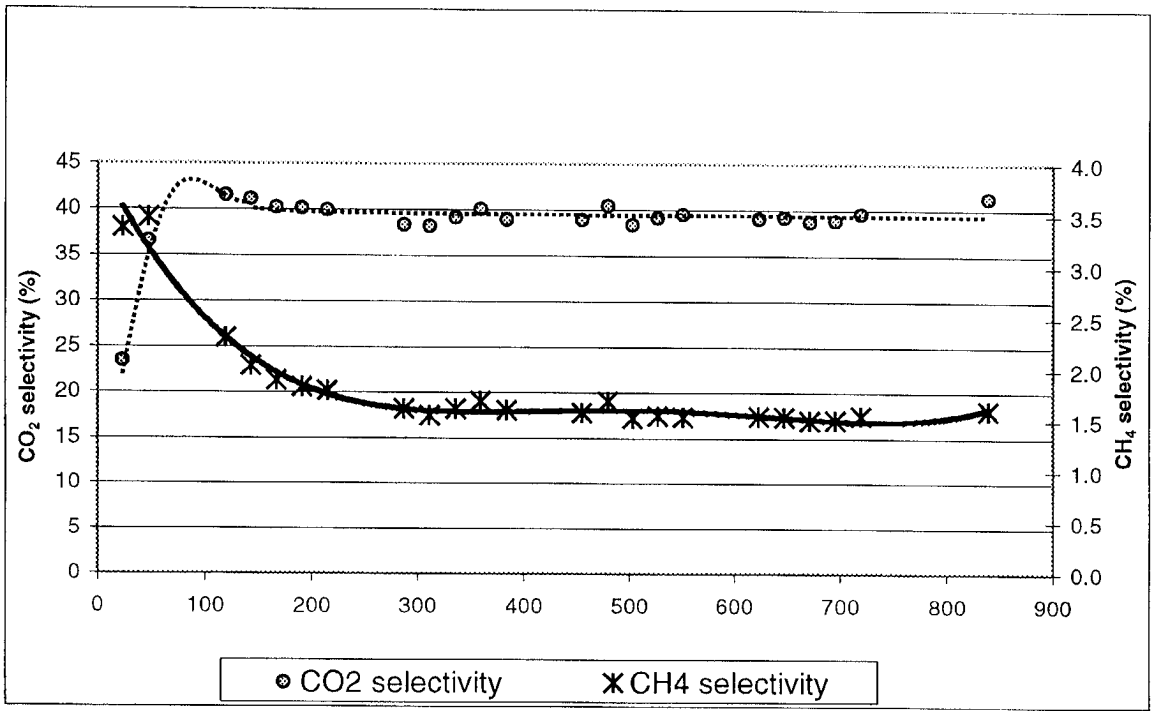

Figure 2. Methane and carbon monoxide selectivity over potassium promoted iron FTS catalyst.

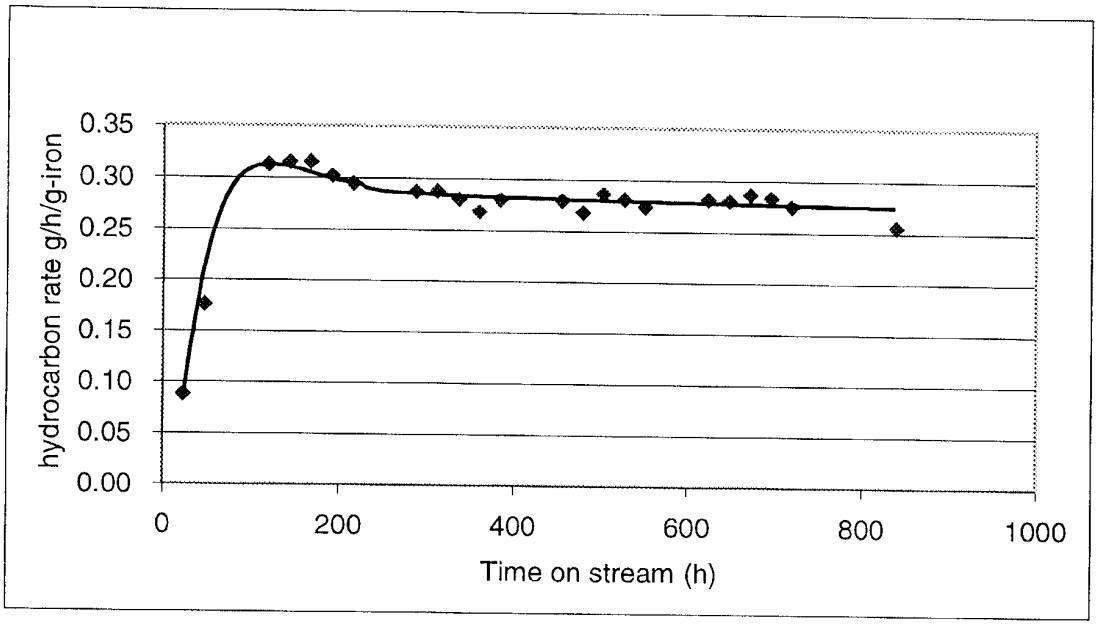

Figure 3. Hydrocarbon rate over potassium promoted iron catalyst.

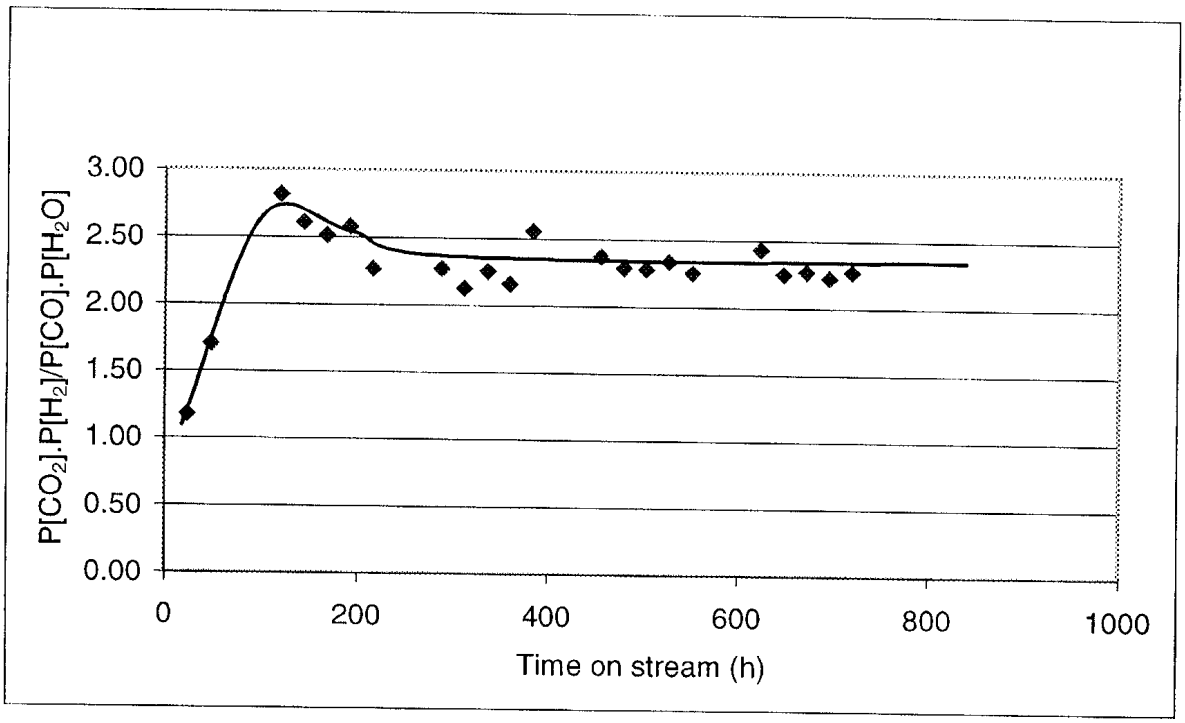

Figure 4. Water-gas shift coefficient over potassium promoted iron FTS catalyst.

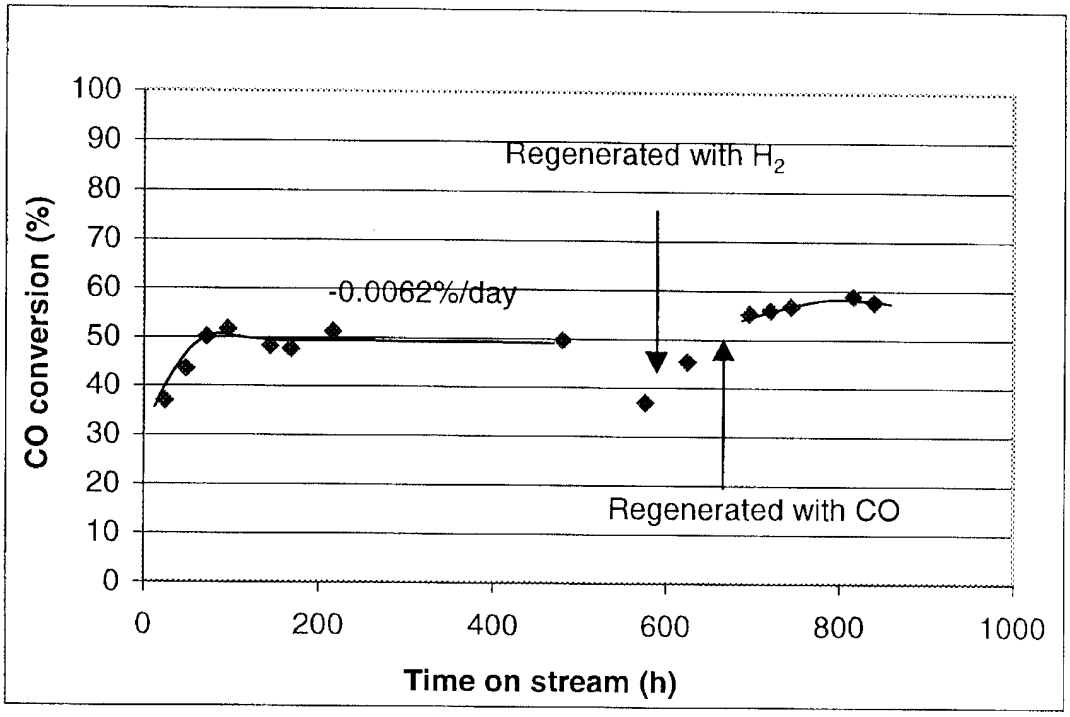

Figure 5. CO conversion over beryllium promoted iron catalyst.

I. OVERVIEW OF REACTORS FOR LIQUID PHASE FISCHER-TROPSCH SYNTHESIS

Abstract

The following overview is divided roughly into three sections. The first section covers the period from the late 1920s when the first liquid-phase synthesis was conducted until about 1960 when the interest in FTS declined because of the renewed view of an abundance of petroleum at a low price. The second period includes the renewed activity that resulted from the oil shortage due to the Arab embargo in 1972 and covers from about 1960 to 1985 when the period of gloomy projections for rapidly increasing prices for crude had faded away. The third section covers the period from when the interest in FTS was no longer driven by the projected supply and/or price of petroleum but by the desire to monetize stranded natural gas and/or terminate flaring the gas associated with petroleum production (1985 to date). These sections are followed by a brief overview of the current status of the scientific and engineering understanding of slurry bubble column reactors.

Introduction

Petroleum refining adjusted its production from kerosine to gasoline following the introduction and rapid acceptance of the auto for personal transportation. During these early years of petroleum usage, the United States was the principal exporter of petroleum crude and refined products (1). During World War I, the Allies had sufficient petroleum supplies for the war effort that was becoming increasingly mechanized; however, Germany was very poor in oil resources and this greatly handicapped their effort. Following the end of WWI, German officials were determined to develop an independent source of transportation fuels that was based on their abundant brown coal resource. The introduction of the Haber process for the high-pressure synthesis of ammonia provided Germany with a leadership role in high-pressure processes,

especially those involving hydrogen. The importance and the scientific advances associated with the ammonia synthesis were recognized and Fritz Haber was awarded the Nobel Prize in 1918.

After much research and development work, the first commercial success in 1925 was with the direct hydrogenation of coal (especially German brown coal) at high-pressure, high-temperature conditions to produce liquids that could be utilized as transportation fuels. This was the Bergius Process and its discoverer, Friedrich Bergius, was awarded the Nobel Prize in 1931. Bergius was led to this effort by his desire to be an entrepreneur and a desire to free Germany from dependence upon external oil supplies for their transportation fuels. I.G. Farbenindustrie (Farben) purchased the rights to the Bergius process. Farben was attracted to this process requiring several conditions, at least in part, because of the expertise they had developed with other high-pressure processes. By 1925, Carl Bosch had risen to a high leadership position in Farben following his successful efforts to commercialize first the ammonia synthesis process, discovered in 1908 by Nobel Laureate Fritz Haber, and then the successful conversion of synthesis gas to methanol. In this work, Farben had become recognized for its ability to produce and utilize hydrogen at high pressures. For his leadership role in developing high-pressure processes and the materials of fabrication that was needed for the processes, Bosch was awarded the Nobel Prize together with Bergius in 1931. In addition to the technical contributions, Bosch was involved in extensive negotiations with the German government that would provide them with the support necessary to conduct the development of their synfuels industry. In addition to his business activities in Germany, Bosch was active at the international levels. The details of his negotiations with the organization that is now Exxon are described in some detail in various sources (e.g., 2,3). In addition, Bosch was in a delicate situation as he negotiated with Nazi government officials as he sought to establish Farben as the lead organization for government

contracts for the production of fuels by both the direct and indirect coal liquefaction processes since he did not join the party.

The first major work on the hydrogenation of carbon monoxide was by Sabatier and his coworkers, and this work was recognized by P. Sabatier being awarded the Nobel Prize in 1912. In 1923, Franz Fischer and Hans Tropsch discovered the production of liquid hydrocarbons from synthesis gas ($CO+H_2$) that could be produced by gasifying coal. Following its discovery, the major advances in the Fischer-Tropsch synthesis (FTS) technology and scientific understanding emanated from Germany. The advances in FTS were concentrated initially in the Kaiser-Wilhelm-Institut (KWI) and then in the German companies selected by the government to commercialize the processes associated with FTS. The companies were supported by the government with a guarantee of a minimum price for the products.

The historical accounts of FTS are far too extensive to be covered adequately in a book, let alone a review paper. Hence, the following will provide a limited survey of the development of the reactors that were used to conduct the reaction in the liquid phase.

“Since 1921 the KWI had been engaged in intensive investigations of the area of gas synthesis, with the goal of producing liquid hydrocarbons. One of the reasons for this activity was the fact that Rhineland-Westphalian heavy industries, a source of financial support for the Institute, were interested in finding ways of utilizing their excess coke-oven off-gases (3).” Fischer and Tropsch were studying as one possible starting point the catalytic preparation of "Synthol," a mixture of liquid hydrocarbon- and oxygen-containing oils described in prewar patents issued to BASF (4,5). Schuster (6) later identified Mittasch and Schmidt as the inventors of these products derived from the reaction of carbon monoxide with hydrogen under high pressure. Much of the initial work was directed toward mechanistic aspects of the process (the

"formate theory"). Nevertheless, Fischer and his co-workers failed to develop a satisfactory scientific explanation of the synthesis, remarking simply in their first publication (7):

> 'We wish therefore to conclude this section regarding the theory of Synthol formation by noting that for the time being we are giving first priority, relative to other possible explanations, to the notion of synthesis through carbon monoxide addition to alcohols, albeit without claiming that we have definitely proven this to be the mechanism.'

The initial mechanism that was widely accepted involved the formation of the metal carbide followed by the hydrogenation of the carbide to produce hydrocarbons. This mechanism became associated with Fischer even though he probably had less to do with its acceptance than others working in the area. By 1950, the bulk carbide mechanism had been shown to be invalid and was replaced by a mechanism that involved a surface oxygenate intermediate. This mechanism received strong support from the results of studies at the U.S. Bureau of Mines and the ^{14}C tracer studies of Emmett and coworkers. By 1980, the results produced using a variety of surface sensitive instruments led to the abandonment of the oxygenate mechanism and the revival of the carbide mechanism which now limited carbide formation to a surface carbon species. This surface carbide mechanism was so strongly supported that it was reproduced on the cover of an issue of Chemical & Engineering News on October 21, 1981. More recently the results of ^{14}C tracer studies indicate that the oxygenate mechanism is more appropriate, at least for the iron catalyst.

In their explanation of the course of the reaction leading to Synthol, Fischer and Tropsch assumed that methane and formaldehyde arose as intermediates, which is a reason why Fischer and coworkers (including the young doctoral candidate Otto Roelen) carried out an extensive series of experiments related to methane combustion and the formation and decomposition of

formaldehyde (8). Despite these efforts, Fischer and his coworkers never succeeded in detecting more than traces of the presumed intermediates (9).

Primarily because of the influence of the management of I. G. Farbenindustrie with the German government and because its ownership of the Bergius direct liquefaction process, the early plants to produce synfuels were for the Bergius process, and not FTS (10,11).

Three reactor types have been utilized for FTS: fixed bed, fluid bed and slurry bubble columns (Figure 1). The fluid bed reactor must be a two phase, solid and gas, system for FTS; if this is not the case liquid will lead to solid agglomeration and loss of the fluid phase. The slurry phase will always be a three-phase system for FTS. Biardi and Baldi (12) have recently reviewed briefly three-phase catalytic reactors and conclude that trickle bed and slurry reactors are the most important. Another review considers the advantages and prospects for FTS in a fixed-bed and slurry reactor but does not conclude that either is the preferred one (13). Reactive distillation tray columns are receiving much attention for some applications (e.g., 14,15) and, in at least a variation, have been applied to FTS. However, the tray columns never received widespread application. The early commercial plants that were operated in Germany utilized fixed bed reactors; however, other reactor types were investigated. The Brownsville, Texas plant utilized a fixed fluid-bed reactor. While the Brownsville plant encountered and overcame many operational problems, ti remained for Sasol to develop the circulating fluid-bed reactors to the point where its operation was reliable. More recently Sasol has replaced the circulating fluid bed reactors with fixed fluid bed reactors. Sasol also operates fixed-bed and slurry reactors but on a smaller scale that the fluid-bed reactors; currently, 90% or more of the Sasol production utilizes fluid bed reactors.

Period I: 1929 to 1965

Work in Germany

Conversions in the liquid phase were initiated in Germany shortly after the discovery of the reaction. The developments progressed from the initial fixed-bed effort at atmospheric pressure to work in a bubble column reactor operated at atmospheric pressure to a large pilot plant that was operated during the 1940-1950s period. The German efforts were extensive and involved work by several companies. These companies added to the complexity faced by a reviewer because of their joint ventures with organizations located outside Germany. Thus, a complete and detailed coverage of the German work is outside the scope of the present manuscript.

Kaiser-Wilhelm-Instituts für Kohlenforschung (KWI)

The Institute, founded in 1913 with Franz Fischer as the director, was established to concentrate its efforts on fundamental studies of coal and its conversion (16). The onset of WWI within months following Fischer's arrival and Germany's need for synfuels led the institute toward more practical accomplishments. Both direct and indirect coal liquefaction studies were undertaken. The indirect approach eventually led to the low-pressure synthesis of predominantly hydrocarbon products, the Fischer-Tropsch synthesis (FTS). The exothermicity of the reaction and the need to provide a uniform temperature in the reactor were quickly recognized.

Fischer and coworkers turned to synthesis in the liquid phase soon after they discovered the FTS reaction. Fischer and Peters (17) evaluated the use of a bubble column reactor (Figure 2) that was operated at atmospheric pressure for the hydrogenation and oligomerization of acetylene and for the hydrogenation of carbon monoxide using a supported nickel catalyst. They indicated that the use of the catalyst in liquid media for these exothermic reactions is advantageous for laboratory and commercial operations because it makes possible close control

of temperature and eliminates overheating as is encountered in fixed-bed reactors. In November 1930 the pilot plant staff attempted to run the F.-T. in the liquid phase, and they were successful in solving the heat flow problem. Fischer and Küster (18) reported results to identify the influence of temperature and pressure on the synthesis. A horizontal stirred silver-lined autoclave was utilized for these studies (Figure 3). The authors found that higher temperatures were needed for liquid phase synthesis because there was no hotspot as was the present for fixed-bed operations. They utilized a catalyst with a composition of 9Co:2Th:1Cu:0.25Ce with an equal mass of Kieselgur as support. However, the typical catalysts of that day had an activity that was too low to have practical commercial interest. They also reported that pressures near atmospheric were preferred since "Synthol" (alcohols, acids, aldehydes, ketones, etc) was formed at higher pressures.

Fischer and Pichler (19) indicated that four approaches were suitable for removing the heat of reaction and for maintaining a uniform temperature in the reactor: (1) circulating oil outside the tube with the catalyst, (2) suspending the catalyst in oil, (3) circulating superheated water outside the catalyst space (e.g., 180^{o}C and 10 atm.) and (4) the suspension of the catalyst in superheated water. Interestingly, they referred to middle-pressure synthesis not as Fischer-Tropsch synthesis but the Fischer-Pichler middle-pressure synthesis. They utilized four catalysts (Ni, Co, Fe and Ru) in a study of middle pressure synthesis in an aqueous phase utilizing a stirred-horizontal autoclave, similar to the one in Figure 3, to effect the synthesis. They found that only Co and Ru were suitable for synthesis since Ni formed the carbonyl and was carried from the vessel while the iron catalyst was too active for the water-gas-shift reaction. The best catalyst was Ru, which was active below 200^{o}C. The amount and kind of products for both Ru and Co were similar to those of the dry synthesis. It was noted that water was effective in removing the heat of reaction and in providing a uniform temperature; this was based on the fact

that the fixed bed catalyst in a reaction tube of the diameter they used would have not produced useful products (i.e., higher hydrocarbons). They indicated that work in the aqueous phase was not suited for scale-up because: (1) the results are not better than operating in the dry phase, (2) a larger reactor volume is needed, (3) the apparatus is more expensive due to the need for an acid resistant reactor liner, (4) considerable expenditure of energy is necessary for stirring to provide the vigorous agitation and (5) the reaction products are not easily removed from the reactor.

Thus, Fischer and coworkers were successful in using liquid-phase synthesis to control the temperature but the reaction velocity with their catalysts was too slow to be of commercial interest. In 1931, they returned to the gas-phase reaction and experiments were conducted with the so-called "moving catalyst" where the catalyst was transported through the heated zone with a screw conveyor. This research also led to results that were unsatisfactory (20).

I. G. Farbenindustrie A. G. (Farben)

Farben utilized two general types of liquid-phase operations: (1) a fixed bed of solid catalysts with liquid and syngas circulating concurrently over the catalyst and (2) a suspension of fine catalyst particles due to the fine bubbles formed when the syngas passed through a ceramic bottom plate with slurry circulation through an external vessel for heat removal. In some versions, they also utilized stirring as a means to maintain the catalyst suspension. Only the fixed-bed version developed beyond the laboratory scale.

The foam process was one variation of the liquid phase synthesis (21-26). During 1939 to 1944 Farben was developing a liquid-phase operation in which iron powder, prepared from iron carbonyl, was mixed with oil and the gas contacted with the liquid suspension (27,28) using a process scheme as outlined in Figure 4.

Michael (28) reports that laboratory reactors of 3 m height and 6.6 and 16.5 cm i.d. were utilized. These reactors were fitted with an internal central tube along the axis of the reactor.

Because the gas bubbles rose in the annular space between the reactor wall and the inner tube, the density of the slurry in the annular space was lower than the essentially gas free slurry inside the smaller tube. The difference in density caused rapid circulation of the slurry within the reactor. In today's language, the inner tube would be a downcomer tube. When they constructed a pilot plant reactor identical to the laboratory reactors except that the volume was 300 L (2.0 m diameter), difficulties were encountered. If the circulation was interrupted for some reason, the catalyst would settle and, upon re-starting, the gas flow was insufficient to cause the catalyst to become uniformly suspended. The concentration of the catalyst at the lower portion of the annular space of the reactor provided a density that was greater than the slurry in the downcomer so that circulation could never be re-started. For this reason, a pump was installed and, for convenience of maintenance, placed outside the reactor vessel as shown in Figure 4. A reactor of this design with a 0.5 m diameter and 8 m tall (1.5 m^3 volume) was constructed and operated satisfactorily. A larger 1.5 m diameter and 8 m tall (14 m^3 volume) reactor was constructed but was not operated because of a shortage of synthesis gas because of wartime problems.

It was found to be difficult to operate the suspended catalyst because the formation of high molecular weight products of limited solubility caused the catalyst particles to agglomerate and settle (21,29). Frequently they experienced thick deposits of iron catalyst around the wall of the reaction vessel, and especially in the upper portions of the reactor.

Duftschmid Process.

One Farben development (30-32) consisted of an oil recycle process in which a cooling oil was passed concurrently with the synthesis gas over granules of an iron catalyst (fused or sintered iron that was doubly promoted with aluminum and potassium oxides, or with titanium, manganese and potassium oxides). Cooling was effected by recycling the oil heated by the exothermic reaction through an external heat exchanger. The process was operated at a pressure

of 20 to 25 atm (2.02-2.53 MPa). and a temperature of 260 to 300ºC in the first stage, and 280 to 330ºC in the second stage when used. The throughput of synthesis gas ($H_2/CO = 0.8$ for this example) was controlled to yield about 0.5 kg of total product per liter of catalyst per day. The yield of C_3+ hydrocarbons was about 150 grams per cubic meter of synthesis gas ($H_2/CO = 1$ for this example) and was distributed as follows: 16% C_3 and C_4 (85% olefins), 40% gasoline boiling to 200ºC (50% olefins), 20% gas oil (25% olefins), 20% paraffin wax and 4% alcohols, largely methanol and ethanol. The crude gasoline had a research octane number of 62 to 65 and the gas oil a cetane number above 70. Some of these patents were assigned to the Standard Catalytic Company. The Standard Catalytic Company was established by six U.S. petroleum companies to develop processes for the production of synthetic fuels, and included an agreement with Farben. Following WWII, legal actions divided the holdings of the Standard-Farben company. Jersey received complete possession of 544 patents and ownership of Standard Catalytic Company. Jersey retained half-ownership of another 254 patents.

Benson et al. (33) report that, after the preliminary work by F. Duftschmid, et al., as described above, a pilot plant with a reactor of 0.2 m diameter and 6 m height (about 0.75 m^3) was constructed during 1936 and 1937 and that it was operated, first at pressures of 100 atm (10.1 Mpa) and then at 15 to 20 atm (1.5 to 2.0 MPa). In 1938, a larger plant with a 0.5 m diameter and 6 m height (4.7 m^3) was operated. The recirculation rate was high, 9-12 reactor volumes of catalyst/oil was recirculated each hour (34). At the end of the war they were planning a 40,000 ton/year (860 bbl/d) plant for this process (34).

The Duftschmid process was consider to be different from the one developed by Ruhrchemie (described below) since the entire bed of solid catalyst is immersed in oil (33). However, Farben obtained a patent (35) in which oil was sprayed onto the catalyst in a fixed bed (Figure 5). The liquid passed in the same direction as the gas. They indicated that, while it was

desirable to always have a thin layer of liquid present on the surface of the catalyst, it may be advantageous to temporarily interrupt the trickling in order to cause a brief increase in the temperature of the catalyst, in effect, a catalyst rejuvenation step.

An early German liquid-phase reactor involved an arrangement of trays, each containing catalyst particles, that were contained in a cylindrical vertical reactor that was fitted at the top with a reflux condenser and an arrangement for removal of liquid at the bottom of the reactor (Figure 6) (32,36). Experiments were conducted in a 7-tray reactor, 4.5 cm diameter and 60 cm tall, with up-flow of the reactant gas.

Another variation of the liquid-phase fixed-bed reactor was developed as shown in Figure 7 (30). A catalyst, K, is placed in an inner tube, which is surrounded by an outside tube. In the example, the reactor was 15 cm in diameter and 5.8 m tall; it was surrounded by a shell that was 20 cm in diameter. An inert liquid from FTS is circulated by a pump, P, through a preheater, H, where it is heated to 240^{o}C and then added through L to the reactor shell held at 120 atm (12.1 MPa). Syngas is preheated by passing through T and then enters through N located below the reactor. Products and recycle solvent exit the top of the reactor and pass through a cooler, S, where liquid products, including water, condense and enter a holding vessel, B. Water and product are withdrawn through D and the oil is recycled. In the example about 6 L of liquid products are formed per hour while 0.75 m^3 of oil is recycled per hour. If the separation vessel, B, has about the volume of the reactor, the recycle volume/reactor volume would be about 10 and the material being withdrawn would contain only about 10% liquid products. It would therefore appear that separation would present major operational problems at the commercial scale. In addition to the reactor configuration shown (Figure 7 (1, 1A)), two other versions were shown: in one the location of the catalyst bed is reversed (Figure 7,(2,2A)) and in the other

multiple catalyst tubes are located within the shell (Figure 7 (3, 3A)). The U.S. patent covering this reactor configuration (30) was assigned to Standard Catalytic Company.

Ruhrchemie

A general license for the FT process developed at KWI was assigned to Ruhrchemie AG in Oberhausen-Holten on October 27, 1934. Independent of this licensing agreement, Ruhrchemie had started construction of a pilot plant on their own and had acquired the services of Otto Roelen, who was glad to leave the KWI since his relationship with Fischer was not entirely satisfactory (16). Roelen is credited with much of the experimental success at both KWI and Ruhrchemie. In addition to his excellent experimental capabilities, Roelen had outstanding scientific and technical abilities. His keen intellectual curiosity led him to discover the oxo process by concluding, correctly and in contrast to the views of others, that the recirculation of ethene to the FT reactor led to the formation of additional C_3-products, especially C_3-oxygenates. This observation led him to the discovery of the oxo process.

Their reactors had a vertical tube 6 m in height that was inside a larger tube where oil circulated to remove the heat of reaction (Figure 8). The reactor volume of one was 55 L and a second reactor had 85L of slurry volume. Because significant quantities of oil were carried over, even with a wider head at the top of the larger reactor, a reflux condenser was operated to return heavier oil to the reactor. Heavy products were withdrawn from the reactor through a filter stick immersed in the slurry. Initially a ceramic plate was used to generate small gas bubbles of feed gas, but the catalyst settled and plugged the plate when the operation had to be interrupted, even temporarily. The plate was replaced by a simple copper capillary tube which never blocked and, based on the conversion, operated to produce fine bubbles of syngas just as well as the ceramic plate.

They indicated that, on a large commercial scale operation, it would be better to limit the conversion in the stage I reactor and to use reactors in series. This operational mode was claimed to limit methane formation and to extend catalyst life.

The usage ratio (the ratio H_2/CO converted), when CO conversion was in the 70-75% range, as when operating a single stage, was usually 1.4-1.5; however, if the reactor was operated at lower conversion levels the usage ratio could be reduced to about 0.9. With two stages together, the usage ratio was 1.24-1.28, which was essentially that of the feed syngas. They had an objective of making the feed and usage ratio the same for each reactor in the series, but apparently never attained this goal. We have reported that this goal can be easily accomplished with a low H_2/CO ratio syngas when using an iron catalyst but that it may be more difficult to accomplish with a high H_2/CO ratio (37).

Ruhrchemie (38) worked to develop a modified liquid-phase process in which finely divided cobalt-thoria-magnesia-kieselguhr catalyst was suspended in oil boiling between 240 and 300^{o}C. During the synthesis, water was injected into the slurry where it vaporized to maintain control of the slurry temperature. The presence of a high water partial pressure, as must be present in this operation, implies that oxidation of their cobalt catalyst did not occur to an extent that it was a problem. An alternative explanation is that the activity of the catalyst was so low that the change could not be detected. With H_2/CO = 2, 10 atm (1.01 MPa) and 2.5 L/gCo/hr at 190-210^{o}C, 172 g of liquid and solid hydrocarbons per cubic meter were produced, with 90% of the liquid product boiling below 300^{o}C. By the end of the war, the work had not progressed to the large-scale pilot plant stage (39).

Ruhrchemie workers also developed a version of the oil recirculation process. Their process utilized a fixed bed of catalyst that was sprayed continuously with an oil that was added through a device that was designed to provide a uniform distribution of oil across the radial

dimension of the catalyst. The intent was to have the oil maintain the catalyst free of wax and to remove the heat of reaction by the latent heat of vaporization of the added oil (34). It was not made clear how the added oil could wash the wax from the catalyst through the bottom of the reactor and, at the same time, evaporated to maintain the temperature.

Rheinpreussen

This company began work on the liquid-phase synthesis about 1937. Most of the work was under the direction of H. Kölbel and the work conducted up to 1945 was summarized by him (34). The composition of most of the catalysts used by Kölbel and coworkers in this early work, as well as in the later pilot plant studies, had a composition of Fe:Cu:K_2O = 100:0.2-0.5:1.0 and was activated 10-20^oC above the synthesis temperature. They used a suspension of 10-20% Fe, a syngas with H_2/CO = 0.5 and a space velocity of 75/hr, a very low value. The early experiments were conducted in a vessel with 15cm id and 3-4 m height with cooling coils either inside or outside. They reported a usage ratio of 0.5, as it was reported that no water was present in the products. In this and other work, Kölbel reported that diesel and the product olefins, and even paraffins, reincorporated extensively to produce heavier products. Excluding the mass of product formed from the diesel recycle fluid, 180 g product was formed from a m^3 of synthesis gas. With this catalyst they reported that no methane was not formed. The synthesis products were obtained by withdrawing oil and catalyst, filtering, and returning the remaining catalyst slurry to the reactor, all operations being conducted under synthesis gas (34).

The claim of paraffin reincorporation is astounding but the data that are reported seem consistent with this claim. Kölbel reported that the great freedom available when operating in the fluid phase process is the reason why the large variation of the primary products, with respect to the variables (temperature, gas composition, catalyst, pressure, residence time, etc.) cannot be approached with other reactors (Table 1) (40). In addition, it is possible that doing the synthesis

in the slurry reactor causes liquid hydrocarbons which were added (recycled is allowed with the German wording) to the reactor, through molecular (reincorporation) of the liquid hydrocarbon that is added back to the reactor, to form hard paraffins (41,42). For this reason, treating the primary product in a secondary process, such as, in general, cracking is not needed. Kölbel explains that this is why this type of process allows one to change the molecular size.

Kölbel and Ackermann (43,44) obtained patents for an apparatus for carrying out gaseous catalytic reactions in liquid medium. The reactions included Fischer-Tropsch synthesis. It was stated that the "[Fischer-Tropsch] synthesis according to known processes is feasible without trouble in a reaction space of up to 20 cm [7.9 in] diameter. With increasing horizontal diameter of the reaction space the amount of gas conversion decreases and it is always more difficult to maintain a constant gas conversion. The larger the horizontal diameter of the reaction space, the more the liquid substance leans toward changing from stationary state to a state of vertical rotation. [Vertical rotation occurs when] the liquid flows downwardly along the surface of the wall and flows along the bottom to the middle of the reaction space, whereby it is drawn out by the gas bubbles leaving at the middle of the bottom. The compressed central gas stream flows along with the liquid toward the top whereby the firmly compressed gas bubbles combine to form large elongated gas bubbles. Only at the upper reversal point of the liquid, in the vicinity of the surface of the column of liquid, the gas spreads out horizontally across the transverse section and the large gas particles are partially decomposed (Figure 9)."

As Kölbel and Ackermann illustrate (Figure 9), the liquid flows upwardly in the interior of the reactor tube and flows downward along the wall side of the reactor. They indicated several disadvantages that accrue from this situation, including: (1) decreased gas conversion, (2) occurrence of secondary reactions, (3) increased catalyst damage, and (4) increased catalyst aging.

These authors state that, for reactions like Fischer-Tropsch synthesis where the gas composition changes with conversion and where the products admix with the unconverted gas, "...the gas conversion should be complete as possible on passing the gas through once..." The authors indicate that, prior to their patent, none of the available operations permit "...maintaining the liquid medium and the suspended catalyst stationary and nevertheless permitting the gas bubbles in uniform size and distribution to pass vertically through the liquid medium at equalized velocity..." The authors indicate that the disadvantages of the liquid and catalyst circulation, as shown in Figure 9 (Figure 1), can be overcome in a cylindrical reactor with a horizontal diameter of more than 30 cm and up to 3 m or more and more than 1.5 m in height, and a gas head space above the liquid at least as large as the reactor diameter. To provide within the reaction zone a stationary catalyst and liquid condition, the large reactor shell is subdivided into similar, vertical shafts which are open at top and bottom that have liquid-tight casings and a diameter of at least 5 cm (Figure 10). The shafts should terminate above the expanded liquid level; i.e., in the free-board gas space. Because of the flows in the bottom of the reactor, it is stated that each of the shafts, in the center as well as at the wall region, receive the same amount gas. While there is circulation of the liquid in the sump (bottom of reactor in Figure 10), "...there are formed in the shafts extremely stationary liquid columns whose expansion depends on the amount of gas."

The authors indicate that in certain cases, as in the Fischer-Tropsch reaction, it may be an advantage to allow the temperature to rise toward the top of the reactor, and provisions are described which would allow for this to occur. Thus, as the partial pressure of the reactants decrease, the higher temperature will be able to compensate, completely or partially, by having the rate increase to compensate for the partial pressure decrease.

Kölbel and coworkers operated a large demonstration plant with a reactor that was 1.55 m in diameter and 8.6 m in height. Until the start-up of the slurry reactor by Sasol, the Rheinpreussen-Koppers demonstration plant was the largest slurry reactor that had been operated successfully. Kölbel states that at the time that most work was conducted using the demonstration plant (1952-53), the operation was confined almost exclusively to the production of gasoline (45). The results of the operation of this plant and the smaller laboratory scale slurry phase reactor produced data that have become the "standard" that is used to compare with other slurry phase studies. As indicated above, a typical catalyst used by Kölbel in this plant would have a composition of Fe:Cu:K_2O = 100:0.1:0.05-0.5; thus, it would be consistent with the objective of producing gasoline range material, and not high molecular weight reactor-wax. The catalyst used by Kölbel would be similar to a low-alpha iron catalyst described in Mobil patents (46,47) and government reports for the Mobil work (48,49) and, except for a much lower copper content, the one used for La Porte run II (50).

At the conversion level shown in Table 2, only 178 g of hydrocarbons were produced per m^3 gas (from the original paper in German, it is not possible for even a native German to tell whether this volume of gas refers to the amount of gas fed or to the amount of gas converted). Even if it is taken as the amount fed, at the 90% conversion level, more than 178 g. of hydrocarbons should have been produced. For example, in the Mobil runs more than 200 g hydrocarbon were produced. Sasol workers indicate that they could not repeat Kölbel's results in their early studies (51). Kölbel et al. report that through polymerization of lower olefins, about 18 g of alkylate gasoline can be produced for each m^3 of syngas that was converted. When this was mixed with the reformed gasoline (112 g/Nm^3 $CO+H_2$), 130 g/Nm^3 $CO+H_2$ of finished gasoline could be produced. For a CO conversion of 91%, the H_2 + CO conversion was 89%; the feed gas ratio was H_2/CO = 0.67. With this gas ratio, based upon our results, the only way that

Kölbel could have obtained such similar high CO and CO + H_2 conversions would be to operate so that the single pass conversion was 50-60% and to recycle the unconverted gas. It has not been widely appreciated that much of the work that Kölbel reports has been conducted under conditions designed to produce gasoline; in this mode the demand on wax/catalyst separation is minimal. Thus, much of Kölbel's work can be viewed as being conducted under conditions that make the operation of a slurry reactor much easier than the current goal of operating to maximize the reactor-wax fraction to subsequently hydrocrack to produce diesel fuel.

Kölbel stressed that the low viscosity and surface tension of the liquid was crucial for maintaining the small bubble size needed to maintain gas-liquid mass transfer. Kölbel maintained the view that it was necessary to establish upper limits upon the solids content of the slurry in order to maintain a low viscosity. Kölbel and coworkers obtained very low methane for the distribution of the other products that they reported. This is illustrated in Figure 11 where the Kölbel data are compared by the author with data obtained by others using bubble column slurry reactors (49). In spite of the question regarding mass balance, Kölbel and coworkers provided a strong scientific and engineering basis for further work.

Another reactor type was constructed along the lines of a modern multi-tray bubble cap distillation tower. Thus, a reactor is fitted with a number of trays that contain catalyst and are fitted with bubble caps arranged to allow vapors, unconverted feed gases and vapor phase products, to be distributed to keep the catalyst in suspension (Figures 12 and 13) (52). Some bubble caps are fitted with downcomers that allow nonvolatile liquid to descent to the bottom of the reactor. In an example, 0.34 lb (0.184 kg) of catalyst was suspended in one gallon (3.79 L) of oil (about 6% slurry) and charged to a reaction chamber containing 50 bubble trays. Other variations were provided (Figures 14 and 15) (31). In these versions, the cooling liquid could be

added at several levels in the reactor to maintain a better control of temperature during startup and synthesis.

The Netherlands

International Hydrocarbon Synthesis Co [N. V. Internationale Koolwaterstoffen Syntheses Maatschappij, The Hague, The Netherlands]

This company was reported to employ a form of the recycle technique that utilized vapor-phase synthesis in the first stage and this stage was followed by a liquid-phase operation that utilized a catalyst suspended in oil. The two reactors were separated by a product condensation unit (53). However, the reference given for this work appears to apply only for an oil recirculation liquid-phase process that has the features of those described above (54). This company obtained many patents covering FTS during the 1930s but only a limited number apply to liquid-phase synthesis.

United Kingdom

The Fuel Research Station at Greenwich first utilized fixed bed reactors that had a reaction space up to 50 liters volume and in 1947 began work on the fluidized bed reactor. In 1949 work began on the liquid-phase technique. Hall et al. (55) compared fixed bed, fluid bed and liquid-phase reactors and in 1952 concluded that the maximum selectivity and flexibility could be obtained with the liquid-phase system. The decision was made to construct a pilot plant, based primarily on the fact that the liquid-phase reactor was the only one that could be operated with the CO-rich gas produced in a slagging coal gasifier. Pilot-scale operations were initiated at Greenwich and transferred to Warren Spring Laboratory in 1958. A plant was to produce up to 385 L of product/day and to operate at pressures up to 20 atm (2.02 MPa) and reaction temperatures to 300^{o}C was operated. The reactor had a 9.75 inch (23.5 cm) internal

diameter and was 28 ft tall (8.5 m), allowing a reactor volume of 273 L. Initial problems were encountered in the settling method they used for wax separation from the catalyst slurry and from carbon formation which increased the viscosity of the reactor contents to the point of near-gellation.

The operation of the British plant was terminated about the time that they had solved most of the operating problems and considered themselves to be at a point where they could operate to produce reliable data. Low catalyst activity and rapid catalyst aging were problems that limited the usefulness of the data produced during the period of operation of the plant.

Dreyfus, a British citizen who assigned U.S. patents to the Celanese Corp., described a liquid phase synthesis for Fischer-Tropsch synthesis (56,57). In his version a catalyst was immersed in a liquid medium which boils at about the temperature of the desired reaction. Syngas is bubbled through the liquid containing the catalyst and fitted with a reflux condenser to maintain the liquid phase. While the inventor indicated that the reaction could be conducted at high pressure, he indicated that it had the greatest value when applied to the synthesis of hydrocarbons under atmospheric pressure. Cobalt catalysts were utilized at a temperature of about 180-200^{o}C and an iron catalyst at a temperature of about 250^{o}C. The example utilized a cobalt catalyst that was promoted with thoria. Excess liquid products are drawn off by an overflow at the desired level, fitted with a liquid seal.

Dreyfus also described the use of liquid-phase synthesis in the range of sub-atmospheric to about 5 atmospheres (5.05 MPa) of pressure (57,58). A feature of this patent was the use of a metal active for Fischer-Tropsch synthesis that was present in a reduced form and at a low concentration. A salt of a reducible metal (especially Co, Ni or Fe) that is soluble in the reaction medium was indicated. A salt of a fatty acid is especially preferred since is very soluble in the

organic medium. Promoters may be included as part of the catalyst system. The metal is reduced in a few hours at the reaction temperature, e.g., 200°C prior to the synthesis.

United States Liquid Phase Work

U.S. Bureau of Mines

The U.S. Bureau of Mines constructed and operated a pilot plant that utilized oil-recycle in a reactor with a 3 inch (7.6 cm) and 8 ft. (2.44 m) tall (33). After several runs during 1946-47 with co-current downflow of gas and liquid over cobalt catalysts, a run was made with the cobalt catalyst completely submerged in liquid and co-current upflow of gas and liquid. After it had been demonstrated that the unit could be operated with the cobalt catalyst, the later runs were made with an iron catalyst. The composition of the cobalt catalyst was $Co:ThO_2:MgO:kieselguhr = 100:7:12:200$. The cobalt catalyst was reduced at atmospheric pressure (0.101 MPa) in the reactor. The temperature was raised to 360°C as rapidly as possible using a hydrogen flow of 10 ft^3/h (1.05 m^3/hr) and then the hydrogen flow was increased to 200 to 400 ft^3/h (21 to 42 m^3/hr) and the reduction continued for 4 h. Since the catalyst bed occupied about 0.25 ft^3 (0.026 m^3), the GHSV was about 800 to 1600 h^{-1} during the reduction at 360°C. Following reduction, the hydrogen flow was reduced to 5 ft^3/h (0.53 m3/hr) and the temperature reduced to 150°C. Nitrogen replaced hydrogen at this point and the pressure was increased to 40 psig (0.28 MPa) . Oil was then admitted to the reactor. After the oil was added, syngas flow of GHSV = 100 h^{-1} was started. The temperature was slowly increased from 150°C while increasing the pressure in small increments, which decreased the rate of evaporation of the cooling oil. The temperature was maintained below 175°C, maintaining a gas contraction of less than 50%, during 48 hours. The temperature was increased to 180°C during the next 24 h., after which the induction was considered complete. The conditions were then adjusted as required to obtain maximum productivity.

The Bureau of Mines also operated a larger 8 inch (20.3 cm) diameter reactor in the oil-recycle mode (Figure 16) (59). These units were operated with a precipitated and a fused iron catalyst that has a very low activity compared to the high surface area precipitated iron catalyst. The fused catalyst was used because it was hard and seemed to have the physical strength needed for slurry operation. Some experimental operating problems made it difficult to maintain constant temperature during significant portions of the runs. While it was demonstrated that this mode of operation was viable, little else was obtained that merit further consideration here.

Standard Oil (Jersey) (Now Exxon Mobil)

In the 1920s it became necessary for Farben to seek funding and partners that were located outside of Germany. One company that was targeted by Bosch, then head of the company, was Exxon. When the top management of Exxon visited the research facilities where Farben was working on the Bergius process and other high pressure hydrogenation and hydroconversion processes, they were sufficiently impressed to enter quickly into a joint effort that was centered on hydrogenation. In the early 1930s Exxon abandoned research on hydrogenation although they had spent more than $30 million on experimental and commercial plants and an additional $35 million payment in Jersey stock to Farben. Larson et al. (60) conclude that, “Perhaps the most important result of the early work in hydrogenation was the interest it stimulated among Jersey researchers in catalysis and catalytic processing...Catalysis research also aroused the company’s interest in the synthesis of hydrocarbons from carbon monoxide and hydrogen derived from natural gas or coal... [Thus,] Jersey sought still other methods [than direct hydrogenation] for making motor fuels of high quality. For example, it investigated the Fischer-Tropsch hydrocarbon synthesis process, developed by Ruhrchemie, A.G., which converted brown coal into liquid fuel. In 1938 and 1939, patents for this process outside Germany were transferred by Ruhrchemie to Hydrocarbon Synthesis Corporation, in

which Standard Oil Development [now Exxon Mobil] took 680 shares, Shell and Kellogg 425 each, and I. G. Farben 170. Both Great Britain and France considered the building of plants using this synthetic process for providing aviation gasoline, but they had been unable to accomplish anything definite by the time the war broke out in Europe in 1939."

It was recognized soon after the discovery of the Fischer-Tropsch synthesis that a reactor employing the catalyst in direct contact with a cooling oil was an attractive approach to maintain temperature control of the exothermic reaction. U.S. patents were obtained by Farben, Standard Oil Development Company and Standard Catalytic Company.

A procedure designed to facilitate removal of the reaction product was to pass the preheated synthesis gas into a 50-bubble tray tower at the rate of 105 m^3/hr. A suspension containing about 0.34 kg of finely divided nickel catalyst activated with magnesium and aluminum oxides per 3.8 L of sulfur-free paraffin was charged through the tower at the rate of 20 L/min. The reaction produced about 385 L of liquid hydrocarbons for each 105 m^3 of gas charged (61).

Texaco

Most of Texaco's attention during this period was directed toward fluid-bed operations such as was utilized at the Brownsville plant. The Brownsville plant was developed by a group of companies and utilized a fixed-fluid bed reactor. The driving force for this plant was Dobie Keith who founded Hydrocarbon Research, Inc. (62). During WWII, Keith was assigned the responsibility for developing the barrier for the separation of the uranium isotopes and the construction for the gaseous diffusion plant at Oak Ridge. He developed an interest in the Fischer-Tropsch synthesis during his work on the Manhattan Project. Three drivers for the Brownsville plant were: (1) the anticipated shortage of petroleum crude, (2) the lack of a pipeline to deliver natural gas to markets, and (3) the development of plants that could be used to produce

oxygen for preparing the syngas. The discovery of the vast quantities of mid-East oil removed the major driving force for the plant just as many of the operating difficulties for the plant were overcome. The scale of the operation was small by today's standards: 900 bbl/day of diesel, 200 bbl/day of fuel oil and 300,000 lb/day of chemicals (63).

Texaco obtained a patent which provided much insight into the operation of a slurry bubble column reactor (Figure 17) (64). While the process equipment and its operation are described in much detail, neither experimental data nor examples are given; thus, it is not certain whether the patent presents a detailed conception or whether it describes equipment that was constructed and operated. The reactor can be viewed as a grouping of tubes inside a shell. The catalyst slurry is circulated through the tubes while the cooling fluid is circulated in the space between the tubes and the shell. Moore cautioned that the height/cross-sectional area should be large and provide an example where the height may range from about 10 to 40 feet (3.1 to 12.2 m) and have an inside diameter of 1 to 6 inches (2.54 to 15.2 cm). Moore taught that the flow of gas should be sufficient such that the "flooding velocity" is exceeded and that diluent gases may be used to accomplish this objective. It was indicated that a light olefin product, e.g., propene, may be used as the diluent and that a portion of the olefin may enter into the conversion, presumably by chain initiation, reincorporation or by hydrogenation. The gas feed rate may be adjusted to give turbulent flow within the tubular reactor tubes. The recycled slurry and dispersed gas flow can be adjusted to give rise through the reactors in "tubular flow." Presumably, tubular flow can be considered to be equivalent to plug flow, as this term is used today. A variety of catalyst formulations were presented, including supported or unsupported cobalt and iron. Separation of wax from the slurry was accomplished external to the reactor and could be operated so that separation was accomplished continuously or by filtering the entire catalyst inventory at one time. The entire recovered catalyst could be regenerated and returned

to the reactor or, as an alternative, regeneration could be effected by discontinuing the CO feed while continuing the H_2 feed to the reactor while the system was held at some elevated temperature.

In another variation, the liquid-phase synthesis is effected in a reactor similar to the one in the above patent but materials are added to alter the surface tension to permit the formation of a froth or foam (65). This was claimed to increase the rate of synthesis by materially increasing the area of the liquid-gas interface. In one variation, water is introduced into the reactor above the entrance of the catalyst/slurry oil entrance. The steam will evaporate and form a foam which will fill the reactor. The foam, after leaving the reactor, is broken and the slurry is separated from the products and recycled.

Another variation of the Texaco liquid-phase synthesis (66) is similar to the Duftschmid process. As shown in Figure 18, a solvent is injected between the catalyst layers of alternating catalyst and noncatalyst solids. Above each stage in the reactor, there is a device for injecting a fluid which, by partial evaporation, effectively removes the heat of the synthesis reaction.

Gulf

Cornell and Cotton (67) patented a reactor that was dramatically different from the others described above. First, the reactor was oriented with its length horizontally rather than vertically (Figure 19). A catalyst bed is located within a tube in a tube (cross-section shown in Figure 20). Located above the catalyst bed and at locations along the length of the reactor are openings to allow syngas to be fed (12) and fans to provide the pressure needed to force the liquid and syngas through the catalyst bed. Along the bottom of the vessel a number of openings allow for the removal of liquid products. Tubes (29) are located below the catalyst bed so that a coolant can be added and withdrawn through openings 31 and 32. A portion of the liquid phase is recirculated around the catalyst through the space between the tube shell containing the catalyst

and the outer shell which depends upon the pressure difference across the catalyst bed that is generated by the series of blowers at near the top of the reactor. This reactor configuration would have intellectual appeal, especially where the height of a reactor is important, as it may be if the reactor is located on a barge. However, it appears that the operation of this plant in a steady-state condition would be an exceptionally demanding task.

In viewing the reactors described for this period, one should keep in mind that the Brownsville plant, at about 7,000 bbl/day, was very large for its time. However, today one thinks of 20-50,000 bbl/day plants so that a design that was reasonable to consider for this period may be impractical when projected to the reactor size needed today.

Period II - 1960-1985

UOP

UOP workers (68) made a comparison of the entrained bed reactor, designed by Kellogg (69) and operated commercially by Sasol, a tube-wall reactor developed by U.S. DOE (70), a slurry reactor, designed by Kölbel (45) and operated on a semi-commercial scale at Rheinpreussen-Koppers, and the ebullating bed reactor, developed by the US Bureau of Mines (33) and utilized by Chem Systems Inc. (71).

It was concluded that, since the FT reactor represents only a small part of the total cost of an indirect liquefaction plant, the value of the products is of primary importance in the selection of a particular reactor (72). These authors also concluded that in spite of uncertainties in the yield structures that have been reported for some reactor systems, the differences in comparing the above reactor systems are large enough to indicate clear advantages for the slurry reactor as it has the lowest investment and catalysts costs. It was expected to give the highest gasoline yields and thermal efficiencies (72). While the slurry reactor seems to be the one currently being

considered by most organizations, it appears that it will be operated to maximize wax yield which will be cracked to diesel fuel with the goal of minimizing the gasoline yields.

Exxon

The patent history indicates that Exxon has exhibited a renewed interest in converting synthesis gas to hydrocarbons. The early work during this period contains numerous examples of syngas conversion at ambient pressures. More recently the data reflect a more sophisticated evaluation of catalysts and a long string of patents that relate to improvements in equipment and its operation. The latter are a result of the operation of a sizable fully integrated pilot facility (200 bbl/day) at their Baton Rouge Laboratory for their AGC-21 process. Because the Exxon work overlaps Periods II and III, and, since there is no logical break in the reports, their work during both periods will be covered in this section.

Slurry Bubble Column Reactor Design

Modified Gas Inlet System. Patents provide claims of methods to improve the axial distribution of catalyst and the mixing of particulate catalyst in the slurry. The methods include adding a secondary gas into the column at locations above, as well as the commonly practiced addition below, the gas distributor plate. The basis of this design is that since solids distribution along the axis of a column is a function of gas velocity in the column, by increasing gas velocity, solids distribution will decrease in the lower part of the column and increase in the upper part. A key to the method disclosed in patents is that introducing a disproportionate share of the gases at an inlet point source close to but above the distributor inlet will reduce the concentration of solids in that particular portion of the reactor and result in an increase in solids concentration in other portions of the reactor. The overall result is a more even distribution of solids in an axial direction.

Downcomers. The patents make a variety of claims regarding the utilization of downcomers to effect catalyst redistribution and/or catalyst rejuvenation. The downcomer is specified as a vertical conduit which is open at both ends, fully submerged in the slurry with the bottom near the bottom of the reactor and the top near the top surface of the slurry. A patent issued to Behrmann et al. (73) claims a method for redistributing catalyst in a slurry reactor by use of a downcomer. The bottom of the downcomer is shielded by a baffle plate to divert gases from rising from the bottom and gas free slurry enters at the top and passes down the conduit and out at the bottom. Most, if not all, Exxon patents utilize downcomers with some attachment to the bottom of the conduit and this feature presumably relates to some finer technical and/or legal features. The preferred cross sectional area of the downcomer should be no more than 2% of the total cross sectional area of the entire reactor. An example is provided using the same equipment described under Pedrick et al. (74) in which the bubble column was run both with and without a downcomer in operation. In both cases rejuvenation tubes were operated in an equivalent manner. The results showed that axial distribution of the catalyst was more uniform when the downcomer was in operation, as shown in Figure 21.

A patent issued to Chang (75) claims a slurry bubble column reactor design incorporating a peripheral downcomer. The reactor comprises a double walled vessel wherein the inner vessel serves as the main reactor zone and the peripheral circumferential top rim of the inner vessel wall, having attached to it an inverted channel having an apex and two edges, being attached to the inner wall along the outer edge of the inverted channel. The second edge of the inverted channel extending over the main reaction zone creating a gas space within its inverted contour with a gas vent extending upward from the inverted channel. A liquid by-pass pipe extends from below the top of the liquid level interface through the inverted channel between the attachment of the inverted channel to the inner reactor wall and the apex of the channel

providing a means through which slurry flows into the peripheral downcomer section. This design is shown in Figure 22 wherein the outer edge 8A of the inverted channel is attached to the top of the inner vessel wall. The innermost edge is in contact with the slurry in the main reaction zone. Gas disengaging from the slurry trapped in the inverted channel exits into the gas disengagement space 5 through line 12 and slurry exits through line 13 onto the top of inverted channel outside the apex 10 through line 13 into the downcomer section 4. The higher density in the downcomer section promotes flow from the top of the vessel to the bottom. A more complete description of this invention can be obtained by referring to the patent specification.

Heat Transfer System. This is illustrated by a patent issued to Stark (76) which claims a method for removing heat from a FT reactor which comprises passing pentane through the tube-side of cooling tubes, vaporizing the pentane to a pressure greater than the pressure in the reaction zone and recovering the vaporized cooling medium. In a preferred embodiment of this invention the vaporized pentane is sent to an expander where the high pressure energy is recovered. The low pressure vapor leaving the expander is fed to a condenser where it is liquified and then pumped up to pressure and fed back to the reactor. The recovered energy can be used to drive compressors for an air separation plant or turbogenerators to generate electricity. A goal is to replace steam so that if a leak develops the cooling fluid will be an inert which will not damage the catalyst whereas steam would in nearly all cases be harmful to the catalyst.

Tube-in-Shell Reactor. A patent issued to Koros (77) claims a slurry FT reactor wherein the slurry catalyst is disposed in a plurality of vertically arranged tubes having a length/diameter ratio of at least 10 with each tube surrounded by a common heat transfer medium disposed within the shell of a shell and tube reactor, the heat transfer medium not in fluid communication with the slurry liquid. The description of the operation of a reactor comprising a 5.76 in (14.6 cm) ID x 50 ft (15.2 m) long pipe mounted in a 12 inch pipe cooling jacket was provided.

Liquid heights varied between 12 and 32 feet (3.66 and 9.75 m) with linear gas velocities up to 7.9 cm/sec. For a 2.1/1 H_2/CO synthesis gas mixture at a superficial velocity of 5 cm/sec, 2200 GHSV, reactor pressure of 285 psig (1.96 MPa), and steam jacket pressure of 140 psig (0.96 MPa), CO conversions in excess of 50% were obtained. The temperature of this run was not given.

Reactor Operation

Setting Operating Conditions. A patent issued to Herbolzheimer and Iglesia (78) claims a method for operating a solid-liquid-gas bubble column having a diameter >15 cm for FT synthesis over a supported cobalt catalyst in which the solids are fluidized by the gas. The invention comprises:

(a) injecting gas at an average gas velocity >2 cm/sec;

(b) fluidizing the particulate catalyst having an average diameter >5 μm in an expanded liquid column >3 meters in height and a particle settling velocity U_s and a dispersion coefficient D, such that (H expanded slurry height):

$$0.5\ (U_s - U_L) \leq \frac{D}{H},\ where\ H>3m$$

where

$$U_s = \frac{1}{18}\ d_p^2 \frac{\rho_s - \rho_l}{\mu}\ gf\ (C)$$

(C_p, catalyst concentration profile; p is density, μ, viscosity of wax; C, volume fraction of slurry; g, gravitational constant; d_p, particle diameter)

(c) operating at plug flow at a gas velocity U_g, expanded liquid height H, and dispersion coefficient D such that

$$U_g \geq 0.2 \frac{D}{H} \text{ where } H > 3\ m, U_g > 2\ cm/\text{sec}.$$

In one example using a Co-Re/TiO_2 catalyst having a density of 2.7 g/cm^3, a liquid density of 0.7 g/cm^3, and a wax viscosity of 0.01 g•cm/sec, the particle settling velocity is:

$$U_s\,(cm/\text{sec}) = 1.1x10^{-4}[d_p(\mu m)^2]$$

For a 60 μm average particle, U_s = 0.39 cm/sec. For a liquid velocity of 0.5 U_s, and a column height of 3 m, a gas velocity of 2 cm/sec provides a Peclet number of 10, which is the minimum gas velocity allowed that would maintain suspension of the solids in the column and maintain a plugflow operation in the column.

This patent and its European counterpart have attracted enormous attention, both technically and in the courts. It appears that enforcement of the patent would prohibit the use of a cobalt catalyst in a slurry bubble column reactor for any conditions that would have appeal for a commercial operation.

Catalyst Activation and Rejuvenation. A patent issued to Mitchell (79) claims a method for activating a fresh, reduced cobalt containing FT catalyst by treating the catalyst with H_2 in hydrocarbon liquids for a period sufficient to increase catalyst productivity. A patent having an identical specification issued to Mitchell (80) claims a process using the method of catalyst activation that is run under FT conditions. The method applies specifically to treating catalysts that had been previously reduced ex situ and exposed to the atmosphere before introduction into

a slurry system. Such catalysts are suspended in a slurry and treated with H_2 at hydrocarbon synthesis temperature and pressure with temperatures no lower than 40°C below hydrocarbon synthesis temperature. Another patent issued to Mitchell (81) claims a method for rejuvenating partially deactivated catalysts which is essentially the same procedure described above. An example for activating a 12% Co-1% Re on a 94% TiO_2-5% Al_2O_3 catalyst by reducing the catalyst with H_2 was given. Following reduction, catalyst was passivated with a CO/H_2 stream. This passivated catalyst was combined with wax in a slurry reactor and treated with H_2. Synthesis gas productivity over the treated catalyst increased to 100% relative to 25-60% productivity for the non-H_2 treated catalyst. The effect of several periods of catalyst rejuvenation during a 50 day run on catalyst productivity following this method is shown in Figure 23.

A patent issued to Pedrick et al. (74) claims a method by which reversibly deactivated particulate hydrocarbon synthesis catalyst in a gas-slurry reactor is rejuvenated and more uniformly distributed in the reactor. A hydrogen rich gas, injected into the bottom of a vertical draft tube which is fully immersed in the slurry, forces the catalyst up the draft tube while concomitantly reactivating the catalyst, which is discharged from the top into the upper portion of the slurry phase. The examples contained results from a series of balances made during a run in a 4 ft (1.2 m) diameter by 35 ft (10.7 m) high reactor that show both activation and axial redistribution of the catalyst. During the run, various combinations of draft tubes fed with H_2, which were commonly referred to as rejuvenation tubes, and draft tubes fed with tail gas, were employed. The maximum flue-gas fed draft tube plus rejuvenation tube cross-sectional area for any of the run conditions was 2.6% of the cross sectional area of the reactor. A feed gas mixture comprising 56% H_2/26% CO/13% CO_2/5% CH_4, by volume, was fed to the reactor containing a 12% Co-1% Re on a 94% TiO_2-5% Al_2O_3 slurry catalyst at 210-230°C and 20 atm (2.02 MPa).

When operating the reactor with two-2 inch (5.08 cm) diameter and two-4 inch (10.2 cm) diameter flue-gas fed draft tubes and one-3 inch (7.62 cm) diameter rejuvenation tube, the superficial velocities in the respective locations were:

inlet,	12-14 cm/sec;
outlet,	10.5-12.1 cm/sec;
draft tubes,	58-60 cm/sec;
rejuvenation tubes,	40-70 cm/sec.

Under these conditions the axial dispersion of the catalyst in the reactor improved significantly (Figure 24) and productivity increased from 41 to 69 (vol CO/hr/vol slurry). The overall reactor temperature differentials from the bottom to the top of the reactor for the individual balances using both lift and rejuvenation tubes was only a couple of degrees.

The effect of rejuvenation tubes on catalyst activity is shown in runs where both flue gas fed draft tubes as well as rejuvenation tubes were used. In a run sequence described in Figure 25, the decline in activity of catalyst was followed for a period of 3 days after which one 3 inch (7.62 cm) rejuvenation tube was brought on line. Immediately upon addition of H_2 an exotherm was observed followed by an immediate increase in catalyst activity recovering its initial activity in 1-2 days, after which it remained constant. After line-out, adding another rejuvenation tube provided no additional benefit. The exotherm in the rejuvenation tube was also used as a method to determine the degree of aging of the catalyst.

The beneficial effect of heating the rejuvenation tube to a temperature higher than the surrounding slurry was also demonstrated. Although the temperature in the rejuvenation tube is typically a few degrees higher than the surrounding slurry, through insulation of the tube and heating with steam, even higher temperatures can be attained. During one period in which the rejuvenation tube was heated sufficiently to raise the temperature an additional 5.6^{o}C, CO

conversion in the reactor increased from 26 to 36% over a 24 hr period whereas in a prior balance period without external heating being applied to the rejuvenation tube, CO conversion had dropped from 32 to 26% over a 12 hr period, as shown in Table 3 (82).

Exxon patents have covered a variety of procedures to effect catalyst rejuvenation that utilize operations within as well as external to the reactor. A number of patents pertain to catalyst rejuvenations that mirror the operations utilized for fluid cracking units. An example is a patent issued to Hsia (83) claims a FT process comprising a slurry reactor design coupled with a continuous rejuvenation reactor. Deactivated catalyst is reactivated and rejuvenated using an external rejuvenation reactor vessel to which catalyst from the synthesis reactor is continuously fed via a downcomer from the top of the slurry bed in the synthesis reactor to the bottom of a slurry bed in the external rejuvenation reactor vessel (see Figure 26). Likewise, rejuvenated catalyst is fed to the synthesis reactor via a downcomer from the top of the slurry bed in the rejuvenation reactor to the bottom of the slurry bed in the synthesis reactor. Slurry flow from synthesis reactor vessel to the rejuvenation vessel and the flow of rejuvenated catalyst back to the synthesis reactor vessel are driven by gravity since both vessels are under the same pressure. A drawing is included but no examples are given.

Removal of Catalyst Fines. A patent issued to Hsu and Robbins (84) claims a method for removing <1 μm particles adhering to catalyst particles containing a Group VIII metal supported on an inorganic refractory oxide. The removal of fines is important for wax separations. The method comprises dispersing the particles to which the <1 μm particles adhere in a liquid comprising a Fischer-Tropsch derived wax, agitating the dispersion and concentrating the <1 μm particles in the supernatant liquid and separating the <1 μm particles by decanting this layer from the larger particle containing phase. Although examples are given in which the liquid used in the particle classification step includes solvents other than Fischer-Tropsch derived wax, the claims

only apply to the latter (see Table 4). Catalysts stirred with FT wax at 130°C gave initially a filtration rate of 0.024L/cm^2/min which decreased to 0.20 cm^3/cm^2/min after stirring for 44 hours. Using the method of this invention of extended stirring and separating the decant after 3 cycles, the filtration rate improved to 0.06L/cm^2/min.

Apparatus for Substantially Plug-Flow, Slurry Phase Synthesis

Koros (77) has patented a slurry apparatus that permits a substantially plug-flow slurry-phase operation in an arrangement of multiple tube reactors in a shell. Thus, the concept of the mechanical part of the tube and shell reactor resembles a Sasol Arge reactor; however, numerous additional features are incorporated to permit slurry-phase operation.

In Figure 27, the syngas is added through 12 and is dispersed through sparger 14 into the liquid slurry medium, held at a level so as to maintain a gas-liquid interface, with the gas held in the space between 15, the slurry-gas interface and 18, a distributor tray.

A series of reactor zones, 20, are arranged within the shell, such as the ones shown by the example in Figure 28.

The reactor tubes are held in place by lower, 22, and upper, 28, tube sheets. The space between the distributor plate, 18, and the lower tube sheet, 22, may or may not contain catalyst in addition to the slurry liquid. A detail of the distribution zone is provided in Figure 29. The bubbly liquid from area 9 enters the tube/bubble cap 19A/19B. The bubble cap is aligned vertically with the reaction zone tube 20. The bubble cap is sized to give a pressure drop and injection velocity sufficient to decrease the size of the bubbles and to suspend the catalyst in the reaction zone (injection velocity about 20 to 100 ft/sec (6 to 30 m/sec)). The gas to liquid transfer rates are at least equal to the conversion rate of the syngas gas.

Preferred slurry materials are stated to be Fischer-Tropsch waxes and C_{16}-C_{18} hydrocarbons. The concentration of solids are usually about 10-50 wt.%, preferably 30-40 wt.% solids.

Catalyst/slurry addition/withdrawal may be effected through line 32. The region between tube sheets, 28 and 30, allows interconnection between the upper ends of the reaction zones for gas, liquid and catalyst. Tube sheet 30 holds filter cartridges, 31, which may be manufactured from sintered metal mesh, woven metal fibers, glass fibers, cloth or fibrous carbon, which can retain the catalyst particles while allowing the wax to pass. The filter cartridges are aligned vertically above each reaction zone. A gas-liquid disengagement zone lies above the filter cartridge tube sheet, and liquid product, separated from catalyst, can be withdrawn through tube 40 and/or 33. A demister, 41, separates gas from liquid droplets; residual gases are withdrawn through tube 42.

During operation the catalyst, 21, is preferably located in the reaction zone although some catalyst may be found in the liquid zones above or below the upper and lower tube sheets.

The catalyst most preferred is cobalt on titania (primarily in the rutile form) with less than about 70 m^2/g. Preferred promoters are stated to be rhenium and hafnium.

It is stated that "...catalyst particle size is not critical..." but is preferably in the 20-150 micron size range.

The example described the operation of a single reactor (6" o.d., 5.76" i.d., 15.24 cm o.d.; 14.63 cm i.d.) about 50 ft. (15.2 m) tall mounted inside a 12" (30 cm) pipe to serve as a cooling jacket. Feed gas to the reactor was preheated.

The catalyst was prepared by impregnating cobalt onto titania extrudates which were crushed and screened to give ca. 30 micron diameter particles (presumably the catalyst contained promoters). The catalyst was reduced in hydrogen in a fluidized bed, and then the slurry wax

was introduced. Following a prescribed procedure of start-up, they attained a CO conversion in excess of 50% at GHSV = 2800. Following a brief reactor upset, the unit was restarted at a higher steam jacket pressure (140 psig; 0.96 MPa) and higher reactor pressure (285 psig, 2.0 MPa at the reactor gas outlet). The reactor maintained CO conversion of 60-70% (2800-3600 hr^{-1}) for nearly seven days of synthesis. This material was stated to be a "...very active HCS catalyst." Methane selectivities were in the range of 2.7 to 3.2%. Assuming the steam jacket pressure represents steam/water, this corresponds to 354°F (178°C); presumably the reactor side would not be at a much higher temperature.

Mobil

The initial runs in the pilot plant (Figures 30 and 31) at Mobil Oil (48,49), based upon the catalyst compositions in Mobil's patents, utilized a catalyst with a composition that resembles the one reported for Kölbel's work and the catalyst used for the La Porte Run II (low, not high, Cu content). Mobil's data from work funded by DOE have become the "standard" for both economic (e.g., 85) and technological evaluations (e.g., 856. The first three runs in the Mobil plant were conducted using a catalyst that produced low molecular weight materials; during the third run a potassium salt was added at 81 days-on-stream and this decreased the methane + ethane production from about 13 to 18 wt.% without significantly lowering the CO conversion; however, operational upsets prevented a valid assessment of the impact of the added alkali (49). The later runs were in the high molecular weight product mode (wax mode). In most runs, Mobil operated with about a 20 wt.% slurry catalyst loading. In run 8, the aging rate of the iron catalyst operated at 250°C, 1.48 MPa and 1.4 NL/gFe-hr was such that half the activity would be lost during 24 days; later in the run the catalyst half-life was 13 days when the temperature and pressure were increased. Mobil workers indicate that the catalyst used in this run was not acceptable because of its high aging rate. In run 9, a surprisingly low methane + ethane make

(about 5.4 wt.%) was obtained. The catalyst was the "same" as had been used in a prior run where this was not observed; the only difference noted was that the low methane + ethane catalyst had a lower surface area. An operational upset terminated the effective operation at day 10. In run 10, Mobil workers reported that the catalyst could not be fully activated at synthesis conditions.

Run 12 was operated for 17 days at constant conditions and "This period represented the finest example of low methane + ethane [4.1 wt.%] mode operation we have ever produced in the pilot plant." Wax production was about 60 wt.%. An operational upset occurred on day 17 and afterwards catalyst settling and low catalyst activity were problems that could not be overcome.

Run 13 was a repeat of run 12 and good operation was accomplished for 35 days-on-stream, after which catalyst settling became a problem. Viewing the pictures of the catalyst, Mobil was utilizing particles in the 1-5 micron range, and the final catalyst particles were considerably larger following removal from the reactor. It is not clear whether this is due to catalyst particle growth or, more likely, cementing together several particles by reactor wax. It is not clear, if wax caused the particle size increase, whether this occurred in the reactor itself or was an artifact introduced during catalyst collection and subsequent treatment.

As stated above, the Mobil data have replaced the Kölbel data as the "standard" for slurry F.-T. operation. Data for reactor wax yield of 46 wt.% are shown in Figure 32. This data has been utilized by Bechtel Corp. for their analysis of slurry F.-T. operations. They consider the data to consist of three regions: methane (α_1) that is higher than ASF; C_2-C_4 (α_2) and reactor wax (α_3). Theoretical curves for reactor wax make of 9.49 wt. % (low alpha data), 46.02 (intermediate alpha data) and 75.95 (high alpha data) are shown in Figure 33.

Thus, the Mobil data, in spite of operational problems, represents the best data that is available in the open literature in sufficient detail that its quality can be adequately judged.

Gulf Oil (Now Part of Chevron)

During this period Gulf Oil conducted a major effort to develop processes that would enable them to convert natural gas to transportation fuels and to petrochemicals. Much of this work was devoted to the development of active catalysts and to the operation of fixed-bed reactors. An outgrowth of this effort was the development of the Gulf-Badger FTS process. Much, if not at all, of the rights to the Gulf FTS technology was obtained by Shell following the incorporation of Gulf Oil into Chevron. Gulf did some work using a slurry bubble column reactor and that is described in the following.

A 1985 patent (87) obtained by Gulf Oil claimed a process for the conversion of synthesis gas using a finely divided catalyst (ca. 10-110 microns) dispersed in a fluid medium. The catalyst consisted essentially of cobalt and ruthenium on a support.

The process is outlined in Figure 34 and does not differ significantly from one used by Kölbel and coworkers (45). In the reactor, the catalyst particles are suspended in a liquid medium having sufficient viscosity to ensure that the particles remain in suspension and having a volatility that is low enough to avoid loss due to vaporization within the reactor. The catalyst is present in the slurry at concentrations from about 2 to 40 wt.%. The catalyst bulk density can be in the range of 0.25 to 0.90. The gas flow enters at a rate sufficient to suspend all of the catalyst particles in the system without settling. The gas flow rate will be selected depending upon the slurry concentration, catalyst density, suspending medium density and viscosity, and particular particle size utilized. Suitable gas flow rates include, for example, from about 2 to 40, preferably from about 6 to 10 cm/sec. The pressure range covered is from about 1 to 70 atm. Light hydrocarbon products, such as C_{20} and below, are withdrawn overhead through a line designated

32 in Figure 34. A portion of the heavier products and catalyst slurry is withdrawn through line 38 and is passed to a separation zone. A concentrated catalyst/slurry fraction is returned to the reactor while a portion of the catalyst/slurry may be passed through a regeneration zone 54 before being returned to the reactor. Heavy products with low catalyst concentration are revolved through line 44. Separation by filtration can be utilized for separating catalyst from the suspending liquid (vessel 40).

The data obtained in the slurry reactor were compared to a run in the fixed bed reactor with the same catalyst formulation. Gas entered the reactor at the bottom through a stainless steel screen in the form of small bubbles. Hydrocarbon was removed from the top through a heated line. The pressure was 160 psig (1.08 MPa) and the gas flow with $H_2/CO = 1.95$ was 1826 cm/s. Initially the temperature was 225°C but was increased and held at several higher temperatures to obtain additional conversion data. The increase in conversion with increasing temperature gives an activation energy of 20.5 kcal/mol (85.7 kJ/mol). At 225°C, methane is 8.4 wt.% of the product and increases to 15.6 wt.% at 240°C. As the temperature increases, the C_5+ fraction gradually decreases (Figure 35) and the C_5-C_{20} fraction increases, indicating that the alpha value decreases with increasing temperature; however, there is not sufficient data to obtain reliable values of alpha (Table 5).

Period III 1985-2000

Sasol

Sasol has reported general, but few specific, details about the development and operation of their slurry reactor operations. Sasol's work on a small scale began in the early 1980s (51). In 1990, a slurry bed with a diameter of about 1 m was commissioned and the results confirmed their early expectations. In a bold move, Sasol decided to construct a commercial scale slurry reactor (5 m diameter, 22 m high) rather than two 5,000 tube tubular-fixed-bed reactors for the

expansion of their low temperature operation. The commercial reactor was commissioned in May 1993 and has been reported to operate successfully since that time.

Sasol uses a separate catalyst pretreatment reactor in which hydrogen reduction (extent of reduction not specified) is used to activate an iron catalyst prior to its introduction into the slurry reactor. During operation, it is understood that an activated catalyst batch is on "stand-by" so that if a significant upset, such as a slug of sulfur to produce severe catalyst poisoning, causes a significant loss in productivity, the reactor is emptied and a fresh catalyst batch added during a short period of a few hours. On-line catalyst removal and additions are reported to be done without difficulty. Based upon reports of the extent of sulfur poisoning in the fixed-bed ARGE reactors, it should not be surprising if Sasol operators had made several replacements of the catalyst inventory during the seven years of commercial operation.

The authors (51) describe the churning nature of the slurry-base bubble interactions, implying that the Sasol operation operates in the bubbly, rather than slug, flow condition. Because of the isothermal nature of the slurry reactor, the operating temperature can be much higher than in a fixed-bed tubular reactor without fear of hot spots leading to carbon formation and break-up of the catalyst. Hot-spots in the fixed-bed reactor presumably allows for the catalyst in the hot-spot to reach a temperature sufficiently above that of the reactor set-temperature so that carbon formation and rapid catalyst deactivation become possible.

It is reported that for an iron catalyst, the product slate is considerable affected by the age of the catalyst, with wax selectivities decreasing with time. However, "by proper scheduling of catalyst renewal, it is possible to maintain a steady selectivity profile for a single reactor while minimizing the catalyst consumption." It therefore appears that the Sasol operation involves a regular schedule of catalyst addition, presumably to replace catalyst that is intentionally withdrawn as well as that which is lost as catalyst fines due to catalyst attrition.

Foam was found to build up in the reactor under certain conditions but it was reported that this could be prevented by modifying operation procedures. "Separation of gas from the entrained slurry was another development that was easily resolved.", implying that slurry carry-over can be a problem if not handled properly.

Several approaches were tried at Sasol in order to effect wax separation form the catalyst containing slurry. These included close attention to the production of the catalyst and its physical characteristics as well as to the separation processes. The technique currently in use in the commercial operation for wax/slurry separation is considered to be proprietary information. The removal of wax, but not catalyst, is a critical aspect of bubble column reactor operation. While Sasol patents address this, the filter operation is poorly described in most of these.

China

The Chinese have operated a two stage process involving slurry F.-T. synthesis with an iron catalyst and fixed-bed cracking/oligomerization processing using a ZSM-5 catalyst to convert the F.-T. product to gasoline range fuels (88). The F.-T. slurry reactor was 4 cm in diameter and 450 cm in height. The reactor, in a schematic form, is very similar to the one used by Mobil Oil (Figures 30 and 31). They used an unsupported precipitated iron catalyst with a typical composition of Fe:Cu:K_2O = 99.5:0.5:0.29. The sample of catalyst used in the slurry reactor had obviously been calcined [based on CAER work, at temperatures of at least 300^oC] since the XRD analysis showed that the main crystal phase was α-Fe_2O_3. The authors indicate that diffusion effects could be neglected for their runs. It appears that they used a slurry that contained 12% catalyst. Most of the published data concerning runs with their pilot plant are for the product following processing with the ZSM-5 catalyst. However, based upon data presumed to be for the F.-T. only operation, the liquid phase is reported to have a composition of approximately 70% C_{5-12}, 27 % C_{13-22} and 3% C_{22+}. Thus, based upon the catalyst composition,

the product distribution would be considered to originate from a low-alpha mode of operation, and the composition of the catalyst is consistent with this. Furthermore, the low-alpha mode would probably be preferred for subsequent conversion of the F.-T. products with a ZSM-5 catalyst in the second stage.

The output during the course of a 1,000 hour (40 day) run declined due to loss of catalyst. From the data published for the Chinese F.-T. only operation, it is difficult to reach definitive conclusions on catalyst performance.

Syntroleum

While Syntroleum began work of FTS earlier than 1985, their visibility dates to this period. Much of the early work they reported did not involve liquid-phase synthesis and will not be covered. The first significant public information for liquid-phase synthesis was the construction and operation of a 70 bbl/day integrated pilot plant at ARCO's Cherry Point Refinery near Bellingham, Washington (89). This project was led by ARCO's upstream technology unit. The individual process units were modular in design, were constructed in Tulsa, Oklahoma, and shipped to the site where they were erected (90). The proprietary reactor design for the autothermal reformer was used to generate syngas from natural gas (actually a refinery dry gas stream substitute) and air. The return to the use of air for the generation of the synthesis gas is a unique feature of the Syntroleum process. For the FTS component, they tested their advanced reactor design and a proprietary cobalt microsphere catalyst. The system is described as, "...a moving bed system, where catalyst microspheres are suspended by the gas in circulating liquid." The catalyst is reported to have high activity, attrition resistance, excellent hydrodynamic properties and is readily separated from the hydrocarbon products. The plant is reported to operate in a turbulent mixing regime that is associated with commercial sized moving bed reactors. After several thousand hours of operation under widely varying conditions, there

was no evidence of significant attrition within the unit while catalyst life and activity maintenance met or exceeded expectations.

A recent patent application describes a Syntroleum liquid-phase system that utilizes a fixed catalyst bed (91). To accomplish this, they employ a catalyst that has a voidage ratio greater than approximately 0.45 or 0.6; in another version of this they utilize a catalyst with a voidage ratio greater than 0.4 and a catalyst concentration in the reactor volume of at least 10%. The catalyst is to have a productivity of 200-4000 vol CO/volume catalyst/hour or greater during at least a 600 hour run. In one version, a saturator precedes the reactor to generate a syngas saturated liquid which is used as the feed to the fixed-bed liquid-phase reactor. Another version utilizes a reactor consisting of tubes in a shell that receives the liquid feed that is saturated with syngas. In another version, the reactor may consist of any version from a single vessel with a length/diameter (L/D) greater than 5 to a shell in a tube vessel with a high L/D that receives liquid and syngas feed streams. In another version, the single vessel reactor is filled with a fixed catalyst bed submerged in a liquid and the feed is only syngas. Another reactor resembles the Dortflund type reactor with a series of fixed catalyst beds within a reactor shell, with each reactor bed having the capability of receiving fresh liquid and syngas feed or not, as desired for the operation (Figure 36). In another version the reactor is essentially the same as in a bubble column reactor except that a fixed catalyst bed is utilized.

Rentech

Rentech reports that they have operated during 1982-1983 a commercial-scale gas to liquids facility. This facility utilized a Pueblo, Colorado landfill to produce gas sufficient for a plant with a capacity of about 235 bbl/day of liquid hydrocarbons. This plant has a capacity that is about the same as the reactor for the demonstration plant that Exxon operated at Baton Rouge,

LA. It was soon learned that the landfill was unable to produce sufficient amounts of gas and the operation was discontinued within three months after attainment of full-scale production.

Rentech has at least nine patents to cover their technology. The bodies of most of these patents are either the same or very similar and provides a concise summary of Fischer-Tropsch synthesis that can serve as an excellent introduction for the novice in this area. The claims are more modest in coverage than the body of the patents. Furthermore, it is sometimes difficult to discern when the cited examples are based on theoretical calculations and when they are based upon data obtained by Rentech.

Rentech has operated a 6 inch (0.15 m) diameter, 8 foot (2.54 m) tall slurry reactor with an iron catalyst. They report that they have designed, built and tested two 6-foot (1.83 m) diameter slurry reactors and have produced catalysts batches of more than 7.5 tons (6810 kg) for use in these reactors (92). The wax/slurry separation, as reported in 1992, was accomplished using an external cross-flow filter. Using this technique, separation was still a problem. They apparently utilized later in their pilot plant studies an external separator that involved gravity settling to concentrate a catalyst/wax slurry for return to the bottom of the reactor; this approach was apparently very similar in design to the one Mobil Oil utilized in the work they conducted for their DOE contracts.

U.S. DOE - La Porte

Air Products operated DOE's Alternative Fuels Development Unit, located in LaPorte, Texas. The unit was initially designed to conduct methanol synthesis in the slurry phase and was later expanded to include development work in FTS liquid-phase operations starting in 1992. The methanol synthesis work was very successful and resulted in a commercial operation (reactor 7.5 ft (2.3 m) diameter and 70 ft (21.3 m) tall) at Tennessee Eastman in Kingsport, Tennessee and the initial commercial scale has now been expanded in size.

Four runs for FTS have been described to date (93). The bubble column reactor is 22.5 inch (0.57 m) and 28.3 feet (8.6 m) top to bottom. The actual slurry space is 20 feet (6.2 m) with the remainder serving as a space for vapor disengagement. One inch (2.54 cm) cooling tubes occupy less than 5% of the reactor cross-section (Figure 37). The first two runs utilized iron catalysts: for Run I a high alpha catalyst was used and slurry/wax separation was a problem (94,95) and for Run II a low alpha catalyst was used (96). Apart from the separations problem, Run I was successful. For Run II, the initial activation was attempted with a 44 wt.% catalyst concentration and the run had to be aborted due to slurry thickening due to carbon formation and particle agglomeration . The second portion of Run II utilized 29 wt.% catalyst concentration and both the activation and synthesis periods followed closely the results from work in a CSTR that were conducted at our lab.

Shell runs at LaPorte. Run III utilized Shell's proprietary catalyst and wax to make a slurry that contained 41.2 wt.% cobalt-based catalyst. During the run a number of operating conditions were to be tested: H_2/CO ratio of 1.18 to 2.07, inlet superficial gas velocity from 0.31 to 0.73 ft/sec (9.5 to 22.3 cm/sec), CO conversion of 80 to 90%, temperature from 210 to 250^{o}C, and pressure from 520 to 710 psig (3.6 to 4.9 MPa). Recycle was utilized to obtain the high total CO conversion levels. During run III a productivity of 126 g hydrocarbon/hr-liter slurry was obtained. Poor catalyst integrity caused slurry thickening and mass transfer limitations. Catalyst break-down limited the operational time for Run II. Run IV was a repeat of run III but with a new catalyst formulation and a proprietary filtration system. Run IV was accomplished successfully and covered the period of time scheduled. It appears that the products were lighter than normally expected for a cobalt catalyst; methane was in the range of 20 wt% of the products and the alpha value was in the 0.85-0.89 range. Using the planned operational conditions, we have estimated the productivity for the run. Assuming a slurry density of 2 g/cm^3 and the reactor

productivity of 150 g hydrocarbon/L reactor volume/hr, we calculate a productivity of 0.18 g hydrocarbon/g catalyst/hr. The same productivity with a 29 wt.% catalyst slurry would provide a productivity of 0.27 g hydrocarbon/g cat/hr. Assuming that the 29 wt.% slurry has a density of only 1 g/cm^3, the productivity would be 0.54 g hydrocarbon/g cat/hr.

Products

Low Temperature vs High Temperature

The product distribution reported by Kölbel was typical of high temperature (low alpha) operation: C_{1-2}:C_{3-4}:gasoline (25-190^{o}C):diesel oil (190-310^{o}C):heavies (>310^{o}C) = 7:17:62:10:3 (97). The olefin content of the C_{2-4}, gasoline and diesel fractions were 72, 74, and 45%, respectively. Kölbel reported in less detail on runs made to produce "medium" and "high" molecular weight products in addition to the ones described above. These products are shown in Table 6. As noted, the production of hydrocarbons per m^3 gas increases as the molecular weight of the products increases; however, in no instance does it approach the theoretical yield of 208 g/m^3. [The theoretical yield is calculated on the basis that all carbon added as CO is converted to hydrocarbons except for the minimum amount of CO that must be shifted by the water-gas shift reaction to produce sufficient hydrogen to augment that of the feed to satisfy the stoichiometry of the synthesis equation.] On the other hand, Mobil runs consistently produced greater than 200 g/m^3. This low hydrocarbon productivity in Kölbel's work is apparently a problem that many investigators have struggled with.

The quality of a diesel fuel can vary considerably. Cetane number is used as one measure of the quality of a diesel fuel much in the same manner as octane number is used for gasoline. However, octane number and cetane may be viewed as opposites. Thus, highly branched paraffins, olefins and aromatics are desirable, and normal paraffins undesirable, components of a fuel if one wants a high octane number; on the other hand, n-paraffins are desirable and highly

branched paraffins, olefins and aromatics are undesirable components for diesel fuel with a high cetane number. In viewing the high molecular weight product slate in Table 6, it is noted that 33% of the product is diesel and 50% is heavier molecular weight material that must ultimately be cracked to produce gasoline and diesel. As produced with an iron catalyst, the diesel fraction of the products (straight-run diesel) contains a significant amount of olefins, and consequently a relatively low cetane number. However, when this fraction is hydrogenated it will contain predominantly (90% or greater) n-paraffins, and this fraction will have a high cetane number (at or greater than 70). Because there is little difference in the ratio of i-/n-paraffin fraction of the hydrogenated straight-run diesel from an iron catalyst and the straight-run diesel from a cobalt catalyst, the straight run diesel produced by either catalyst will be the same, or very similar. Furthermore, it requires the same amount of hydrogen to produce a paraffin irrespective of whether it is produced indirectly by hydrogenating an initially formed olefin produced by iron catalysis or produced directly using a cobalt catalyst. Based upon straight-run diesel, there should therefore be no difference in the quality of the materials produced using either catalyst. Likewise, the >450^{o}C fraction of the iron and cobalt catalyst is composed essentially of n-paraffins, either before or following a hydrogenation step, so that, while the quality of the diesel fuel produced by hydrocracking may depend upon the hydrocracking process utilized, it should not depend upon whether the >450^{o}C fraction is obtained by iron or cobalt catalysis.

It cannot be overemphasized that diesel is not a sufficient specification to use to compare catalysts and/or processes. Straight-run diesel and diesel obtained from hydrocracking will not, in general, have the same properties even when both are composed only of paraffins. The major reason for this is that hydrocracking normally produces a significant fraction of monobranched paraffins; in fact, the classical bifunctional hydrocracking mechanism would produce an i-/n-paraffin ratio of 1 or even greater. Thus, it is important, when discussing cetane number, to

specify whether one refers to what is straight-run diesel, diesel produced by hydrocracking or some blend of these two products. For blending with petroleum-derived diesel to produce a more environmentally friendly transportation fuel, it is desirable that the F.-T. product have the highest possible cetane number. From the point of view of obtaining a superior diesel for blending with petroleum-derived diesel, it appears that straight-run F.-T. diesel would be preferred over hydrocracked diesel when the decision is based on cetane number.

In considering the medium and high molecular weight cases shown above, an equal amount of blended diesel would be produced by combining the straight-run and hydrocracked diesel fraction only if the hydrocracking selectivity was such that it produced only 32 % diesel fraction. The selectivity for hydrocracking is much greater than 32% so that it is obvious that more diesel will be produced from the "high" operation in Table 6. However, for a run at La Porte to generate diesel to make a large-scale test, both straight-run and hydrocracked diesel could be produced using either the medium or high molecular weight mode of operation. For the medium molecular weight case the straight-run fraction would dominate over the hydrocracked diesel whereas the opposite would result from the high molecular weight mode of operation.

Wax/Slurry Separation

In general, there are two approaches to this task: in-reactor separators that retain the slurry while allowing clean wax to pass and external separators where slurry is removed from the reactor and separation is effected in an external separator. Both of these approaches were utilized by Kölbel in his work in the 1950s.

Wax/slurry separation is not needed for fluid bed reactor operation since wax cannot form without causing agglomeration of the catalyst with loss of fluidization. Robust iron catalysts have been formulated for operation in fluid beds and are in commercial operation at Sasol. Presumably supported cobalt catalysts could be operated in this reactor type since fluid

catalytic cracking catalysts have been formulated with the necessary robustness and some form of these materials could be utilized as support for cobalt catalysts (98).

Separation of wax from supported cobalt catalysts is much easier than for an unsupported iron catalyst. A major reason for this is that the support material (alumina, silica, titania, etc) can usually be prepared so that it has the attrition resistance that is required for operation in a fixed or slurry bubble column reactor. While there were problems with one supported cobalt catalyst during operations at the La Porte facility, an improved version of the catalyst could be separated successfully in an external separator that utilized a cross flow filter with slurry circulation using a pump (99). However, operating the same plant with spray dried iron catalyst, the filter became plugged within a few hours or days of operation (100).

Mobil utilized an external system in which slurry is circulated by density differences and the time in the separator is sufficient for the slurry to settle so that solids-rich and a nearly solids free zones are formed; the clean wax is removed from the solids free zone and the solids rich fraction is returned to the bottom of the column. A similar apparatus has been utilized by Rentech, at least in their smaller pilot plant. A number of external filtration systems as, for example, (101) have been patented.

While separation devices have been described in the body of several patents, fewer patents describe filtration devices within the reactor. Most of the patents that describe a reactor mention internal or external separation but usually do not provide details. Statoil patents (102,103) describe a vertical cylindrical filter element in the form of a fine meshed screen, although alternatives could be used, located inside the reactor within the slurry. In the examples, models are used for the separation rather than a working reactor. Sasol has described in some detail their operation in a large pilot plant with a slurry bubble column reactor using a separation

procedure, in one particular case, a spiral wound (candle) filter (104). An improved candle filter has also been described (105).

A process for the separation of a catalyst from FT slurry has been patented by US DOE (106) This process separates the catalyst from the wax product using a dense gas and/or liquid extraction in which the organic compounds in the wax are dissolved and carried away from the insoluble inorganic catalyst particles. This work utilized wax/slurry generated at the LaPorte facility and the separation work was conducted by Kerr-McGee Corp (107). The use of near-critical fluid extraction to remove wax product to provide a solids enriched stream to return to the reactor has also been studied and has shown promise (108). For the latter technique, the extraction would likely be effected at temperatures above the reactor temperature and how this impacts the catalyst remains to be determined.

In summary, the separation of wax from a supported cobalt catalyst slurry will be much easier than from an unsupported iron catalyst. The unsupported iron catalyst rapidly attrits to produce small (1-3 micron) particles (109) that blind the pore openings of the filter. It would therefore be desirable to develop a filter material that can handle the 1-3 micron sized particles without blinding.

In the British work at Greenwich, the catalyst, after "break-in," was 1-3 μm in size. A liquid slip-stream was withdrawn continuously from the reactor and catalyst was recovered in a multiple-stage, gravity-settling apparatus. Because of the relatively rapid catalyst aging rates as well as significant coke formation, reliable data for wax/catalyst separation is not available from this work.

A finely divided powder catalyst was utilized by Kölbel and coworkers (45); the starting material has a particle size <30μm but sizes during or after use are not provided. The liquid level in the reactor was maintained by a float-device. A slip-stream, utilized when excess liquid

was produced, allowed for wax/catalyst separation by pressure filtration. Kölbel operated most of the times under conditions where the liquid inventory of the reactor could be maintained **only by adding** heavier liquid products along with the synthesis gas and wax/catalyst separation was not a problem. As an alternative, wax/catalyst separation could be effected by centrifugation. Capability for replacement of the catalyst was included in the process although catalyst replacement rates are not given. Data are not available to enable one to reach valid conclusions about the effectiveness of the wax/catalyst separation because of the lack of knowledge of catalyst addition rates. Based on the data in Table 6 for the "low" operating conditions, an upper limit of 15% reactor-wax removal can be set, and in practice it should have been much lower.

Supercritical Phase Fischer-Tropsch Synthesis

While supercritical phase synthesis is not strictly a liquid phase synthesis, it approaches liquid phase when operating at higher densities. It is claimed that three main advantages of the supercritical synthesis are: (1) rapid diffusion of reactants, (2) effective removal of reaction heat and (3) effective extraction of wax, α-olefins and water. Thus, the supercritical operation could, if item 3 is accomplished, decrease or eliminate secondary reactions.

Yokota et al. (110) compared the results of the operation of three types of reactors: fixed-bed, liquid and supercritical. In order to make an effective comparison the feed consisted of 22-36 % synthesis gas with the remainder being diluent (nitrogen for the fixed-bed, hexadecane and nitrogen for the liquid, and n-hexane for the supercritical). An iron catalyst was utilized and had the following composition by wt. fraction: Fe, 83.5; Ca, 2.1; Al, 1.5; Si, 0.4; K, 0.5 or Fe, 99; Cu, 0.3; K, 0.3. Thus, both iron catalysts were of the low alpha type utilized by Mobil Oil and La Porte Run II. The total pressure was 5 MPa, 270^{o}C, $H_2/CO = 1$ and W/F ($CO + H_2$) = 10 g-cat h/mol. Each run was conducted for 6 hours. Under no circumstances should it be considered that a steady-state operation was attained.

The authors show the CO conversion, CO_2 yield and chain-growth probabilities for the fixed-bed, supercritical and slurry phase reactors as 33.0, 30.2 and 27.9; 8.65, 7.52 and 9.15; and 0.84, 0.83 and 0.80, respectively. They considered these differences to be significant and attribute the lower CO_2 yield for the supercritical operation as being due to the increased removal of water from the reactor. The reported chain growth probabilities appear high for an iron catalyst that contains such a low level of potassium. These data may be viewed as suggestive.

Fujimoto et al. (111) report that the addition of a small amount of heavy 1-alkene in a supercritical-phase or liquid-phase F.-T. reaction medium greatly enhanced the selectivity of wax products, along with increased CO conversion and suppressed methane selectivity. A cobalt-silica catalyst that contained La was used. The authors reported that the addition of 1-tetradecene or 1-hexadecene significantly decreased the hydrocarbon production for carbon-number products lower than that of the added alkene, and increased significantly the production rate of the carbon-number products with higher carbon numbers that the added alkene (Figure 38). The data shown in Figure 38 are astounding. When alkenes were not added the production rate of the products above carbon number 15 decreased with increasing carbon number; this is expected and observed in normal F.-T. synthesis. However, when the alkene is added, the hydrocarbon production with carbon-numbers above that of the added alkene become essentially constant; i.e., independent of carbon number. It appears that this requires the added alkene to initiate chain growth that differs from that of the F.-T. reaction. If the only impact of the alkene was to initiate additional growing chains, the product distribution above the carbon number of the added alkene should be determined by the Anderson-Schulz-Flory distribution; i.e., the rate of production of all higher carbon-number products may increase but the products should still be produced in the same ratio as they were when no alkene was added. Thus, the amounts of higher carbon-number products may increase but the alpha value should be the same as when the alkene

was not added. The data obtained when 1-heptene, in contrast to 1-tetradecene or 1-hexadecene, was added is in better agreement with the expectation.

Lang et al. (112) utilized a precipitated iron catalyst in a fixed-bed reactor and found that the catalyst activity and lumped hydrocarbon product distribution under the supercritical conditions were similar to those obtained during reaction at the baseline (non-supercritical) conditions. This is in contrast to the views expressed above. Lang et al., (112) reported slightly higher selectivities for the 1-alkenes during supercritical operation (Figure 39). This suggests to them that the F.-T. reaction is not diffusionally limited under their reaction conditions. The higher alkene production during supercritical operation was due to higher diffusivities and desorption rates of the high molecular weight olefins relative to those under normal F.-T. conditions.

Summary

The major attention, both industrial and academic, during the past 10 years, has been given to the slurry bubble column reactor. The slurry phase methanol process has been developed and operated in a commercial setting (113-115). Deckwer has published a major treatise on bubble column reactors (116). Saxena (117) has recently reviewed the use of bubble column reactors in FTS. The reader is referred to these for description of reactor details.

Two major types of slurry bubble column reactors are possible and these are illustrated in Figure 40 (77,118). The reactor containing cooling coils immersed in the slurry is the one that is most frequently encountered (77,78,92,105,118-123). The concept of one type of reactor patented by Exxon has many similarities to the Arge fixed bed reactor except the fixed catalyst bed has been replaced with a slurry catalyst; both utilize the “tube-in-a-shell” reactor concept (77).

As with the three-phase slurry reactor in other applications, the distributor plate is treated as a proprietary topic. Kölbel contends that when the bubble column reactor is operated in the proper gas flow range the bubbles within the reactor will be in dynamic equilibrium with the formation of larger bubbles and their spontaneous break-up.

For modeling, the bubbles within the slurry are usually considered to have a spherical shape, their size distribution taken as some average size, and their breakup and reformation are neglected. The work conducted at Ohio State show that the bubbles are clearly not spherical but are as shown in Figure 41 (124). The influence of elevated pressure and temperature on the shape and rise velocity of a single bubble in a liquid-solid suspension has been investigated in a unique experimental setup (e.g., 125). For very low flows (gas velocity of 0.01 m/s) it is possible to have a reasonably uniform distribution of small (less than 5 mm) bubbles that rise vertically (126) and can be modeled as plug flow. However, to operate in the small bubble, plug flow regime DeSwart et al. (126) calculates that it would require seventeen (17) 11 m diameter reactors to produce the same amount of product as could be produced in four 7.5 m diameter reactors that operate in the churn turbulent slurry regime.

It is found that the bubble rise velocity decreases with increasing pressure and with decreasing temperature. This is mainly due to the changes in the densities of the gas and the liquid velocity. Not only do the bubbles have a shape like a comet with a tail of smaller bubbles, they also do not rise straight to the vertical but exhibit a corkscrew path to the top of the reactor, leaving regions rich in bubbles and regions with a lower concentration (Figure 42) (127). The bubble shape is frequently modeled with variable aspect ratios as cross sections of ellipsoids (128). A representative status of the activities in this research area may be obtained from recent references (124,129-140).

The US DOE has a major effort to understand the many variables affecting the performance of a bubble column reactor. Dudukovic and Toseland (141) outlined the cooperative study by Air Products & Chemicals (APC), Ohio State University (OSU), Sandia National Laboratory (SNL) and Washington University (WU); this program is outlined in Figure 43. The efforts of this group have developed valuable unique experimental techniques for the measurement of gas holdup, velocity and eddy diffusivities in bubble columns. They have obtained data that allows improved insight in churn-turbulent flow and have assessed the impact of various effects (internals, solids concentration, high gas velocity, pressure, etc.). General ideal flow pattern based models do not reflect bubble column reality; to date the models are based on a combination where some parameters are evaluated from first principles and some from the data base.

It has been observed that the time-dependent flow behavior in a cylindrical column is chaotic and not predictable. However, some periodic structures may be detected in the velocity time series in the axial and tangential direction the may lead to some kind of periodicity (142). It has been reported that the transition from the homogeneous to the heterogeneous flow regime in bubble columns can be quantitatively found with high accuracy by analyzing the chaotic characteristics of the pressure fluctuation signal. A distinctive feature of the pressure signal from bubble columns is that it is composed of two different parts: a low frequency part resulting from the motion of the large bubbles and a high frequency part resulting from all other processes (coalescence, collapse, breakup, etc) (143). Delnoij (144) conducted an extensive study and concluded that their computed flow structures resembled the experimentally observed patterns although the time-dependent behavior predicted by the model differed from that observed in their bubble column.

The extensive theoretical and experimental data for bubble column reactors has been applied to situations that are applicable to FTS. Inga and Morsi (86,145) have constructed a 0.3 m diameter, 2.8 m tall slurry bubble column reactor and have operated this in the churn-turbulent regime with catalyst concentrations up to 50 wt.% and pressures to 8 bars. The impact of gas velocity, pressure and catalyst concentration on gas holdup (V_G) has been determined and it was found that under given operating conditions, the gas bubbles can be classified into "small" and "large" bubbles (86,145). The "large" bubbles exhibit plug flow behavior but the "small" bubbles recirculated with the liquid. The gas holdup, (V_G), increases with superficial gas velocity and pressure and decreases with catalyst concentration. At high catalyst loading, coalescence of gas bubbles increased, reducing the number of small bubbles, and the gas interfacial area. The gas/liquid mass transfer coefficient ($k_i a$) values follow the trends of the gas/liquid interfacial area (146).

Van der Laan (147) reported attempts to model FT in a bubble column reactor. His model exhibits well mixed liquid and two gas bubble regimes: small bubbles that are well mixed and large bubbles that exhibit plug flow behavior (Figure 44). Van der Laan also provides a summary of bubble column reactor models that others have utilized (Tables 7 and 8). He concluded that the FT SBCR is reaction controlled due to the low activity of the iron catalyst and the volumetric mass transfer coefficient of the large bubbles due to frequent bubble coalescence and breakup.

Groups are now beginning to apply multicomponent reaction engineering models for FTS in bubble column reactors. Recent examples can be found in the references (147-149). Van der Laan (147) provides the following summary of slurry bubble column reactors:

> "A number of patents deal with modifications of Fischer-Tropsch slurry bubble column reactors to reduce the back-mixing of both the liquid and the gas phase

(124,150-152) described the influence of various degrees of back-mixing on the selectivity and productivity based on kinetic data obtained over a Co/TiO_2 catalyst, both in plug flow (fixed bed), bubble column and completely mixed reactors (CSTR). Arcuri (150) claimed that the productivity in a slurry bubble column is equal to or greater than for plug flow, and the same selectivity is obtained for the completely mixed system. Koros (151) reported the invention of a slurry bubble column multi-tubular slurry bubble column reactor with cooling medium around the tubes. The example presented shows a reaction tube of 0.15 m mounted inside a 0.30 m pipe that served as a cooling jacket. According to our opinion, this reactor configuration has several disadvantages: (1) possibility of slug flow conditions, 2) large gas holdup due to the influence of the column diameter on the large gas bubble holdup (152), 3) possibility of maldristribution of the gas, the liquid and the catalyst phases, and 4) low specific cooling area relative to, for example, 1.5 inch cooling tubes. A better option is staging the slurry bubble column horizontally as proposed earlier by Graaf (153) for slurry phase methanol synthesis. Maretto and Piccolo (154) reported the effect of staging a slurry bubble column. The temperature in each stage could be controlled separately. Their model assumed plug flow of the gas phase and complete mixing of the slurry in each stage. Maretto and Piccolo (154) claimed that the liquid phase in the multistage reactor may approach plug flow behavior, resulting in an increase of the synthesis gas conversion with increasing the number of stages. Our model can easily be extended to incorporate the effect of staging of a slurry bubble column. In addition to the study of Maretto and Piccolo (154), extension of the model presented will also predict the effect of staging on

the product selectivity. Maretto and Piccolo (154) did not report on the engineering details of staging bubble columns. One of the possibilities would be the application of horizontal gauzes or perforated plates (155,156). These plates decrease the bubble size of large gas bubbles and slugs which results in a higher gas holdup and improvement of the plug flow characteristics of the gas and liquid phase."

Acknowledgment

This work was supported by U.S. DOE contract number DE-FC26-98FT40308 and the Commonwealth of Kentucky. The preparation of this manuscript was made easier by the information contained on a web site (Fischer-Tropsch.org) maintained by the Syntroleum Corp. The author is deeply indebted to Drs. Attilio Bisio and Keith Lawson for the improvements their comments provided to the manuscript.

References

1. H. F. Williamson, R. L. Andreano, A. R. Daum and G. C. Klose, The American Petroleum Industry. The Age of Energy 1899-1959, Northwestern University Press, Evanston, 1963.
2. J. Blorkin, "The Crime and Punishment of I. G. Farben," Barnes and Noble, New York, 1997.
3. M. Rash,, Geschichte des Kaiser-Wilhelm-Institute für Kohlenforschung 1912-1943, VCH, Weinheim, 1989, p 159 ff.
4. BASF, DRP 293,787, 1913.
5. BASF, DRP 660,619, 1924.
6. C. Schuster, Fortschr. Chem. Forsch., 311-74, 1951, CA46, 886g.
7. F. Fischer and H. Tropsch, Brenst. Chem, 4 (1923) 276.
8. H. Tropsch and O. Roelen, Gesammelte Abh. Kemt. Kohle, 7 (1925) 15.
9. B. Cornils, W. A. Herrmann and M. Rash, Angew. Chem. Int. Ed. Engl., 33, **1994,** 2144-2163.)
10. A. Krammer, Technology & Culture, 19, 394-422 (1978).
11. R. C. Stokes, Business History Rev., 59, 254-277 (1985).
12. G. Biardi and G. Baldi, *Catal. Today*, **1999**, 52, 223-234.
13. E. V. Slivinskii, G. A. Kliger, A. E. Kuz'min, A. V. Abramova, A. N. Shuikin, *Kinetics and Catalysis*, **1999**, 40, 338-344.
14. A. P. Higler, R. Taylor, R. Krishna, *Chem. Eng. Sci*., **1999**, 54, 2873-288.
15. J. Ellenberger, R. Krishna, *Chem. Eng. Sci*., **1999**, 54, 1339-1345.

16. M. Rasch, Geschichte des Daiser-Wilhelm-Instituts für Kohlenforschung: 1913-1943, VCH, Weinheim, 1989.

17. F. Fischer and K. Peters, Brenstoff-Chemie, **12**, 286-293 (1931).

18. Fischer and Kuster, Brenstoff-Chemie, 14, 3-8 (1933).

19. F. Fischer and H. Pichler, Brennstoff-Chemie, 20, 247 (1939).

20. M. Rash,, Geschichte des Kaiser-Wilhelm-Institute für Kohlenforschung 1912-1943, VCH, Weinheim, 1989, p 129 ff.

21. W. F. Faragher and W. A. Horne, "Interrogation of Dr. Pier and Staff at I. G. Farbenindustrie A. G., Ludwigshafen and Oppau, Supplement II," U. S. Bureau of Mines I.C. 7376, August 1946.

22. I. G. Farbenindustrie, "Hydrocarbons," British Patent 449,274, June 24, 1936; British Patent 468,434, June 29, 1937.

23. I. G. Farbenindustrie, "Converting CO and H into Hydrocarbons," British Patent 516,352, Jan 1, 1940; British Patent 516,403, Jan 1, 1940.

24. F. Duftschmid, E. Lindth and F. Winlder, "Production of valuable hydrocarbons and their derivatives containing oxygen," US 2,159,077, May 23, 1939.

25. "Improvements in the manufacture and production of hydrocarbons and their derivatives from CO and H_2," British Appl. 29636, Oct. 29, 1937 (from ref. 21)..

26. H. Tramm and W. Wischermann, "Hydrogenation of CO in a liquid medium over suspended catalysts," German Patent 744,185, Jan 26, 1944.

27. H V Atwell, A. R. Powell and H H Storch, "US Government Technical Oil Mission, Fischer-Tropsch Report One," TOM Report July 5, 1945, 66 pp, Office of publication board report 2051, 1945, 45 pp.

28. W. Michael, Brennstoff-Chemie, 37, 171 (1956).

29. R. Holroyd, “Report on Investigations by Fuels and Lubricants teams at the I.G. Farbenindustrie A.G. Works, Ludwigshafen and Oppau,” Bureau of Mines IC 7375, 1946, p 42.

30. F. Duftschmid, E. Linckh and F, Winkler, "Synthesis of hydrocarbons," U.S. Patent 2,287,092, June 23, 1942.

31. F. Duftschmid, E. Linckh and F, Winkler, "Synthesis of hydrocarbons," U.S. Patent 2,318,602, May 11, 1943.

32. F. Duftschmid, E. Linckh and F, Winkler, "Preparation of products containing valuable hydrocarbons or their derivatives,” U.S. Patent 2,207,581, July 9, 1940.

33. H. E. Benson, J. H. Field, D. Bienstock, R. R. Nagel, L. W. Brunn, C. O. Hawk, H. H. Crowell and H. H. Storch, "Development of the Fischer-Tropsch Oil-Recycle Process," Bureau of Mines Bulletin 568, 1957.

34. C. C. Hall and S. R. Craxford, “Additional information concerning the Fischer-Tropsch process and its products,” B.I.O.S. Final Report No. 1722, Item No. 22, British Intelligence Objectives Sub-committee.

35. Great Britain Patent 464,308, April 15, 1937.

36. F. Duftschmid, E. Linckh and F, Winkler, "Production of valuable hydrocarbons and their derivatives containing oxygen," U.S. Patent 2,159,077, May 23, 1939.

37. L. Xu, S. Bao, R. J. O'Brien, A. Raje and B. H. Davis, *Chemtech*, **28**, 47 (1998).

38. “Office of Publication Board Report 412,” May 15, 1945.

39. E. Reichl, “U. S. Technical Mission in Europe; Technical Report No. 248-45, The Synthesis of Hydrocarbons and Chemicals from CO and H_2,” September 1945.

40. Kölbel, H., Die Fischer-Tropsch-Synthese, "Chemische Technologie, Band 3: Organische Technologie I", K. Winnacker and L. Kuchler, Eds., Carl Hanser Verlag, Munchen, 1959, pp. p. 495.

41. H. Kölbel and P. Ackermann, Chemie.-Ing.-Techn., **28**, 381 (1956).

42. H. Kölbel and E. Ruschenburg, Brennstoff-Chem., **35**, 161, (1954).

43. H. Kölbel and P. Ackermann, "Apparatus for carrying out gaseous catalytic reactions in liquid phase," U.S. Patent 2,853,369, Sept. 23, 1958.

44. H. Kölbel and P. Ackermann, "Apparatus for carbon monoxide hydrogenation,"U.S. Patent 2,868,627, Jan. 13, 1959.

45. H. Kölbel and M. Ralek, *Catal. Rev.-Sci. Eng.*, **21** (1980) 225.

46. W. K. Bell and W. O. Haag, "Method for preparing a promoted iron catalyst and catalyst prepared by the method for conversion of synthesis gas to liquid hydrocarbons," U.S. Patent 4,994,428, February 19, 1991.

47. W. K. Bell and W. O. Haag, "Conversion of synthesis gas to liquid hydrocarbons," U.S. Patent 4,978,689, December 18, 1990.

48. J. C. W. Kuo, "Slurry Fischer-Tropsch/Mobil two state process of converting syngas to high octane gasoline," Final Report, DOE/PC/30022-10 (DE84004411), June 1983.

49. J. C. W. Kuo, "Two-Stage process for conversion of synthesis gas to high quality transportation fuels," Final Report, Appendix, DOE/PC/60019-9, October 1985.

50. B. L. Bhatt, Liquid phase Fischer-Tropsch (II) Demonstration in the LaPorte Alternative Fuels Development Unit, Topical Report, Final, Volume VII: Appendix, September 1995, DOE/PC/90018-T13.

51. B. Jager and R. Espinoza, *Catal. Today*, **23** (1995) 17.

52. E. B. Peck, "Method of controlling exothermic reactions, U.S. Patent 2,161,974, June 13, 1939.

53. H. V. Atwell, A. R. Powell and H. H. Storch, “US Government Technical Oil Mission, Fischer-Tropsch Report One,” TOM Report July 5, 1945, 66 pp, Office of publication board report 2051, 1945, 45 pp.

54. International Hydrocarbon Synthesis Co., “H_2-CO Synthesis,” French patent 860,360, Jan. 13, 1941.

55. G. C. Hall, D. Gall and S. L. Smith, *J. Inst. Petrol.*, **38**, 845 (1952).

56. H. Dreyfus, "Improvements in or relating to the manufacture of hydrocarbons and other products from carbon monoxide and hydrogen,” British 505,121, November 6, 1937.

57. H. Dreyfus (assigned to Celanese Corp. of America), "Production of organic compounds,” U.S. Patent 2,361,997, November 7, 1944.

58. British Patent 564,730, October 11, 1944.

59. H. H. Storch, N. Golumbic and R. B. Anderson, “The Fischer-Tropsch and related synthesis,” John Wiley & Sons, New York, 1951.

60. H. M. Larson, E. H. Knowlton and C. S. Popple, "New Horizons, History of Standard Oil Company (New Jersey), 1927-1950," Harper & Row, New York, 1971, p. 169.

61. Standard Oil Development Co., “Catalytic Apparatus and Process,” British Patent 496,159, Jan 3, 1938.

62. S. Groueff, “Manhattan Project: The Untold Story of the Making of the Atomic Bomb,” Little, Brown & Co., Boston, 1967.

63. G. Weber, *Oil & Gas J.*, March 24, 1949, p 248.

64. F. J. Moore, “Methods of effecting catalytic reactions,” U. S. Patent 2,440,109, April 20, 1948.

65. M. M. Stewart, R. C. Garrett and E. E. Sensel, “Method of effecting catalytic reaction between carbon monoxide and hydrogen,” U.S. Patent 2,433,072, December 23, 1947.

66. H. V. Atwell, “Method for synthesizing hydrocarbons and the like,” U.S. Patent, 2,433,255, December 23, 1947.

67. P. W. Cornell and E. Cotton, “Catalytic reaction,” U.S. Patent 2,585,441, February 12, 1952.

68. M. L. Riekena, A. G. Vickers, E. C. Haun, R. C. Koltz, CEP, April 1982, pp. 86-90.

69. P. Kellogg, “Synthol Feasibility Study for Standard Oil Company (Indiana) - Base Case,” J-5109, Revised Version, October, 1977.

70. W. P. Haynes, M. J. Baird, R. R. Schehl, M. F. Zarowchak, “Fischer-Tropsch Studies in a Bench-Scale Tube-Wall Reactor Using Magnetite Raney Iron, and Taconite Catalyst,” ACS Meeting, Anaheim, March 12-17, 1978.

71. D. B. Blum, M. B. Sherwin, M. E. Frank, “Liquid-Phase Methanation of High Concentration CO Synthesis Gas,” *ACS Adv. Chem. Series*, **1974**, 146, 149-159.

72. G. J. Thompson, M. L. Riekena and A. G. Vickers, “Comparison of Fischer-Tropsch reactor systems. Phase I., Final Report,” DOE/ET/10159-T2, September 1981.

73. W. C. Behrmann, C. H. Mauldin, L. E. Pedrick, “Hydrocarbon synthesis reactor employing vertical downcomer with gas disengaging means,” U.S. Patent 5382748, January 17, 1995.

74. L. E. Pedrick, C. H. Mauldin, W. C. Behrmann, “Draft Tube for Catalyst Rejuvenation and Distribution,” U.S. Patent 5268344, December 7, 1993.

75. M. Chang, “Enhanced gas separation for bubble column draft tubes,” U.S. Patent 5332552, July 26, 1994.

76. T. M. Stark, “Pentane energy transfer medium in gas conversion,”U.S. Patent 5409960, April 25, 1995.

77. R. M. Koros, “Bubble column, tube side slurry process and apparatus,”U.S. Patent 5384336, January 24, 1995.

78. E. Herbolzheimer, E. Iglesia, “Slurry Bubble Column,’ U.S. Patent 5348982, September 20, 1994.

79. W. N. Mitchell, “Activation of Hydrocarbon Synthesis Catalyst,” U.S. Patent 5292705, March 8, 1994.

80. W. N. Mitchell, “Activation of hydrocarbon synthesis catalyst,” U.S. Patent 5389690, February 14, 1995.

81. W. N. Mitchell, “Rejuvenation of hydrocarbon synthesis catalyst,” U.S. Patent 5283216, February 1, 1994.

82. E. Iglesia and R. Madon, “Reducing methane production and increasing liquid yields in FT reactions,” U.S. Patent 4,754,092, June 1988.

83. S. J. Hsia, “External Catalyst Rejuvenation System for the Hydrocarbon Synthesis Process,” U.S. Patent 5260239, November 9, 1993.

84. E. C. Hsu, J. L. Robbins, “Catalyst pretreatment method,” U.S. Patent 5070064, December 3, 1991.

85. J. M. Fox, III and S. S. Tam, *Topics in Catal.*, **2** (1995) 285.

86. J. R. Inga and B. I. Morsi, “Effect of catalyst loading on gas/liquid mass transfer in a slurry reactor: a statistical approach,” 13th Ann. Int. Pittsburgh Coal Conf., 1996, pp. 924-929.

87. H. Beuther, T. P. Kobylinski, C. E. Kibby and R. B. Pannell, "Conversion of synthesis gas to diesel fuel in controlled particle size fluid system," South Africa Application No. 85/5317, July 15, 1985.

88. Bijang Zhang, "Synthesis of Liquid Fuels From Coal," Science and Technology Publishing Corp., Shanxi Province, China, 1993.

89. Syntroleum press release, July 28, 1999.

90. K. Agee, K. B. Arcuri and P. F. Schubert, Preprint, ACS Div. Petroleum Chem., 45, 268 (2000).

91. K. B. Arcuri, K. L. Agee and M. A. Agee, WO 00/34414, June 15, 2000.

92. C. B. Benham and M. S. Bohn, “A decade of research and development in Fischer-Tropsch applications,” Pittsburgh Coal Conf., October 15, 1992.

93. B. L. Bhatt and P. J. A. Tijm, “Slurry Phase Fischer-Tropsch Synthesis Process Development,” 15th Ann. Pittsburg Coal Conf. Proceedings, 1998.

94. B. L. Bhatt, R. Frame, A. Hoek, K. Kinnari, V. U. S. Rao and F. L. Tungate, “Catalyst and Process Scale-up for Fischer-Tropsch Synthesis, 1994 ACS Meeting, San Diego, CA (March 15-17, 1994).

95. B. L. Bhatt, R. Frame, A. Hoek, K. Kinnari, V. U. S. Rao, F. L. Tungate, *Topics in Catal.*, **2**, 235-257 (1995).

96. B. L. Bhatt, “Liquid Phase Fischer-Tropsch (II) Demonstration in the LaPorte Alternative Fuels Development Unit,” Topical Report prepared by Air Products and Chemicals for U.S. DOE, Contract No. DE-AC22-91PC90018, September 1995.

97. M. L. Poutsma, “Assessment of advanced process concepts for liquefaction of low H_2/CO ratio synthesis gas based on the Kölbel slurry reactor and the Mobil-gasoline process,” ORNL-5635, February, 1980.

98. S. A. Butler, F. V. Hanson, H. S. Sherry, “Conversion of synthesis gas with cobalt-containing fluid catalyst,” U.S. 4,207,248, June 10, 1980.

99. B. L. Bhatt, P. J. A. Tijm, “Slurry phase Fischer-Tropsch synthesis process development,” 15th Ann. Pitt. Coal Conf. Proc., 1998.

100. B. L. Bhatt, “Liquid phase Fischer-Tropsch (II) demonstration in the LaPorte alternative fuels development unit, Topical Report, FINAL” (Volume I/II: Main Report), September 1995, Contract No. DE-AC22-90018.

101. C. W. Degoeorge, M. Chang, “Slurry hydrocarbon synthesis with external product filtration,” U.S. 5,770,629, June 23, 1998.

102. E. Rytter, P. Lian, T. Myrstad, P. T. Roterud, A. Solbakken, “Method of conducting catalytic converter multi-phase reaction,” U.S. 5,422,375, Feb. 24, 1993.

103. E. Rytter, P. Lian, T. Myrstad, P. T. Roterud, A. Solbakken, “Catalytic multi-phase reactor, WO 93/16795, Sept. 2, 1993.

104. B. Jager, A. P. Steynberg, J. R. Inga, R. C. Kelfkens, M. A. Smith, F. E. J. Malherbe, “Process for producing liquid and, optionally, gaseous products from gaseous reactants,” U.S. 5,599,849, February 4, 1997.

105. C. D. Ackerman, “Process for performing reactions in a liquid-solid catalyst slurry,” U.S. 5,527,473, June 18, 1996.

106. C. M. White, M. S. Quiring, K. L. Jensen, R. F. Hickey, L. D. Gillham, “Separation of catalyst from Fischer-Tropsch slurry,” U.S. 5,827,903, Oct. 27, 1998.

107. C. M. White, K. L. Jensen, P. C. Rohar, J. P. Tamilia, L. J. Shaw, R. F. Hickey, *Energy & Fuels*, **8**, 1067 (1996).

108. J. M. Brioles, Y. D. Wan, P. K. Kilpatric, G. W. Roberts, *Energy & Fuels*, **13**, 667 (1999).

109. R. Srinivasan, L. Xu, R. L. Spicer, F. L. Tungate, B. H. Davis, *Fuel Sci. & Tech. Intl.*,**14**, 1337 (1996).

110. K. Yokota, Y. Hanakata and K. Fujimoto in "Natural Gas Conversion," (A. Holmen et al., Eds.), Elsevier, Amsterdam, (1991), pp. 289-295.

111. K. Fujimoto, L. Fan and K. Yoshii, *Topics in Catal.*, **2** (1995) 259.

112. X. Lang, A. Akgerman and D. B. Bukur, *Ind. Eng. Chem. Res.*, **34** (1995) 72.

113. Anonymous, "Design and fabrication of the first commercial-scale liquid phase methanol (LPMEOH^{TM}) reactor, Topical Report, DE-FC22-92PC90543, October, 1998.

114. Y. Wu, D. Gidaspow, *Chem. Eng. Sci*., **55**, 573 (2000).

115. K. A. Shollenberger, T. J. O'Hern, "Characterization of slurry-phase flow in the LaPorte Alternative Fuels Development Unit (AFDU) using differential pressure measurements, SAND97-0530, Sandia National labs, 1997.

116. W-D. Deckwer, "Reaktionstechnik in Blasensaeulen," Otto Salle Verlag GmbH & Co, Frankfurt am Main Verlag Sauerlaender AG, Aarau, Switzerland; W.-D. Deckwer, "Bubble Column Reactors," (translated by Valeri Cottrell), John Wiley and Sons, New York, (1992).

117. S. C. Saxena, *Catal. Rev.-Sci. Eng*., **37**, 227 (1995).

118. R. L. Espinoza, J. L. Visagie, P. J. van Berge and F. H. Bolder, "Catalysts," U.S. Patent 5,733,839, March 31, 1998.

119. E. Rytter, P. Lian, T. Myrstad, P. T. Roterud, A. Solbakken, "Method of conducting catalytic converter multiphase reaction," U.S. 5,422,375, June 6, 1995.

120. R. C. Ryan, "Slurry phase syngas process," U.S. 4,472,534, September 18, 1984.

121. B. Jager, “Sasol’s advanced commercial Fischer-Tropsch process,” AIChE, 1997 Spring National Meeting, Houston, March 9-13, 1997, N.27c.

122. P. Chaumette, P. Boucot, P. Galtier, “Procedure for conversion of synthesis in liquid phase,” EP 0753 562, A1, July 3, 1996.

123. C. Maretto, P. Vincenzo, “Fischer-Tropsch process with a multistage bubble column reactor,” US 5,827,902, October 27, 1998.

124. W. Luewisuthichat, A. Tsutsumi, K. Yoshida, *J. Chem. Eng. Japan*, **29**, 675 (1996).

125. X. Luo, J. Zhang, K. Tsuchiya, L-S. Fan, *Chem. Eng. Sci*., **52**, 3693 (1997).

126. J. W. A. DeSwart, R. Krishna, S. T. Sie, *Natural Gas Conversion IV*, **107**, 213 (1997).

127. W. M. Ohkawa, N. Kawata, S. Uchida, *Chem. Eng. Sci*., **54**, 2711 (1999).

128. F. Raymond, J-M. Rosant, *Chem. Eng. Sci.*, **55**, 943 (2000).

129. W. Luewisuthichat, A. Tsutsumi, K. Yoshida, *J. Chem. Eng. Japan*, **30**, 461 (1997).

130. J. W. A. DeSwart, R. Krishna, *Trans. Inst. Chem. Eng*., **73**, 308 (1995).

131. H. Z. Li, *Chem. Eng. Sci*., **54**, 2247 (1999).

132. A. Sokolichin, G. Eigenberger, *Chem. Eng. Sci*., **54**, 2273 (1999).

133. R. Krishna, M. I. Urseanu, J. M. van Baten, J. Ellenberger, *Chem. Eng. Sci*, **54**, 171 (1999).

134. R. Krishna, M. I. Urseanu, J. M. van Baten, J. Ellenberger, *Chem. Eng. Sci*, **54**, 4903 (1999).

135. R. F. Mudde, H. E. A. van Den Akker, *Chem. Eng. Sci*., **54**, 4921 (1999).

136. G. Eigenberger, *Chem.-Ing.Tech*., **71**, 852 (1999).

137. E. Delnoij, J. Westerweel, N. G. Deen, J. A. M. Kuipers, W. P. M. van Swaaij, *Chem. Eng. Sci*, **54**, 5159 (1999).

138. R. C. Chen, J. Reese, L-S. Fan, *AIChEJ*, **40**, 1093 (1994).

139. D. Colella, D. Vinci, R. Bagatin, M. Masi, E. Abu Bakr, *Chem. Eng. Sci*., **54**, 4767 (1999).

140. L-S. Fan, G. Q. Yang, D. J. Lee, K. Tsuchiya, X. Luo, *Chem. Eng. Sci*., **54**, 4681 (1999).

141. M. P. Dudukovic, B. A. Toseland, DOE Meeting, Sept. 22, 1999, Cincinnati, Ohio..

142. S. Becker, H. De Bie, J. Sweeney, *Chem. Eng. Sci*., **54**, 4929 (1999).

143. H. M. Letzel, J. C. Schouten, R. Krishna, C. M. van den Bleek, *Chem. Eng. Sci*., **52**, 4447 (1997).

144. E. Delnoij, "Fluid Dynamics of Gas-Liquid Bubble Columns: A Theoretical and Experimental Study," Ph.D. thesis, Twente University, Enschede, The Netherlands, 1999.

145. J. R. Inga, B. I. Morsi, "Novel approach for scale-up and scale-down of slurry bubble column reactors," 15th Proc. Annual Intl. Pittsburgh Coal Conf., 1998, 124-137.

146. J. R. Inga, Scaleup and scaledown of slurry reactors: a new methodology," Ph.D. thesis, University of Pittsburgh, 1997.

147. G. van der Laan, Ph.D. thesis, University of Groningen, 1999.

148. S. T. Sie, R. Krishna, *Appl Catal A: General*, **186**, 55 (1999).

149. C. Maretto, R. Krishna, *Catal Today*, **52**, 279 (1999).

150. K. B. Arcuri, EP 0 450 861m A2, 1999.

151. R. M. Koros, EP 0 592 176 A1, 1992.

152. C. Maretto, V. Piccolo, EP 0 923 470 A1, 1998.

153. R. Krishna, J. W. A. DeSwart, J. Ellenberger, G. B. Martina, C. Maretto, *AIChEJ*, **43**, 311 (1997).

154. G. H. Graff, Ph.D. thesis, University of Groningen, The Netherlands, 1988.

155. B. H. Chen, N. S. Yang, *Ind. Eng. Chem. Res.*, **28**, 1405 (1989).

156. J. Voight, K. Schugerl, *Chem. Eng. Sci*, **34**, 1221 (1979).

Table 1

Flexibility of Product Composition by Liquid Phase Synthesis (data from ref. 40).

Synthesis based on molecular size	Low	Low	Medium	High
Hydrocarbon Product - C_3+ ($g/m^3 CO+H_2$)	162	166	175	182
	Wt.%	Wt.%	Wt.%	Wt.%
$C_3 + C_4$	29.6	18.1	6.9	2.2
C_5+ to 190°C (C_5 to C_9)	63.0	68.0	40.0	7.1
190-310°C (C_9 to C_{17})	6.2	10.9	25.7	8.3
320-450°C (C_{17} to C_{31})	1.2	2.4	18.3	33.0
> 450°C (C_{31}+)	-	0.6	9.1	49.4
Alpha values	α_1,0.68	α_1,0.68	α_1,0.69 α_2,0.92	α_1,0.40 α_2,0.95
Fraction of product from α_2	---	---	0.17	0.50

1. Calculated by author from data above.
2. Calculated by author assuming two alpha distribution with α_2 representing the higher carbon number products.

Table 2

Operating Data and Results of Liquid-Phase Synthesis for One-Step Operation with a Single Passage of the Gas Over Iron Catalysts (from ref. 45)

	Demonstration Plant (a)	Laboratory Plant (b)
Effective reaction space (volume suspension including dispersed gas) (L)	10,000	6
Catalyst (kg Fe)	800	0.4
Synthesis gas pressure (bar)	12	11
Synthesis gas (volume ratio, $CO:H_2$)	1.5	1.5
Quantity of synthesis gas (Nm^3/hr)	2,700	1.3
Linear velocity of the compressed gases at operating temperature referred to the free reactor cross section (cm/sec)	9.5	3.5
Total $CO + H_2$ used (Nm^3/hr) Per m^3 of reaction chamber (Nm^3/hr) Per kg of Fe (Nm^3/hr)	2,300 230 2.6	1.1 183 2.45
Average synthesis temperature, °C	268	266
CO conversion, %	91	90
$CO + H_2$ conversion, %	89	88
Synthesis products referred to $CO + H_2$ used: Hydrocarbons C_1^+ (g/Nm^3) $C_1^+ + C_3$ (g/Nm^3) C_3^+ (g/Nm^3)	 178 12 166	 176 11 165
O-containing products in the synthesis water (g/Nm^3)	3	2
Space-time yield of C_3^+ products including O-products in 24 hr (kg/m^3 of reaction chamber)	930	740

Table 3

Effect of heating rejuvenation tubes on catalyst activation (from ref. 81).

Heat addition	no	Yes
Gas rate in tube, scfh	5100	4800
Avg reactor temp, ^{o}F	427	427
Avg rejuvenation temp, ^{o}F	430	440
CO conv, start to end of run, %	32 to 26 (over 12 hrs)	26 to 36 (over 24 hrs)
Conv, change/day	-12.4	+10.4

Table 4

Improvement in Catalyst/wax Separation in Slurry FT Processes by Removal of Catalyst Fines (from ref. 83)

Classification Solvent	Catalyst/solvent wt/wt	Other	Cycles	Acetone cycles	Filter time	Filter rate	
						(gm/min)	gal/ft^2/min
0.45 μm Millipore filter paper							
Blank	-	-	-	-	95.0	0.5	
Water	15/85	-	6	2	0.9	55.0	
i-C_3H_6OH/n-C_7H_{16} (1/9)	10/150	1% Oleic acid added	7	2	1.0	50.0	
i-C_3H_6OH/n-C_7H_{16} (1/9)	10/150	1% Aerosol OT-100 added	7	2	1.0	50.0	
0.3 μm glass fiber filter							
FT wax @ 130°C	2/98	Stirred 5 min	none	none	-	-	5.8 @ 14 psig
		Stirred 44 hrs	none	none	-	-	0.05 @ 14 psig
FT wax @ 120°C	2/98	Stirring per cycle19/48/24	3	none	-	-	14.5 @ 14 psig

Table 5

Conversion Data for Syngas Conversion Using Fixed-Bed and Slurry Reactors (from ref. 86)

Test Number	1	2	3	4	5
Reactor Type	fixed-bed	slurry	slurry	slurry	slurry
Temperature, ^{o}C	215	225	230	235	240
CO Conversion rate (ccCO/g/h)	215	649	808	992	1210
CO Conversion, %	45.3	8.4	10.4	12.8	15.6
Product Yields, Methane, wt. %	26.6	10.5	11.5	12.5	14.0
C_5-C_{20} (mg/g/h)	67	325	400	478	560
C_5+, wt.%	60.0	79.0	78.0	76.0	73.0

Table 6

Variations in Product Composition from the Kölbel Reactor (data from ref. 40)

Molecular Weight Goal	"Low"	"Medium"	"High"
Single-pass C_3^+ product yield (g/m^3 feed)[a]	166	175	182
Distribution of C_3^+ products (%)			
C_{3-4}	18	7	2
Gasoline (C_5-190°C)	68	40	7
Diesel fuel (190-310°C)	11	26	8
310-450°C	2.5	18	33
> 450°C	0.5	9	50

Table 7

Comparison of Reaction Engineering Models for the Fischer-Tropsch Synthesis in Slurry Bubble Column Reactors (from ref. 146)

Reference	Gas Phase	Liquid Phase	Catalyst Distribution	Energy Balance	Components	FT (Table 8)	WGS (Table 8)
Calderbank, et al.	PF	PF	uniform	isothermal	H_2	1	---
Satterfield, et al.	PF	PM	uniform	isothermal	H_2	1	---
Deckwer, et al.	PF	PM	uniform	isothermal	H_2	1	---
Deckwer, et al.	AD	AD	non-uniform	non-isothermal	H_2	1	---
Bukur	PF	PF,PM	uniform	isothermal	H_2	1	---
Stern, et al.	PF	PM	uniform	isothermal	H_2,CO,CO_2,H_2O	1	---
Kuo	PF	PM,PF, AD	non-uniform	isothermal	C_5,H_{10}	1	---
Kuo	PF	PF	non-uniform	isothermal	H_2	2	2
Stenger, et al.	AD	AD	non-uniform	isothermal	H_2,CO,CO_2,H_2O,C_{1-3}	1	1
Prakash, et al.	AD	AD	non-uniform	isothermal	H_2,CO,CO_2,H_2O,C_{1-3}	2	2
Prakash	AD	AD	non-uniform	isothermal		2	2
DeSwart[1]	AD	AD	non-uniform	non-isothermal	H_2	1	---
DeSwart[2]	PF	PM	uniform	isothermal	H_2	1	---
Mills, et al.	AD	AD	non-uniform	non-isothermal	H_2	1	---
Inga, et al.	PF	MC	uniform	isothermal	H_2,CO,H_2O	1,3	2
Krishna, et al.[2]	PF	PM	uniform	isothermal	H_2,CO	3	---
Our Model	PF	PM	uniform	isothermal	H_2,CO,CO_2,H_2O,N_2,C_{1-100}		

PF: plug flow; PM: perfectly mixed; MC: mixing cells, AD: axial dispersion.
1 Heterogeneous flow regime: large bubbles: PF, small bubbles and liquid: AD.
2 Heterogeneous flow regime: large bubbles: PF, small bubbles and liquid: PM.

Table 8 Kinetic Models for Table 7 (from ref. 146)	
FT Kinetic Expressions	WGS Kinetic Expressions
1 $kC_{H_2,L}$	1 $k(C_{CO,L}C_{H_2O,L} - C_{CO_2,L}C_{H_2O,L}/K_p)$
2 $\frac{k_{C_{H_2,L}}C_{CO,L}}{C_{CO,L} + aC_{H_2O}}$	2 $\frac{k(C_{CO,L}C_{H_2O,L} - C_{CO_2,L}C_{H_2O,L}/K_p)}{P_{CO} + aP_{H_2O}}$
3 $\frac{k_{C_{H_2,L}}C_{CO,L}}{(1 + aC_{CO,L})^2}$	

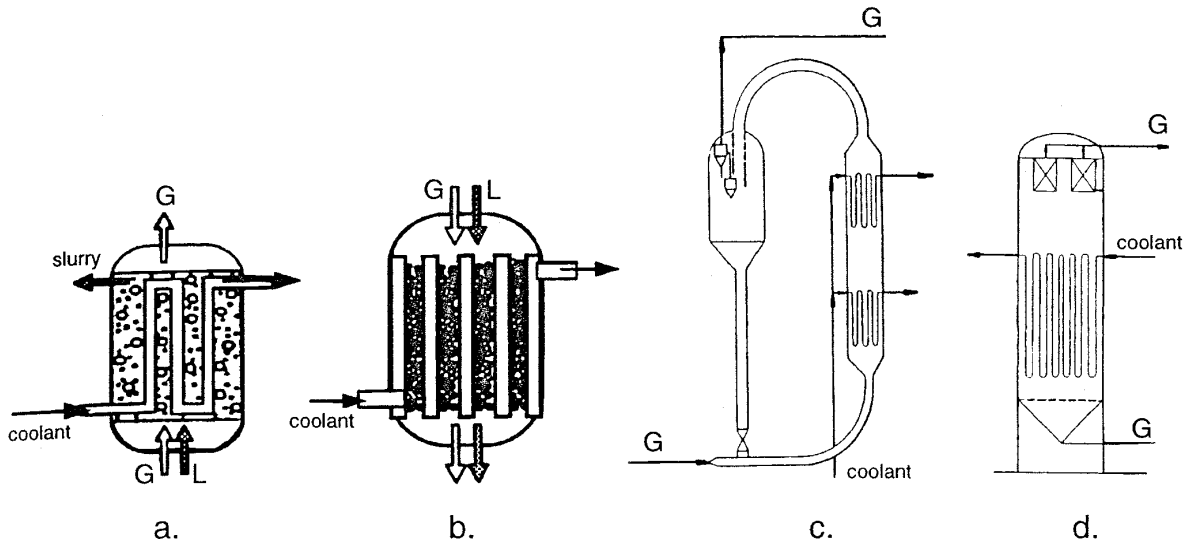

Figure 1. Possible reactors for Fischer-Tropsch synthesis. (a) slurry bubble column reactor, (b) multitubular trickle bed reactor, (c) circulating - and, (d) fluidized-bed reactor.

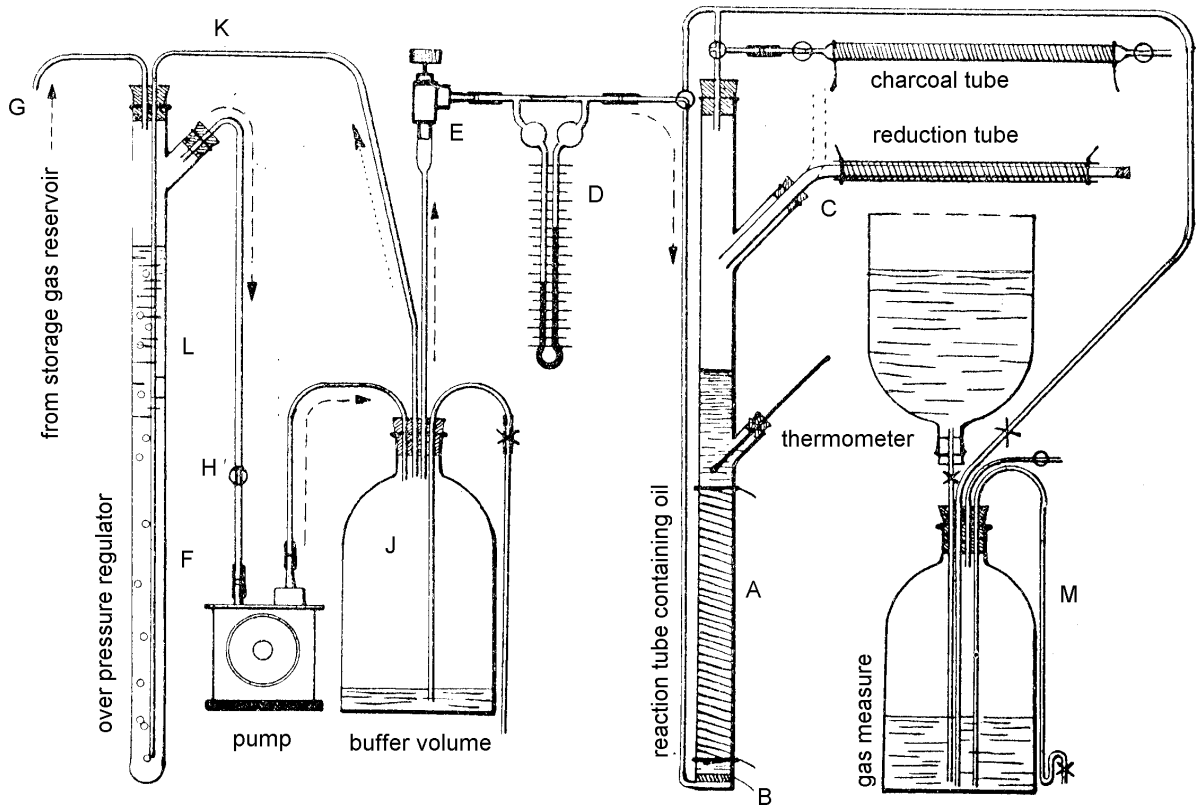

Figure 2. Slurry phase catalytic reactor for FTS (from ref. 17).

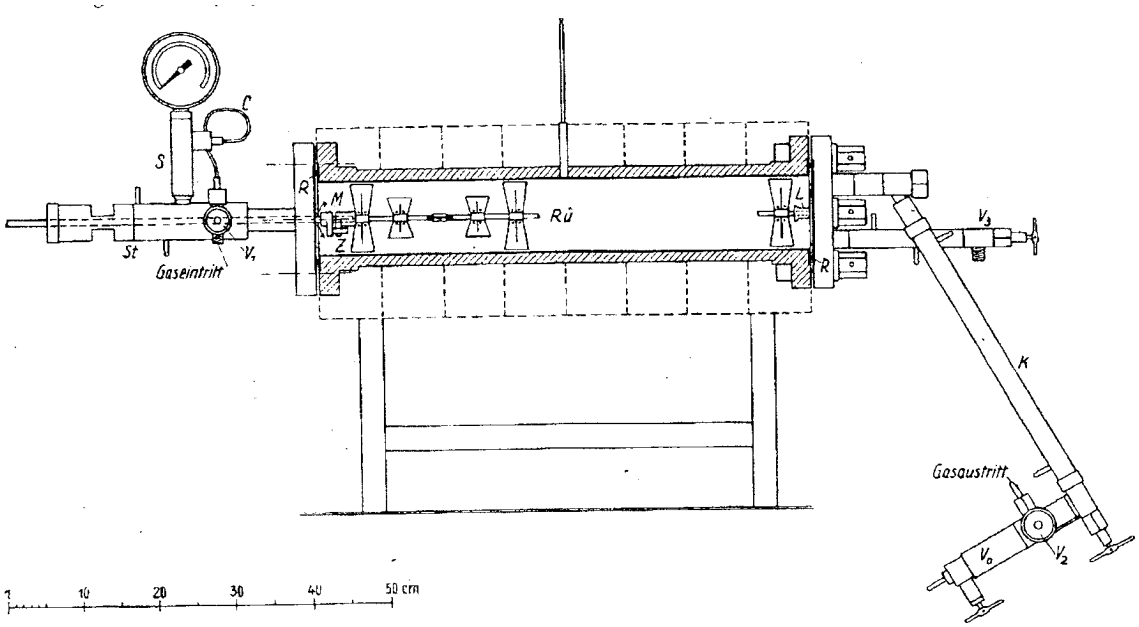

Figure 3. Tubular stirred autoclave with silver cladding (from ref. 18).

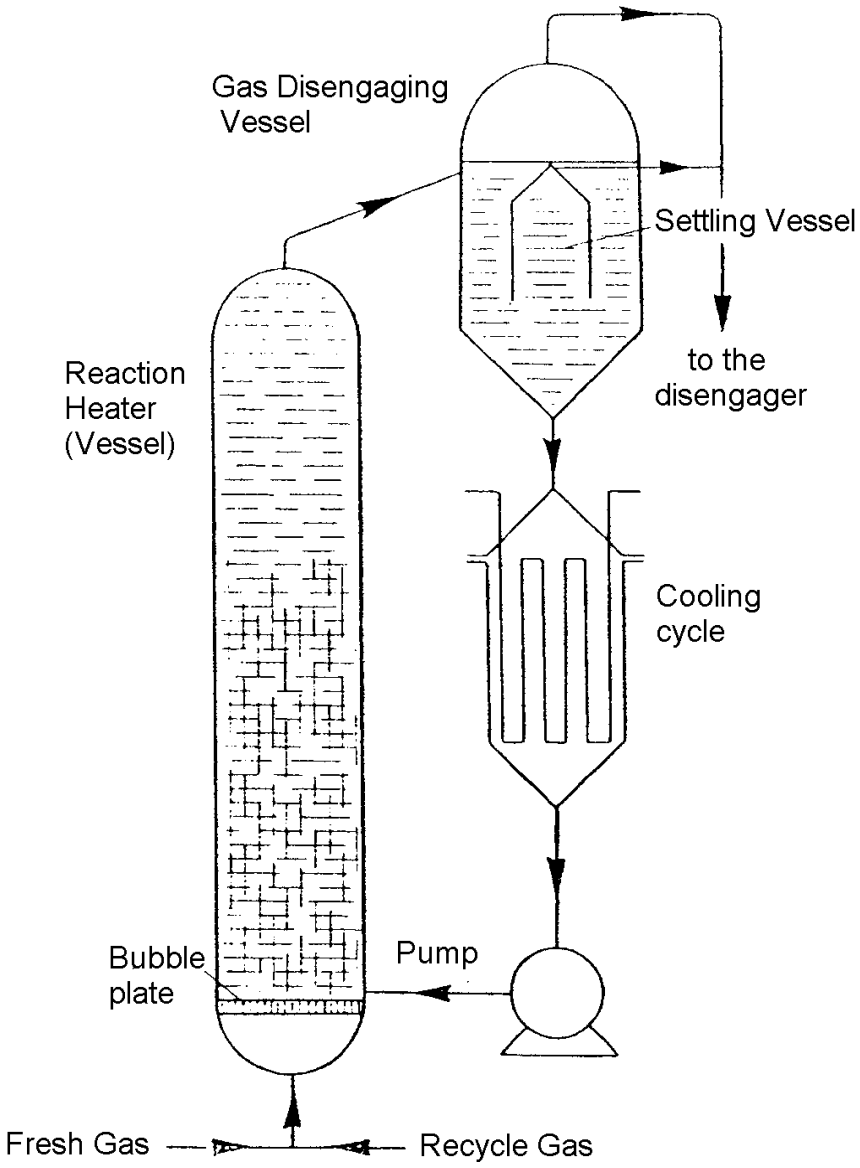

Figure 4. Schematic of the FTS reactor unit for the foam process (from ref. 28).

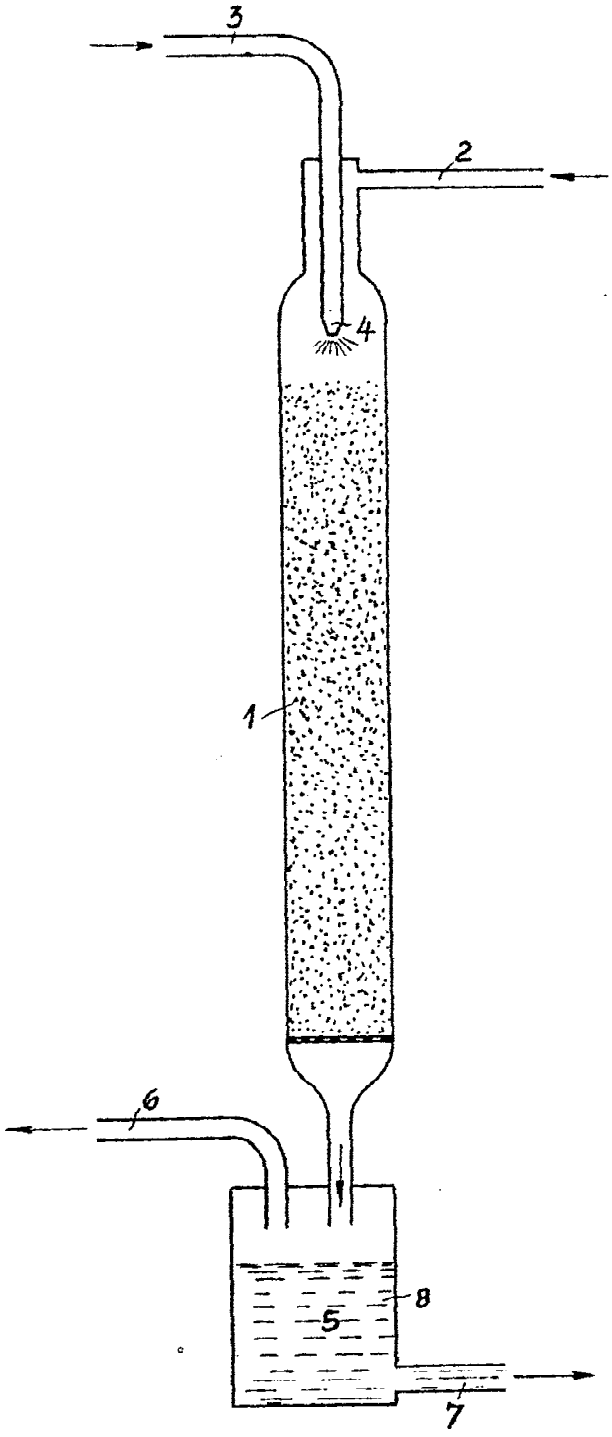

Figure 5. I. G. Farben fixed bed FTS reactor with oil sprayer for cooling (from ref. 35).

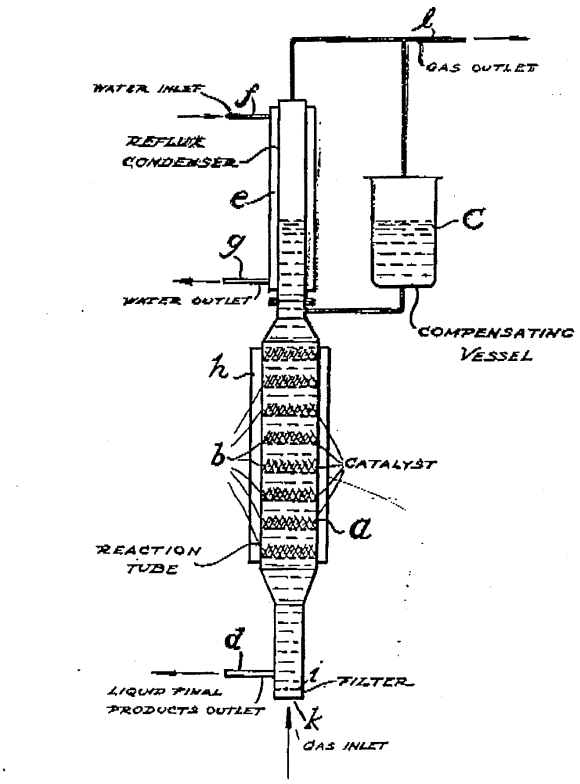

Figure 6. Schematic reactor fitted with catalyst trays for the preparation of hydrocarbons from synthesis gas in slurry reactor (from ref. 36).

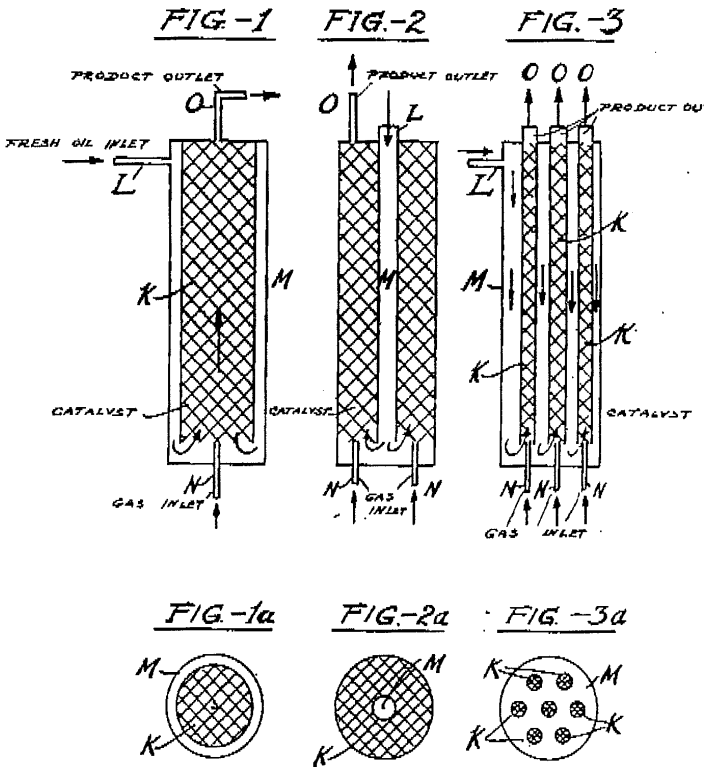

Figure 7. Schematic of slurry reactor tube subdivided into cells to modify liquid flow patterns (from ref. 30).

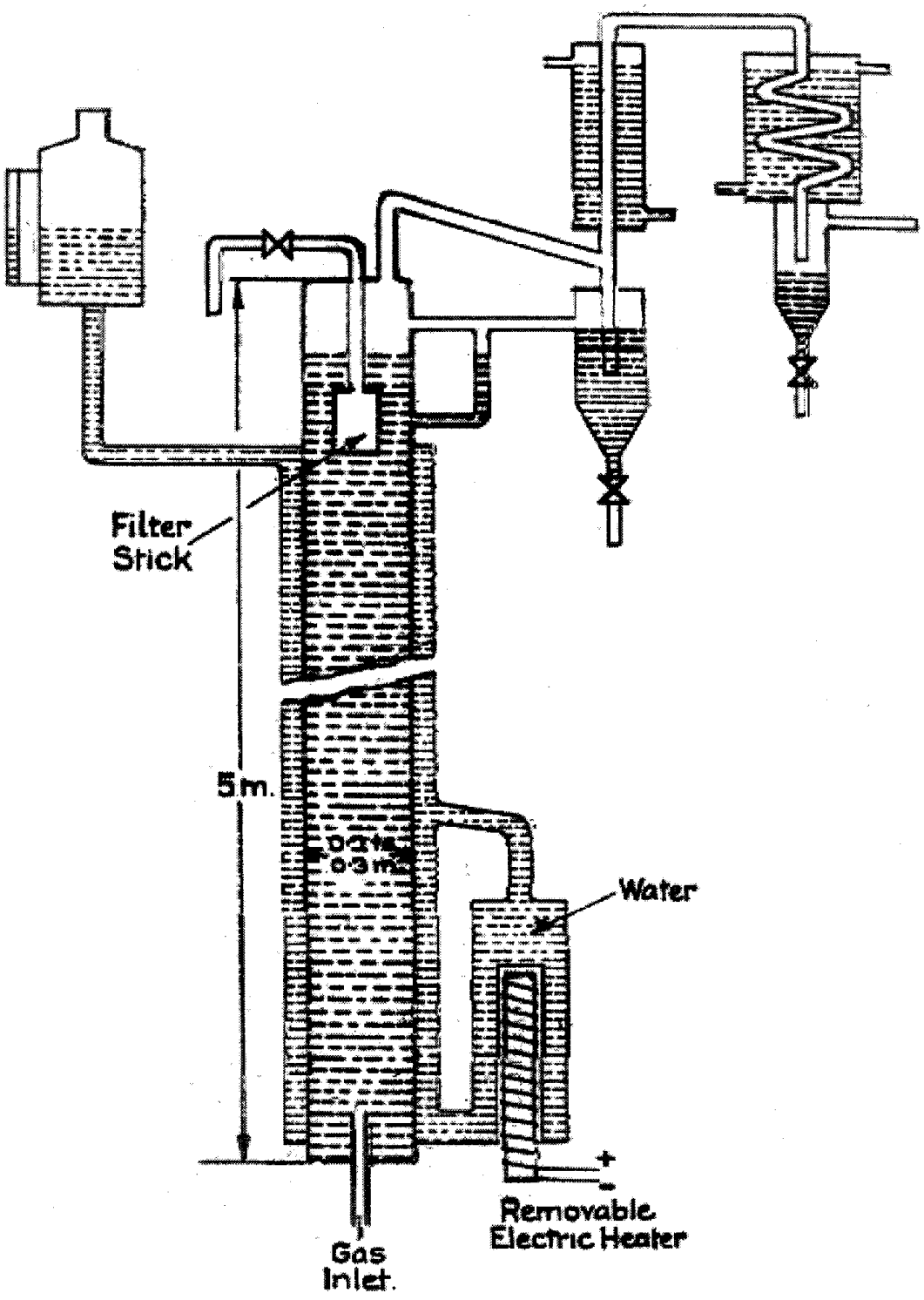

Figure 8. Liquid phase synthesis apparatus (from ref. 34).

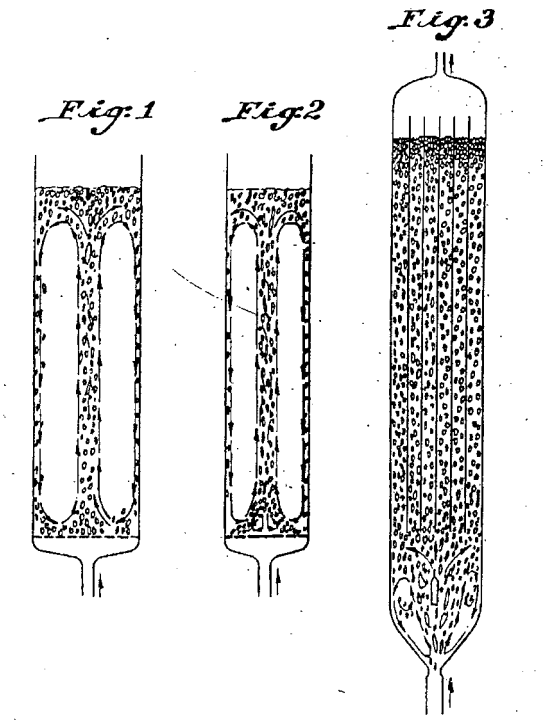

Figure 9. Schematic of oil recirculation within slurry reactor (Figures 1 and 2 of Figure 9) and the elimination of recirculation by adding shafts (tubes) (Figure 3) (from ref. 43).

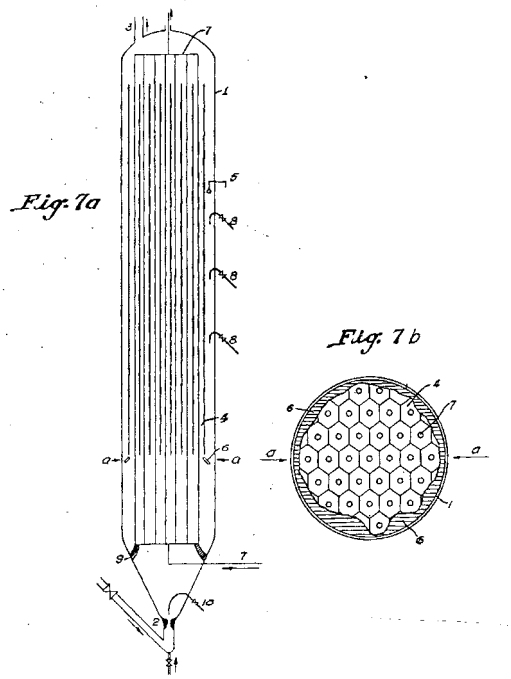

Figure 10. Schematic of slurry reactor with shafts (open at top and bottom) to subdivide reactor shell to establish reactor zone with stationary catalyst and liquid condition (from ref. 44).

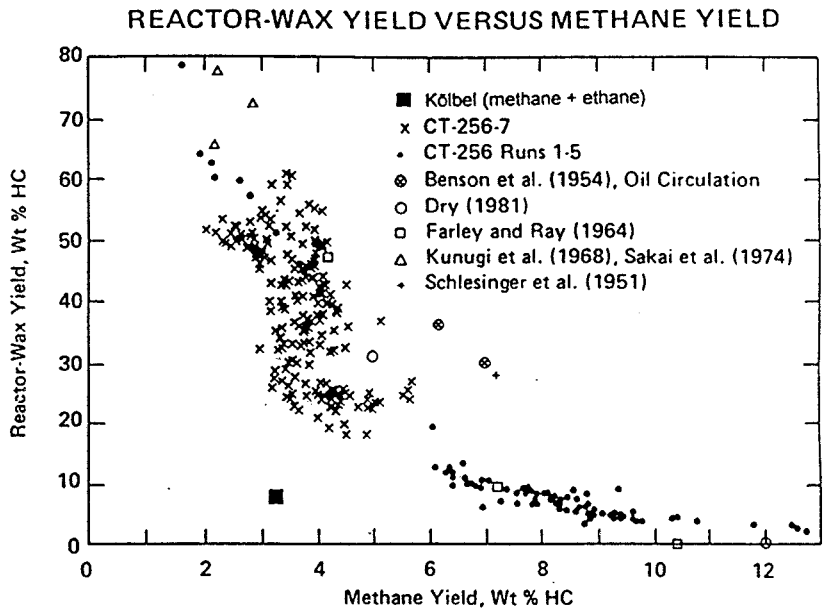

Figure 11. Reactor wax yield versus methane yield with data from ref. 45 and 49 (redrawn by author).

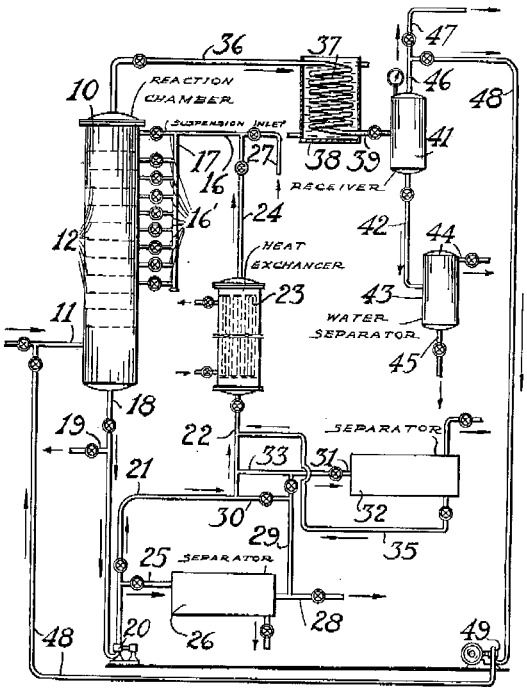

Figure 12. Reactor fitted with catalyst trays, each containing bubble caps, to effect slurry phase synthesis of hydrocarbons (from ref. 52).

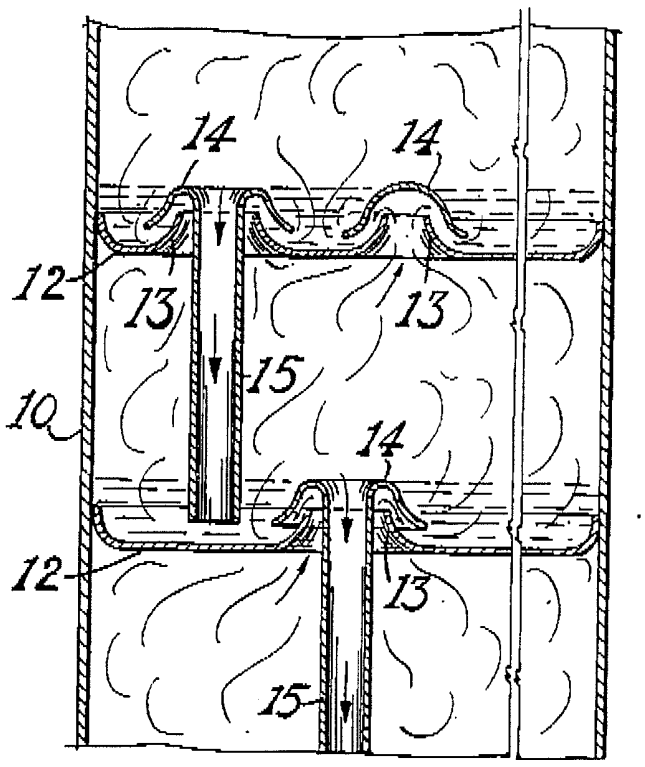

Figure 13. Schematic of bubble caps and gas transport columns for trays in reactor shown in Figure 12 (from ref. 52).

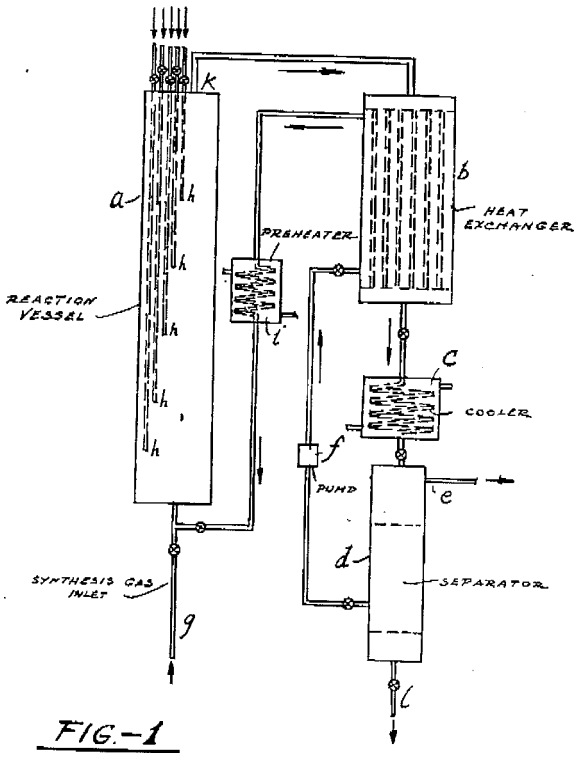

Figure 14. Schematic of slurry reactor with capability of adding preheated liquid as several levels within the reactor (from ref. 31).

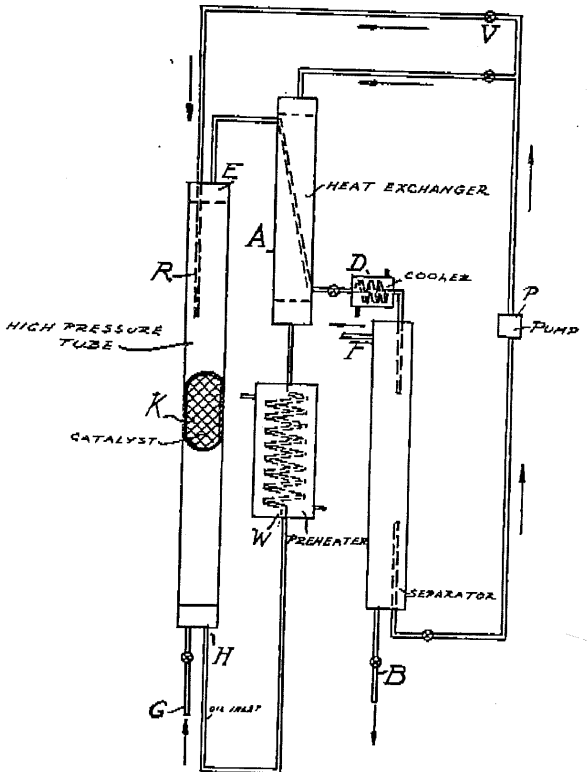

Figure 15. Schematic of slurry reactor with recycle of oil to the reactor (from ref. 31).

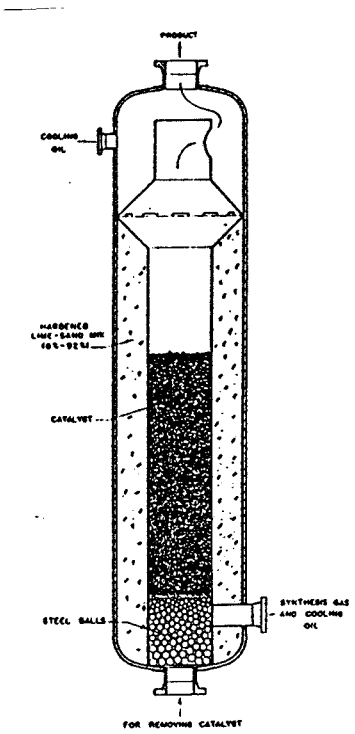

Figure 16. Synthesis reactor at Bureau of Mines, Louisiana, Missouri plan (from ref. 59).

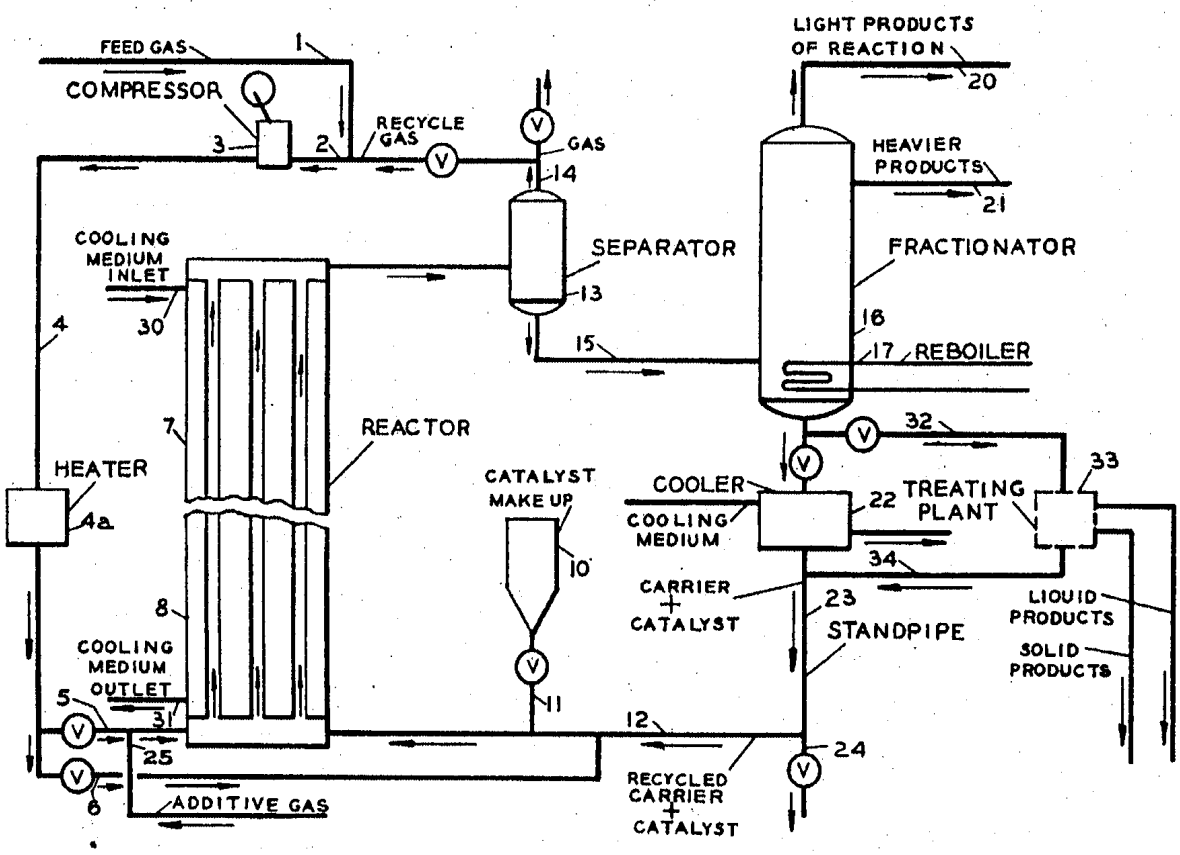

Figure 17. Method of effecting catalytic reactions (from ref. 64).

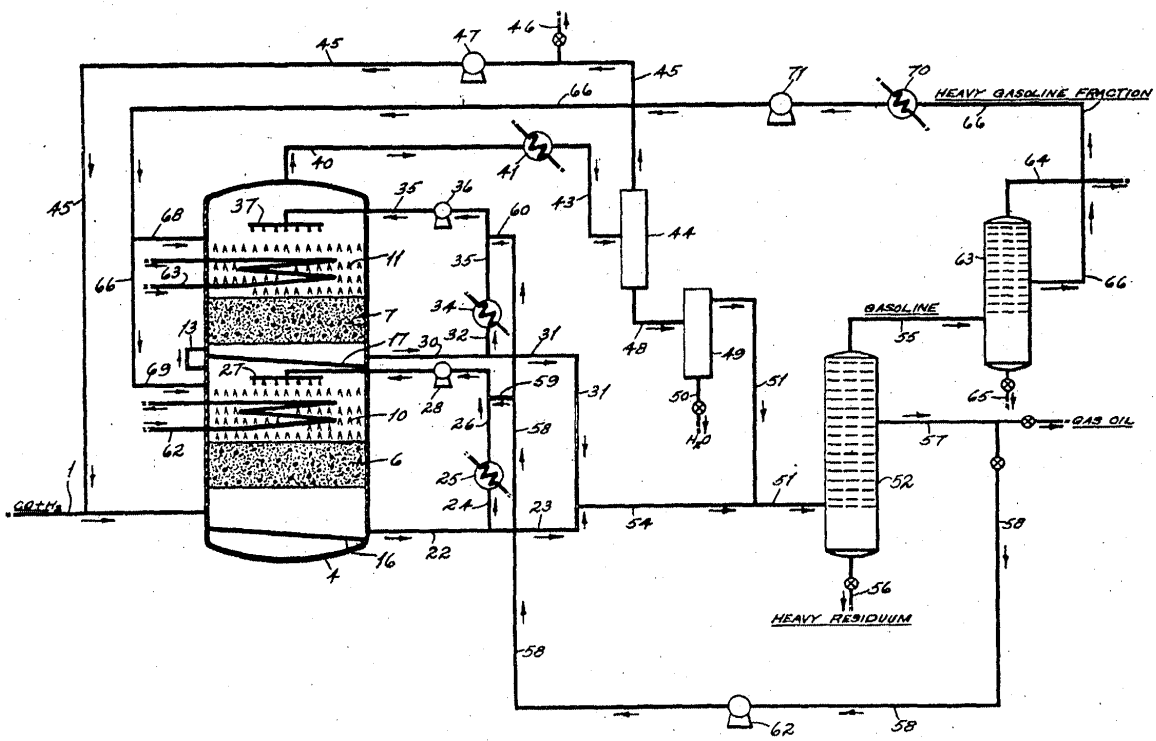

Figure 18. Method for synthesizing hydrocarbons and the like (from ref. 66).

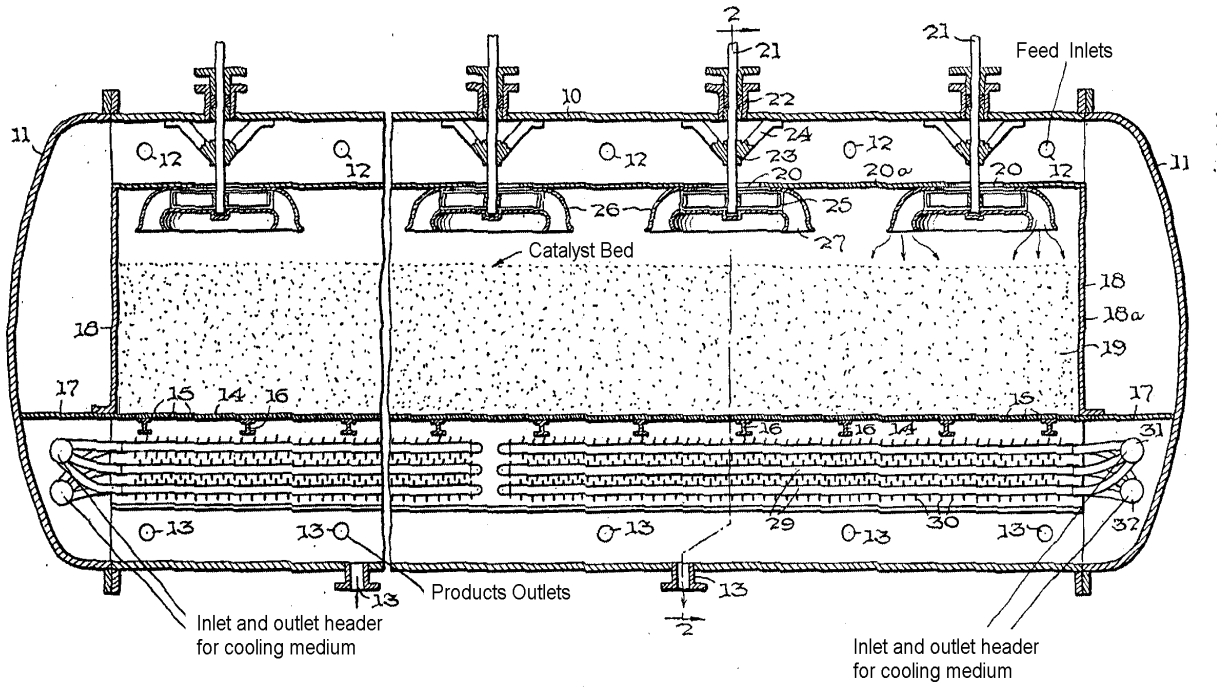

Figure 19. Catalytic reactor for liquid-phase synthesis (from ref. 67).

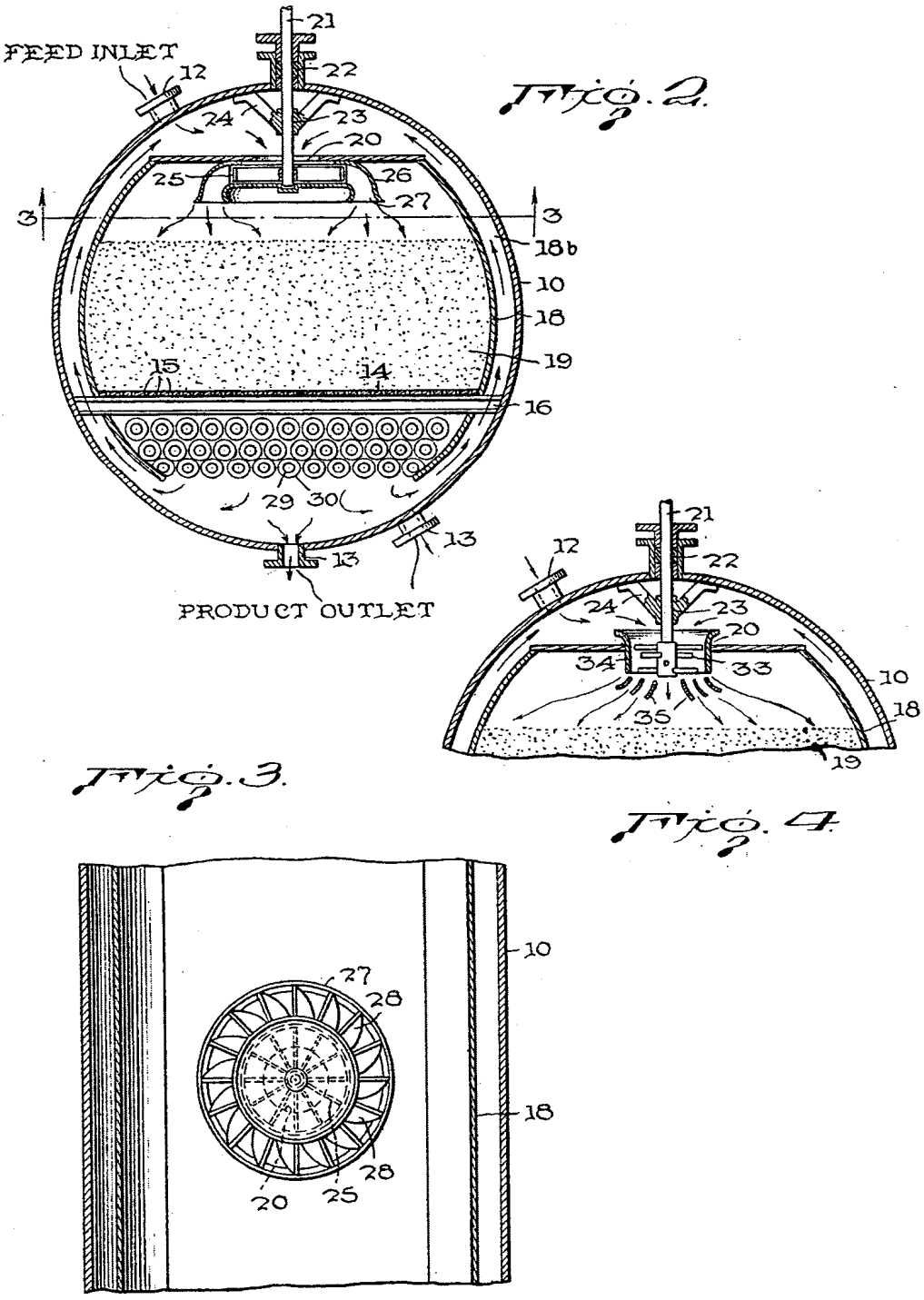

Figure 20. Cross sectional views of reactor in Figure 19 (from ref. 67).

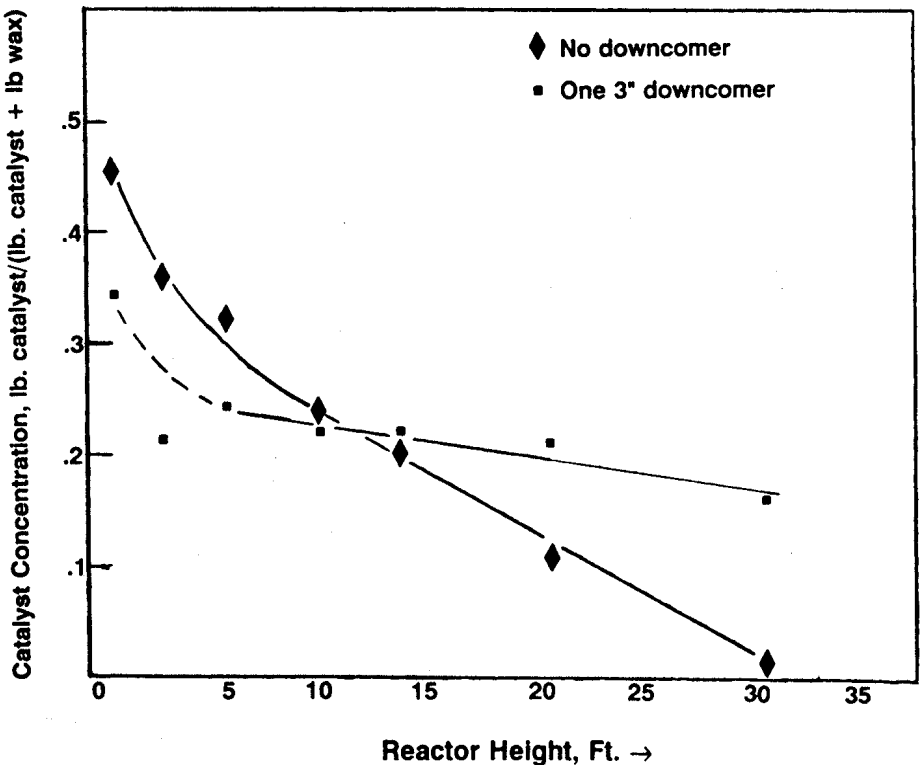

Figure 21. Catalyst concentration versus reactor height for (!) no downcomer and for one 3" downcomer (Q) (from ref. 74).

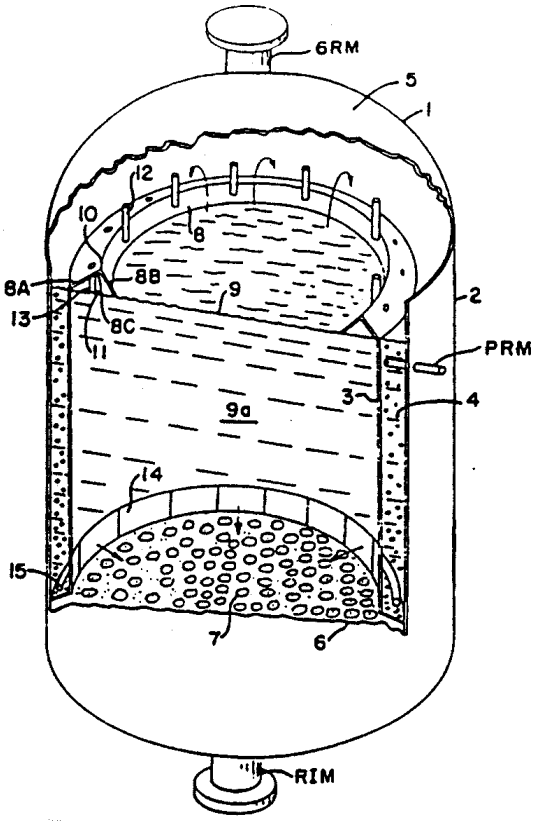

Figure 22. Schematic of reactor for enhanced gas separation for bubble column draft tubes (from ref. 75).

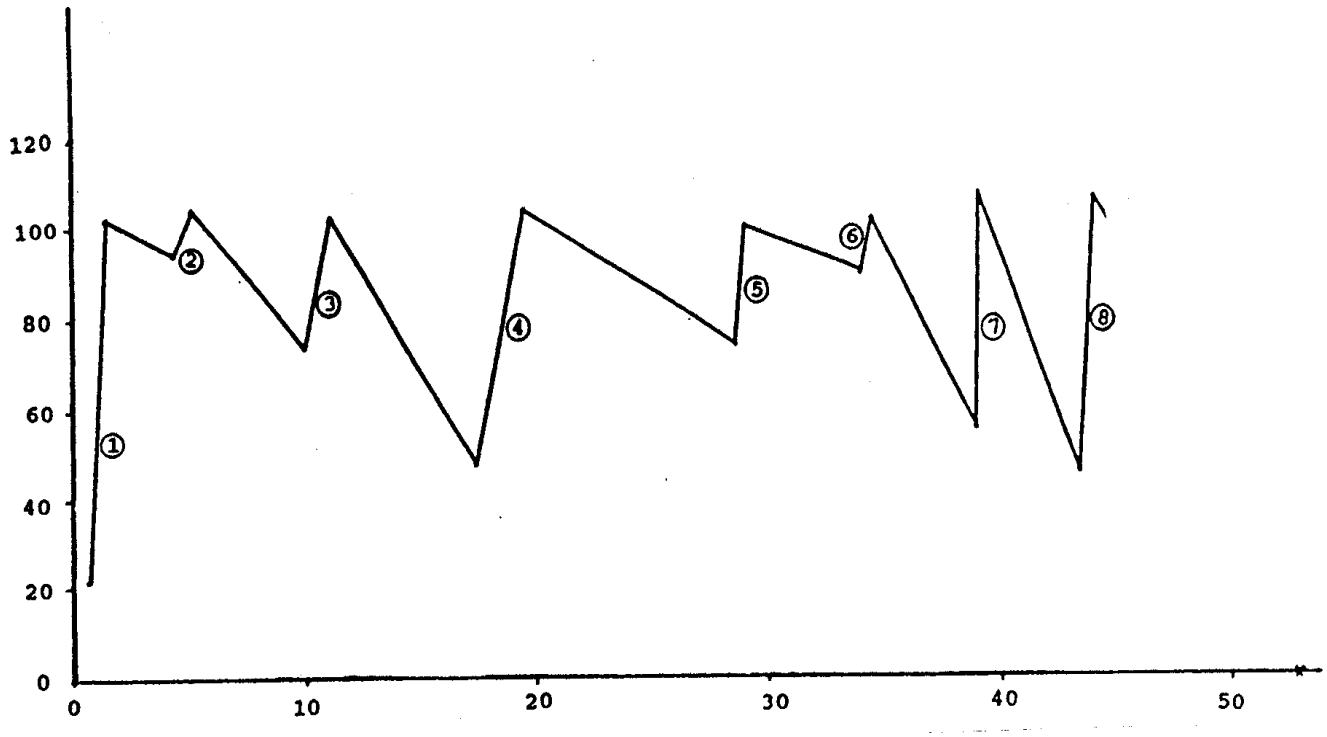

Figure 23. Relative volumetric productivity represented by activity with days on stream with intervals of hydrogen rejuvenation (12 wt.% Co on titania with 6 wt.% Al_2O_3 as binder (from ref. 81).

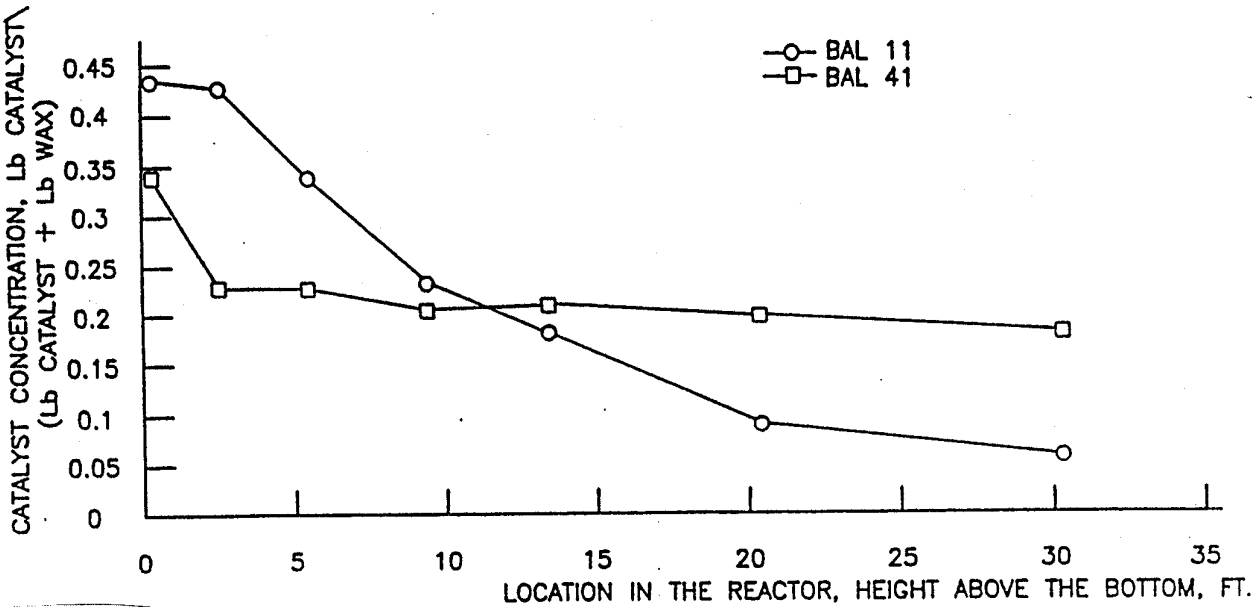

Figure 24. Catalyst concentration versus elevation in the reactor with (Q) and without (F) use of draft tubes (from ref. 74).

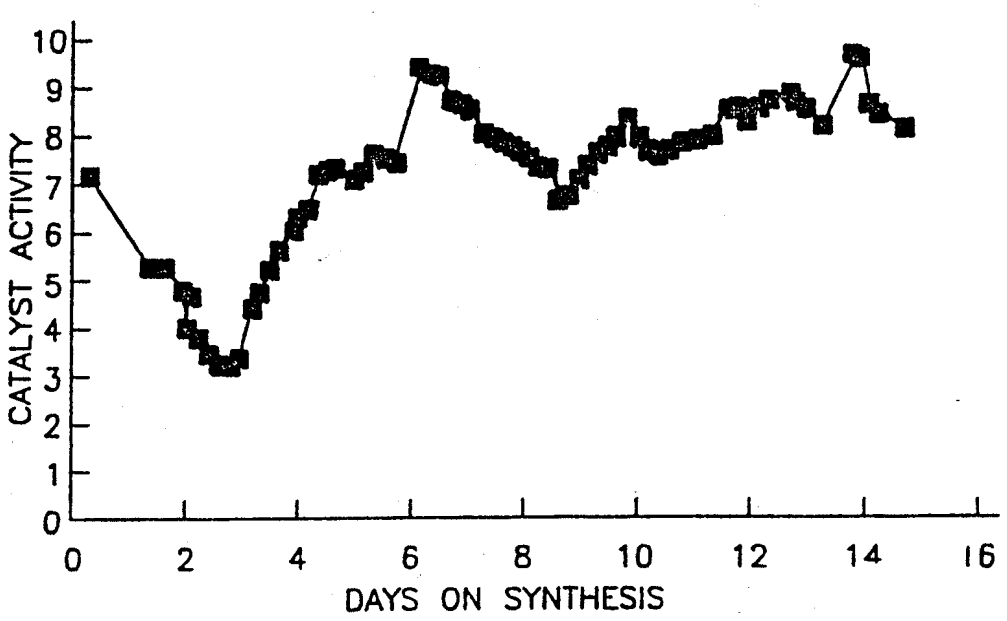

Figure 25. Conversion using hydrogenation rejuvenation (to day 3 no rejuvenation; rejuvenation after day 3) (from ref. 82).

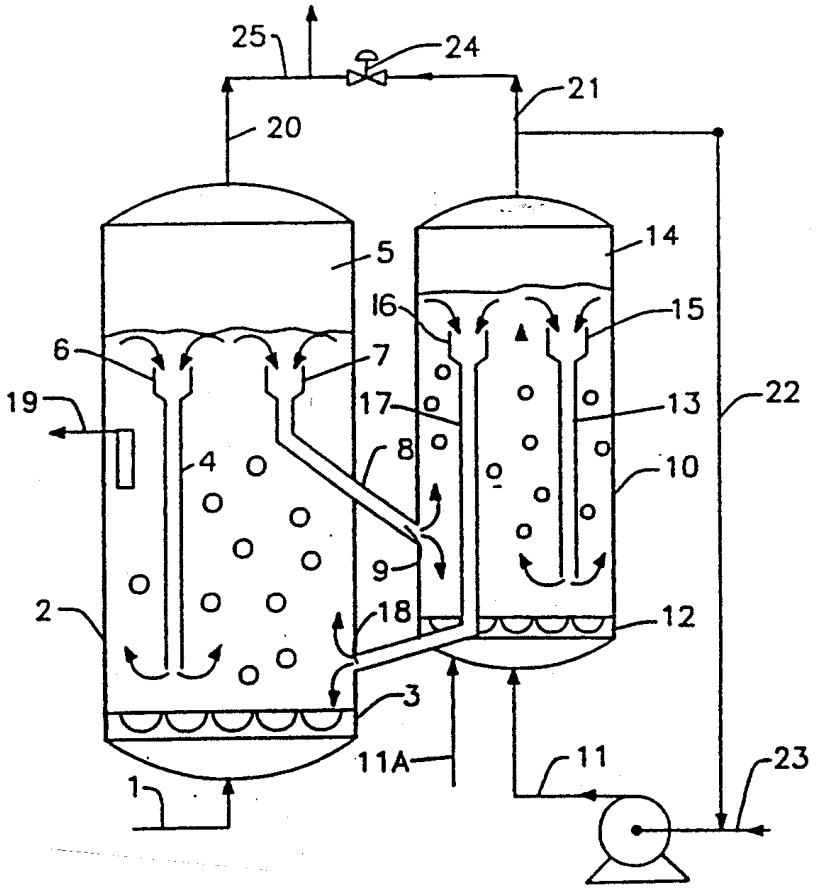

Figure 26. Schematic of multiple vessels for catalyst rejuvenation (from ref. 83).

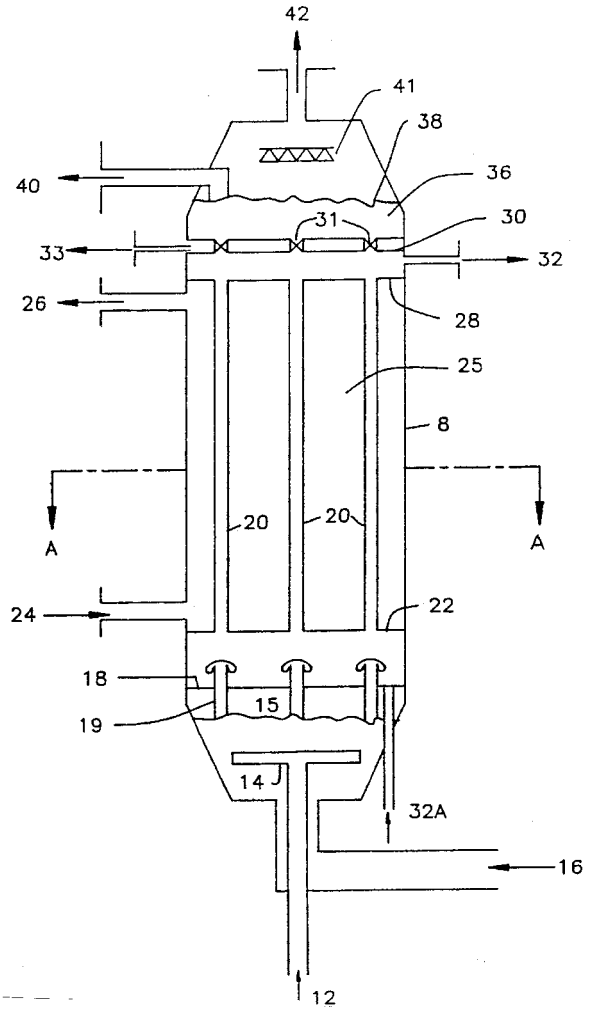

Figure 27. Elevation of a shell and tube reactor arrangement showing the gas, liquid, catalyst interconnection both above and below the upper and lower tube sheets (from ref. 77).

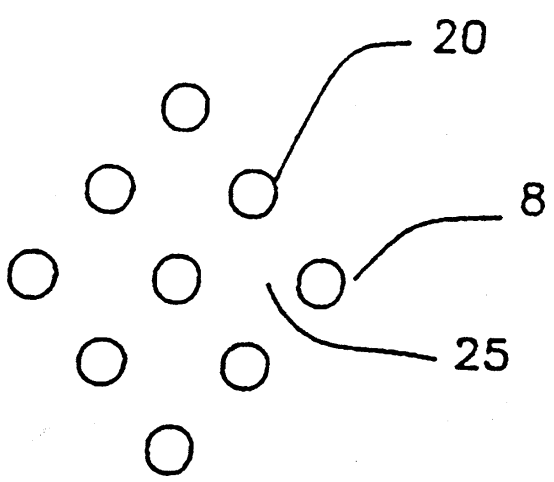

Figure 28. Horizontal Section A - A through the elevation of Figure 29 showing a possible arrangment of tubes, that is, reaction zones (from ref. 77).

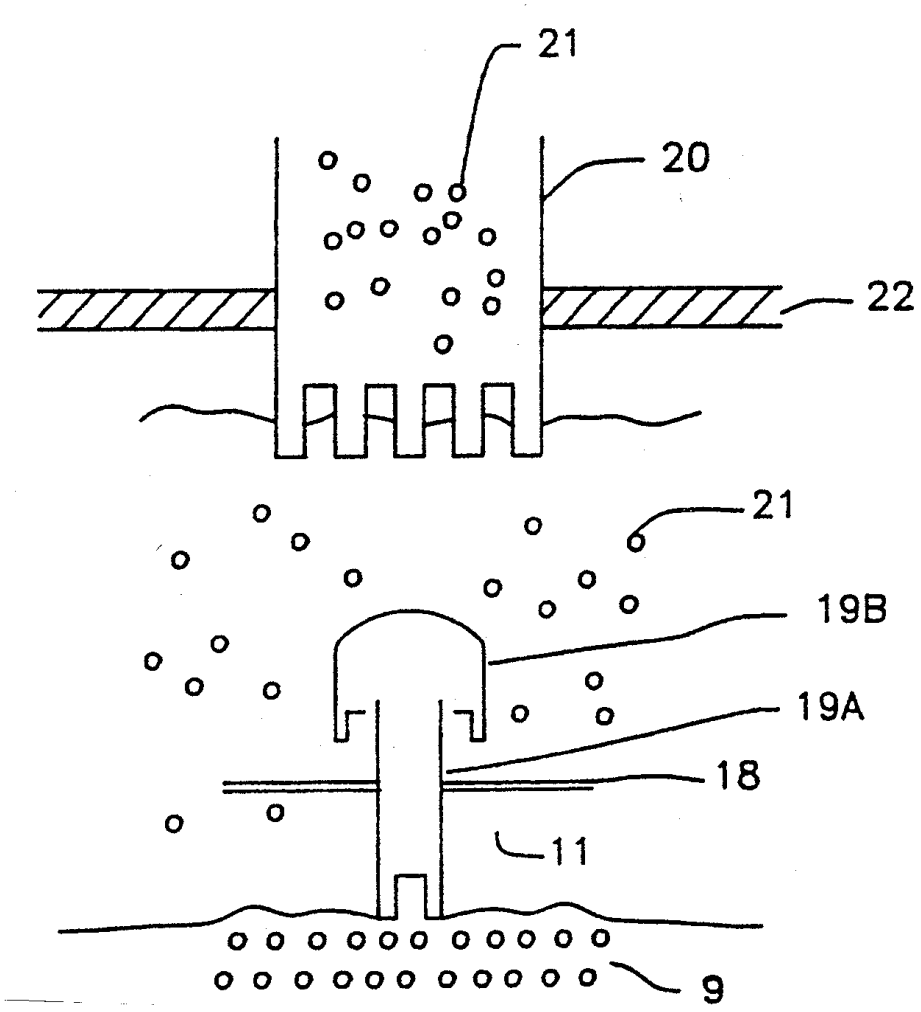

Figure 29. Detail of a possible distribution zone for one reaction tube/zone (from ref. 77).

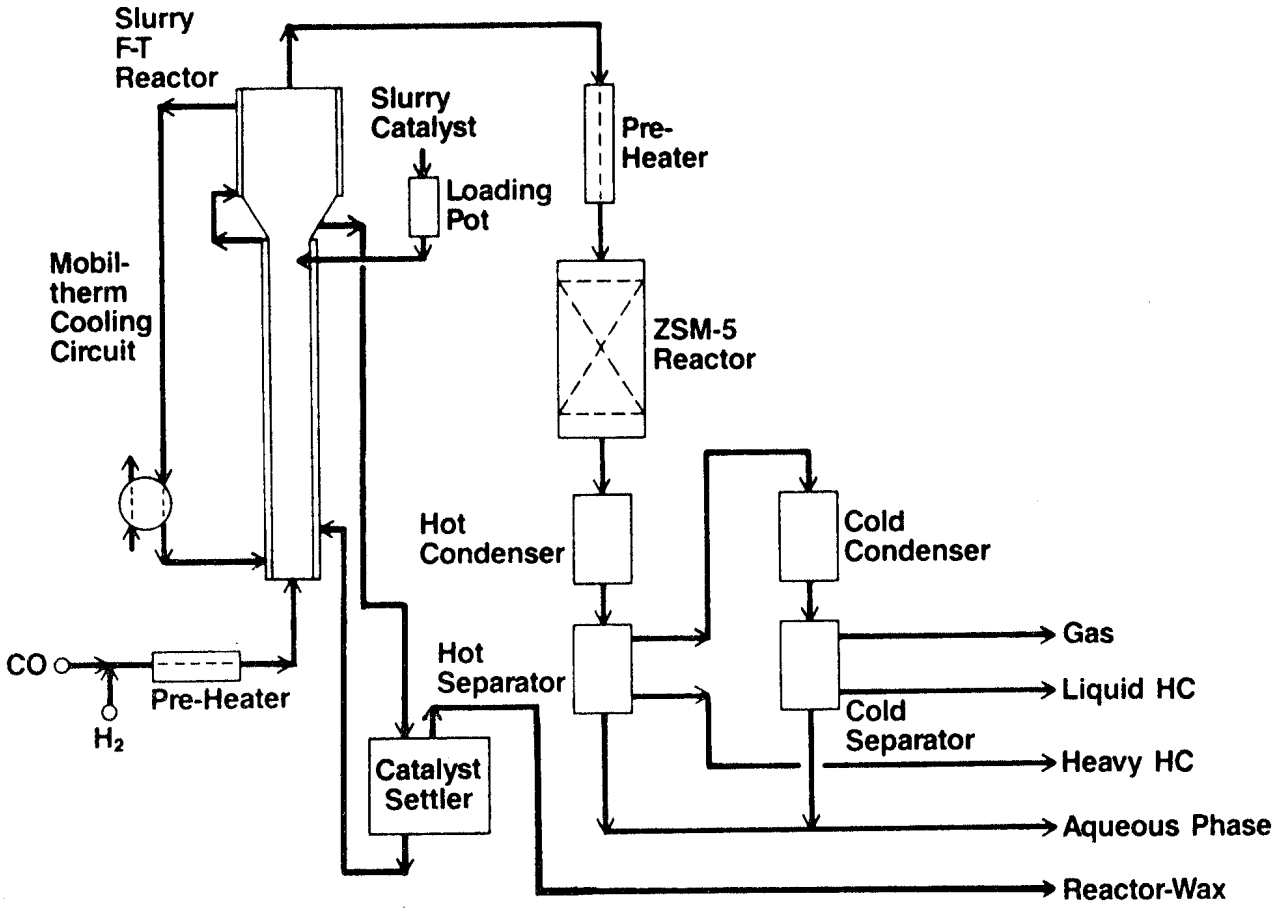

Figure 30. Simplified flow diagram of the Mobil Oil two-stage plant for synthesis gas conversion (from ref. 48).

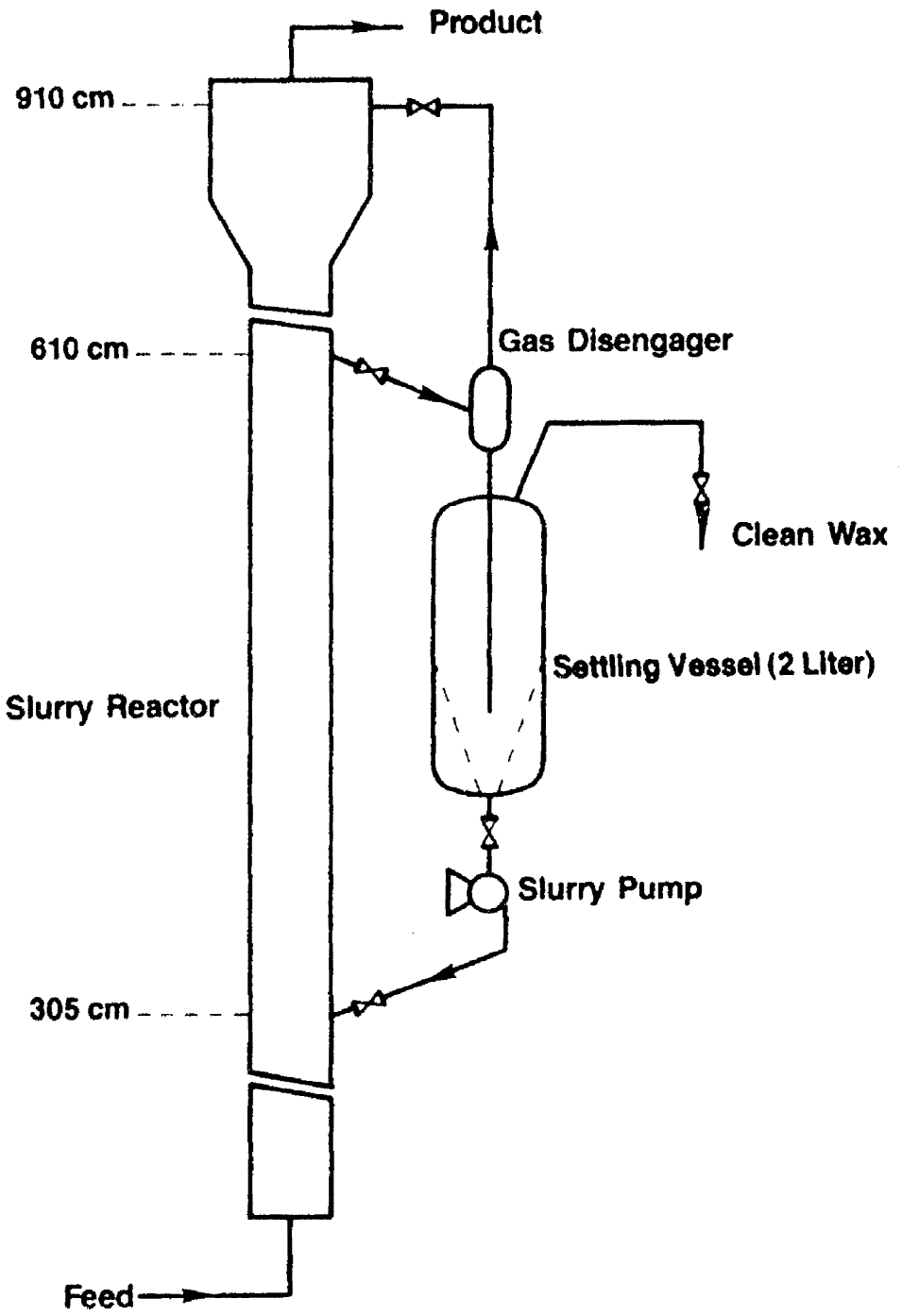

Figure 31. Schematic diagram of the continuous settling system for catalyst/wax separation (from ref. 48).

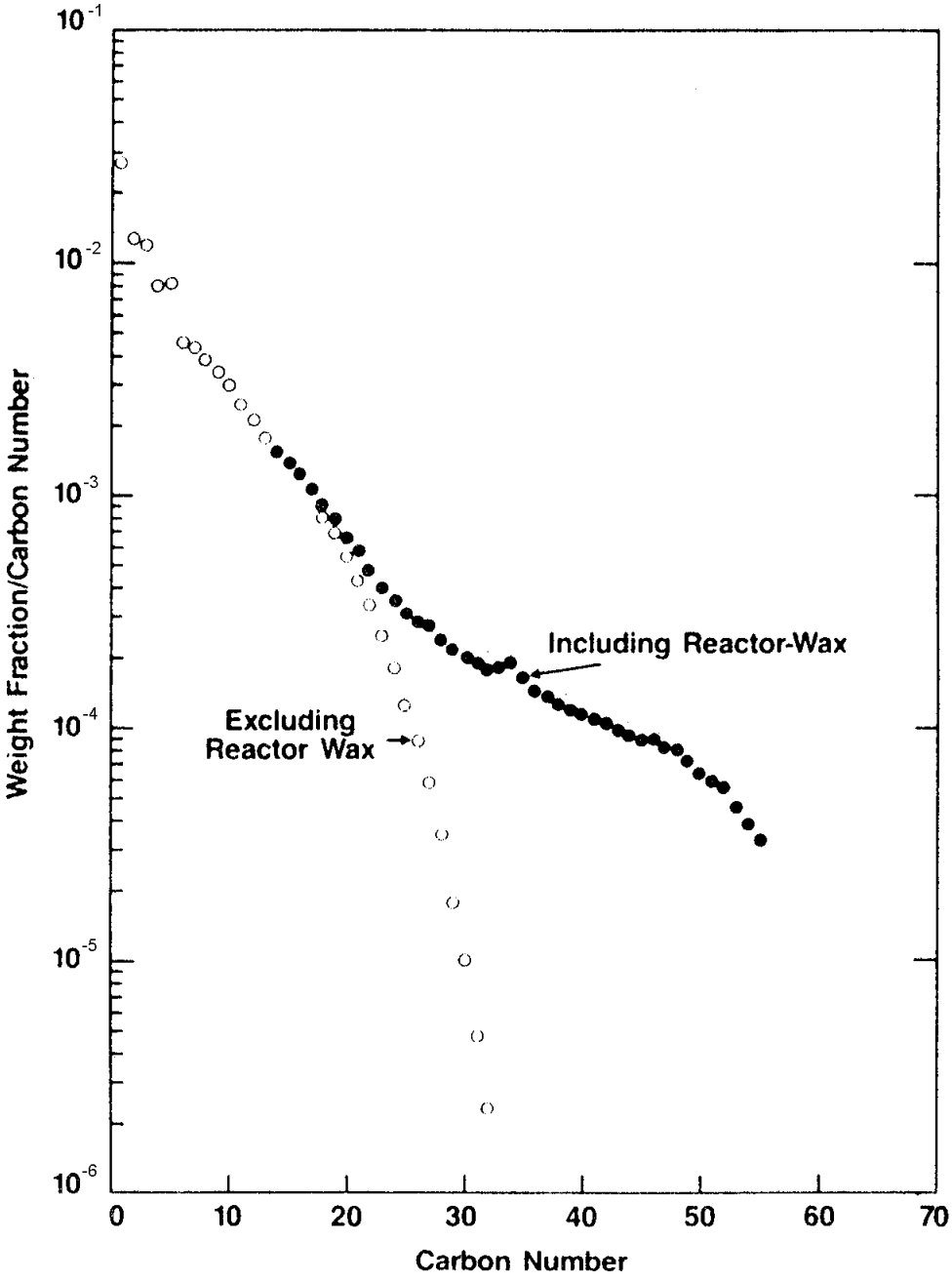

Figure 32. Schulz-Flory distribution for the first stage Fischer-Tropsch products obtained by Mobil Oil at a reactor wax yield of 46 wt.% (from ref. 49).

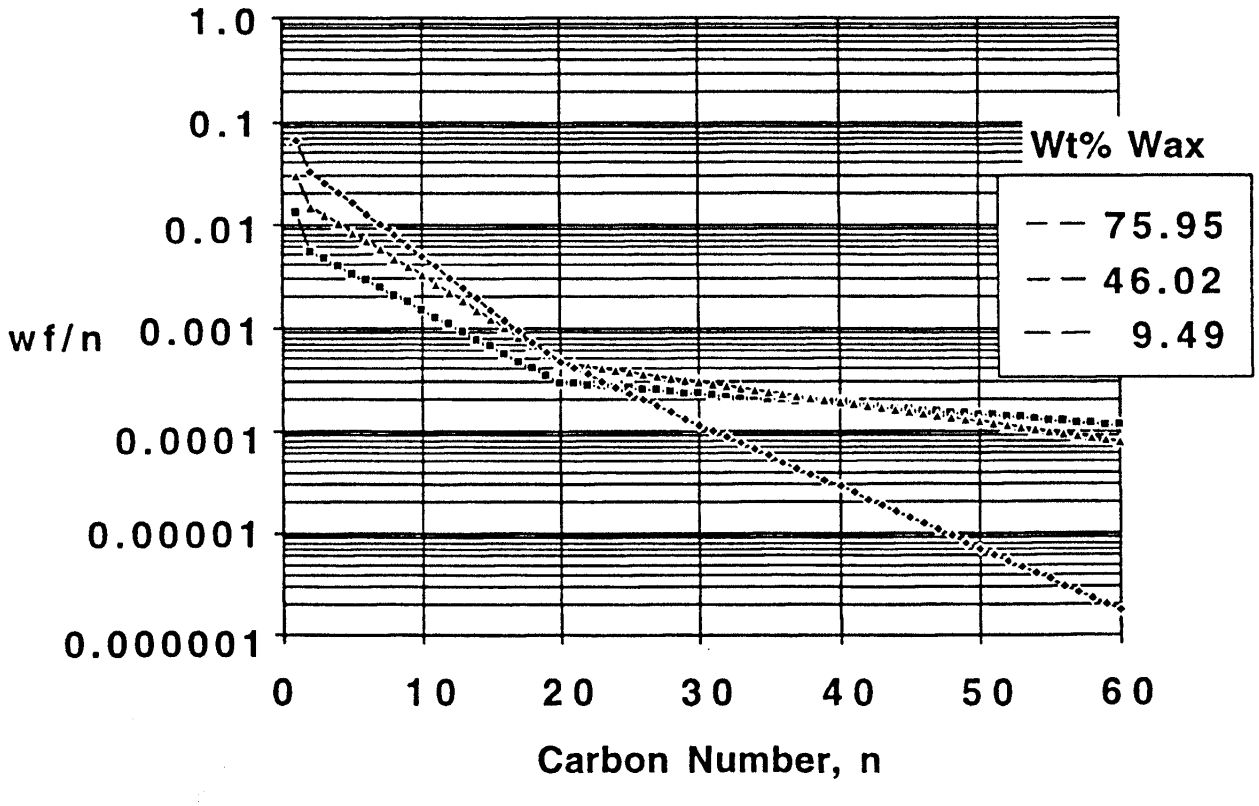

Figure 33. Schulz-Flory distribution based on Mobil Oil data at low, intermediate and high alpha synthesis conditions (from ref. 85).

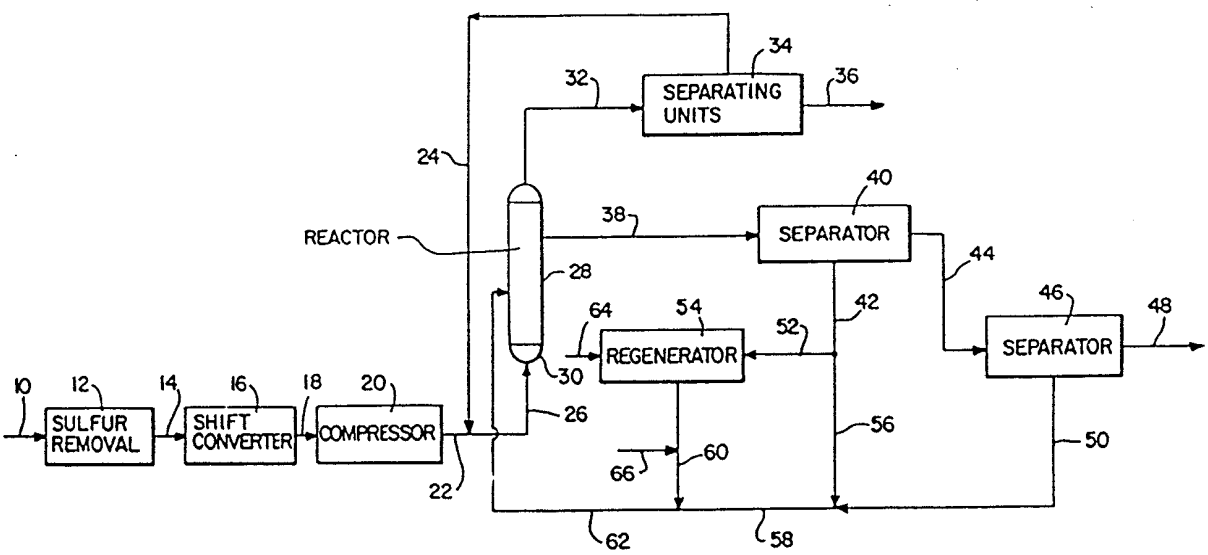

Figure 34. Process schematic for slurry reactor system using cobalt catalyst (from ref. 87).

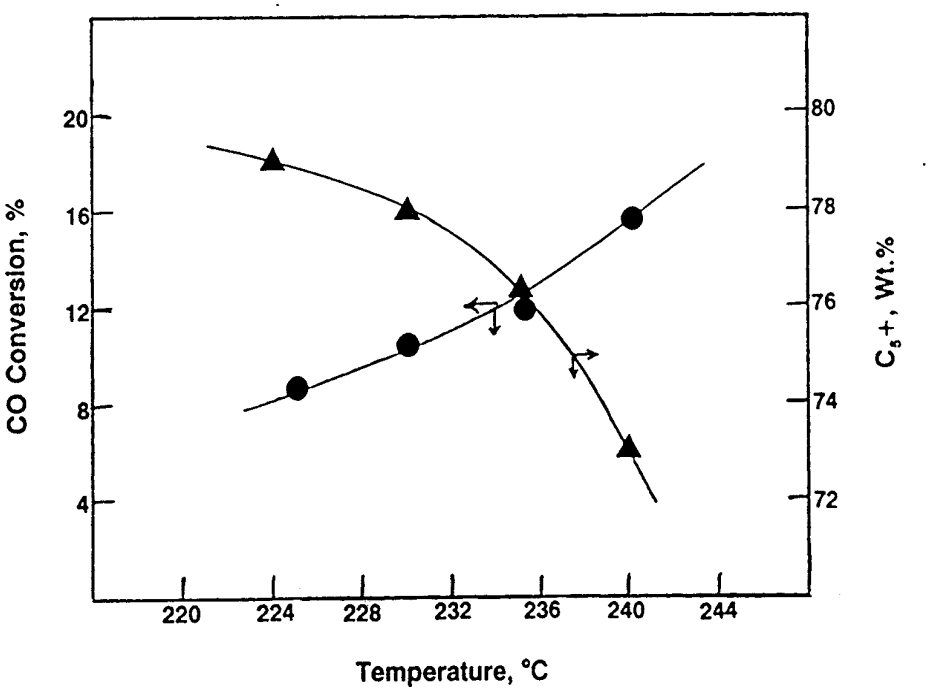

Figure 35. CO conversion and C_5+ product selectivity for FTS using slurry reactor and cobalt catalyst (data from ref. 87).

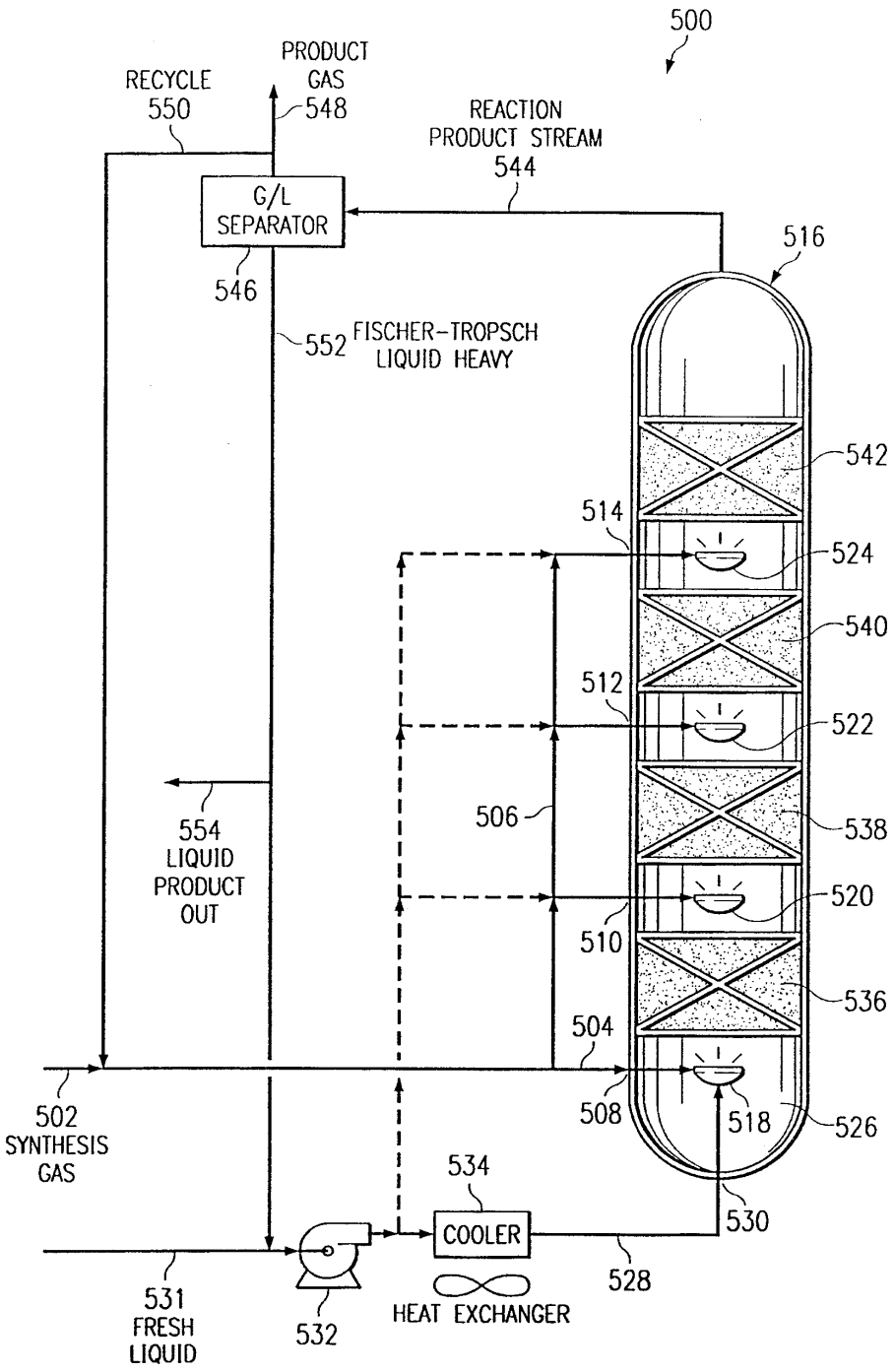

Figure 36. System liquid-phase fixed catalyst bed reactor with gas and/or liquid addition as one or more catalyst trays (from ref. 91).

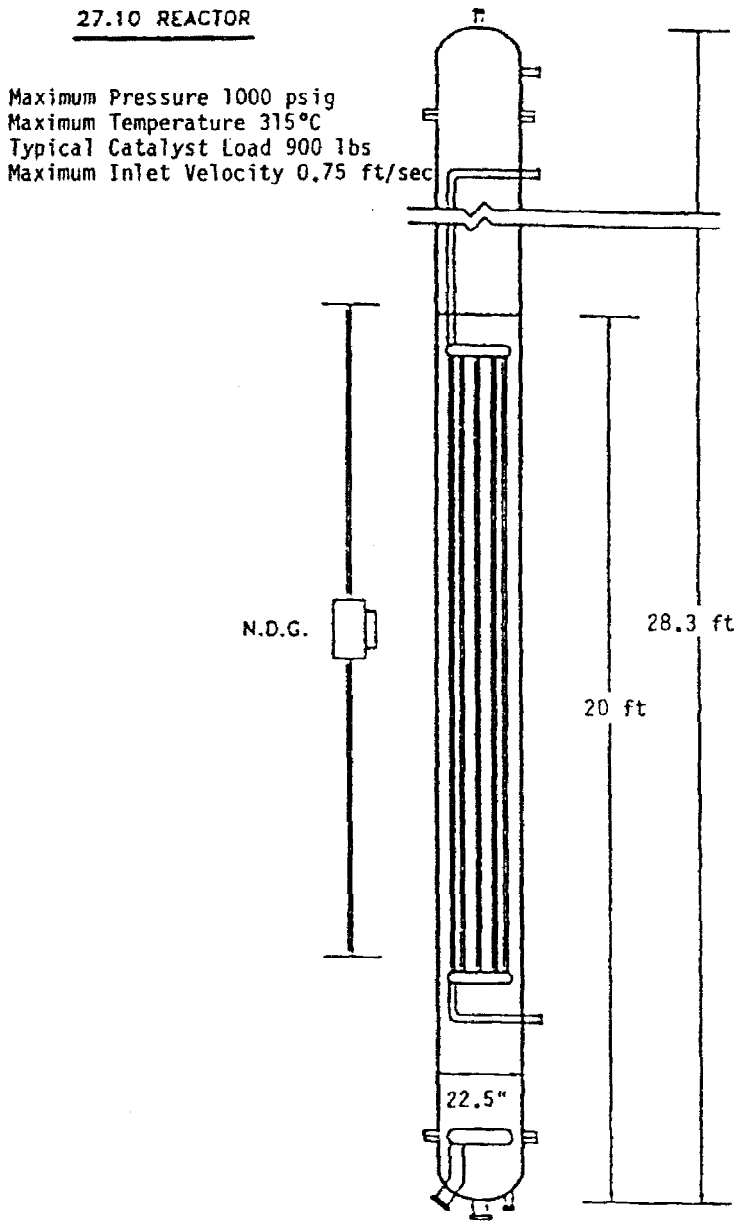

Figure 37. Bubble column reactor (27.10) at La Porte (from ref. 93).

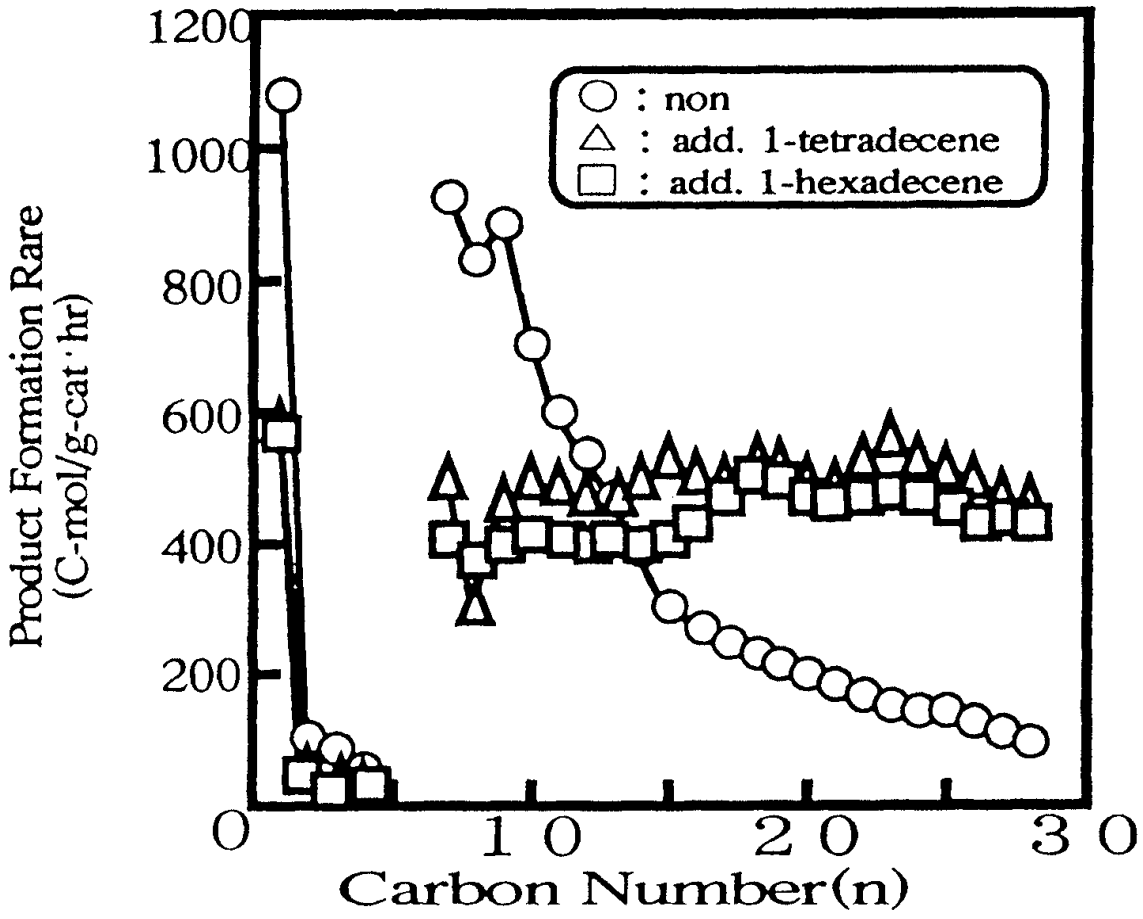

Figure 38. Product distribution in the olefin-added supercritical phase FT reaction with a cobalt catalyst: (F) no olefin added; (△) 1-tetradecene added; (G) 1-hexadecene added (from ref. 111).

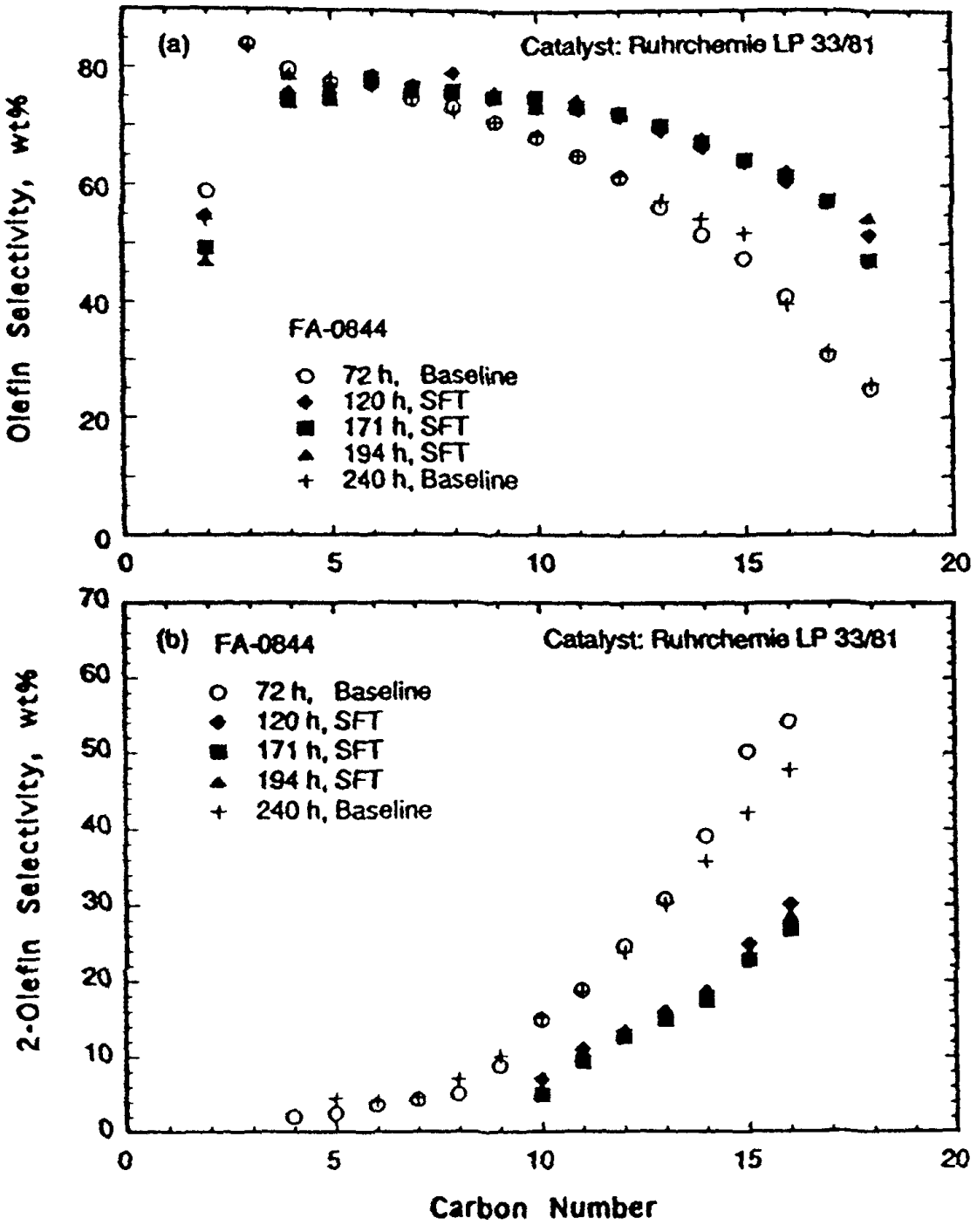

Figure 39. Effect of supercritical FT synthesis on α-olefin (a) and 2-olefin (b) selectivity using an iron catalyst (from ref. 112).

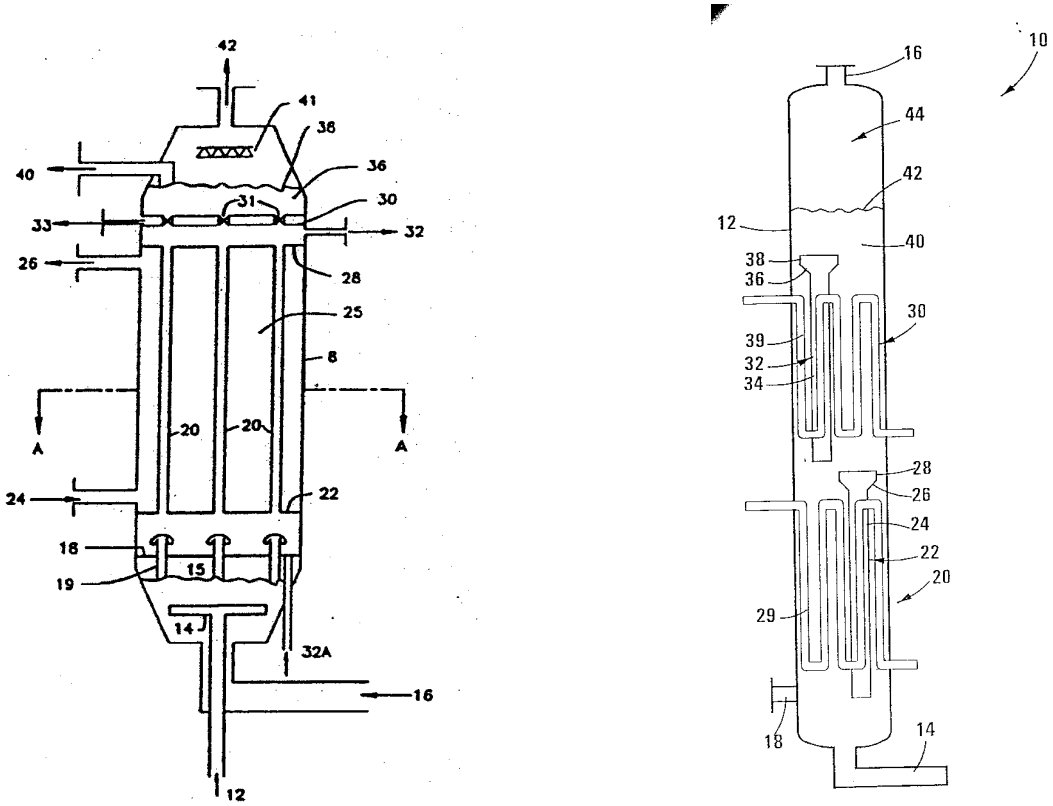

Figure 40. (left) Schematic of Exxon slurry phase reactor (ref. 77); (right) schematic of Sasol slurry bubble column reactor (ref. 118).

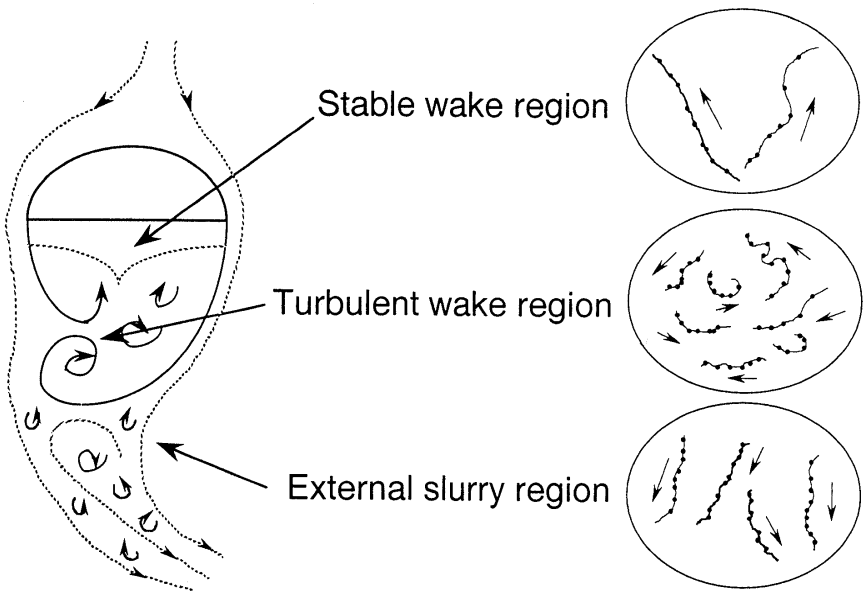

Figure 41. Typical particle trajectories within three different flow regions around a rising bubble (ref. 124).

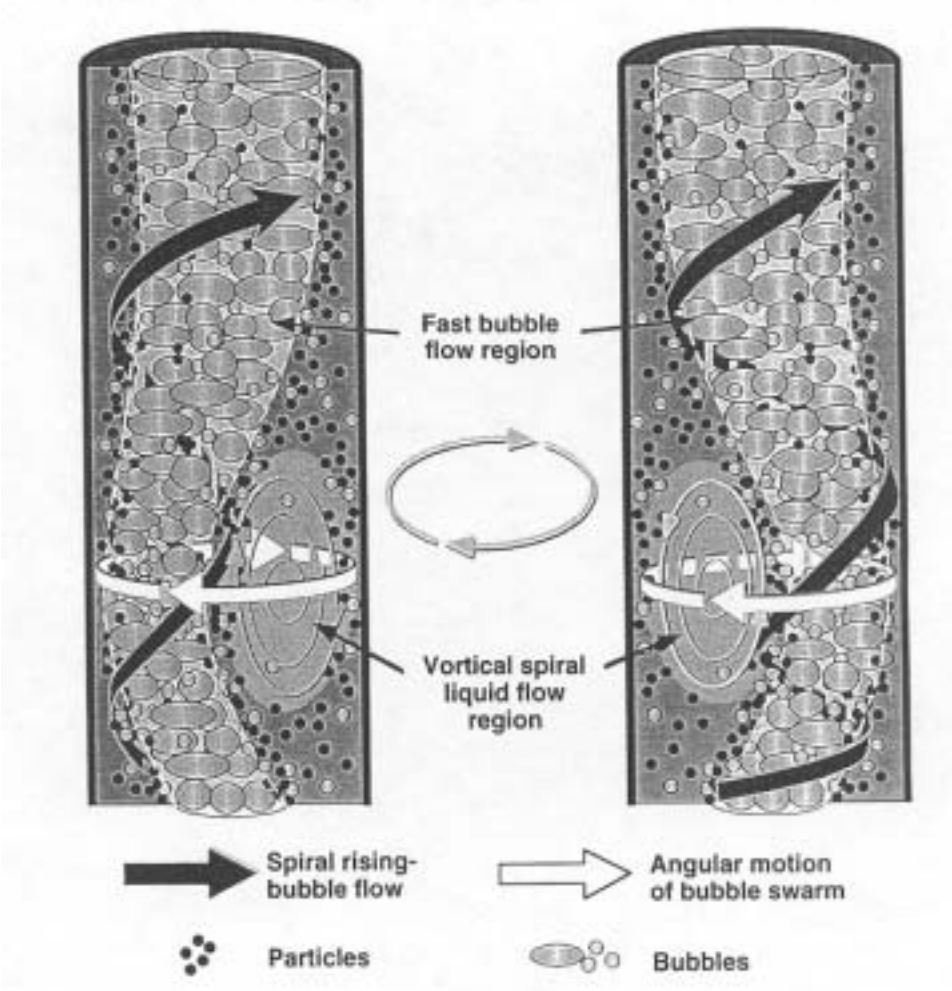

Figure 42. Model of flow scheme in the slurry bubble column (from ref. 127).

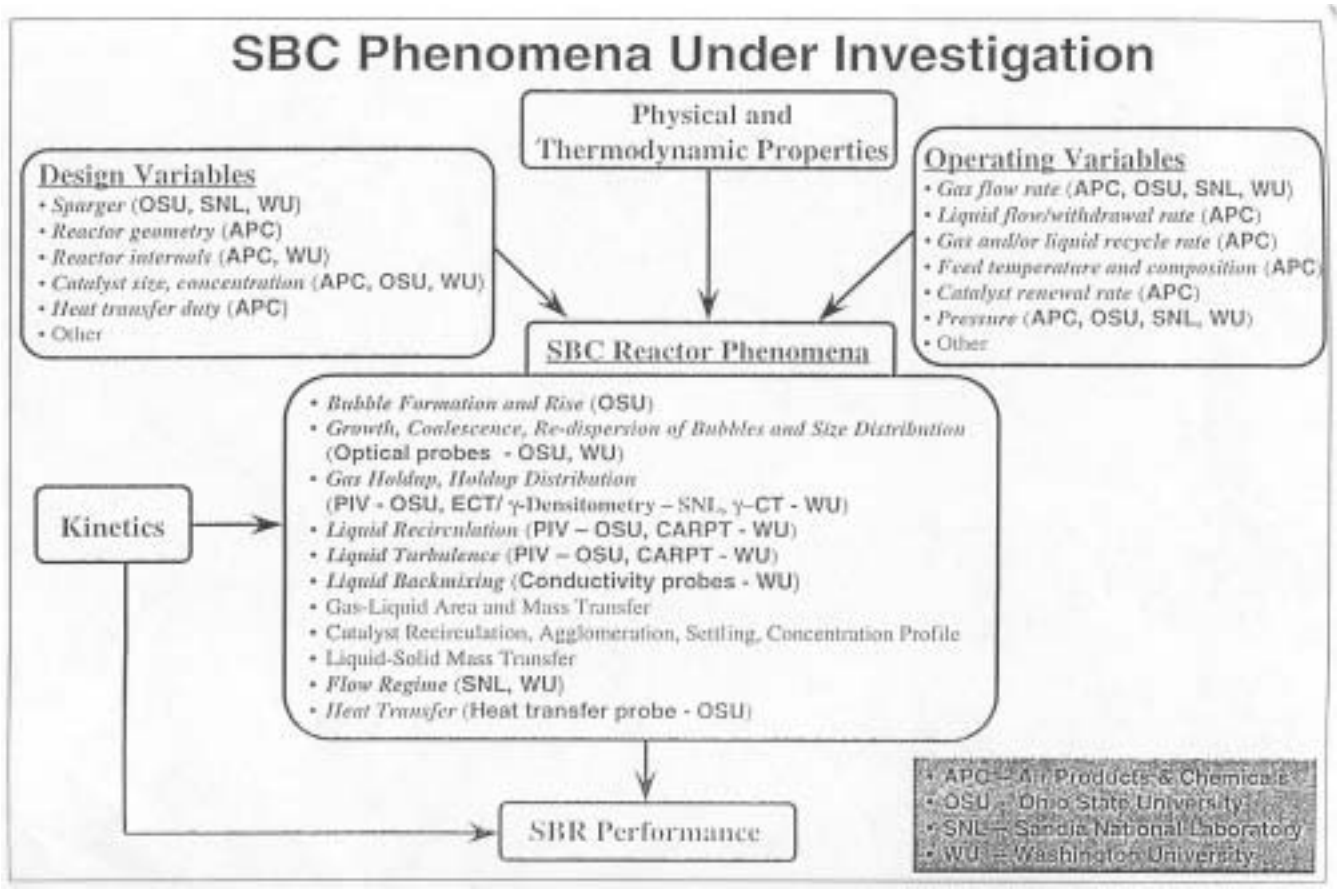

Figure 43. SBC phenomena under investigation (ref. 141).

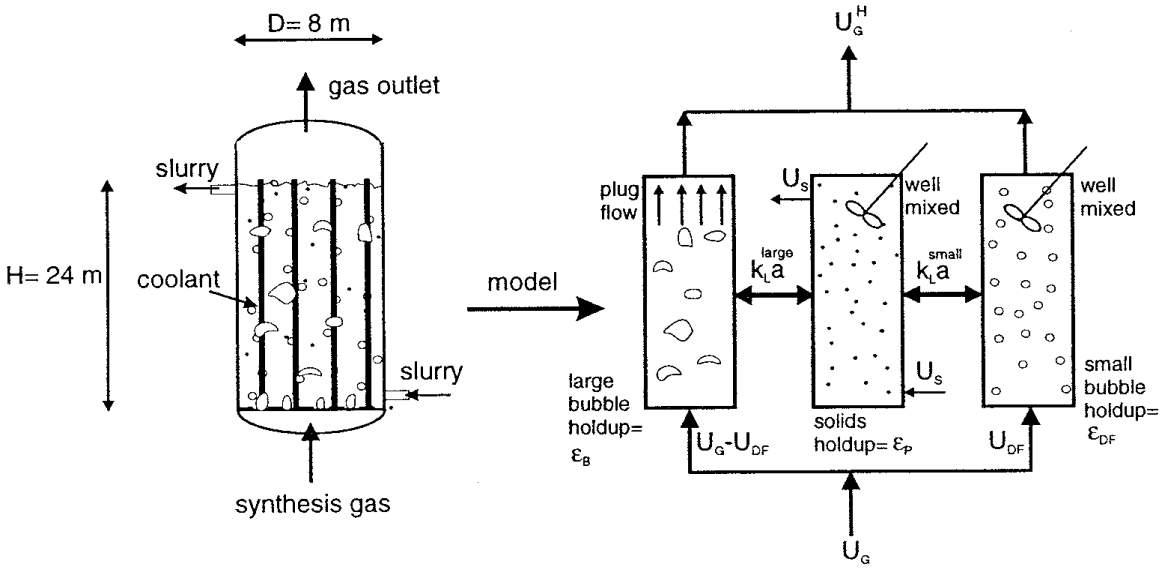

Figure 44. Hydrodynamic model of slurry bubble column reactor in the heterogeneous flow regime (ref. 147).

J. Slurry Bubble Activities

Executive Summary

A Slurry Bubble Column Reactor (SBCR) is a gas-liquid-solid reactor in which the finely divided solid catalyst is suspended in the liquid by rising gas bubbles. The synthesis gas flows in a bubble phase through the catalyst/wax suspension. A gas distributor located in the bottom of the reactor produces the bubbles that rise inside the reactor. The volatile products are removed over together with unconverted gases, and the liquid products are separated from the catalyst suspension through a filter.

A considerable interest has been expressed in using SBCRs to carry out Fischer-Tropsch Synthesis (FTS), particularly for the conversion of stranded natural gas into liquids. Historically, wall effects in small-scale SBCR reactors (diameters less than 30 cm) have presented many challenges with regard to interpretation of kinetic/conversion data for process scale-up. In this paper, we describe a novel 5-cm diameter SBCR system that incorporates a natural slurry recirculation loop that minimizes wall effects and promotes plug-flow behavior in the liquid phase. Conversion performance, catalyst activity decline, and attrition of a precipitated Fe/K FTS catalyst in the improved SBCR is compared to that of a CSTR run using the same catalyst and operating conditions.

Slurry back-mixing in the improved SBCR was significantly reduced by the addition of the down-comer/dip-tube flow path; consequently, the gas and liquid phases likely exhibited more plug-flow behavior. Thus, for a given space velocity, the enhanced SBCR yielded a higher conversion than that of the CSTR. The activity decline measured in the revamped SBCR system was shown to be similar to that of the CSTR experiments. Attrition tests in the SBCR system indicated that the most of the catalyst breakdown occurred between the time period of loading and activation; however, further research will be required to investigate the possibility of particle

size classification/segregation at the sampling points. After activation, the catalyst particle mean diameter decreased in an exponential decay fashion.

Introduction

The Prototype Integrated Process Unit (PIPU) is a pilot plant system built in the early 1980s at the University of Kentucky for studying a multitude of synthetic fuel/chemical processes. Recently, a direct coal liquefaction reactor within the PIPU plant was reconfigured as a SBCR for FTS studies (see Figure 1.). The reactor was originally designed to operate with coarse catalyst pellets (>500 μm). Consequently, the reactor system did not contain a wax separation system sufficient for smaller catalyst particles that are typically used in FTS. Therefore, a slurry accumulator and a batch wax filtration system were installed.

Early attempts to operate the pilot-scale reactor in a F-T mode were successful in that a clear wax product could be obtained. However, the initial activity observed in the bubble column was about 10-15% less than that of comparable CSTR runs. Also, the rate of conversion decline (and apparent catalyst deactivation) in the SBCR was much greater than that observed in the CSTR. It was hypothesized that the apparent increased deactivation rate in the SBCR was caused by the depletion of catalyst inventory due to the nature of the wax/catalyst separation system.

The CAER SBCR plant was overhauled and redesigned to incorporate automatic slurry level control and wax filtration systems. These design changes allowed for a more constant inventory of the catalyst to be maintained in the reactor while reducing slurry hold-up in the catalyst/wax separation system. In addition, the wax filtration system was rearranged to accept a variety of filter elements. These additions were meant to enhance the stability of the reactor operation so that long-term tests can be conducted to study catalyst deactivation and attrition under real-world conditions.

In the following discussion, we will detail the results and operational experiences of a catalyst attrition test with the enhanced SBCR system. Objectives of the study were to: Compare the performance of a precipitated Fe/K Fischer Tropsch Synthesis (FTS) catalyst in the enhanced SBCR and a continuous stirred tank reactor (CSTR); and Determine change of the catalyst distribution within the reactor system due to particle attrition effects.

Experimental

All FTS runs were conducted in either CSTR or SBCR systems. Activation and synthesis conditions for both reactor configurations are listed in Table 1. A precipitated iron catalyst having atomic composition of 100 Fe/4.4 Si/1K was used for this series of experiments.

Table 1. Operating Conditions for SBCR and CSTR Comparison Experiments.

	SBCR	CSTR
H_2/CO Ratio	0.7	0.7
Gas Space Velocity (SL/hr-g Fe)	5.0	5.15
Temperature (^oC)	270	270
Pressure (Mpa)	1.21	1.21
Gas Superficial Velocity (cm/s)	3	750 RPM

CSTR Apparatus. The one-liter CSTR used in this study has been described in detail in the literature [1-2]. The following is a brief description of the reactor system.

The synthesis gas was delivered to the catalyst slurry via a sparger tube located below an impeller blade turning at 750 rpm. The reactor effluent exited the reactor and passed sequentially through two traps maintained at 333 and 273 K. Accumulated reactor wax was removed daily through a tube fitted with a porous metal filter. A dry flow meter was used to measure the exit gas flow rate.

SBCR Apparatus. A schematic of the SBCR apparatus is shown in Figure 1. In the current configuration, the bubble column has a 5.08 cm diameter and a 2 m height with an effective reactor volume of 3.7 liters. The synthesis gas was passed continuously through the

reactor and distributed by a sparger near the bottom of the reactor vessel. The product gas and slurry exit the top of the reactor and pass through an overhead receiver vessel where the slurry was disengaged from the gas-phase. Vapor products and unreacted syngas exit the overhead vessel, enter a warm trap (333 K) followed by a cold trap (273 K). A dry flow meter down stream of the cold trap was used to measure the exit gas flow rate.

A dip tube was added to the reactor vessel so that the F-T catalyst slurry could be recycled internally via a natural convection loop. The unreacted syngas, F-T products, and slurry exited into a side port near the top of the reactor vessel and entered a riser tube. The driving force for the recirculation flow was essentially the difference in density between the fluid column in the riser (slurry and gas) and that of the dip-tube (slurry only). The dip tube provided a downward flow path for the slurry without interfering with the upward flow of the turbulent syngas slurry mixture. Thus, to some degree, back mixing of the slurry phase and wall effects in the narrow reactor [3] tube were minimized.

Based upon the analysis of the initial SBCR pilot plant runs, several more design changes were carried out to the system to increase the conversion stability. An automatic level controller was added to the overhead slurry/gas separation tank. This insured a constant inventory of catalyst particles was being maintained in the reactor vessel if the superficial gas velocity within the column was constant.

Originally, the overhead separator vessel was designed to enhance settling of the catalyst particles. Thus, slurry to be filtered was extracted near the top of the vessel where the catalyst concentration would be lower than that near the bottom. Unfortunately, this approach required a large hold-up volume of slurry outside the reactor (greater than the reactor volume itself). Hold-up of slurry outside the reactor was lowered by decreasing the volume of the overhead vessel from 18 to 4 liters.

The sintered metal filter tube was moved to the liquid down comer below the overhead separation vessel. Currently, the filter is a flow-through device having a sintered metal tube in a shell. Filtered wax was extracted radially through the tube while slurry flows downward in the axial direction. The shear force of the axial slurry flow prevented excessive caking of the catalyst around the filter media. Filtered wax was metered into a storage tank through a let-down valve operated by the overhead liquid level controller. Pressure drop across the filter media can be varied manually by varying the wax storage tank pressure. The filter assembly was configured such that the filter media could be replaced on-line, without aborting or interrupting the reactor run.

The level or volume of the slurry within the receiver was continuously monitored by measuring the differential pressure across the height of the vessel. Argon was purged through each of the pressure legs to keep the lines free of slurry. Slurry volume within the receiver was controlled to be no more than 1.3 liters by removing wax from the reactor system via the level control valve. The unfiltered slurry flowed back to the reactor via a natural convection loop through a dip-tube exiting near the bottom of a reactor.

Samples of the unfiltered slurry were taken from the bottom of the reactor vessel and the overhead receiver tank on a daily basis. Wax products were Soxhlet extracted according to the method of McCartney [4]. The particle size distributions of the extracted catalyst particles were quantified using a light scattering technique by a Cilas 1064 liquid/particle analyzer.

Results and Discussion

SBCR Conversion Comparisons between CSTR and SBCR runs. One of the objectives of the run was to compare the performance of the enhanced SBCR with that of a CSTR configuration. It was anticipated that the modified SBCR system performance, in terms of catalyst deactivation, would be comparable to that of the CSTR experiments. The run/activation

conditions for the enhanced SBCR system along with the comparison SBCR and CSTR conditions are listed in Table 1.

The CO gas conversions versus time-on-stream for the SBCR and CSTR systems are displayed in Figure 2. The CO conversion for the enhanced SBCR with level control reached a maximum of 78% after 72 hours time-on-stream (TOS). After this catalyst initiation period, the gas conversion started to steadily decline to about 72% after 192 hours TOS.

Slurry back-mixing in the SBCR is significantly reduced by the addition of the down-comer/dip-tube flow path; consequently, the gas and liquid phases likely exhibited more Aplug-flow@ behavior. Thus, for a given space velocity, the enhanced SBCR should yield a higher conversion than that of a CSTR [5]. Differences in conversion between the enhanced SBCR and CSTR reactor types may also be caused by the dissimilarity of heat and mass transfer phenomena.

SBCR Catalyst Attrition. Heavy wax products must be separated from catalyst particles before being removed from the reactor system. Achieving an efficient wax product separation from the catalyst is one of the most challenging technical problems associated with slurry-phase F-T. The breakdown of the catalyst particles and the production of heavy wax using high alpha catalysts can further exasperate the filtration problem. Thus, designing a physically robust catalyst without compromising activity is an important factor for a stable and economical F-T process. However, small-scale catalyst attrition tests may not be adequate in simulating the environment within a bubble column reactor. In previous studies [6,7] by Jothimurgean and Zhao an air-jet attrition tester as outlined in the ASTM-D-5757-95 test method was used to compare the relative breakdown resistance of catalysts. This method is useful in comparing the relative strength between catalyst candidates; however, it does not yield information as to the rate of attrition during synthesis. Attrition data in CSTR systems are compromised by the

extreme impact and shear forces from the impeller blade on catalyst particles. In contrast, the SBCR unit does not utilize any mechanical pumping devices that could alter the size distribution of the catalyst. Consequently, SBCR particle attrition will depend mainly on chemical changes within particles and perhaps some particle/wall or particle/particle mechanical abrasion.

Figure 3 shows the changing distribution of catalyst concentration with TOS. During the start of activation, only a small fraction of catalyst fines were detected in the reactor effluent stream. However, near the bottom of the reactor the concentration of catalyst particles was greater than 25 wt%. This indicated the liquid recirculation rate was not sufficient to fully entrain the largest (>23 mm) catalyst particles. As the activation process was completed (TOS = 0), the slurry effluent contained about 5 wt% of catalyst fines. Thereafter, the solids concentration of the reactor effluent increased linearly with TOS.

The mean particle size of the reactor bottom and effluent streams are shown in Figure 4. The dotted horizontal line represents the initial mean particle size of the raw catalyst. Physical classification of the catalyst particles was apparent as evidenced by the mean particle size of slurry in the bottom being greater than that of the raw catalyst. As the synthesis progressed, the mean particle size in the reactor dropped below the baseline (23 mm) after only 40 hours TOS. In summary, the data shown in Figures 3 and 4 indicate that a significant portion of the catalyst exited the reactor system due to particle attrition after 40 hours of TOS. Considering the slurry hold-up outside the reactor was maintained at less than 1 liter, the percentage of catalyst lost after 40 hours TOS was less than 20 wt%. Therefore, this lost catalyst must be considered when calculating the space velocity.

Conclusions

Tight control of catalyst distribution within SBCRs should be maintained in order to quantify activity decline, especially for small pilot plant systems. Transient problems with

previous SBCR experiments were caused by a maldistribution of catalyst between the reactor and slurry filtration system. The level indication/control system installed in an enhanced SBCR was robust and effective in maintaining a steady inventory of catalyst slurry in contact with the gas-phase. Measured deactivation rates in the enhanced SBCR system were comparable to that of CSTR experiments under similar conditions.

Attrition tests in the SBCR system indicated that the most of the catalyst breakdown occurred during catalyst activation and the initial synthesis stage; however, further research will be required to investigate the possibility of particle size classification/segregation at the sampling points. After activation, the catalyst particle mean diameter decreased in an exponential decay fashion. Attrition effects must be considered in order to accurately estimate the space velocity in pilot-scale SBCRs.

References

1. R. J. O'Brien, R., L.Xu, D. Milburn, Y. Li, K. Klabunde, and B. Davis, *Top. Catal.*1995, 2, 1.
2. O'Brien, R., L. Xu, R. L. Spicer, and B. H. Davis, *Energy & Fuels*, 10 (1996) 921.
3. Marretto, C. and R. Krishna, AModeling of Bubble Column Slurry Reactor for Fischer-Tropsch Synthesis@, *Catalysis Today* 52 (1999) 279-289.
4. McCartney, J.T., L. Hofer, B. Seligan, J. Lecky, W. Peebles, and W. Anderson, *J. Phys. Chem.* 1953, 57, 730.
5. Fogler, H., Elements of Chemical Reaction Engineering, 1st Edition, pgs. 273-278, Prentice-Hall, Englewood Cliffs, New Jersey 07632, 1986, ISBN 0-13-263476-7.
6. Jothimurugesan, K., J. Goodwin, Jr., S. Gangwal, and J. Spivey, "Development of Fe Fischer-Tropsch Catalysts for Slurry Bubble Column Reactors", *Catalysis Today* 58 (2000) 335-344.
7. Zhao, R., J. Goodwin, Jr., K. Jothimurugesan, S. Gangwal, J. Spivey, "Spray-Dried Iron Fischer-Tropsch Catalysts. 1. Effect of Structure on the Attrition Resistance of the Catalysts in the Calcined State", *Ind. Eng. Chem. Res.* 2001, 1065-1075.

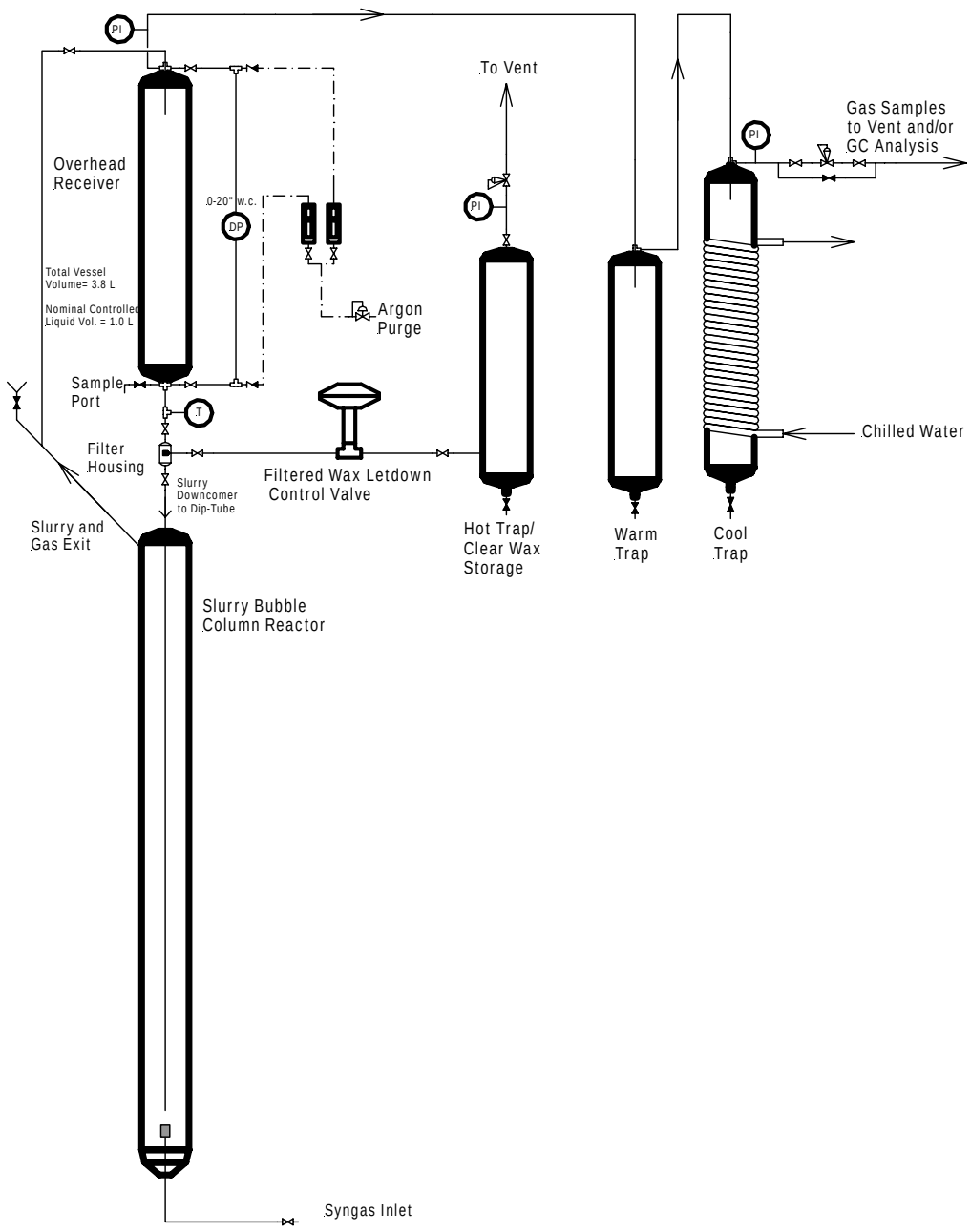

Figure 1. Schematic of SBCR pilot plant system.

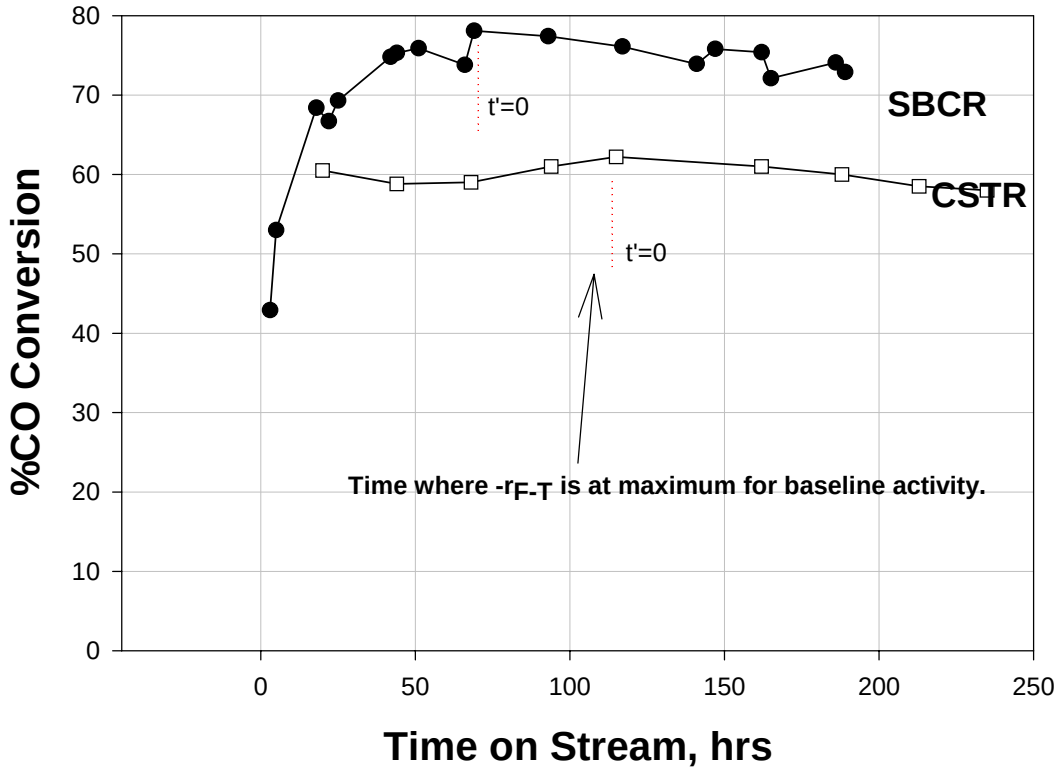

Figure 2. CO conversion comparison between reactor types.

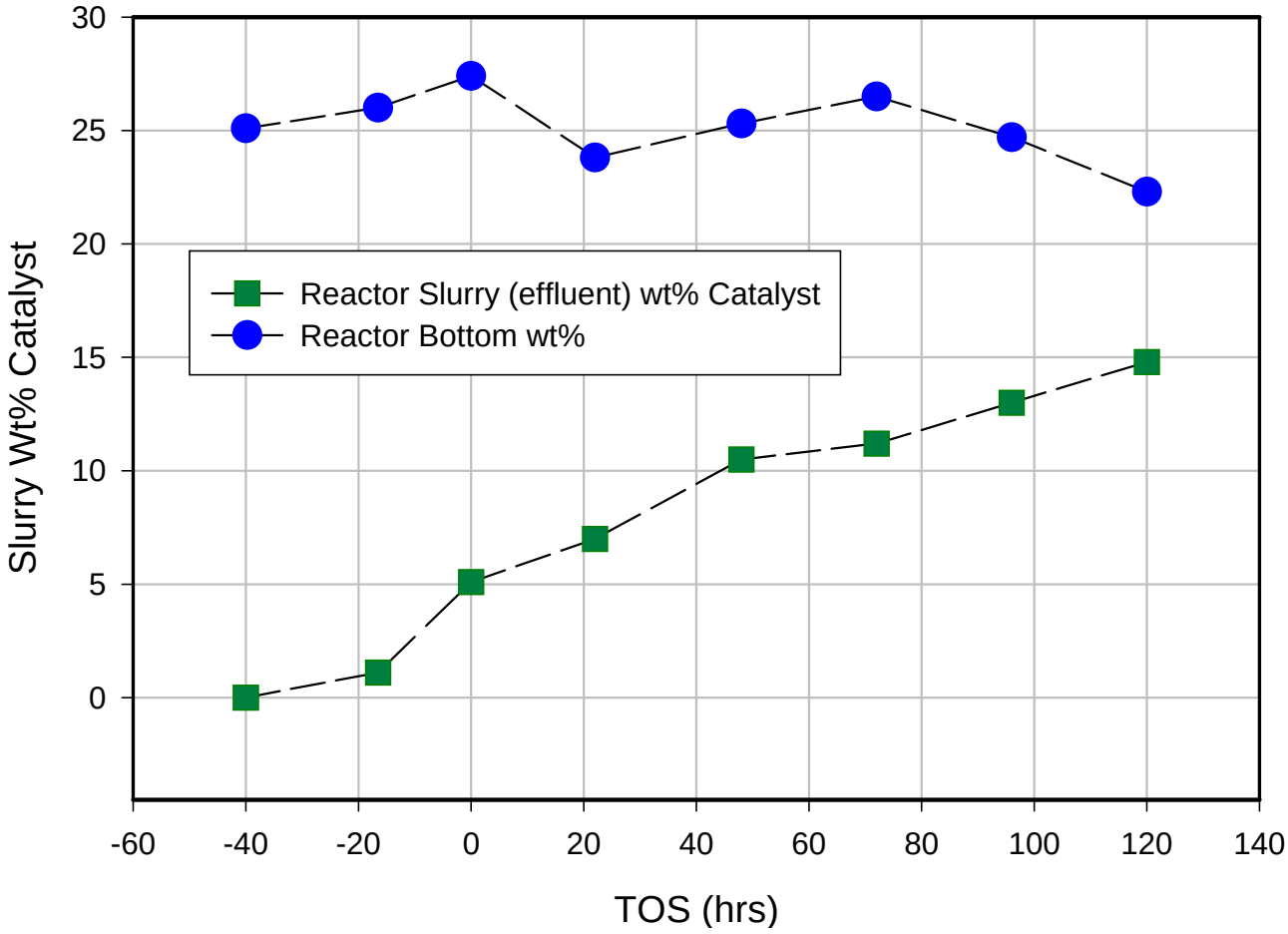

Figure 3. Catalyst solids distribution (reactor and reactor effluent) versus time-on-stream.

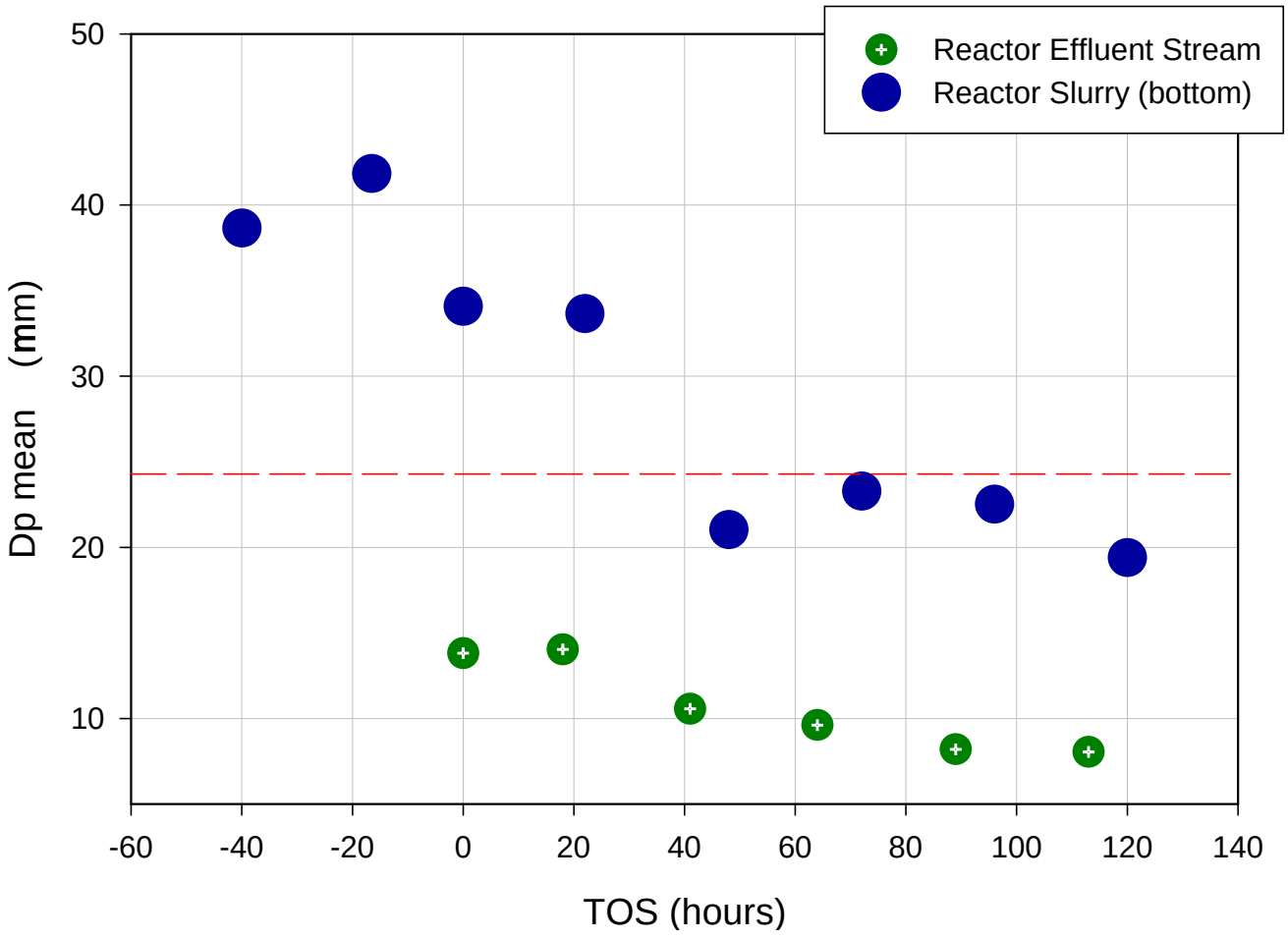

Figure 4. Mean particle size in the catalyst slurry versus time-on-stream (reactor and reactor effluent).